AN INTRODUCTION TO THE MATHEMATICAL THEORY OF DYNAMIC MATERIALS

Advances in Mechanics and Mathematics

VOLUME 15

AN INTRODUCTION TO THE MATHEMATICAL THEORY OF DYNAMIC MATERIALS

By

KONSTANTIN A. LURIE
Worcester Polytechnic Institute, Worcester, MA

Springer

Library of Congress Control Number: 2006940343

ISBN-10: 0-387-38278-X e-ISBN-10: 0-387-38280-1

ISBN-13: 978-0-387-38278-4 e-ISBN-13: 978-0-387-38280-7

Printed on acid-free paper.

AMS Subject Classifications: 35L05, 35L70, 49S05, 49K20, 78A40, 78A48

9 8 7 6 5 4 3 2 1

springer.com

To the memory of Ella

Contents

List of Figures

Preface

This book has emerged from the study of a new concept in material science that has been realized about a decade ago. Before that, I had been working for more than 20 years on conventional composites assembled in space and therefore adjusted to optimal material design in statics. The reason for that adjustment is that such composites appeared to become necessary participants in almost any optimal material design related to a state of equilibrium.

A theoretical study of conventional composites has been very extensive over a long period of time. It received stimulation through many engineering applications, and some of the results have become a part of modern industrial technology. But again, the ordinary composites are all about statics, or, at the utmost, are related to control over the free vibration modes, a situation conceptually close to a static equilibrium.

The world of dynamics appears to be quite different in this aspect. When it comes to motion, the immovable material formations distributed in space alone become insufficient as the elements of design because they are incapable of getting fully adjusted to the temporal variation in the environment. To be able to adequately handle dynamics, especially the wave motion, the material medium *must itself be time dependent*, i.e. its material properties should vary in space and time alike. Any substance demonstrating such variation has been termed a *dynamic material* [1].

The wave propagation through dynamic materials may be accompanied by a number of special effects that are unthinkable with regard to purely *static materials* mentioned above. In general, dynamic materials may be thought of as assemblages of conventional materials distributed in *space and time*; particularly, they may be involved in their own material motion. When such assemblage is furnished with a microstructure, we may call it a *dynamic composite*, or a *spatio-temporal composite*, contrary to its conventional (i.e. static) counterpart.

Unlike conventional composites, dynamic materials are rarely found in mother nature: all of them known so far have come into the scene as the products of modern technology. The only exception, though of extreme signif-

icance, is a living tissue. There is one fundamental feature that brings the two substances together: they both participate in a permanent exchange of energy and momentum with the environment and therefore appear to be thermodynamically open systems. Due to this exchange, the dynamic materials represent a suitable environment for dynamics, especially for the wave propagation. This particular feature adds much to the resources available to a designer because it makes it possible to establish an effective control over both spatial and temporal behavior of a dynamic system.

Regardless of a material implementation, it is now the time to investigate some general features of dynamic materials mathematically. A general scheme for such investigation may be similar to the one successfully tested with regard to ordinary static composites. One of the most exciting problems that received solution in this connection is the problem of material mixing in space. A study of this problem has put forth a special concept of a G-closure (GU) of the original set U of materials [2],[3],[4]. A G-closure is defined as a set of the effective properties of all mixtures that are produced when the original materials become intermingled on a microscale, regardless of a structural geometry. Clearly, $U \in GU$. The G-closures were found explicitly for a number of sets U with regard to some important elliptic differential operators arising in electrostatics and in the theory of elasticity. Analytically, all of the G-closures known so far have been found with the aid of a special technique named the translation method [3]; it has been worked out specifically for this purpose. The knowledge of a G-closure is sufficient for a correct formulation of many design problems that remain ill-posed without such knowledge.

The idea of a G-closure has emerged from the desire to make a set of available materials complete, simply by adding all possible mixtures to it. This idea surely persists in a hyperbolic context, too, and it has been an intriguing task to investigate G-closures produced by some typical hyperbolic operators governing the non-stationary phenomena developing in dynamic materials. Some results of such studies are included into this book. The analysis is related to a simple wave operator

$$(\rho u_t)_t - (k u_z)_z, \tag{0.1}$$

with coefficients ρ, k being both t and z-dependent. The problem is therefore two dimensional, with one spatial coordinate z and time t. The operator (1) serves as a good model, similar to that given by the operator

$$\mathrm{div}\mathcal{D}\mathrm{grad}u, \quad \mathcal{D} = \mathcal{D}(x, y), \tag{0.2}$$

in a relevant elliptic situation. Many features of hyperbolic G-closures revealed through the study of (1) are quite special and substantially different from the properties of the G-closures associated with (2). These differences are likely to be even more pronounced in the case of higher spatial dimensions. The latter has not been investigated in detail in this introductory text; however, the very notion of a dynamic material, as well as the procedure of material

mixing in space-time received a clear mathematical implementation in many spatial dimensions as well. Remarkably there is a fundamental physical theory, namely Maxwell's theory for moving dielectrics, that perfectly embodies dynamic materials as a natural dielectric medium capable of conducting electromagnetic waves. It was rewarding to find such a theory, so to speak, on the surface, because it immediately offered a natural classification of dynamic materials produced by two conceptually different ways of mixing in space-time. The reader will find a brief account of these ideas on the opening pages of the main text.

I fully realize that the presentation below is a first step towards an extensive theory that should unveil in the future. My purpose was to try to get a clear vision of the base ideas, and I believe that an interested reader will be able to share the excitement that I experienced while working on this beautiful subject.

Acknowledgments

This text would probably not appear without invaluable support that I had from many people. My thanks go to my dear colleague and friend, Dr. Suzanne L. Weekes, whose contribution to this new field is quite solid; many of her results are included into the text as its indefeasible part. Dr. Brian King of the Department of Electrical and Computer Engineering in Worcester Polytechnic Institute has contributed most of the text of sections 1.3, 1.4 of Chapter 1. Colleen Lewis and Elizabeth Teixeira of the Department of Mathematical Sciences in Worcester Polytechnic Institute did a magnificent job on typing and graphics. Major inspiration has come from discussions that I had with my old friend Professor Ilya I. Blekhman at all stages of this work. I am deeply obliged to my colleagues and friends for their remarkable effort.

My special thanks and admiration go to my wife Sonia, to my son Dmitri and daughter Aleksandra whose exceptional perseverance gave me inspiration and force to go through a difficult time when this text was written.

Support for the study of dynamic materials given through NSF Grants DMS-9803476, DMS-0204673, and DMS-0350240 is gratefully acknowledged.

Worcester, Massachusetts The Author
December 2005

References

1. Blekhman, I.I., and Lurie, K.A.: On dynamic materials. Proceedings of the Russian Academy of Sciences (Doklady) **37**, 182–185 (2000)
2. Lurie, K.A.: Applied Optimal Control of Distributed Systems, Plenum Press, 499 pp (1993)
3. Lurie, K.A., and Cherkaev, A.V.: The effective characteristics of composite materials and optimal design of constructions. Advances in Mechanics (Poland), vol. 9, 3–81 (in Russian) (1986)
4. Cherkaev, A.V.: Variational Methods for Structural Optimization, Springer Verlag, xii + 627 pp (2000)

1

A General Concept of Dynamic Materials

1.1 The idea and definition of dynamic materials

The idea of composites is one of the key ideas in material science. When different substances are used as primary elements through the constructing of material assemblages, these new formations may demonstrate properties that are alien to original constituents. Of such properties, the structural anisotropy is probably the most critical. This property is created artificially, through making composites, thanks to their special microgeometry; an anisotropic composite may thus be built from isotropic original constituents. Anisotropy is vitally important for optimal design: every such design is a custom-tailored formation built purposefully to fit in the environment peculiar to a concrete working situation. Examples illustrating this are numerous; they may be found in many texts, (see, e.g., [1],[2],[3]).

Until recently, the concept of composites has been viewed as essentially static: a composite that is ordinary in a conventional sense, is assembled once and for all in space, and this assemblage remains invariable in time. This concept fits well into the problems related to a static equilibrium; however, it fails to be adequate with regard to a dynamic environment.

To work effectively in a dynamic world, a material medium should be responsive to dynamic disturbances allowing for the energy and momentum exchange take place between various parts of the system on a suitable spatio-temporal scale. It should be able to maintain selective interaction between the material property patterns and dynamic disturbances, i.e. such interaction should occur wherever and whenever necessary. This fundamental requirement could be met if we resort to a special material arrangement termed a *dynamic material*.

Dynamic materials are defined as formations assembled from ordinary materials distributed in space *and* time. When such formation is allotted with a microstructure, a dynamic material becomes a dynamic (spatio-temporal) composite. The appearance of time is special: it serves as an additional fast

variable. The presence of such a variable combined with the fast variable spatial coordinate, transforms an ordinary composite assembled in *space alone*, into a dynamic composite distributed in *space and time*.

The dynamic disturbances whose spatio-temporal scale is much greater than the corresponding scale of the assemblage, may perceive this one as a new material allotted its own effective properties. By changing the material parameters of original substances, as well as the microgeometry, we shall be able to selectively control the dynamic processes by creating effects that are unattainable so far as we operate with ordinary materials or composites.

One may set a difference between various types of dynamic materials, and we will introduce their formal classification in Chapter 3. At the same time, such materials share one special feature that is common to all of them: they universally appear to be substantially non-equilibrium formations. To create a dynamic material, we have to maintain the energy exchange between it and its surroundings. Energy should either be pumped into the medium, or it should be extracted from it. The effective properties of dynamic materials are therefore specifically affected by the relevant energy flows. For this reason, dynamic materials themselves appear to be thermodynamically open systems; only a combination of such material and the environment may be considered as closed.

To some extent, dynamic materials fall outside a stock notion of a material as of something that can be taken into your hands, stored, moved, manufactured once for all, individualized by placing some "indelible" labels, etc. There is no such thing as "a piece of dynamic material". Instead, they would rather be "brought into the scene" and exist with the environment. For example, a TV screen on which a movie is demonstrated represents a dynamic material: our eye perceives it, through a movie performance, as a plane with the reflection properties variable in space and time. A human mechanism of vision implements a spatio-temporal averaging of a pattern of rapidly alternating sequences and thereby detects a "slow motion" carrying information stored in the movie.

The concept of dynamic materials appears to be a special realization of the idea of *smart* materials, i.e. substances able to respond to environmental variations by changing their properties, structure or composition, or their function both in space and time.

1.2 Two types of dynamic materials

Dynamic materials have originally been introduced in [4], [5] in both mechanical and electromagnetic contexts. They have been classified into two major categories termed *activated* and *kinetic* materials. The difference between such categories is fundamental, and it is best illuminated by examples.

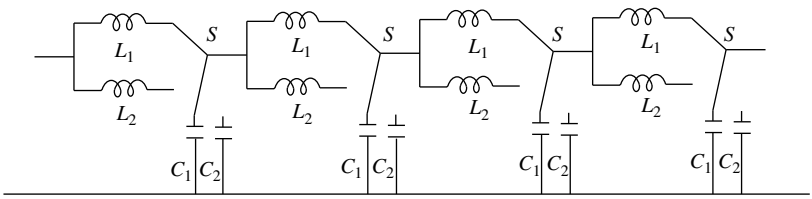

Fig. 1.1. A discrete version of a transmission line.

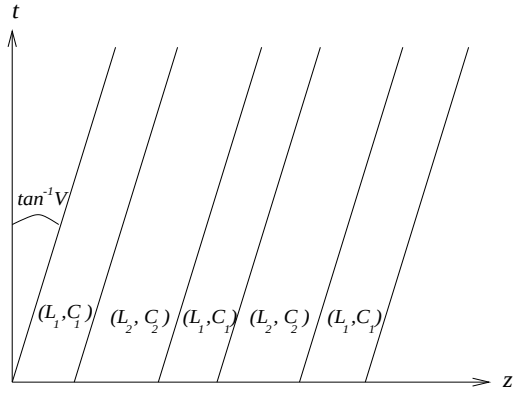

Fig. 1.2. A moving (LC)-property pattern - an activated composite.

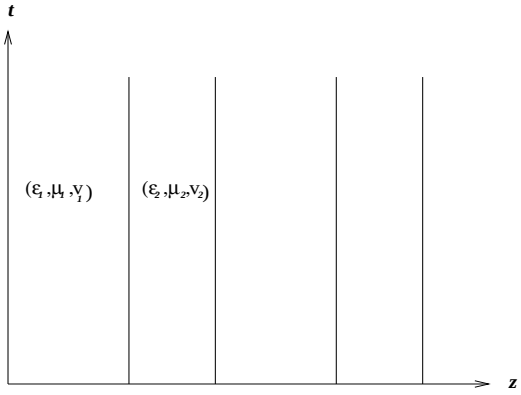

Fig. 1.3. An immovable material pattern with moving original substances - a kinetic composite.

Consider a transmission line. Its discrete version may be interpreted as an array of LC-cells connected in series (Fig. 1.1). Assume that each cell offers two possibilities: (L_1, C_1) and (L_2, C_2), turned on/off by a toggle switch S. If the cells are densely distributed along the line, then, by due switching, the linear inductance L and capacitance C of the line may become, with any desired accuracy, almost arbitrary functions of a spatial coordinate z along the line, and time t. In particular, we may produce in a (z, t)-plane a periodic LC-laminate assembled from segments with properties (L_1, C_1) and (L_2, C_2), respectively (Fig. 1.2). In this figure, a periodic pattern of such segments is shown moving along the z-axis at velocity V, and this motion creates a laminated structure in space-time. It is essential that this construction does not include any motion of the material itself; what is allowed to move, is the *property pattern* alone. This is a pure case of activation, and *activated*

materials appear as a result of a standard homogenization procedure applied to this type of construction.

As another example, consider a dielectric rod assembled from alternating segments occupied by isotropic dielectrics with material constants (ϵ_1, μ_1) and (ϵ_2, μ_2), respectively (Fig. 1.3); we term these dielectrics materials 1 and 2. Within each segment, the material may be brought into its individual material motion along the z-axis at velocities v_1 (material 1) and v_2 (material 2). A discontinuous velocity pattern may be implemented either through the use of a special "caterpillar construction" introduced in [6] and described in Chapter 3, or, approximately, by a fast periodic longitudinal vibration of a dielectric continuum in the form of a standing wave. Contrary to the case of activation, the property pattern, i.e. the set of segments, now remains immovable in a laboratory frame; what is moving, is the *dielectric material itself* within the segments. This is a pure case of kinetization; a *kinetic* material appears after we apply homogenization to this type of construction.

In particular, when materials 1 and 2 are identical, the kinetic material turns out to be a spatio-temporal assemblage of fragments of the same original dielectric, with each fragment brought into its own individual motion. For reasons explained in Chapter 3, this type of kinetic material will be termed a spatio-temporal polycrystal.

In both activated and kinetic laminates, homogenization introduces an averaged characterization of the composite material in terms of its effective constants. This characterization is valid for disturbances whose wavelengths are long compared to the period of the material pattern.

The following example gives an additional illustration of the contrast between activated and kinetic composites. Consider an activated laminate in one spatial dimension, as shown in Fig. 1.4. For a laboratory observer, materials 1 and 2 are kept at rest within the layers, while the property pattern is travelling at velocity V. As we know, that particular feature is characteristic of activation.

A different situation arises if we assume that the same material assemblage is brought *as a whole into a material motion* at the same velocity V along the z-axis; the property pattern will then also travel at velocity V. Clearly, the microstructure in the (z, t)-plane will be given by Fig. 1.4 also. The difference is that, in the second case, a laboratory observer sees the layers occupied by the *moving* materials though there is no motion of such materials relative to one another. The second case therefore appears to be a combination of *activation* produced by the *pattern moving* at velocity V, and of *kinetization* produced by a *material motion* occuring at the same velocity V, identical for both materials.

When we apply homogenization in either of these cases, the effective material is viewed by a laboratory observer as a composite substance moving at some velocity w, generally not the same as V. The effective parameters of this substance will come into the scene if we manage, in a sense, to bring the substance to rest.

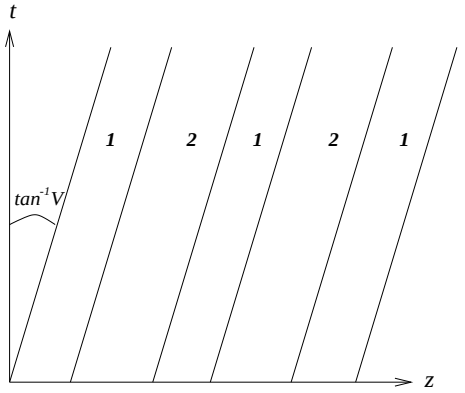

Fig. 1.4. Material laminate in space-time.

To this end, we introduce a *proper* frame travelling at velocity w relative to the laboratory frame. The velocity w is so chosen as to reduce the homogenized equations to a canonical form, through diagonalization of the corresponding matrix of the effective material coefficients. If such a frame exists, i.e. if the required velocity w is real, then the composite will be characterized in this frame by two parameters $\mathcal{E}, M$ - the effective permittivity and permeability of a (homogenized) dynamic dielectric material. In the first case (pure activation) listed above, $w \neq V$, and the effective parameters depend on V. In the second case (activation plus kinetization), an observer moving at velocity $w = V$ perceives the assembly as immovable, and for this reason, its effective parameters prove to be the same as they are for a static composite with $V = 0$, in other words, those parameters appear to be independent of V. A proper frame moving at velocity w then becomes identical with a *co-moving* frame travelling at velocity V. We conclude that, in the second case, the V-dependency of the effective parameters is removed by the counter balancing effect of the material motion that occurs within layers at the same velocity V as the motion of the property pattern itself. These observations will receive a formal implementation in the following chapters. However, it already becomes clear that a material motion plays the same role in spatio-temporal composites as an ordinary rotation plays in conventional (purely spatial) assemblages. Technically, both operations work towards bringing the relevant equations to a canonical form, through diagonalizing the corresponding material tensors. For a dynamic case, diagonalization occurs due to the transition to a proper coordinate frame.

Conceptually, the treatment of a material motion as rotation obtains an ultimate disclosure in electrodynamics. Such a treatment is intrinsic in a relativistic concept which forms a foundation of Maxwell's theory. We shall see in Chapter 3 that this concept provides a perfect framework for the idea of a dynamic material as a spatio-temporal composite. From this standpoint, the

dynamic materials unveil themselves, rigorously speaking, as conceptually relativistic formations, though it would certainly be erroneous to say that they do not display their special features in non-relativistic material motion.

1.3 Implementation of dynamic materials in electronics and optics

It will be important to demonstrate that the mathematical theory and analysis of dynamic materials will correctly model the true natural phenomena. To that end, we must physically assemble proof-of-concept metamaterials and experimentally measure and compare the behavior to the predicted results. In this section we discuss issues specific to implementation and construction of devices that exhibit the desired spatio-temporal behavior.

Effective implementation of the desired temporal switching requires very abrupt changes in the material's permeability (through induced magnetic moments) and permittivity (through induced electric dipole moments). There are numerous ways to temporally adjust both material parameters and we consider the most applicable methods in the following subsections.

1.3.1 Ferroelectric and ferromagnetic materials

Ferroelectric materials respond to an external electric field by producing a spontaneous electric polarization [15],[13],[8],[16]. The polarization results in a modification of the permittivity constitutive relation between the electric field ($\mathbf{E}(x,t)$) and the displacement field ($\mathbf{D}(x,t)$) throughout the material. The effect is characterized by a change in the material's permittivity tensor, $\boldsymbol{\epsilon}$:

$$\begin{aligned}\mathbf{D}(x,t) &= \epsilon\mathbf{E}(x,t) + \epsilon\mathbf{P}(x,t)\\ &= \epsilon\mathbf{E}(x,t) + \epsilon p(\mathbf{E}_A(x,t))\mathbf{E}(x,t)\\ &= \boldsymbol{\epsilon}\mathbf{E}(x,t),\end{aligned}$$

where $\boldsymbol{\epsilon}$ is the effective permittivity tensor due to an applied field $\mathbf{E}_A(x,t)$.

In addition to the spontaneous polarization in ferroelectrics, the material also demonstrates hysteresis as the induced polarization interacts with the applied electric field. As the applied electric field is increased the polarization achieves a saturation value. Fig. 1.5 shows some example hysteresis loops for ferroelectric materials adapted from [11].

Ferromagnetic materials [7],[21] behave very similarly to ferroelectric materials, except that an applied magnetic field produces a magnetic polarization that modifies the relation between the magnetic field ($\mathbf{H}(x,t)$) and the magnetic induction field ($\mathbf{B}(x,t)$) through the permeability tensor, $\boldsymbol{\mu}$:

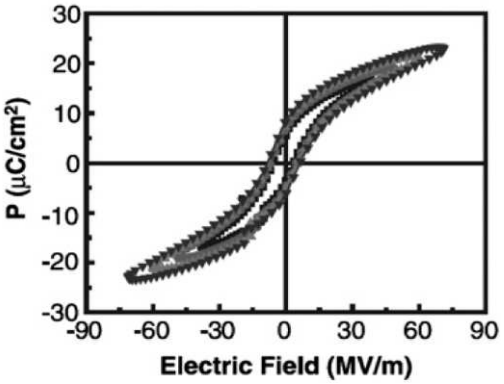

Fig. 1.5. E-P hysteresis curve for ferroelectric materials.

$$\begin{aligned}\mathbf{B}(x,t) &= \mu\mathbf{H}(x,t) + \mu\mathbf{M}(x,t)\\ &= \mu\mathbf{H}(x,t) + \mu m(\mathbf{H}_A(x,t))\mathbf{H}(x,t)\\ &= \boldsymbol{\mu}\mathbf{H}(x,t),\end{aligned}$$

where $\boldsymbol{\mu}$ is the effective permeability tensor due to an applied magnetic field $\mathbf{H}_A(x,t)$. Fig. 1.6 shows some example hysteresis loops for ferromagnetic materials adapted from [11] where Gaussian units are used.

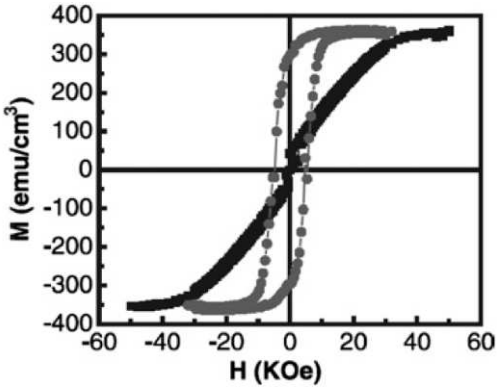

Fig. 1.6. H-M hysteresis curve for ferromagnetic materials

For both ferromagnetic and ferroelectric materials the creation of electric/magnetic dipole moments occurs through distortion of the electron orbitals and through local distortions in atomic spacing. As a consequence, the rate at which the permittivity and permeability are affected due to an applied electric or magnetic field can be extremely fast [20], [14].

It is also possible to produce composite materials that simultaneously have both a ferromagnetic and ferroelectric response [11],[12],[17],[20]. The material response time for an applied magnetic or electric field remains extraordinarily fast. One example of a candidate ferroelectric/ferromagnetic material operating at high switching speeds has been demonstrated in [17]. For the ferroelectric switching, speeds of up to 1 GHz were demonstrated. For the ferromagnetic switching, speeds of up to 10 MHz were demonstrated.

We can harness this material for our spatio-temporal application. Fig. 1.7 shows a single tunable cell. Electrodes 1 and 2 on the sides of the ferroelectric/ferromagnetic (FEFM) material produce an **E** field in the x-direction and determine the applied **E** field across the material. The ferroelectric behavior of the material induces the corresponding change in the **D** field and hence the material's permittivity. The current loop on the top of the material introduces a magnetic **H** field in the y-direction which couples through the ferromagnetic effect to change the permeability of the sample. The two fields can be independently controlled and switched on a scale necessary to maintain the desired material constants for the propagating wave that is traveling in the z-direction. Multiple cells are stacked together in the z-direction to implement the waveguide. Fig. 1.8 shows this configuration. The FEFM material can be one continuous material with electrodes and current loops attached to delineate the waveguide into discrete cells. Research and numerical simulation of the electrodynamics will be necessary to improve the structures response near the cell borders as a sharp transition from the material properties in one cell to the next is desired.

For medium-scale-integration (MSI) the smallest dimensions of the device are in millimeters. For this size scale the device could be constructed in a properly equipped machine shop with simple placement of the necessary electrical contacts. The FEFM material can be fabricated in a variety of ways. [17] describes one feasible method requiring the use of a fully equipped chemistry laboratory.

For very-large-scale-integration (VLSI) the critical dimensions are on the order of micrometers. In this case conventional lithography techniques used to manufacture semiconductor chips could be applied to create the waveguide. Reactive ion etching can be used to pattern the FEFM material. Chemical polishing will smooth the surfaces of the material to a sufficient degree (optical flatness is not required). Next a thin layer of SiO_2 could be sputtered or deposited onto the material followed by deposition of the electrodes and bonding pads.

Precise control of the etching process for the uncommon FEFM material at the micron scale would be difficult and requires some clever work, but it should prove feasible after a concerted effort.

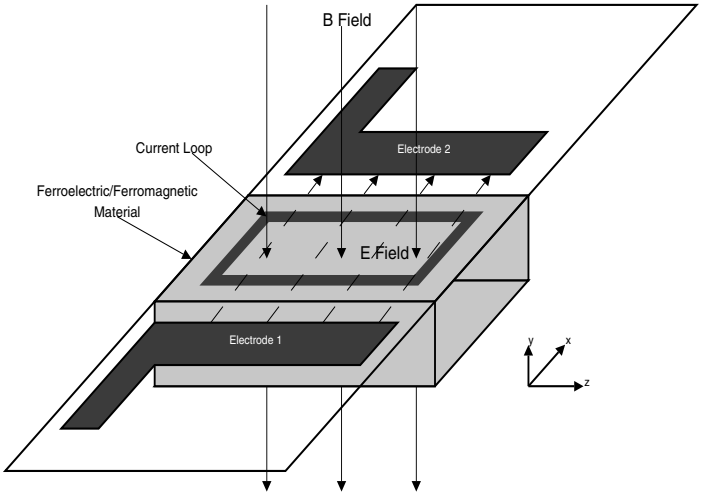

Fig. 1.7. Single cell of ferroelectric/ferromagnetic material.

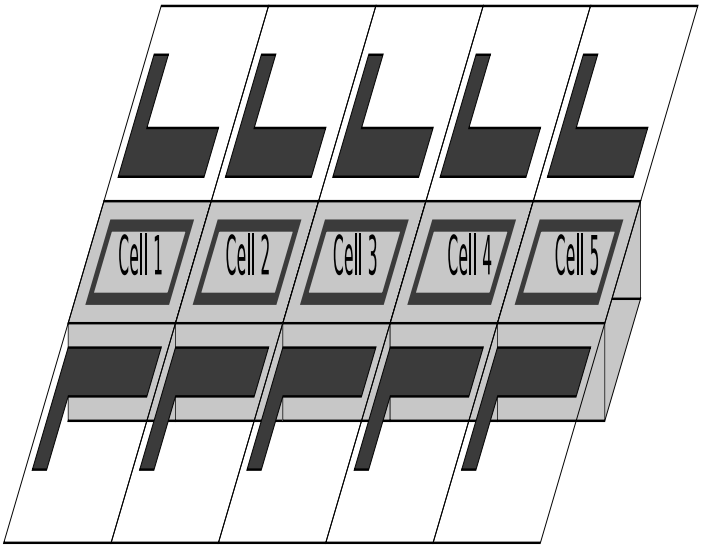

Fig. 1.8. Multiple cells of ferroelectric/ferromagnetic material.

1.3.2 Nonlinear optics

One possible limitation of the ferroelectric/ferromagnetic approach is that it will not be possible to achieve switching speeds on the order of the optical fre-

quencies. Using electronics to create drive signals at rates approaching optical frequencies is not feasible. For this range of optical frequencies (on order of 100 THz or above), it will be necessary to produce the permittivity and permeability switching through all-optical methods. Interference patterns from a coherent laser source can be used to generate dynamic periodic intensity patterns at the desired high frequencies. A single laser would generate a stationary intensity profile. If two lasers are used, then the intensity pattern will move at a velocity determined by the difference of the two laser frequencies.

In order to convert the optical intensity into a perturbation of the permittivity it is necessary for the material to have at least a second-order nonlinear electro-optic response. For nonlinear optical materials, the polarization induced by an applied electric field varies nonlinearly with the strength of the applied electric field. For third order materials, the polarization can be expressed as

$$\mathbf{P} = \epsilon_0 \chi \mathbf{E} + 2d \mid \mathbf{E} \mid^2 + 4\chi^{(3)} \mid \mathbf{E} \mid^3,$$

where d and $\chi^{(3)}$ are material-specific coefficients determining the magnitude of the second and third order effects, respectively. For centrosymmetric materials, the inversion symmetry of the structure forces $d = 0$, producing a lowest order nonlinearity of third order. These materials are referred to as Kerr materials. The second and third order coefficients are typically very small (d varies on the order of 10^{-24} to $10^{-21} A \cdot s/V^2$, and $\chi^{(3)}$ varies on the order of 10^{-34} to 10^{-29}) [18] and will require an intensive pump beam to provide the energy necessary to modulate the material properties.

While the above method will allow for direct optical control of the material permittivity, it will not allow tuning of the magnetic permeability. To modulate the permeability, it will still be necessary to use drive electronics to produce a current which will induce a magnetic field in the ferromagnetic material. The magnetic field will adjust the permeability according to the $B - H$ curve of the ferromagnetic material. In this case, the permittivity (electrical property) will be modulated at optical frequencies (100 THz) while the permeability (magnetic property) will be controlled at a comparatively slow frequency of around 10 GHz (radio frequency).

1.4 Some applications of dynamic materials

Left-handed metamaterials (materials with negative effective values of both permittivity and permeability) are possible with the proposed structure. It has been demonstrated that static structures such as photonic crystals (periodic 1D, 2D, or 3D metal or dielectric structures) can also produce left-handed metamaterials [9]. With the proposed spatio-temporal materials a wider class of left-handed or negative-index materials (NIMs) becomes accessible. We briefly mention below some of the more promising applications to be investigated.

Property 1: Imaging resolution beyond diffraction-limited sizes. An imaging system is limited in resolution due to the exponential decay of the higher-order spatial frequency components as the distance from the source increases. NIMs can couple the decaying evanescent waves through a set of plasmon resonances in the material. As a consequence it is possible to image the source at a resolution not limited by propagation. Applications of this property include semiconductor fabrication wherein significantly smaller feature sizes can be imaged without requiring more exotic shorter wavelength laser sources and focusing materials. This technique will demonstrate a more practical way to dramatically improve transistor density through an improved optical photolithography method.

Property 2: Flat metamaterial surface could result in flat lens imaging beyond diffraction limit. The small form factor and rectangular shape of the imaging metamaterial allows for ultra-high density data storage (next-generation optical data storage, next-generation hard drive data storage).

Property 3: *Tunable* left-handed metamaterials. Because the switching rate and duty cycle are temporally controlled, the left-handed properties can be tuned over some limited range. The tunability can be exploited to change system properties such as focus for the imaging modality. Applications such as medical imaging could be significantly enhanced by this feature. Tunable focus allows for 2D and 3D non-destructive imaging via techniques such as confocal microscopy and optical coherence tomography.

In addition to acting as a left-handed material, a number of other unique properties exist.

Property 4: Optical pumping. Due to the energy exchange required for the dynamic switching, an incident beam can be pumped to higher power levels by propagation through the proposed metamaterial. This feature is useful in applications such as long-distance communication networks (telcomm), and nondestructive non-invasive medical imaging.

Property 5: High-energy pulse compression. Due to the properties of the limit cycles arising in spatio-temporal checkerboard structures (see Chapter 5), optical pulses can be compressed spatially, as well as being optically pumped, to produce pulses with extraordinarily high power densities. Efficient methods of creating high-energy pulses have numerous applications from material processing to medical diagnostics and treatment.

1.5 Dynamic materials and vibrational mechanics

Dynamic materials, or more specifically, kinetic dynamic materials, may be examined through the framework of a special branch of general mechanics - i.e. *vibrational mechanics*. Introduced in the early and mid-fifties in the works of I.I. Blekhman and many of his colleagues and followers, this theory emerged from the study of nonlinear effects as well as from the analysis of parametric excitation of vibration. It offers a solid conceptual background for numerous

remarkable phenomena observed in daily life, such as stabilization of inverted pendulum by a high frequency vertical vibration of its pivot, vibrational lifting of a massive body along the inclined plane, vibrational dipping of piles into a solid ground, etc. In all of those phenomena, a *background fast variable vibration* affects a slow motion by changing both the environment and material properties of a moving system. A background motion is often interpreted as a factor *hidden within a system*; an observer watching an inverted pendulum or a body moving upward along the inclined plane may not even notice a small high frequency background vibration. He will ascribe his observations to the presence of additional forces acting upon the system, as well as to accumulative change in its material parameters, such as the inertial coefficients and the stiffnesses.

These factors affect the *slow* motion of a system, occurring at frequencies that are low compared to the frequency of a background *fast* vibration. We shall see that dynamic materials basically implement the same idea: the disturbances occurring on a spatio-temporal scale much greater than the scale of a background property pattern may perceive the medium as having some effective material parameters.

In the case of kinetization, this occurrence is due to a relative material motion that may, in particular, be vibrational. An interested reader is referred to many original contributions by I.I. Blekhman and other authors (see [22] and additional references therein).

2

An Activated Elastic Bar: Effective Properties

2.1 Longitudinal vibrations of activated elastic bar

Consider an immovable elastic bar distributed along the z-axis; the longitudinal wave propagation along the bar is governed by the second order hyperbolic equation

$$(\rho u_t)_t - (k u_z)_z = 0. \tag{2.1}$$

Here, $u = u(z,t)$ denotes a small horizontal displacement depending on z and t, and $\rho = \rho(z,t)$, $k = k(z,t)$ denote, respectively, the (positive) linear density and stiffness (Young modulus) of the bar.

We shall examine the wave propagation along the bar with variable material parameters ρ and k. More specifically, we assume that this dependency is characterized by the following features:

(i) both ρ and k are space *and* time dependent;
(ii) at each point (z,t) the pair (ρ, k) may take either the values (ρ_1, k_1), or the values (ρ_2, k_2);
(iii) these admissible values are taken within alternating layers in the (z,t)-plane having the slope $dz/dt = V$ so chosen as to ensure a regular transition of dynamic disturbances $u(z,t)$ across the interface from one layer to another. In other words, both kinematic and dynamic compatibility conditions must be observed across the interface.

The spatio-temporal variability of both ρ and k may be achieved if we attach (release) some portions of material to (from) the bar wherever and whenever necessary. To illustrate this operation, consider the interface separating materials 1 and 2; this interface is moving from left to right with velocity V. Let the point P in Fig. 2.1 indicate position of the interface at time t. From the right of P there arrives, per unit time, the mass $\rho_2 V$ with velocity u_{2t} and momentum $\rho_2 V u_{2t}$. At the instant $t - 0$, an additional mass $\rho_* V$, with absolute velocity V_0 and momentum $\rho_* V V_0$, is attached to $\rho_2 V$. The combined momentum then becomes equal to $\rho_2 V u_{2t} + \rho_* V V_0$.

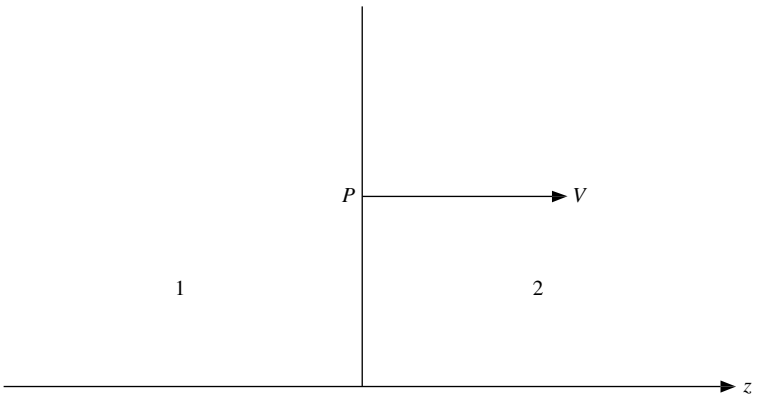

Fig. 2.1. A moving interface.

At time $t + 0$, we have a joint mass $(\rho_2 + \rho_*)V = \rho_1 V$ moving with velocity u_{1t} and carrying momentum $(\rho_2 + \rho_*)Vu_{1t} = \rho_1 Vu_{1t}$. The difference of momenta

$$\rho_1 Vu_{1t} - \rho_2 Vu_{2t} - \rho_* VV_0$$

is equal to the resultant force acting upon the mass, i.e.

$$k_2 u_{2z} - k_1 u_{1z}.$$

We shall assume that $V_0 = 0$, i.e. let the additional mass be immovable in a laboratory frame. Then the balance of momenta asserts that

$$\rho_1 Vu_{1t} + k_1 u_{1z} = \rho_2 Vu_{2t} + k_2 u_{2z};$$

in other words, the resultant momentum of the restoring force and the force of inertia (taken with minus sign) should be continuous across the interface. If we replace the equation (2.1) by an equivalent system

$$v_t = ku_z, \quad v_z = \rho u_t, \tag{2.2}$$

then the balance of momenta will be expressed as the continuity of the derivative $v_t + Vv_z$ taken along the trajectory of the interface in the (z,t)-plane:

$$v_{1t} + Vv_{1z} = v_{2t} + Vv_{2z}; \tag{2.3}$$

we may say that this condition is equivalent to the continuity of v. A similar condition holds for the derivative $u_t + Vu_z$:

$$u_{1t} + Vu_{1z} = u_{2t} + Vu_{2z}; \tag{2.4}$$

this condition expresses the continuity of the displacement u across the interface.

Equations (2.2) should now be complemented by compatibility conditions (2.3), (2.4). The system (2.2) is hyperbolic, and caution should be taken to guarantee existence of a desired continuous solution. The problem that arises may be illustrated if we consider, as an example, the case of an *immovable* interface: $V = 0$ (Fig. 2.2).

In order to observe both of the compatibility conditions, we have to make sure that there are precisely two characteristics of the system (2.2) that *depart* from the interface. On the interface $V = 0$, we have two characteristics, with the slopes $\pm a_1$, at the side occupied by material 1, and two characteristics with the slopes $\pm a_2$, at the opposite side occupied by material 2; here, a_i, $i = 1, 2$, denotes the phase velocity $\sqrt{k_i/\rho_i}$ of waves in material i; we assume below, without sacrificing generality, that $a_2 > a_1$. Clearly, two out of the four characteristics, specifically, those with slopes a_2 and $-a_1$, *depart* from the interface. We conclude that the interface with $V = 0$ is *admissible*, i.e. it allows for a desired continuous solution.

Consider now a *moving* interface ($V \neq 0$), with materials 1 and 2 on either side of it preserved immovable. Instead of Fig. 2.2, we now refer to Fig. 2.3 as illustration; in this one, the interface is making the angle $\tan^{-1} V$ with the t-axis. Nothing dramatic happens while $\mid V \mid$ remains less than the least of the phase velocities: $\mid V \mid < a_1$; if, however, $\mid V \mid$ falls into the interval (a_1, a_2), then the balance of characteristics becomes violated: we have either three (Fig. 2.4) or one (Fig. 2.5) departing characteristic. In the first case, we have non-uniqueness, in the second case - non-existence of a continuous solution. The balance will, however, be restored as $\mid V \mid$ becomes greater then both of the phase velocities: $\mid V \mid > a_2$; this case is illustrated by Fig. 2.6. We conclude that the condition

$$(V^2 - a_1^2)(V^2 - a_2^2) > 0, \tag{2.5}$$

is necessary for the existence of a required solution. This condition imposes substantial restrictions on spatio-temporal material assemblages, in fact, it becomes violated by microgeometries that are quite habitual in statics. An example is given by a matrix structure in space-time illustrated in Fig. 2.7. In this figure, the matrix and the oval-shaped (shaded) inclusions are occupied by two different materials. Along the oval interfaces, there will always

be parts where ineqs. (2.5) are violated. On the other hand, a rectangular microstructure shown in Fig. 5.1 is admissible because (2.5) is satisfied on both horizontal and vertical interfaces.

For a laminate of the type shown in Fig. 1.4, ineqs. (2.5) become satisfied by a due choice of V; bearing this in mind, we shall now calculate the effective parameters of an activated elastic bar.

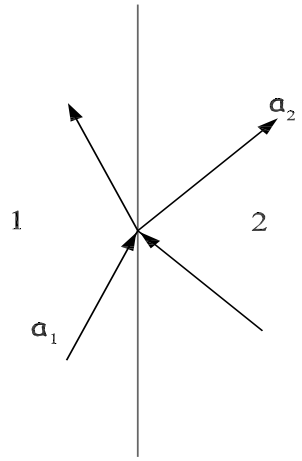

Fig. 2.2. An immovable interface: $V = 0$.

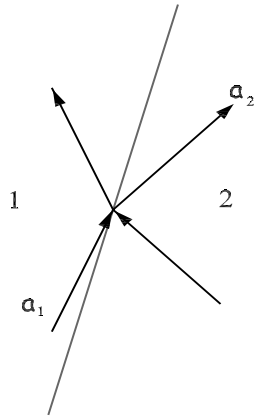

Fig. 2.3. A moving interface: $\mid V \mid < a_1$.

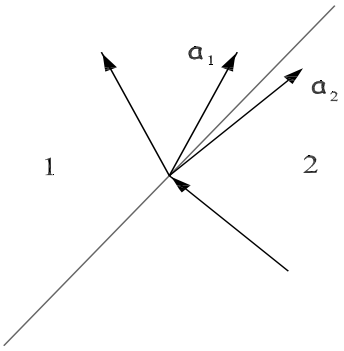

Fig. 2.4. A moving interface: $a_1 < V < a_2$.

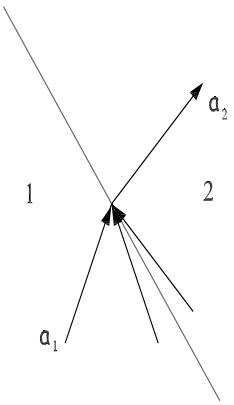

Fig. 2.5. A moving interface: $-a_2 < V < -a_1$.

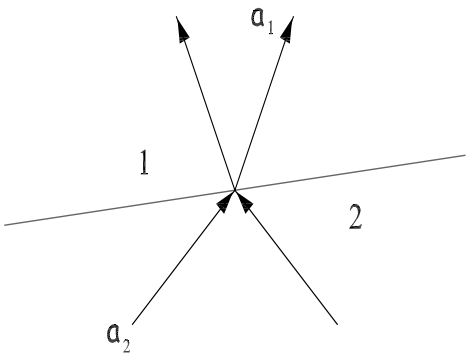

Fig. 2.6. A moving interface: $\mid V \mid > a_2$.

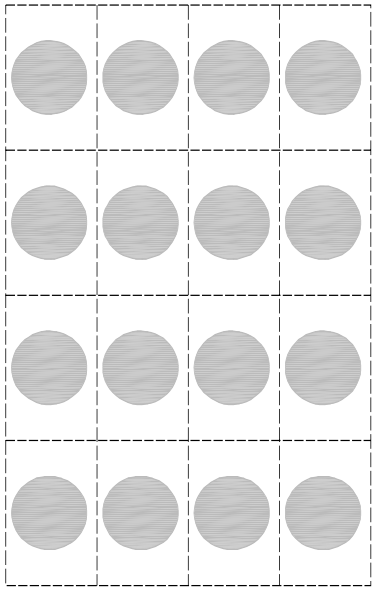

Fig. 2.7. A matrix microstructure in space-time violating ineqs. (2.5).

2.2 The effective parameters of activated laminate

To determine them, we apply homogenization to the system (2.2) with the observance of conditions (2.3)-(2.5). The analysis will be simplified if we introduce, instead of (z,t), the Galilean coordinate frame (ζ,τ) specified by

$$\zeta = z - Vt, \quad \tau = t; \tag{2.6}$$

this *co-moving* frame is travelling with velocity V in the positive z-direction.

By using obvious relations

$$\partial/\partial z = \partial/\partial\zeta, \quad \partial/\partial t = \partial/\partial\tau - V\partial/\partial\zeta, \tag{2.7}$$

we reduce the system (2.2) to the form

$$\rho u_\tau = \rho V u_\zeta + v_\zeta, \quad v_\tau = k u_\zeta + V v_\zeta;$$

on denoting

$$\Delta = V^2 - a^2, \quad a^2 = k/\rho, \tag{2.8}$$

we rewrite this as

$$u_\zeta = \frac{V}{\Delta}u_\tau - \frac{1}{\rho\Delta}v_\tau, \quad v_\zeta = -\frac{k}{\Delta}u_\tau + \frac{V}{\Delta}v_\tau. \tag{2.9}$$

Conditions (ii), (iii), section 2.1, indicate that parameters ρ, k depend on the argument $z - Vt = \zeta$; we shall assume that these parameters are periodic functions, with a unit period, of the *fast variable* $\xi = \zeta/\delta$, $\delta \to 0$. Equations (2.9) will now be averaged over the unit period in ξ. Introduce the symbol $\langle\cdot\rangle = m_1(\cdot)_1 + m_2(\cdot)_2$ for the arithmetic mean of $(\cdot)$, with materials 1 and 2 represented in a unit period at the volume fractions $m_1, m_2 \geq 0$ $(m_1 + m_2 = 1)$. We apply averaging to equations (2.9) bearing in mind that derivatives u_τ, v_τ are continuous across the interfaces ζ=const immovable in a new frame; for this reason, they remain unaffected by averaging: $\langle u_\tau\rangle = u_\tau$, $\langle v_\tau\rangle = v_\tau$. Preserving symbols $u_\zeta, u_\tau, v_\zeta, v_\tau$ for the averaged quantities $\langle u_\zeta\rangle, \langle u_\tau\rangle, \langle v_\zeta\rangle, \langle v_\tau\rangle$, we arrive at the system

$$u_\zeta = BVu_\tau - Cv_\tau, \quad v_\zeta = -Du_\tau + BVv_\tau,$$

where we introduced notation

$$B = \left\langle \frac{1}{\Delta} \right\rangle, \quad C = \left\langle \frac{1}{\rho\Delta} \right\rangle, \quad D = \left\langle \frac{k}{\Delta} \right\rangle. \tag{2.10}$$

We now go back to z, t, with the reference to (2.6), (2.7); after some calculation, we arrive at the system

$$v_t = pu_z - qu_t, \quad v_z = qu_z + ru_t. \tag{2.11}$$

The coefficients p, q, r are given by the formulae

$$p = V^2 D - \frac{A^2}{C}, \quad q = -V\left(D - \frac{AB}{C}\right), \quad r = \frac{B^2V^2}{C} - D, \tag{2.12}$$

with the symbol A defined as

$$A = BV^2 - 1 = \left\langle \frac{a^2}{V^2 - a^2} \right\rangle. \tag{2.13}$$

A direct calculation shows that

$$\begin{aligned}
A &= \frac{a_1^2 a_2^2}{\Delta_1 \Delta_2}\left[V^2\left(\frac{\bar{1}}{a^2}\right) - 1\right], \\
B &= \frac{1}{\Delta_1 \Delta_2}(V^2 - \overline{a^2}), \\
C &= \frac{1}{\rho_1 \rho_2 \Delta_1 \Delta_2}(V^2\bar{\rho} - \bar{k}), \\
D &= \frac{k_1 k_2}{\Delta_1 \Delta_2}\left[V^2\left(\frac{\bar{1}}{k}\right) - \left(\frac{\bar{1}}{\rho}\right)\right].
\end{aligned}$$

Here, we applied notation

$$\bar{(\cdot)} = m_1(\cdot)_2 + m_2(\cdot)_1, \tag{2.14}$$

and an obvious symbol (see (2.8)) $\Delta_i = V^2 - a_i^2, \quad i = 1, 2.$

We shall also use parameters α, β, θ defined by the formulae

$$\begin{aligned}
\alpha &= \frac{A}{C} = \frac{\left\langle \frac{a^2}{\Delta} \right\rangle}{\left\langle \frac{1}{\rho\Delta} \right\rangle} = k_1 k_2 \frac{V^2\left(\frac{\bar{1}}{a^2}\right) - 1}{V^2\bar{\rho} - \bar{k}}, \\
\beta &= \frac{BV}{C} = V\frac{\left\langle \frac{1}{\Delta} \right\rangle}{\left\langle \frac{1}{\rho\Delta} \right\rangle} = \rho_1\rho_2 V\ \frac{V^2 - \overline{a^2}}{V^2\bar{\rho} - \bar{k}}, \\
\theta &= \frac{C}{D} = \frac{\left\langle \frac{1}{\rho\Delta} \right\rangle}{\left\langle \frac{k}{\Delta} \right\rangle} = \frac{1}{k_1 k_2 \rho_1 \rho_2}\ \frac{V^2\bar{\rho} - \bar{k}}{V^2\left(\frac{\bar{1}}{k}\right) - \left(\frac{\bar{1}}{\rho}\right)}.
\end{aligned} \tag{2.15}$$

The symbols p, q, and r are linked with α, β, θ through the following relations (c.f. (2.12))

$$p = \frac{V^2 - \theta\alpha^2}{\theta(\beta V - \alpha)}, \quad q = -\frac{V - \theta\alpha\beta}{\theta(\beta V - \alpha)}, \quad r = -\frac{1 - \theta\beta^2}{\theta(\beta V - \alpha)}. \tag{2.16}$$

We now get back to equations (2.11). This system appeared as a result of homogenization applied to (2.2); the relevant composite is a spatio-temporal

laminate in (z,t) of the type illustrated in Fig. 1.4. We wish to determine the effective parameters of this laminate.

Consider first the case $V = 0$ when the laminate becomes *static*. Then $q = 0$, and p, r become defined as

$$p = \alpha = \frac{1}{\left\langle \frac{1}{\rho a^2} \right\rangle} = \frac{1}{\left\langle \frac{1}{k} \right\rangle} = \langle k^{-1} \rangle^{-1}, \quad r = \frac{1}{\theta \alpha} = \left\langle \frac{k}{a^2} \right\rangle = \langle \rho \rangle. \tag{2.17}$$

Because $q = 0$, we conclude, by comparing (2.11) and (2.2), that parameters p and r specified by (2.17), may be treated, respectively, as the effective stiffness K and density P of a static laminate. When $V = 0$, the matrix

$$\begin{vmatrix} p & -q \\ q & r \end{vmatrix} \tag{2.18}$$

of the coefficients in (2.11) becomes diagonal, and its elements are then qualified as effective constants. Another extreme case $V = \infty$ corresponds to what we term a *temporal* laminate. In this case, the terms with q in (2.11) drop out compared with terms containing p, r; these parameters become specified as

$$p = \langle k \rangle, \quad r = \frac{1}{\left\langle \frac{1}{\rho} \right\rangle} = \langle \rho^{-1} \rangle^{-1}, \tag{2.19}$$

with a similar interpretation as the effective stiffness K and density P. The matrix (2.18) may also be treated as diagonal in this case.

With V being neither zero nor infinity, we diagonalize the matrix (2.18) by introducing a new Galilean frame η, τ through the formulae

$$\eta = z - wt, \quad \tau = t. \tag{2.20}$$

The frame η, τ is moving along the z-axis with the velocity w specified below. In a new frame, the system (2.11) takes on the form

$$\begin{aligned} v_\tau &= (p + 2qw - rw^2)u_\eta - (q - wr)u_\tau, \\ v_\eta &= (q - wr)u_\eta + ru_\tau. \end{aligned} \tag{2.21}$$

If we now define w as

$$w = q/r, \tag{2.22}$$

then equations (2.21) are reduced to

$$v_\tau = (1/\theta r)u_\eta, \quad v_\eta = ru_\tau. \tag{2.23}$$

Here, we used an easily checked relation (c.f. (2.16))

$$pr + q^2 = 1/\theta. \tag{2.24}$$

The frame (2.20) with w specified by (2.22) with be called a *proper frame*. The matrix (2.18) takes in this frame the diagonal form

$$\begin{vmatrix} \theta^{-1}r^{-1} & 0 \\ 0 & r \end{vmatrix},$$

with the effective stiffness K and density P specified as (c.f. (2.2))

$$K = \theta^{-1}r^{-1}, \quad P = r\,. \tag{2.25}$$

Notice that the product of these parameters equals θ^{-1}:

$$KP = \theta^{-1}. \tag{2.26}$$

The symbols p, q, r may be expressed directly through the material parameters ρ_1, k_1, ρ_2, k_2, the velocity V, and the volume fraction m_1. After some calculation in which we use (2.15), we arrive at the formulae:

$$\begin{aligned}
\frac{1}{\theta(\beta V - \alpha)} &= \frac{k_1 k_2}{\Delta_1 \Delta_2}\left[V^2\left(\bar{\frac{1}{k}}\right) - \left(\bar{\frac{1}{\rho}}\right)\right], \\
V^2 - \theta\alpha^2 &= \frac{\Delta_1\Delta_2}{F}\bar{\rho}\left(\bar{\frac{1}{k}}\right)\left[V^2 - \frac{1}{\bar{\rho}\left(\bar{\frac{1}{k}}\right)}\right], \\
V - \theta\alpha\beta &= V\frac{\Delta_1\Delta_2}{F}\left[\bar{\rho}\left(\bar{\frac{1}{k}}\right) - \left(\bar{\frac{1}{a^2}}\right)\right], \\
1 - \theta\beta^2 &= -\frac{\Delta_1\Delta_2}{F a_1^2 a_2^2}\left[V^2 - \bar{k}\left(\bar{\frac{1}{\rho}}\right)\right].
\end{aligned} \tag{2.27}$$

Here, we used notation (c.f. (2.8))

$$\begin{aligned}
\Delta_i &= V^2 - a_i^2, \quad i = 1, 2, \\
F &= (V^2\bar{\rho} - \bar{k})\left[V^2\left(\bar{\frac{1}{k}}\right) - \left(\bar{\frac{1}{\rho}}\right)\right].
\end{aligned} \tag{2.28}$$

Referring to (2.16), we obtain the following expressions for p, q, r, and θ :

$$\begin{aligned}
p &= k_1 k_2 \bar{\rho}\left(\bar{\frac{1}{k}}\right)\ \frac{V^2 - \frac{1}{\bar{\rho}\left(\bar{\frac{1}{k}}\right)}}{V^2\bar{\rho} - \bar{k}} = \langle k\rangle \frac{V^2 - \frac{1}{\bar{\rho}\left(\bar{\frac{1}{k}}\right)}}{V^2 - \frac{\bar{k}}{\bar{\rho}}}, \\
q &= -Vk_1k_2\ \frac{\bar{\rho}\left(\bar{\frac{1}{k}}\right) - \left(\bar{\frac{1}{a^2}}\right)}{V^2\bar{\rho} - \bar{k}} = -V\ \frac{k_1k_2}{\bar{\rho}}\ \frac{\bar{\rho}\left(\bar{\frac{1}{k}}\right) - \left(\bar{\frac{1}{a^2}}\right)}{V^2 - \frac{\bar{k}}{\bar{\rho}}}, \\
r &= \rho_1\rho_2\ \frac{V^2 - \bar{k}\left(\bar{\frac{1}{\bar{\rho}}}\right)}{V^2\bar{\rho} - \bar{k}} = \frac{\rho_1\rho_2}{\bar{\rho}}\ \frac{V^2 - \bar{k}\left(\bar{\frac{1}{\rho}}\right)}{V^2 - \frac{\bar{k}}{\bar{\rho}}}, \\
\theta &= \frac{\bar{\rho}}{\rho_1\rho_2\langle k\rangle}\ \frac{V^2 - \frac{\bar{k}}{\bar{\rho}}}{V^2 - \frac{\left(\bar{\frac{1}{\rho}}\right)}{\left(\bar{\frac{1}{k}}\right)}}.
\end{aligned} \tag{2.29}$$

These formulae show that the velocity $w = q/r$ of a proper frame (2.20) is not equal to V unless $V = 0$.

2.3 The effective parameters: homogenization

To confirm the results of the previous section, we apply a standard homogenization procedure [1] to the system (2.9). It is more convenient, however, to work with an equivalent equation (2.1) in which the coefficients ρ and k are defined as fast periodic functions of the argument $\xi = (z - Vt)/\delta, \quad \delta \to 0$. The period in ξ is taken equal to 1.

We look for solution to (2.1) represented in the form of a power series over δ:

$$u = u_0(z,t,\xi) + \delta u_1(z,t,\xi) + \delta^2 u_2(z,t,\xi) + \dots \tag{2.30}$$

where $u_i, \quad i = 0, 1, 2, \dots$ are assumed 1-periodic in ξ.

The derivatives that participate in (2.1) should be recalculated by the rule of differentiating composite functions:

$$\begin{aligned} \frac{d}{dz}F(z,t,\xi) &= F_z + \delta^{-1}F_\xi, \\ \frac{d}{dt}F(z,t,\xi) &= F_t - V\delta^{-1}F_\xi. \end{aligned} \tag{2.31}$$

The subscripts in these formulae denote partial differentiation over the relevant variables.

By virtue of (2.30), (2.31), we obtain the formulae

$$\begin{aligned} \frac{du}{dz} &= u_{0z} + \delta u_{1z} + \delta^2 u_{2z} + \dots + \delta^{-1}(u_{0\xi} + \delta u_{1\xi} + \delta^2 u_{2\xi} + \dots), \\ \frac{du}{dt} &= u_{0t} + \delta u_{1t} + \delta^2 u_{2t} + \dots - V\delta^{-1}(u_{0\xi} + \delta u_{1\xi} + \delta^2 u_{2\xi} + \dots), \\ \frac{d}{dt}\left(\rho(\xi)\frac{du}{dt}\right) &= \left(\rho(\xi)\frac{du}{dt}\right)_t - V\delta^{-1}\left(\rho(\xi)\frac{du}{dt}\right)_\xi \\ &= [\rho(\xi)(u_{0t} + \delta u_{1t} + \delta^2 u_{2t} + \dots) \\ &\quad - V\delta^{-1}\rho(\xi)(u_{0\xi} + \delta u_{1\xi} + \delta^2 u_{2\xi} + \dots)]_t \\ &\quad - V\delta^{-1}[\rho(\xi)(u_{0t} + \delta u_{1t} + \delta^2 u_{2t} + \dots) \\ &\quad - V\delta^{-1}\rho(\xi)(u_{0\xi} + \delta u_{1\xi} + \delta^2 u_{2\xi} + \dots)]_\xi. \end{aligned} \tag{2.32}$$

A similar expansion for

$$\frac{d}{dz}\left(k(\xi)\frac{du}{dz}\right)$$

appears as we formally apply k instead of ρ, and set $V = -1$ in (2.32).

By using these expansions in the lhs of (2.1), we express this one as a power series over δ; we require that the coefficients of powers of δ be set equal to zero. This requirement, applied to the coefficient of the lowest power, δ^{-2}, means that

$$V^2(\rho u_{0\xi})_\xi - (k u_{0\xi})_\xi = 0. \tag{2.33}$$

The similar conditions related to the coefficients of δ^{-1} and δ^0, produce the following equations:

$$-V(\rho u_{0\xi})_t - V(\rho u_{0t})_\xi + V^2(\rho u_{1\xi})_\xi - (k u_{0\xi})_z - (k u_{0z})_\xi - (k u_{1\xi})_\xi = 0, \tag{2.34}$$

$$\begin{aligned}(\rho u_{0t})_t - V(\rho u_{1\xi})_t - V(\rho u_{1t})_\xi + V^2(\rho u_{2\xi})_\xi \\ - (k u_{0z})_z - (k u_{1\xi})_z - (k u_{1z})_\xi - (k u_{2\xi})_\xi = 0.\end{aligned} \tag{2.35}$$

We now consider the consequences of (2.33)-(2.35). Integration of (2.33) reveals that

$$(V^2\rho - k)u_{0\xi} = m(z,t).$$

Because u_0 should be 1-periodic in ξ, we get

$$m(z,t)\int_0^1 \frac{d\xi}{V^2\rho - k} = 0,$$

i.e. $m(z,t) = 0$, since the integral equals a non-zero constant C given by (2.10). We conclude that, unless $V^2\rho - k = 0$, u_0 is independent of the fast variable ξ: $u_0 = u_0(z,t)$.

Bearing this in mind and integrating (2.34), we arrive at the relation

$$-V\rho u_{0t} - k u_{0z} + (V^2\rho - k)u_{1\xi} = n(z,t),$$

or, equivalently,

$$u_{1\xi} = \frac{n}{V^2\rho - k} + \frac{V\rho}{V^2\rho - k}u_{0t} + \frac{k}{V^2\rho - k}u_{0z}.$$

We demand, as before, that u_1 be 1-periodic in ξ; this requirement defines n as

$$n = -V\frac{B}{C}u_{0t} - \frac{A}{C}u_{0z},$$

with A, B, C given by (2.13) and (2.10). The expression for $u_{1\xi}$ now takes the form

$$u_{1\xi} = Pu_{0t} + Qu_{0z}, \tag{2.36}$$

with P, Q defined by

$$P = \frac{V}{V^2\rho - k}\left(\rho - \frac{B}{C}\right), \quad Q = \frac{1}{V^2\rho - k}\left(k - \frac{A}{C}\right). \tag{2.37}$$

Note that

$$\int_0^1 P d\xi = \int_0^1 Q d\xi = 0.$$

We also mention the formulae

$$\begin{aligned} X &= u_{1t} - V u_{2\xi} = -\frac{1}{V^2\rho - k}(kS + VT), \\ Y &= u_{1z} + u_{2\xi} = \frac{1}{V^2\rho - k}(\rho V S + T), \end{aligned} \tag{2.38}$$

where

$$S = \int_0^\xi (N_t - M_z) d\xi, \quad T = \int_0^\xi (-\rho M_t + k N_z) d\xi, \tag{2.39}$$

with M, N defined as

$$\begin{aligned} M &= u_{0t} - V u_{1\xi} = u_{0t}(1 - VP) - u_{0z} V Q, \\ N &= u_{0z} + u_{1\xi} = u_{0t} P + u_{0z}(1 + Q). \end{aligned} \tag{2.40}$$

Eqs. (2.38)-(2.40) are produced by the same technique as that applied toward obtaining (2.36), (2.37).

By integrating (2.35) over the period 1 in ξ and by using the 1-periodicity of u_1 and u_2, we arrive at the relation:

$$\begin{aligned} (\langle\rho\rangle u_{0t})_t - V \left\langle \frac{V\rho}{V^2\rho - k}\left(\rho - \frac{B}{C}\right) u_{0t} + \frac{\rho}{V^2\rho - k}\left(k - \frac{A}{C}\right) u_{0z} \right\rangle_t \\ - (\langle k\rangle u_{0z})_z - \left\langle \frac{Vk}{V^2\rho - k}\left(\rho - \frac{B}{C}\right) u_{0t} + \frac{k}{V^2\rho - k}\left(k - \frac{A}{C}\right) u_{0z} \right\rangle_z = 0. \end{aligned}$$

The symbol $\langle\cdot\rangle$ has been defined in section 2.2 as $m_1(\cdot)_1 + m_2(\cdot)_2$. Bearing in mind that $u_0 = u_0(z,t)$ and that ρ, k depend on ξ alone, we rewrite the last equation in the form:

$$\left(\frac{B^2V^2}{C} - D\right) u_{0tt} - 2V\left(D - \frac{AB}{C}\right) u_{0zt} - \left(V^2 D - \frac{A^2}{C}\right) u_{0zz} = 0$$

In view of (2.12), this is reduced to

$$r u_{0tt} + 2q u_{0zt} - p u_{0zz} = 0, \tag{2.41}$$

which is equivalent to the system (2.11). Now it is easy to see that $S(0) = T(0) = S(1) = T(1) = 0$ and, as a consequence,

$$X(0) = X(1) = Y(0) = Y(1) = 0.$$

2.4 The effective parameters: the Floquet theory

Because of a special assumption made about ρ, k as 1-periodic functions of a single argument $\xi = \zeta/\delta$, the system (2.9) may be viewed as a linear system with coefficients that are periodic in ζ with period δ. We shall apply the Floquet theory to this system to obtain its exact solution; the results of sections 2.2, 2.3 will follow from this solution in a low frequency asymptotic limit.

We first eliminate the τ-variable by applying the Laplace transform:

$$\bar{u}(\zeta, s) = \int_0^\infty e^{-s\tau} u(\zeta, \tau) d\tau.$$

Equations (2.9) then take on the form

$$\begin{aligned} \bar{u}_\zeta - \frac{s}{V^2 - a^2}\left(V\bar{u} - \frac{1}{\rho}\bar{v}\right) = 0, \\ \bar{v}_\zeta + \frac{s}{V^2 - a^2}(k\bar{u} - V\bar{v}) = 0, \end{aligned} \tag{2.42}$$

where a^2 is defined as k/ρ (see (2.8)).

Assume that $\zeta \geq 0$, and that material 1 occupies the intervals

$$(n - m_1)\delta \leq \zeta \leq n\delta, \quad n = 0, 1, 2, \ldots, \tag{2.43}$$

while material 2 is concentrated within supplementary intervals

$$n\delta \leq \zeta \leq (n + m_2)\delta, \quad n = 0, 1, \ldots \ . \tag{2.44}$$

Here m_1 and m_2 denote, as before, the volume fractions of materials 1 and 2 in the laminate; clearly, $m_1 + m_2 = 1$.

A general solution to the system (2.42) is given by

$$\begin{aligned} \bar{u} = A_1 e^{\mu_1 \zeta} P(\mu_1, \zeta) + A_2 e^{\mu_2 \zeta} P(\mu_2, \zeta), \\ \bar{v} = A_1 e^{\mu_1 \zeta} Q(\mu_1, \zeta) + A_2 e^{\mu_2 \zeta} Q(\mu_2, \zeta), \end{aligned} \tag{2.45}$$

with $P(\mu_1, \zeta), \ldots, Q(\mu_2, \zeta)$ being δ-periodic in ζ. In (2.45), A_1 and A_2 denote the coefficients to be determined by the boundary conditions, and μ_1, μ_2 represent the Floquet characteristic exponents given by the formula (see Appendix 1)

$$\mu_{1,2}\delta = V(\theta_1/a_1 + \theta_2/a_2) \pm \chi. \tag{2.46}$$

Here, the upper (lower) sign is related to $\mu_1(\mu_2)$, and parameters θ, χ are defined as

$$\begin{aligned} &\theta_i = s\delta\phi_i, \quad \phi_i = m_i a_i/(V^2 - a_i^2), \quad i = 1, 2, \\ &\cosh\chi = \cosh\theta_1 \cosh\theta_2 + \sigma \sinh\theta_1 \sinh\theta_2, \\ &\sigma = (\gamma_1^2 + \gamma_2^2)/2\gamma_1\gamma_2, \\ &\gamma_i = k_i/a_i = \rho_i a_i = \sqrt{k_i \rho_i}, \quad i = 1, 2 \ . \end{aligned} \tag{2.47}$$

Clearly, $\sigma \geq 1$. Consider the low frequency case $\mid s\delta/a_i \mid \ll 1$; equation (2.47) then specifies χ approximately as

$$\chi = s\delta\sqrt{\phi_1^2 + \phi_2^2 + 2\sigma\phi_1\phi_2}. \tag{2.48}$$

By (2.5), the quantities ϕ_1, ϕ_2 should be of the same sign; because $\sigma > 0$, the square root in (2.48) is real.

If $s = i\omega$ with ω real, then

$$\cosh\chi = \cos\omega\delta\phi_1 \cos\omega\delta\phi_2 - \sigma \sin\omega\delta\phi_1 \sin\omega\delta\phi_2.$$

If the absolute value of the rhs of this equation exceeds 1, then the roots χ have non-zero real parts, and solution (2.45) contains exponentially increasing terms.

This cannot happen in the low frequency approximation $\omega\delta/a_i \ll 1$, and the corresponding values of χ, as well as μ_1, μ_2, are in this case imaginary.

The functions $P(\mu, \zeta)$ and $Q(\mu, \zeta)$ in (2.45) are given by the formulae

$$P(\mu,\zeta) = \begin{cases} e^{-\left(\mu - \dfrac{s}{V-a_1}\right)(\zeta - n\delta)} + Ee^{-\left(\mu - \dfrac{s}{V+a_1}\right)(\zeta - n\delta)}, & \zeta \in (2.43) \\ Ge^{-\left(\mu - \dfrac{s}{V-a_2}\right)(\zeta - n\delta)} + He^{-\left(\mu - \dfrac{s}{V+a_2}\right)(\zeta - n\delta)}, & \zeta \in (2.44) \end{cases}$$

$$Q(\mu,\zeta) = \begin{cases} \gamma_1 \left[e^{-\left(\mu - \dfrac{s}{V-a_1}\right)(\zeta - n\delta)} + Ee^{\left(\mu - \dfrac{s}{(V+a_1)}\right)(\zeta - n\delta)} \right], & \zeta \in (2.43) \\ \gamma_2 \left[-Ge^{-\left(\mu - \dfrac{s}{V-a_2}\right)(\zeta - n\delta)} + He^{-\left(\mu - \dfrac{s}{V+a_2}\right)(\zeta - n\delta)} \right], & \zeta \in (2.44) \end{cases}$$

The constants E, G, and H in these formulae are defined as solutions to the system

$$\begin{aligned} -E + G + H &= 1, \\ E + (G - H)(\gamma_2/\gamma_1) &= 1 \\ -Ee^{\theta_1} + Ge^{\theta_2 \mp \chi} + He^{-\theta_2 \mp \chi} &= e^{-\theta_1}, \end{aligned} \tag{2.49}$$

with upper (lower) sign related to $\mu = \mu_1(\mu_2)$. For derivation of (2.49), see Appendix 1.

Both $P(\mu, \zeta)$ and $Q(\mu, \zeta)$ are δ-periodic in ζ; these functions actually depend on $\zeta - n\delta$, this argument falling into the range $[-m_1\delta, 0]$ for (2.43), and into $[0, m_2\delta]$ for (2.44):

$$-m_1 \le \frac{\zeta - n\delta}{\delta} \le 0 \text{ for (2.43)}; \;\; 0 \le \frac{\zeta - n\delta}{\delta} \le m_2 \;\; \text{for (2.44)}.$$

In both cases, the difference $\zeta - n\delta$ is of order δ. The functions $\bar{u}, \bar{v}$ given by (2.45) have the form of modulated waves; when $s = i\omega$ and $\omega\delta/a_i \ll 1$, then $e^{\mu\zeta}$ appears to be the long wave modulation factor, while $P(\mu,\zeta), Q(\mu,\zeta)$ represent the short wave carriers. By averaging $\bar{u}$ and $\bar{v}$ over the period δ, we perform homogenization; this operation eliminates the short wave carriers P, Q, and detects the long wave envelopes $e^{\mu\zeta}$. These envelopes give birth to the original $u(\zeta,\tau)$ taking the form of the d'Alembert waves $f(\zeta + \frac{s}{\mu_{1,2}}\tau)$ in the coordinate frame (ζ,τ) linked with the laboratory frame (z,t) through (2.6). In this latter frame, the waves take on the form $f(z-(V-\frac{s}{\mu_{1,2}})t)$, with phase velocities $V - \frac{s}{\mu_{1,2}}$.

In Appendix 1, these velocities are calculated for $s = i\omega$, $\omega\delta/a_i \ll 1$; they are specified as

$$v_{1,2} = V - \frac{s}{\mu_{1,2}} = -Va_1^2a_2^2\frac{\bar{\rho}\left(\frac{\bar{1}}{k}\right) - \left(\frac{\bar{1}}{a^2}\right)}{V^2 - \bar{k}\left(\frac{\bar{1}}{\rho}\right)} \pm a_1a_2\frac{\sqrt{(V^2\bar{\rho} - \bar{k})\left(V^2\left(\frac{\bar{1}}{k}\right) - \left(\frac{\bar{1}}{\rho}\right)\right)}}{V^2 - \bar{k}\left(\frac{\bar{1}}{\rho}\right)}; \tag{2.50}$$

as before, the upper (lower) sign is related to $\mu_1(\mu_2)$.

On the other hand, if we go back to equation (2.41) and look for its solution $f(z-vt)$, then the phase velocities $v_{1,2}$ appear to be the roots of the equation

$$rv^2 - 2qv - p = 0. \tag{2.51}$$

Referring to (2.29), we conclude that $v_{1,2}$ are identical with the expressions given by (2.50).

2.5 The effective parameters: discussion

Equations (2.25) define the effective parameters K, P of an activated laminate in (z,t). Material properties k, ρ are assumed positive for both of the original substances; with no loss of generality, we set $a_2^2 > a_1^2$, i.e. $k_2/\rho_2 > k_1/\rho_1$. Then it is easily checked that, apart from obvious inequalities

$$\bar{\rho}\left(\frac{\bar{1}}{\rho}\right) \ge 1,$$
$$\bar{k}\left(\frac{\bar{1}}{k}\right) \ge 1, \tag{2.52}$$

we have

$$a_1^2 \le \frac{\bar{k}}{\bar{\rho}} \le a_2^2,$$
$$a_1^2 \le \frac{\left(\frac{\bar{1}}{\rho}\right)}{\left(\frac{\bar{1}}{k}\right)} \le a_2^2. \tag{2.53}$$

Also,

$$\frac{1}{\bar{\rho}\left(\frac{\bar{1}}{k}\right)} \le a_2^2,$$
$$a_1^2 \le \bar{k}\left(\frac{\bar{1}}{\rho}\right). \tag{2.54}$$

From this point on, we shall distinguish between two possible situations:

$$(i) \quad k_2 > k_1, \quad \rho_2 < \rho_1; \tag{2.55}$$

this possibility will be referred to as the *regular* case;

$$(ii) \quad \text{either} \quad k_2 > k_1, \quad \rho_2 > \rho_1, \qquad \text{or} \qquad k_2 < k_1, \quad \rho_2 < \rho_1; \tag{2.56}$$

both of the latter possibilities will be termed *irregular*.

In a regular case, inequalities (2.54) will be complemented by the following:

$$a_1^2 \le \frac{1}{\bar{\rho}\left(\frac{\bar{1}}{k}\right)}, \qquad \bar{k}\left(\frac{\bar{1}}{\rho}\right) \le a_2^2. \tag{2.57}$$

In irregular case, however, there exists the range of parameters ρ, k, and m_1, such that

$$\frac{1}{\bar{\rho}\left(\frac{\bar{1}}{k}\right)} \le a_1^2, \tag{2.58}$$

and the range for which

$$a_2^2 \le \bar{k}\left(\frac{\bar{1}}{\rho}\right). \tag{2.59}$$

Indeed, we have

$$\frac{1}{\bar{\rho}\left(\frac{\bar{1}}{k}\right)} - a_1^2 = \frac{k_1 k_2}{\bar{\rho}\langle k\rangle} - \frac{k_1}{\rho_1} = \frac{k_1}{\rho_1 \bar{\rho}\langle k\rangle}\left[k_2\rho_1 - (m_1k_1 + m_2k_2)(m_1\rho_2 + m_2\rho_1)\right]$$
$$= \frac{m_1 k_1}{\rho_1 \bar{\rho}\langle k\rangle}\left[\rho_1 \Delta k - k_1 \Delta\rho - m_2 \Delta k \Delta\rho\right]; \tag{2.60}$$

$$a_2^2 - a_1^2 = \frac{k_2}{\rho_2} - \frac{k_1}{\rho_1} = \frac{1}{\rho_1\rho_2}(\rho_1\Delta k - k_1\Delta\rho) \geq 0; \tag{2.61}$$

here we applied notation $\Delta(\cdot) = (\cdot)_2 - (\cdot)_1$. It is clear that the difference $1/\bar{\rho}\left(\frac{\bar{1}}{\bar{k}}\right) - a_1^2$ is positive in the regular case when $\Delta k > 0, \Delta\rho < 0$; however, in irregular case, when the signs of Δk and $\Delta\rho$ are the same, this difference may become negative. For example, if $k_2 = 10, \quad \rho_2 = 9, \quad k_1 = \rho_1 = 1$, then $\rho_1\Delta k - k_1\Delta\rho - m_2\Delta k\Delta\rho = 9 - 8 - 72m_2$, and this is ≤ 0 if $m_2 \geq 1/72$. At the same time, the difference $k_2/\rho_2 - k_1/\rho_1$ is positive by (2.61), i.e. k/ρ increases as we go from material 1 to material 2. Combined with $\Delta k\Delta\rho > 0$ (irregular case), this means that the increase may be due to that in k and to the less intensive increase (not a decrease) in ρ, or due to the decrease in ρ and the less intensive decrease (not an increase) in k. The possibility for inequality (2.59) to hold is illustrated quite similarly. We calculate the difference

$$\begin{aligned}\bar{k}\left(\frac{\bar{1}}{\rho}\right) - a_2^2 &= \frac{\bar{k}\langle\rho\rangle}{\rho_1\rho_2} - \frac{k_2}{\rho_2} = -\frac{1}{\rho_1\rho_2}\left[k_2\rho_1 - (m_1k_2 + m_2k_1)(m_1\rho_1 + m_2\rho_2)\right] \\ &= -\frac{m_2}{\rho_1\rho_2}\left[\rho_1\Delta k - k_1\Delta\rho - m_1\Delta k\Delta\rho\right]; \end{aligned} \tag{2.62}$$

this difference is negative in a regular case, and may become positive in irregular case. Indeed, for an example cited above ($k_2 = 10, \quad \rho_2 = 9, \quad k_1 = \rho_1 = 1$), the difference becomes positive if $m_1 \geq 1/72$, i.e. $m_2 \leq 71/72$. We conclude that, for this example, both inequalities (2.58), (2.59) will hold once m_2 falls into the range $(1/72, 71/72)$.

If, as assumed,

$$a_2^2 > a_1^2, \tag{2.63}$$

then, for inequalities (2.58), (2.59) to hold, it is necessary that Δk and $\Delta\rho$ should *both* be non-zero. So the situation in which the original substances differ in *only one* material constant, can never involve (2.58), (2.59).

On making these observations, we may discuss the formulae (2.25) for K and P. Inequality (2.5) outlines two admissible ranges for V^2 : the *slow* range

$$V^2 < a_1^2, \tag{2.64}$$

and the *fast* range

$$V^2 > a_2^2. \tag{2.65}$$

The last formula (2.15) shows that $\theta \geq 0$ for both ranges once k, ρ are of the same sign for all participating materials. As to the values of r (see (2.29)), they are always positive for the slow range (2.64), but may become negative in the irregular case for the fast range (2.65). Indeed, for this range the denominator $V^2\bar{\rho} - \bar{k}$ in (2.29) is positive by (2.53), while the numerator $V^2 - \bar{k}\left(\frac{\bar{1}}{\rho}\right)$ may become negative for the fast range: to this end, we should choose V^2 within the interval $\left(a_2^2, \bar{k}\left(\frac{\bar{1}}{\rho}\right)\right)$; as stated above (see (2.59)), this interval may come to existence in the irregular case.

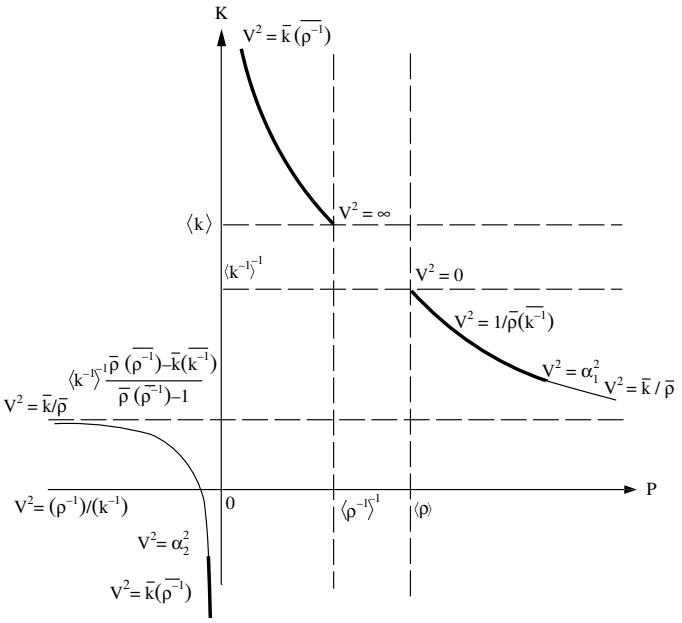

Fig. 2.8. Effective parameters K versus P with variable V (case $\bar{\rho}\left(\frac{\bar{1}}{\rho}\right) - \bar{k}\left(\frac{\bar{1}}{k}\right) \geq 0$).

The plots of K versus P with V variable along the curves are given, respectively, by Fig. 2.8 (case $\bar{\rho}\left(\frac{\bar{1}}{\rho}\right) - \bar{k}\left(\frac{\bar{1}}{k}\right) \geq 0$), and Fig. 2.9 (case $\bar{\rho}\left(\frac{\bar{1}}{\rho}\right) - \bar{k}\left(\frac{\bar{1}}{k}\right) \leq 0$). Both curves have parametric equations (with parameter V) following from (2.25) and (2.29):

$$K = \langle k \rangle \frac{V^2 - \frac{\left(\frac{\bar{1}}{\rho}\right)}{\left(\frac{\bar{1}}{k}\right)}}{V^2 - \bar{k}\left(\frac{\bar{1}}{\rho}\right)}, \quad P = \frac{\rho_1 \rho_2}{\bar{\rho}} \frac{V^2 - \bar{k}\left(\frac{\bar{1}}{\rho}\right)}{V^2 - \frac{\bar{k}}{\bar{\rho}}}.$$

Only those parts of the curves are realizable that are consistent with the admissible ranges $V^2 \leq a_1^2, , \ V^2 \geq a_2$ of V^2 (see (2.5)); the relevant segments are marked boldface in the figures.

The "averaged" d'Alembert waves, i.e. the low frequency envelopes introduced in section 2.4, propagate with the phase velocities $v_{1,2}$ specified by (2.50). By (2.51), the product of these velocities equals $-p/r$, or, with reference to (2.29),

$$v_1 v_2 = -\bar{\rho}\left(\frac{\bar{1}}{k}\right) a_1^2 a_2^2 \frac{V^2 - \frac{1}{\bar{\rho}\left(\frac{\bar{1}}{k}\right)}}{V^2 - \bar{k}\left(\frac{\bar{1}}{\rho}\right)}. \tag{2.66}$$

Given the observations made earlier in this section, we conclude that v_1 and v_2 should have opposite signs in a regular case. As to an irregular case,

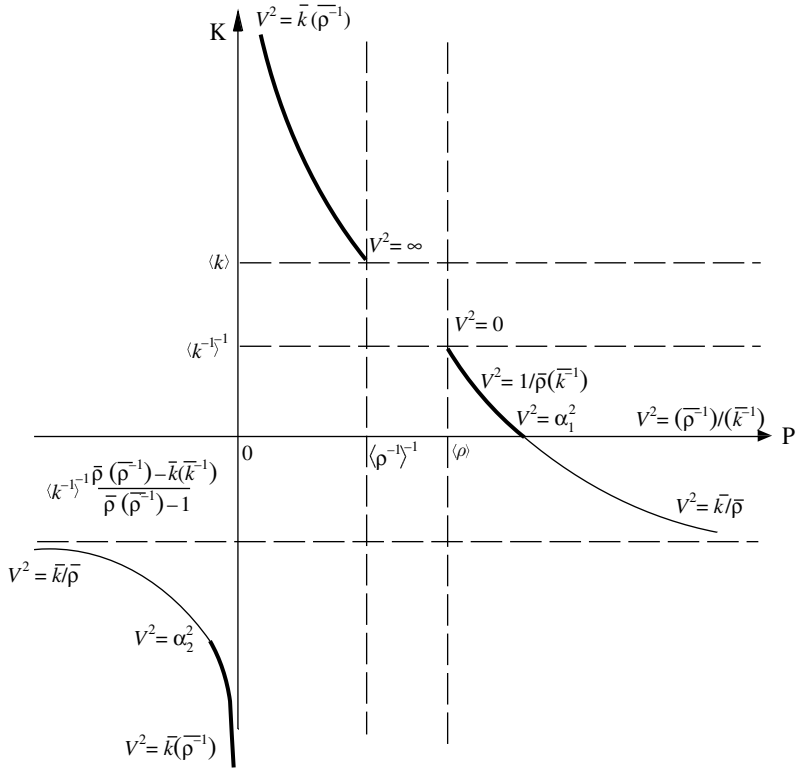

Fig. 2.9. Effective parameters K versus P with variable V (case $\rho\left(\frac{1}{\rho}\right) - k\left(\frac{1}{k}\right) \leq 0$).

the signs of v_1 and v_2 are the same if V^2 is taken within the interval

$$\left(\frac{1}{\bar{\rho}\left(\frac{\bar{1}}{\bar{k}}\right)}, a_1^2\right) \quad \text{for the slow range,} \tag{2.67}$$

and within the interval

$$\left(a_2^2, \bar{k}\left(\frac{\bar{1}}{\rho}\right)\right) \quad \text{for the fast range.} \tag{2.68}$$

We have seen in (2.58) and (2.59) that such intervals may exist in the irregular case. For each of them, the homogenized waves propagate in the *same* direction relative to a laboratory frame; this direction may be switched to opposite as we go from V to $-V$. We thus arrive at what will be termed *coordinated wave propagation*. The possibility of coordinated wave motion is peculiar to the dynamic materials; this option does not arise if we apply

conventional (static) composites. The effects achieved through the use of this phenomenon may be quite unusual as seen from the following example.

Assume that we have a laminate in space-time offering a coordinated wave propagation with both low frequency waves travelling from left to right; we shall term such material a *right* laminate. By switching V to $-V$, the direction of coordinated waves is also switched to opposite, so we obtain a *left* laminate. Now consider the material arrangement produced by placing the left (right) laminate to the left (right) of the point $z = 0$ (see Fig. 2.9 representing the relevant families of characteristics).

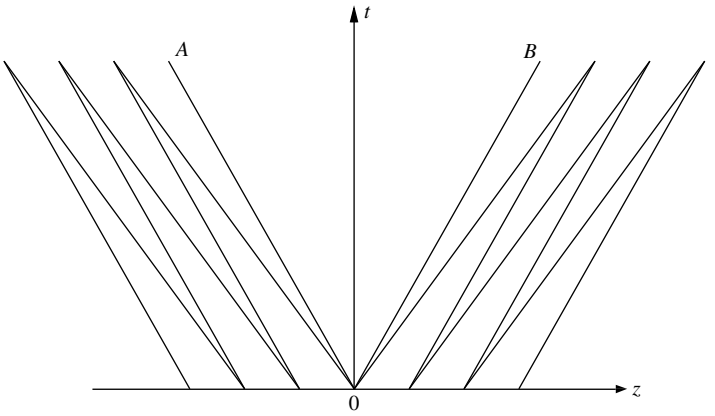

Fig. 2.10. Screening effect produced by a shadow zone.

It is clear that an initial disturbance gives rise to two pairs of d'Alembert waves propagating each in the relevant quadrant of the (z, t)-plane along the characteristics. The interior of the angle AOB in a (z, t)-plane then appears to be a "shadow zone" free from any initially applied disturbance since they will be unable to enter this domain due to a special geometry of characteristics. By controlling such geometry, we will selectively screen large domains in space-time from the invasion of long wave dynamic disturbances. With ordinary (static) composites, this *screening* effect is impossible.

Remark 2.1. The velocities $v_{1,2}$ specified by (2.50) are the phase velocities of the envelopes $e^{\mu\zeta}$ of the modulated waves that represent the Floquet solutions to equations (2.9); these velocities are defined by (2.50) in a low frequency limit $\omega \to 0$. In this capacity, they represent the group velocities of the low frequency waves propagating through an activated dynamic lamination.

When $V = 0$ (a static laminate), the velocities become $\pm v_{st}$, where, by (2.17),

$$v_{st}^2 = \langle k^{-1} \rangle^{-1} / \langle \rho \rangle = a_1^2 a_2^2 / \bar{k} \left(\frac{\bar{1}}{\rho} \right). \tag{2.69}$$

When $V = \infty$ (a temporal laminate), the velocities become $\pm v_{temp}$, where, by (2.19),

$$v_{temp}^2 = \langle k \rangle / \langle \rho^{-1} \rangle^{-1} = a_1^2 a_2^2 \bar{\rho} \left(\frac{\bar{1}}{k} \right). \tag{2.70}$$

Inequalities (2.54) now show that always

$$v_{st}^2 \le a_2^2, \quad v_{temp}^2 \ge a_1^2.$$

For a regular case, as seen from (2.57),

$$v_{st}^2 \ge a_1^2, \ \ v_{temp}^2 \le a_2^2,$$

whereas for an irregular case, (2.58) and (2.59) show that it is possible that

$$v_{st}^2 \le a_1^2, \ \ v_{temp}^2 \ge a_2^2.$$

Combining these inequalities, we conclude that, in a regular case, both v_{st} and v_{temp} fall into the interval (a_1, a_2), whereas in an irregular case, they may fall outside this interval: v_{st} may become less than a_1, and v_{temp} - greater than a_2.

Remark 2.2. Consider a special case when the acoustic impedance $\gamma = \sqrt{k\rho}$ takes the same values for both materials; this case belongs with a regular range (2.55). The formula (2.50) for the effective velocities may then be illustrated by the following elementary argument.

When $\gamma_1 = \gamma_2$, then, at each encounter with the interface separating two adjacent materials in a laminate, an incident wave propagating through material 1 generates *only one* secondary wave, i.e. a transmitted wave travelling in material 2. The waves propagate through ith material ($i = 1, 2$) with velocity $\pm a_i - V$ measured in the frame (2.6) where the interfaces stay immovable. An elementary calculation now specifies the average velocity of waves passing through a unit period in ξ in this frame:

$$\frac{1}{\frac{m_1}{\pm a_1 - V} + \frac{m_2}{\pm a_2 - V}} = \frac{(V \mp a_1)(V \mp a_2)}{\pm \bar{a} - V}. \tag{2.71}$$

On the other hand, when $\gamma_1 = \gamma_2$, then a direct inspection indicates that equation (2.50) defines the difference $v_{1,2} - V$ as

$$v_{1,2} - V = \frac{1}{(\bar{a})^2 - V^2} (V \pm \bar{a})(V \mp a_1)(V \mp a_2); \tag{2.72}$$

this difference characterizes the effective velocities of waves measured in the frame (2.6). We see that the values given by (2.71) and (2.72) are identical.

In a laboratory frame (z,t), the effective velocities take the values

$$\frac{(V\mp a_1)(V\mp a_2)}{\pm\bar{a}-V}+V=\frac{a_1a_2\mp V\langle a\rangle}{\pm\bar{a}-V}.$$

Particularly, for $V=0$ we obtain

$$v_{st}=\pm\langle a^{-1}\rangle^{-1},$$

whereas for $V=\infty$

$$v_{temp}=\pm\langle a\rangle\ .$$

These expressions are identical with those following from the formulae (2.69) and (2.70) for v_{st} and v_{temp} when we apply them to the case $\gamma_1=\gamma_2$.

2.6 Balance of energy in longitudinal wave propagation through an activated elastic bar

The differential equation (2.1) governing the wave propagation through an immovable elastic bar represents an Euler equation generated by the action density

$$\Lambda=\frac{1}{2}\ \rho\ \left(\frac{\partial u}{\partial t}\right)^2-\frac{1}{2}\ k\ \left(\frac{\partial u}{\partial z}\right)^2. \tag{2.73}$$

This density defines components of the energy-momentum tensor W according to the formulae

$$\begin{aligned}
W_{tt}&=\frac{\partial u}{\partial t}\ \frac{\partial\Lambda}{\partial\left(\frac{\partial u}{\partial t}\right)}-\Lambda=\frac{1}{2}\rho\left(\frac{\partial u}{\partial t}\right)^2+\frac{1}{2}k\left(\frac{\partial u}{\partial z}\right)^2-\text{the energy density},\\
W_{tz}&=\frac{\partial u}{\partial t}\ \frac{\partial\Lambda}{\partial\left(\frac{\partial u}{\partial z}\right)}=-k\frac{\partial u}{\partial t}\ \frac{\partial u}{\partial z}-\text{the energy flux density},\\
W_{zt}&=\frac{\partial u}{\partial z}\ \frac{\partial\Lambda}{\partial\left(\frac{\partial u}{\partial t}\right)}=\rho\frac{\partial u}{\partial t}\ \frac{\partial u}{\partial z}-\text{the momentum density},\\
W_{zz}&=\frac{\partial u}{\partial z}\ \frac{\partial\Lambda}{\partial\left(\frac{\partial u}{\partial z}\right)}-\Lambda=-\frac{1}{2}\rho\left(\frac{\partial u}{\partial t}\right)^2-\frac{1}{2}k\left(\frac{\partial u}{\partial z}\right)^2-\text{the momentum flux density}.
\end{aligned} \tag{2.74}$$

These components satisfy the equations

$$\frac{\partial}{\partial t}\ W_{tt}+\frac{\partial}{\partial z}W_{tz}=-\frac{1}{2}\left[\frac{\partial\rho}{\partial t}\left(\frac{\partial u}{\partial t}\right)^2-\frac{\partial k}{\partial t}\left(\frac{\partial u}{\partial z}\right)^2\right], \tag{2.75}$$

$$\frac{\partial}{\partial t}\ W_{zt}+\frac{\partial}{\partial z}W_{zz}=-\frac{1}{2}\left[\frac{\partial\rho}{\partial z}\ \left(\frac{\partial u}{\partial t}\right)^2-\frac{\partial k}{\partial z}\ \left(\frac{\partial u}{\partial z}\right)^2\right], \tag{2.76}$$

following directly from (2.1), (2.74).

At the lhs of equation (2.75) we have the rate of increase $\frac{DW_{tt}}{Dt}$ of the energy of a unit segment of the bar; this rate is calculated as the sum of the local change $\frac{\partial W_{tt}}{\partial t}$ and the energy $\frac{\partial W_{tz}}{\partial z}$ that is brought into a unit segment through its endpoints per unit time. The net increase $\frac{DW_{tt}}{Dt}$ is equal to the work

$$-\frac{1}{2}\left[\frac{\partial \rho}{\partial t}\left(\frac{\partial u}{\partial t}\right)^2 - \frac{\partial k}{\partial t}\left(\frac{\partial u}{\partial z}\right)^2\right], \tag{2.77}$$

produced, per unit time, by an external agent against the variable property pattern. Equation (2.75) thus expresses the energy balance in the system; the balance of momentum is reflected in equation (2.76).

In this section, we shall see in detail how the energy-momentum balance manifests itself through homogenization. To this end, we apply the analysis of section 2.3 in order to find an asymptotic form of equations (2.75), (2.76).

For reasons explained in section 2.3, the derivatives $\partial/\partial t, \partial/\partial z$ entering these equations should be replaced, respectively, by $d/dt, d/dz$, and these latter derivatives calculated by (2.31). We thus reduce (2.75), (2.76) to the following form

$$\begin{aligned}(W_{tt})_t + (W_{tz})_z - V\delta^{-1}(W_{tt})_\xi + \delta^{-1}(W_{tz})_\xi \\ = \frac{1}{2}V\delta^{-1}\left[\rho_\xi(u_t - V\delta^{-1}u_\xi)^2 - k_\xi(u_z + \delta^{-1}u_\xi)^2\right],\end{aligned} \tag{2.78}$$

$$\begin{aligned}(W_{zt})_t + (W_{zz})_z - V\delta^{-1}(W_{zt})_\xi + \delta^{-1}(W_{zz})_\xi \\ = -\frac{1}{2}\delta^{-1}[\rho_\xi(u_t - V\delta^{-1}u_\xi)^2 - k_\xi(u_z + \delta^{-1}u_\xi)^2].\end{aligned} \tag{2.79}$$

Here, as in section 2.3, we assume that $u = u(z,t,\xi)$, $\rho = \rho(\xi)$, $k = k(\xi)$, $\xi = (z - Vt)/\delta$, with δ being a small parameter; the symbols $(\cdot)_z$, $(\cdot)_t$, $(\cdot)_\xi$ stand for the relevant partial derivatives. We now introduce an asymptotic expansion (2.30) for $u(z,t,\xi)$; as shown in section 2.3, the function $u_0(z,t,\xi)$ does not depend on ξ, and the derivatives $u_{1\xi}, u_{2\xi}$ are given, respectively, by (2.36) and (2.38).

Bearing this in mind along with (2.32), we reduce the densities W_{tt} and W_{tz} to the form

$$\begin{aligned}W_{tt} = \frac{1}{2}\rho(u_{0t} - Vu_{1\xi})^2 + \frac{1}{2}k(u_{0z} + u_{1\xi})^2 \\ + \delta[\rho(u_{0t} - Vu_{1\xi})(u_{1t} - Vu_{z\xi}) \\ + k(u_{0z} + u_{1\xi})(u_{1z} + u_{2\xi})] + \ldots,\end{aligned} \tag{2.80}$$

$$\begin{aligned}W_{tz} = -k(u_{0t} - Vu_{1\xi})(u_{0z} + u_{1\xi}) - \delta k[(u_{0t} - Vu_{1\xi})(u_{1z} + u_{2\xi}) \\ + (u_{0z} + u_{1\xi})(u_{1t} - Vu_{2\xi})] + \ldots\ .\end{aligned} \tag{2.81}$$

The expression for W_{zt} is produced if we replace k by $-\rho$ in (2.81); the expression for W_{zz} appears to be the negative of W_{tt}.

In (2.80) and (2.81), the dots stand for terms of order δ^2 and higher. We drop such terms because we want to calculate both sides of (2.78) up to terms of order δ^0. We also need the expansions

$$\begin{aligned}(u_t - V\delta^{-1}u_\xi)^2 &= [u_{0t} + \delta u_{1t} + \ldots - V\delta^{-1}(\delta u_{1\xi} + \delta^2 u_{2\xi} + \ldots)]^2 \\ &= (u_{0t} - Vu_{1\xi})^2 \\ &\quad + 2\delta(u_{0t} - Vu_{1\xi})(u_{1t} - Vu_{2\xi}) + \ldots, \end{aligned} \tag{2.82}$$

$$(u_z + \delta^{-1}u_\xi)^2 = (u_{0z} + u_{1\xi})^2 + 2\delta(u_{0z} + u_{1\xi})(u_{1z} + u_{2\xi}) + \ldots \ . \tag{2.83}$$

Now as we apply (2.80)-(2.83) towards (2.78), the latter equation includes terms of order $\delta^{-1}, \delta^0, \delta$, etc. The coefficients of such terms taken on both sides of (2.78), should be set equal to each other. We are particularly interested in the coefficients of δ^0 because they carry information about the energy flows as we pass to the limit $\delta \to 0$. The balance of δ^{-1} terms yields the equation

$$\begin{aligned}&- V\frac{\partial}{\partial\xi}\left[\frac{1}{2}\rho(u_{0t} - Vu_{1\xi})^2 + \frac{1}{2}k(u_{0z} + u_{1\xi})^2\right] - \frac{\partial}{\partial\xi}k(u_{0t} - Vu_{1\xi})(u_{0z} + u_{1\xi}) \\ &= \frac{1}{2}V\rho_\xi(u_{0t} - Vu_{1\xi})^2 - \frac{1}{2}Vk_\xi(u_{0z} + u_{1\xi})^2, \end{aligned} \tag{2.84}$$

whereas the balance of δ^0-terms is expressed by

$$\begin{aligned}&\frac{1}{2}\frac{\partial}{\partial t}\left[\rho(u_{0t} - Vu_{1\xi})^2 + k(u_{0z} + u_{1\xi})^2\right] - \frac{\partial}{\partial z}\left[k(u_{0t} - Vu_{1\xi})(u_{0z} + u_{1\xi})\right] \\ &- V\frac{\partial}{\partial\xi}\left[\rho(u_{0t} - Vu_{1\xi})(u_{1t} - Vu_{2\xi}) + k(u_{0z} + u_{1\xi})(u_{1z} + u_{2\xi})\right] \\ &- \frac{\partial}{\partial\xi}\left[k(u_{0t} - Vu_{1\xi})(u_{1z} + u_{2\xi}) + k(u_{0z} + u_{1\xi})(u_{1t} - Vu_{2\xi})\right] \\ &= V\left[\rho_\xi(u_{0t} - Vu_{1\xi})(u_{1t} - Vu_{2\xi}) - k_\xi(u_{0z} + u_{1\xi})(u_{1z} + u_{2\xi})\right]. \end{aligned} \tag{2.85}$$

Referring to (2.36)-(2.39), we conclude, after some calculation, that both (2.84) and (2.85) are identically satisfied.

Before we discuss the specifics of such cancellations, it will be appropriate to clarify the physical meaning of various terms participating in (2.85). The first term at the lhs side of (2.85) expresses the local increase of the energy density of *a slow motion*; by (2.80) and (2.40), this density is calculated as

$$\begin{aligned}T_{tt} &= \frac{1}{2}\left[\rho(u_{0t} - Vu_{1\xi})^2 + k(u_{0z} + u_{1\xi})^2\right] \\ &= \frac{1}{2}\left(\rho M^2 + kN^2\right) = \frac{1}{2}\left[\rho(1 - VP)^2 + kP^2\right]u_{0t}^2 \\ &\quad - [\rho VQ(1 - VP) - kP(1 + Q)]u_{0t}u_{0z} \\ &\quad + \frac{1}{2}\left[\rho V^2Q^2 + k(1 + Q)^2\right]u_{0z}^2. \end{aligned} \tag{2.86}$$

The second term reflects contribution due to the energy flux density of a slow motion; by (2.81) and (2.40), this density is represented as

$$T_{tz} = -k(u_{0t} - Vu_{1\xi})(u_{0z} + u_{1\xi}) = -kMN = -k\{P(1-VP)u_{0t}^2 + [(1-VP)(1+Q) - VPQ]u_{0t}u_{0z} - VQ(1+Q)u_{0z}^2\}. \tag{2.87}$$

The term in the second line at the lhs of (2.85),

$$-V\frac{\partial}{\partial\xi}\left[\rho(u_{0t} - Vu_{1\xi})(u_{1t} - Vu_{2\xi}) + k(u_{0z} + u_{1\xi})(u_{1z} + u_{2\xi})\right] = -V\frac{\partial}{\partial\xi}\left[\rho MX + kNY\right], \tag{2.88}$$

represents the local increase of the energy density of a *fast motion*, and the term in the third line

$$-\frac{\partial}{\partial\xi}\left[k(u_{0t} - Vu_{1\xi})(u_{1z} + u_{2\xi}) + k(u_{0z} + u_{1\xi})(u_{1t} - Vu_{2\xi})\right] = -\frac{\partial}{\partial\xi}[k(MY + NX)] \tag{2.89}$$

reflects contribution due to the energy flux density of such a motion. By the last equation of section 2.3 we conclude that the averaged values (over period 1) of the terms (2.88) and (2.89) responsible for a fast motion are both equal to zero. As to the rhs of (2.85), it defines the work produced, per unit time, by an external agent against the variable property pattern. This agent is responsible for an external force working against elastic deformations.

When we implement differentiation $\partial/\partial\xi$ in (2.88) and (2.89) and refer to (2.40) and (2.38), there emerge terms with factors ρ_ξ, k_ξ, as well as the terms without such factors. The factored terms are counter-balanced by the rhs of (2.85). The remaining (nonfactored) terms precisely match the expressions in (2.85) generated by (2.86) and (2.87) combined.

All of those reductions occur term-wise, with no averaging operation applied whatsoever. The relevant (somewhat cumbersome) calculation is left to the reader.

These observations show that the work of an external force produced over a period is equal to the net increase of the energy of a slow motion.

So far in this section we never referred to the homogenized equation (2.41). This equation appears to be an Euler equation produced by an *effective action density*

$$\bar{\Lambda} = \frac{1}{2}(ru_{0t}^2 + 2qu_{0t}u_{0z} - pu_{0z}^2). \tag{2.90}$$

As in the beginning of this section, this function generates components of an *effective energy-momentum tensor* $\bar{W}$:

$$\begin{aligned}
\bar{W}_{tt} &= u_{0t}\,\frac{\partial \bar{\Lambda}}{\partial u_{0t}} - \bar{\Lambda} = \frac{1}{2}(ru_{0t}^2 + pu_{0z}^2),\\
\bar{W}_{tz} &= u_{0t}\,\frac{\partial \bar{\Lambda}}{\partial u_{0z}} = qu_{0t}^2 - pu_{0t}u_{0z},\\
\bar{W}_{zt} &= u_{0z}\,\frac{\partial \bar{\Lambda}}{\partial u_{0t}} = ru_{0t}u_{0z} + qu_{0z}^2,\\
\bar{W}_{zz} &= u_{0z}\,\frac{\partial \bar{\Lambda}}{\partial u_{0z}} - \bar{\Lambda} = -\frac{1}{2}(ru_{0t}^2 + pu_{0z}^2).
\end{aligned} \tag{2.91}$$

These components satisfy the system

$$\begin{aligned}
\frac{\partial}{\partial t}\bar{W}_{tt} + \frac{\partial}{\partial z}\,\bar{W}_{tz} = 0,\\
\frac{\partial}{\partial t}\,\bar{W}_{zt} + \frac{\partial}{\partial z}\,\bar{W}_{zz} = 0,
\end{aligned} \tag{2.92}$$

following from (2.41).

Contrary to (2.75), (2.76), the system (2.92) has zero rhs because the coefficients r, q, p in (2.41) are constant while the ρ, k in (2.1) are ξ-dependent. Equations (2.92) therefore express conservation of both energy and momentum for an *effective* motion governed by (2.41). We want to see how the system (2.92) is linked with (2.75), (2.76). To this end, we first rewrite the expression (2.90) for an effective action density in a more convenient form.

Consider the expression

$$\frac{1}{2}[\rho(u_{0t} - Vu_{1\xi})^2 - k(u_{0z} + u_{1\xi})^2] = \frac{1}{2}(\rho M^2 - kN^2). \tag{2.93}$$

Referring to (2.40), we transform it to

$$\begin{aligned}
&\frac{1}{2}\left\{u_{0t}^2[\rho(1-VP)^2 - kP^2] - 2u_{0t}u_{0z}[\rho VQ(1-VP) + kP(1+Q)]\right.\\
&-\left. u_{0z}^2[k(1+Q)^2 - \rho V^2Q^2]\right\}.
\end{aligned} \tag{2.94}$$

By direct inspection and with reference to (2.37), we get

$$\begin{aligned}
\rho(1-VP)^2 - kP^2 &= \frac{1}{V^2\rho - k}\left(\frac{B^2}{C^2}\,V^2 - k\rho\right),\\
-[\rho VQ(1-VP) + kP(1+Q)] &= \frac{V}{V^2\rho - k}\left(\frac{AB}{C^2} - k\rho\right),\\
k(1+Q)^2 - \rho V^2Q^2 &= \frac{1}{V^2\rho - k}\left(k\rho V^2 - \frac{A^2}{C^2}\right).
\end{aligned} \tag{2.95}$$

Now, by averaging both sides of every equation (2.95) over the period 1 in ξ and by referring to (2.10), (2.12), and (2.13), we write

$$\langle \rho(1-VP)^2 - kP^2 \rangle = \frac{B^2V^2}{C} - D = r,$$
$$-\langle \rho VQ(1-VP) + kP(1+Q) \rangle = V\left(\frac{AB}{C} - D\right) = q,$$
$$\langle k(1+Q)^2 - \rho V^2 Q^2 \rangle = V^2 D - \frac{A^2}{C} = p. \tag{2.96}$$

Combining (2.93), (2.94) and (2.96), we finally obtain

$$\frac{1}{2}\langle \rho M^2 - kN^2 \rangle = \frac{1}{2}(ru_{0t}^2 + 2qu_{0t}u_{0z} - pu_{0z}^2),$$

i.e. the effective action density (2.90).

The quantity $\bar{W}_{tt}$ defined by (2.91) may be interpreted as an *effective energy density* measured in the laboratory frame. Given (2.96), this density takes on the form

$$\bar{W}_{tt} = \frac{1}{2}\langle \rho(1-VP)^2 - kP^2 \rangle u_{0t}^2 + \frac{1}{2}\langle k(1+Q)^2 - \rho V^2 Q^2 \rangle u_{0z}^2. \tag{2.97}$$

We now observe that an effective energy density $\bar{W}_{tt}$ is generally *not equal* to the *averaged energy density* $\langle T_{tt} \rangle$ of the slow motion calculated as (c.f. (2.86))

$$\langle T_{tt} \rangle = \frac{1}{2}\langle \rho(1-VP)^2 + kP^2 \rangle u_{0t}^2 - \langle \rho VQ(1-VP) - kP(1+Q) \rangle u_{0t}u_{0z} + \frac{1}{2}\langle k(1+Q)^2 + \rho V^2 Q^2 \rangle u_{0z}^2. \tag{2.98}$$

The difference between the two densities

$$\bar{W}_{tt} - \langle T_{tt} \rangle = -\langle kP^2 \rangle u_{0t}^2 + \langle \rho VQ(1-VP) - kP(1+Q) \rangle u_{0t}u_{0z} - \langle \rho V^2 Q^2 \rangle u_{0z}^2 = \langle \rho VQMu_{0z} - kPNu_{0t} \rangle$$

vanishes when $V = 0$, i.e. for a static laminate.

This difference is non-zero because of a temporal activation. We therefore expect that if we go to a *co-moving* coordinate frame τ, η in which an interface between layers in an activated composite remains immovable, then the difference between $\bar{W}_{\tau\tau}$ and $\langle T_{\tau\tau} \rangle$ evaluated for this system, may vanish.

The required frame is given by (2.20) with $w = V$; in it, the components of the energy-momentum tensor are expressed by the formulae:

$$\begin{aligned} W_{\tau\tau} &= W_{tt} + VW_{zt}, \\ W_{\tau\eta} &= W_{tz} + VW_{zz} - V\left(W_{tt} + VW_{zt}\right), \\ -W_{\eta\tau} &= W_{zt}, \\ W_{\eta\eta} &= W_{zz} - VW_{zt}. \end{aligned} \tag{2.99}$$

An asymptotic expression for W_{zt} is produced, as mentioned above, if we replace k by $-\rho$ in (2.81). The term T_{zt} in this expression will be defined as ρMN, similarly to the quantity T_{tz} introduced in (2.87). This term takes the form (c.f. (2.87))

$$T_{zt} = \rho MN = \rho\{P(1-VP)u_{0t}^2 + [(1-VP)(1+Q) - VPQ] \\ u_{0t}u_{0z} - VQ(1+Q)u_{0z}^2\}; \tag{2.100}$$

we may call it the momentum density of a slow motion.

Introduce the quantity similar to $W_{\tau\tau}$:

$$T_{\tau\tau} = T_{tt} + VT_{zt};$$

by direct inspection, with reference to (2.10), (2.13). (2.37), (2.97) and (2.98), we show that

$$\langle T_{\tau\tau}\rangle = \bar{W}_{\tau\tau}. \tag{2.101}$$

By a similar argument, for the quantity

$$T_{\tau\eta} = T_{tz} + VT_{zz} - V(T_{tt} + VT_{zt}), \tag{2.102}$$

we obtain

$$\langle T_{\tau\eta}\rangle = \bar{W}_{\tau\eta}. \tag{2.103}$$

The effective energy density (flux)thus appears to be the same as the averaged energy density (flux) of a slow motion in a co-moving coordinate frame in which the interface remains immovable. We could expect that if we noticed that

$$\frac{\partial}{\partial t}(W_{tt} + VW_{zt}) + \frac{\partial}{\partial z}(W_{tz} + VW_{zz}) = 0, \tag{2.104}$$

because of (2.75), (2.76) and due to a supposed dependency of ρ and k on the argument $z - Vt$.

As shown at the end of section 2.2, a co-moving frame never becomes proper except in a trivial case $V = 0$. Eqn. (2.104) is now rewritten as

$$\frac{\partial W_{\tau\tau}}{\partial \tau} + \frac{\partial W_{\tau\eta}}{\partial \eta} = 0; \tag{2.105}$$

it shows that the energy is preserved in a co-moving frame.[1]

We will now discuss the momentum equation taking the form (2.79) in a laboratory frame. Following remarks made after eqn. (2.81), we reproduce an asymptotic version of (2.79) expressing the balance of δ^0-terms:

[1] The conservation of energy in a co-moving frame (2.20) follows from the Noether theorem applied to the variational principle of stationary action with the action density (2.73). For a laminate, the material coefficients ρ and k depend on η and do not depend on τ, which means the conservation of energy in a co-moving frame.

$$\frac{\partial}{\partial t}\rho MN - \frac{1}{2}\frac{\partial}{\partial z}(\rho M^2 + kN^2) - V\frac{\partial}{\partial \xi}[\rho(MY + NX)] - \frac{\partial}{\partial \xi}(\rho MX + kNY)$$
$$= -(\rho_\xi MX - k_\xi NY). \tag{2.106}$$

As for the energy equation, we use the momentum density T_{zt} of a slow motion defined by (2.100), as well as the momentum flux density T_{zz} of the same motion defined as (see (2.86))

$$T_{zz} = -T_{tt} = -\frac{1}{2}(\rho M^2 + kN^2).$$

The third term at the lhs of (2.106) represents contribution due to the momentum density of a fast motion whereas the fourth term reflects a similar contribution produced by the momentum flux density. The averaged (over period 1) values of both terms are equal to zero, just as the averaged values for similar terms (2.88) and (2.89).

Desiring to arrive at the second formula (2.92), we rewrite (2.106) in the following equivalent form:

$$\left(\frac{\partial}{\partial t} + V\frac{\partial}{\partial z}\right)(\rho MN) - \frac{\partial}{\partial z}\left[\frac{1}{2}(\rho M^2 + kN^2) + \rho VMN\right]$$
$$-V\frac{\partial}{\partial \xi}[\rho(MY + NX)] - \frac{\partial}{\partial \xi}(\rho MX + kNY)$$
$$+\rho_\xi MX - k_\xi NY = 0. \tag{2.107}$$

Before applying averaging to (2.107), observe that, by (2.99)-(2.101), we have

$$\left\langle \frac{1}{2}\rho(M^2 + kN^2) + \rho VMN \right\rangle = \langle -T_{zz} + VT_{zt}\rangle = \langle -T_{\eta\eta}\rangle = \langle T_{\tau\tau}\rangle$$
$$= \bar{W}_{\tau\tau} = -\bar{W}_{\eta\eta}.$$

Eqn. (2.107) is now reduced to

$$\left(\frac{\partial}{\partial t} + V\frac{\partial}{\partial z}\right)\langle \rho MN\rangle + \frac{\partial \bar{W}_{\eta\eta}}{\partial z} + \langle \rho_\xi MX - k_\xi NY\rangle = 0 \tag{2.108}$$

The sum of the first and the last terms in the lhs becomes, after some calculation, equal to

$$\frac{\partial \bar{W}_{\eta\tau}}{\partial t} + V\frac{\partial \bar{W}_{\eta\tau}}{\partial z} = \frac{\partial \bar{W}_{\eta\tau}}{\partial \tau},$$

where $\bar{W}_{\eta\tau} \neq \langle \rho MN\rangle = \langle T_{\eta\tau}\rangle$. For example, when $V = 0$, we have $\bar{W}_{\eta\tau} = \langle \rho\rangle u_{0t}u_{0z}$, whereas $\langle \rho MN\rangle = \left\langle \frac{\rho}{k}\right\rangle \frac{1}{\left\langle \frac{1}{k}\right\rangle} u_{0t}u_{0z}$. We conclude that the last term in (2.108), i.e. the momentum applied by an external agent, substantially contributes to an effective momentum density making it *not equal* to the averaged momentum density even in a co-moving coordinate frame.

In this particular frame, only three components $\bar{W}_{\tau\tau}, \bar{W}_{\tau\eta}, \bar{W}_{\eta\eta}$ of an effective energy-momentum tensor appear to be the same as the averaged values $\langle T_{\tau\tau}\rangle, \langle T_{\tau\eta}\rangle, \langle T_{\eta\eta}\rangle$ of the relevant quantities related to a slow motion. The component $\bar{W}_{\eta\tau}$ is *not equal* to $\langle T_{\eta\tau}\rangle$, and it *is directly influenced by an external agent.* Of course, this contribution affects the entire energy-momentum tensor.

References

1. Bakhvalov, N.S., and Panasenko, G.P.: Homogenization: Averaging Processes in Periodic Media - Mathematical Problem in the Mechanics of Composite Materials. Kluwer, Dordrecht, 408 pp (1989)

3

Dynamic Materials in Electrodynamics of Moving Dielectrics

3.1 Preliminary remarks

The analysis given in Chapter 2 may be treated as introductory. We applied the model of a thin elastic bar to illustrate the concept of activated dynamic material. Within this concept, we defined the effective material parameters of a spatio-temporal composite, specifically, a laminate in one spatial dimension and time. Such parameters emerge as we introduce a proper coordinate frame in which the homogenized system is reduced to a canonical form, with diagonal matrix of the effective material constants. This approach obtains a rigorous and universal formulation as we resort to a tensor language to generate a covariant description of the relevant dynamic phenomena. An adequate example illuminating the basic features of the unveiling theory is given by electrodynamics of moving dielectrics. Created by Maxwell and Minkowski, it naturally applies to activated and kinematic composites; particularly, it reveals the conceptual difference between those types of dynamic materials and elucidates the role they play in a general framework of spatio-temporal material assemblages. We begin this chapter with a brief account of the fundamentals of Maxwell's theory (see e.g. [7]); the presentation in sections 3.2-3.4 follows the paper [8].

3.2 The basics of electrodynamics of moving dielectrics

The main object of Maxwell's theory is the electromagnetic field. This one is defined as a set of four vectors $\mathbf{E}, \mathbf{B}, \mathbf{H}, \mathbf{D}$, termed, respectively, the electric field, the magnetic induction, the magnetic field, and the electric displacement. These vectors satisfy the fundamental system of Maxwell's equations, which, in the absence of currents and charges, come up in two basic pairs:

$$\mathrm{curl}\mathbf{E} = -\mathbf{B}_t, \quad \mathrm{div}\mathbf{B} = 0, \tag{3.1}$$

$$\mathrm{curl}\mathbf{H} = \mathbf{D}_t, \quad \mathrm{div}\mathbf{D} = 0. \tag{3.2}$$

The second equation in each pair represents an initial condition for $\mathbf{B}$ and $\mathbf{D}$, respectively, so we ultimately have six equations for four 3D-vectors. To make the Maxwell's system complete, we need six additional equations. They appear as the material relations which, in a classical theory, take the form of two linear equations incorporating the field vectors. For isotropic dielectrics immovable in a laboratory frame x, y, z, t, the classical Maxwell's relations are represented by the formulae

$$\mathbf{D} = \epsilon\mathbf{E}, \quad \mathbf{B} = \mu\mathbf{H}, \tag{3.3}$$

with scalar coefficients ϵ, μ termed, respectively, the dielectric permittivity and the magnetic permeability of a material. For ordinary dielectrics, these coefficients are positive. We shall assume in what follows that they are also frequency independent, i.e. the material has no dispersion.[1]

In special circumstances, the system (3.1)-(3.3) may be reduced to (2.2). To illustrate this, consider a partial solution of (3.1)-(3.3) known as the plane electromagnetic wave. This one appears as we specify the vectors $\mathbf{E}, \ldots, \mathbf{D}$ as

$$\mathbf{E} = E\mathbf{j}, \;\; \mathbf{B} = B\mathbf{i}, \;\; \mathbf{H} = H\mathbf{i}, \;\; \mathbf{D} = D\mathbf{j}, \tag{3.4}$$

with components $E, \ldots, D$ depending on a single spatial coordinate z and time t. The Maxwell's equations (3.1) and (3.2) then yield

$$E_z = B_t, \;\; H_z = D_t. \tag{3.5}$$

This system will be satisfied if we introduce potential functions u, v by setting

$$E = u_t, \;\; B = u_z, \;\; H = v_t, \;\; D = v_z. \tag{3.6}$$

Material relations (3.3) are then reduced to

$$v_t = \frac{1}{\mu}\, u_z, \quad v_z = \epsilon u_t; \tag{3.7}$$

these equations become identical with (2.2) if we apply replacements

$$\frac{1}{\mu} \to k, \quad \epsilon \to \rho. \tag{3.8}$$

Equations (3.3) hold for a medium that is at rest in a laboratory frame (x, y, z, t); they are not valid for a moving medium. Specifically, if the material motion occurs with a uniform velocity $\mathbf{V}$ relative to the (x, y, z, t)-frame, then, *in this frame*, the modified material relations take the form

[1] For our purposes, it is sufficient to assume that ϵ and μ are frequency independent for the frequencies below $\bar{\omega}$, the characteristic frequency of the microstructure.

$$\mathbf{D} + \frac{1}{c^2}\,\mathbf{V} \times \mathbf{H} = \epsilon(\mathbf{E} + \mathbf{V} \times \mathbf{B}),$$
$$\mathbf{B} - \frac{1}{c^2}\,\mathbf{V} \times \mathbf{E} = \mu(\mathbf{H} - \mathbf{V} \times \mathbf{D}). \tag{3.9}$$

Here, c means the velocity of light in a vacuum. The electromagnetic field in a dielectric medium moving with velocity $\mathbf{V}$ relative to a laboratory frame is governed by the system (3.1), (3.2), (3.9). The effects produced by a material motion are then registered by a laboratory observer.

Equations (3.9) are due to Minkowski. Like (3.3), they are linear in the field vectors, though more complicated algebraically.

The system (3.1), (3.2), (3.9) is nothing but the system (3.1)-(3.3) formulated in a moving coordinate frame. This observation has been used by Minkowski when he introduced equations (3.9) in his paper of 1908 [9]. Minkowski's results follow directly from the special theory of relativity established by Einstein in his seminal paper [10] of 1905, three years before Minkowski published his work.

3.3 Relativistic form of Maxwell's system

It will be convenient to introduce the Minkowskian coordinates $x_1 = x,\ \ x_2 = y,\ \ x_3 = z,\ \ x_4 = ict$, and the orthonormal system $\mathbf{e}_1, \mathbf{e}_2, \mathbf{e}_3, \mathbf{e}_4\ \ (\mathbf{e}_i \cdot \mathbf{e}_k = \delta_{ik})$ of unit vectors of the relevant axes in 4-space. The x_4-coordinate in this list is special because it is imaginary while the other coordinates are real. The group of rotations in this space is called the Lorentz group. It involves, as elements, the purely spatial (Euclidean) rotations, with no participance of the x_4-coordinate, and the spatio-temporal rotations that incorporate x_4. The group of Euclidean rotations participates, as a subgroup, in a more general Lorentz group of *all* rotations in 4-space.

Consider a spatial rotation affecting only x_1, x_2 (this rotation may be thought of as occurring "about the (x_3, x_4)-plane"). The relevant coordinate transformation is given by the formulae

$$x_1' = x_1 \cos\phi + x_2 \sin\phi,\ \ x_2' = -x_1 \sin\phi + x_2 \cos\phi,\ \ x_3' = x_3,\ \ x_4' = x_4,$$

where ϕ is the angle of rotation. Once ϕ is real, then x_1' and x_2' are real as well.

A similar set of relations characterizes the spatio-temporal rotation that involves the x_4-coordinate. Assume that such rotation occurs "about the (x_1, x_2)-plane", and, consequently, affects x_3, x_4. We may write

$$x_1' = x_1,\ \ x_2' = x_2,\ \ x_3' = x_3 \cos\phi + x_4 \sin\phi,\ \ x_4' = -x_3 \sin\phi + x_4 \cos\phi. \tag{3.10}$$

The "angle of rotation" ϕ introduced here obtains a clear interpretation within a relativistic concept. We first observe that x_3' and x_3 should both be

real while x'_4 and x_4 should both be imaginary. This requirement means that the angle ϕ should be imaginary, and we simply replace it by $i\phi$. We obtain, instead of (3.10),

$$x'_1 = x_1,\ x'_2 = x_2,\ x'_3 = x_3\cosh\phi + ix_4\sinh\phi,\ x'_4 = -ix_3\sinh\phi + x_4\cosh\phi. \tag{3.11}$$

On the other hand, the special relativity introduces the *Lorentz transform* that links coordinates x'_1, x'_2, x'_3, x'_4, and x_1, x_2, x_3, x_4 of two frames of which the first is moving with uniform velocity $\mathbf{V}$ relative to the second. In particular, if $\mathbf{V} = V\mathbf{k} = V\mathbf{e}_3$, then the Lorentz transform is expressed by the formulae

$$x'_1 = x_1,\ x'_2 = x_2,\ x'_3 = \Gamma(x_3 + i\frac{V}{c}\,x_4),\ x'_4 = \Gamma\left(-i\frac{V}{c}\,x_3 + x_4\right). \tag{3.12}$$

Here, the symbol Γ is defined as

$$\Gamma = \frac{1}{\sqrt{1 - V^2/c^2}}.$$

By comparing this with equations (3.11) we notice that the symbol ϕ in the latter should be specified by

$$\tanh\phi = \frac{V}{c}. \tag{3.13}$$

We conclude that the motion of a new ("primed") frame $(x'_1,\ x'_2,\ x'_3,\ x'_4)$ relative to the laboratory ("non-primed") frame $(x_1,\ x_2,\ x_3,\ x_4)$ that occurs with velocity V along the x_3-axis is equivalent to rotation of the x_3- and x_4-axes about the (x_1, x_2)-plane by the angle $i\phi$, with ϕ defined by (3.13). This interpretation of a motion as a *spatio-temporal rotation in Minkowskian 4-space* appears to be especially helpful towards an adequate interpretation of the effective properties of spatio-temporal material composites.

The unit vectors $\mathbf{e}_1, \ldots, \mathbf{e}_4$ are transformed by the same formulae as coordinates $x_1, \ldots, x_4$. Particularly, if $\mathbf{V} = V\mathbf{e}_3$, then (c.f. (3.11))

$$\mathbf{e}'_1 = \mathbf{e}'_1,\ \mathbf{e}'_2 = \mathbf{e}_2,\ \mathbf{e}'_3 = \mathbf{e}_3\cosh\phi + i\mathbf{e}_4\sinh\phi, \mathbf{e}'_4 = -i\mathbf{e}_3\sinh\phi + \mathbf{e}_4\cosh\phi, \tag{3.14}$$

etc. We observe that the vectors $\mathbf{e}_i$ are generally complex. The inverse formulae are produced if we replace ϕ by $-\phi$.

The Maxwell's theory establishes relations that express the electromagnetic field vectors $\mathbf{E}', \ldots, \mathbf{D}'$ measured by an observer moving with the "primed" frame in terms of the vectors $\mathbf{E}, \ldots, \mathbf{D}$ measured by a laboratory observer. The relevant formulae may be obtained if we introduce matrices

$$F = (c\mathbf{B}, -i\mathbf{E}) = \begin{pmatrix} 0 & cB_3 & -cB_2 & -iE_1 \\ -cB_3 & 0 & cB_1 & -iE_2 \\ cB_2 & -cB_1 & 0 & -iE_3 \\ iE_1 & iE_2 & iE_3 & 0 \end{pmatrix}, \tag{3.15}$$

$$f = (\mathbf{H}, -ic\mathbf{D}) = \begin{pmatrix} 0 & H_3 & -H_2 & -icD_1 \\ -H_3 & 0 & H_1 & -icD_2 \\ H_2 & -H_1 & 0 & -icD_3 \\ icD_1 & icD_2 & icD_3 & 0 \end{pmatrix}, \tag{3.16}$$

and interpret their elements as components of two skew-symmetric tensors F and f of the second rank in Minkowski's 4-space. These tensors are known as the electromagnetic tensors. Every such tensor may be expanded over six linearly independent tensors a_{ik} $(i, k = 1, 2, 3, 4)$ specified by the formulae

$$\begin{aligned} a_{12} = (1/\sqrt{2})(\mathbf{e}_1\mathbf{e}_2 - \mathbf{e}_2\mathbf{e}_1),\ a_{13} &= (1/\sqrt{2})(\mathbf{e}_1\mathbf{e}_3 - \mathbf{e}_3\mathbf{e}_1), \\ a_{14} &= (1/\sqrt{2})(\mathbf{e}_1\mathbf{e}_4 - \mathbf{e}_4\mathbf{e}_1), \\ a_{23} = (1/\sqrt{2})(\mathbf{e}_2\mathbf{e}_3 - \mathbf{e}_3\mathbf{e}_2),\ a_{24} &= (1/\sqrt{2})(\mathbf{e}_2\mathbf{e}_4 - \mathbf{e}_4\mathbf{e}_2), \\ a_{34} &= (1/\sqrt{2})(\mathbf{e}_3\mathbf{e}_4 - \mathbf{e}_4\mathbf{e}_3); \end{aligned} \tag{3.17}$$

these tensors constitute an orthonormal basis in the space of skew-symmetric second rank tensors in 4-space:

$$a_{ik} : a^T_{\ell m} = \begin{cases} 1,\ i = \ell, k = m, \\ 0 \ \text{ otherwise.} \end{cases} \tag{3.18}$$

For F and f we obtain, respectively,

$$F = \sqrt{2}(cB_3a_{12} - cB_2a_{13} - iE_1a_{14} + cB_1a_{23} - iE_2a_{24} - iE_3a_{34}), \tag{3.19}$$

$$f = \sqrt{2}(H_3a_{12} - H_2a_{13} - icD_1a_{14} + H_1a_{23} - icD_2a_{24} - icD_3a_{34}). \tag{3.20}$$

The basic tensors a_{ik} are transformed by the formulae that follow from (3.17), (3.18), and from the relevant relations for $\mathbf{e}_i$. In particular, when $\mathbf{V} = V\mathbf{e}_3$, then we apply equations (3.14) and conclude that all tensors a_{ik} except a_{12} and a_{34} become affected by the transform. These formulae also indicate how the transform changes the field components. To illustrate this, consider the plane electromagnetic wave (3.4); the relevant tensors F and f are given by

$$F = \sqrt{2}(cBa_{23} - iEa_{24}), \quad f = \sqrt{2}(Ha_{23} - icDa_{24}). \tag{3.21}$$

Because, by (3.14) and (3.17),

$$a_{23} = a'_{23}\cosh\phi - ia'_{24}\sinh\phi, \quad a_{24} = ia'_{23}\sinh\phi + a'_{24}\cosh\phi, \tag{3.22}$$

we rewrite (3.19) and (3.20) as

$$\begin{aligned} F &= \sqrt{2}[(cB\cosh\phi + E\sinh\phi)a'_{23} - i(cB\sinh\phi + E\cosh\phi)a'_{24}], \\ f &= \sqrt{2}[(H\cosh\phi + cD\sinh\phi)a'_{23} - i(H\sinh\phi + cD\cosh\phi)a'_{24}] \end{aligned} \tag{3.23}$$

The coefficients of a'_{23}, a'_{24} in the square brackets are now interpreted as $cB', -iE'$, etc. (see (3.21)). We obtain

$$B' = B\cosh\phi + \frac{1}{c}E\sinh\phi, \quad H' = H\cosh\phi + cD\sinh\phi, \tag{3.24}$$

etc. These formulae represent the Lorentz transform applied to the field components. Generally, for the field components parallel ($\mathbf{E}_\parallel, \ldots$) and perpendicular ($\mathbf{E}_\perp, \ldots$) to $\mathbf{V}$, we obtain the following transformation formulae:

$$\mathbf{E}'_\parallel = (\mathbf{E} + \mathbf{V}\times\mathbf{B})_\parallel, \;\; \mathbf{E}'_\perp = \Gamma(\mathbf{E} + \mathbf{V}\times\mathbf{B})_\perp, \tag{3.25}$$

$$\mathbf{B}'_\parallel = (\mathbf{B} - \frac{1}{c^2}\mathbf{V}\times\mathbf{E})_\parallel, \;\; \mathbf{B}'_\perp = \Gamma(\mathbf{B} - \frac{1}{c^2}\mathbf{V}\times\mathbf{E})_\perp, \tag{3.26}$$

$$\mathbf{H}'_\parallel = (\mathbf{H} - \mathbf{V}\times\mathbf{D})_\parallel, \;\; \mathbf{H}'_\perp = \Gamma(\mathbf{H} - \mathbf{V}\times\mathbf{D})_\perp, \tag{3.27}$$

$$\mathbf{D}'_\parallel = (\mathbf{D} + \frac{1}{c^2}\mathbf{V}\times\mathbf{H})_\parallel, \;\; \mathbf{D}'_\perp = \Gamma(\mathbf{D} + \frac{1}{c^2}\mathbf{V}\times\mathbf{H})_\perp. \tag{3.28}$$

Note that all expressions of the type $(\mathbf{V}\times\mathbf{A})_\parallel$ are equal to zero.

These relations allow us to give a direct derivation of Minkowski's material equations (3.9) for a moving medium. To this end, consider an observer moving with the "primed" frame that is "frozen" into a moving material. Because the material is now immovable relative to the observer, he will apply, in a "primed" frame, the formulae

$$\mathbf{D}' = \epsilon\mathbf{E}', \;\; \mathbf{B}' = \mu\mathbf{H}', \tag{3.29}$$

identical with (3.3). By using equations (3.25)-(3.28) in (3.29), we arrive at (3.9).

These equations may be incorporated into a single tensor relation. To this end, let us consider tensors a_{ik} of the set (3.17) and introduce the elementary symmetric functions of the second degree of those tensors. We obtain as many as 21 such functions, given by the following table:

$$\left.\begin{array}{l}
a_{12}a_{12}, \quad a_{12}a_{13} + a_{13}a_{12}, \\
\quad a_{12}a_{14} + a_{14}a_{12}, \quad a_{12}a_{23} + a_{23}a_{12}, \; a_{12}a_{24} + a_{24}a_{12}, \; a_{12}a_{34} + a_{34}a_{12}, \\
a_{13}a_{13}, \\
\quad a_{13}a_{14} + a_{14}a_{13}, \quad a_{13}a_{23} + a_{23}a_{13}, \; a_{13}a_{24} + a_{24}a_{13}, \; a_{13}a_{34} + a_{34}a_{13}, \\
\qquad\quad a_{14}a_{14}, \quad a_{14}a_{23} + a_{23}a_{14}, \; a_{14}a_{24} + a_{24}a_{14}, \; a_{14}a_{34} + a_{34}a_{14}, \\
\qquad\qquad\quad a_{23}a_{23}, \; a_{23}a_{24} + a_{24}a_{23}, \; a_{23}a_{34} + a_{34}a_{23}, \\
\qquad\qquad\qquad\quad a_{24}a_{24}, \; a_{24}a_{34} + a_{34}a_{24}, \\
\qquad\qquad\qquad\qquad\quad a_{34}a_{34}.
\end{array}\right\} \tag{3.30}$$

The most general linear form of these functions represents the second rank symmetric tensor in the space of skew-symmetric tensors a_{ik} treated as primary entities; with respect to the original vector space $\mathbf{e}_i$, this form represents the 4th rank tensor with a special symmetry of indices.

A unit tensor e in the space of skew-symmetric second rank tensors a_{ik} is given by

$$e = -a_{12}a_{12} - a_{13}a_{13} - a_{14}a_{14} - a_{23}a_{23} - a_{24}a_{24} - a_{34}a_{34}. \tag{3.31}$$

Introduce the tensor

$$s = -\frac{1}{\mu c}(a_{12}a_{12} + a_{13}a_{13} + a_{23}a_{23}) - \epsilon c(a_{14}a_{14} + a_{24}a_{24} + a_{34}a_{34}); \quad (3.32)$$

then the relation

$$f = s \ : \ F \quad (3.33)$$

turns out to be equivalent to the system (3.3). We check this by a direct inspection, with a reference to (3.18)-(3.20). The tensor s given by (3.32) is therefore interpreted as a material tensor for an isotropic dielectric immovable in the laboratory frame.

Equation (3.33) is a linear relation between the tensors F and f in a 4-space. For this reason, it may be applied toward an isotropic medium moving relative to a laboratory ("non-primed") frame. Desiring to study the electromagnetic phenomena in such a medium from the standpoint of a laboratory observer, we still use equations (3.19) and (3.20) for F and f; as to the tensor s, we apply for it the equation (3.32), with tensors a_{ik} replaced by $a'_{ik} = (1/\sqrt{2})(\mathbf{e}'_i\mathbf{e}'_k - \mathbf{e}'_k\mathbf{e}'_i)$:

$$s = -\frac{1}{\mu c}(a'_{12}a'_{12} + a'_{13}a'_{13} + a'_{23}a'_{23}) - \epsilon c(a'_{14}a'_{14} + a'_{24}a'_{24} + a'_{34}a'_{34}). \quad (3.34)$$

The equation (3.33) then becomes equivalent to Minkowski's relations (3.9). To show this, it is enough to expand tensors F and f over the tensor basis a'_{ik}; the relevant formulae will be the same as (3.19), (3.20), with a_{ik} replaced by a'_{ik}, and coefficients B, E, H, D replaced by the primed symbols B', E', H', D'. Equation (3.33) then reduces to (3.29) which confirms the desired result.

The Maxwell's system (3.1), (3.2) allows for a very compact formulation in terms of the electromagnetic tensors F and f. Apply double indexation for components of F and f listed in their matrices (3.15), (3.16); then the first pair (3.1) is replaced by a single tensor equation

$$\frac{\partial F^*_{ik}}{\partial x_k} = 0, \quad (3.35)$$

where F^*_{ik} is a tensor dual to F_{ik}, i.e.

$$F^*_{ik} = \frac{1}{2}e_{ikln}F_{ln}.$$

Here, e_{ikln} is a completely antisymmetric tensor of the fourth rank; we apply a standard rule of summation over repeated indices.

The second pair (3.2) is incorporated in the equation

$$\frac{\partial f_{ik}}{\partial x_k} = 0. \quad (3.36)$$

This equation says that the tensor f is divergence free, whereas (3.35) characterizes the dual tensor F^* also as a divergence free tensor. Because of the

tensor character of equations (3.35), (3.36), they preserve their form as we go from a non-primed to a primed coordinate frame. To summarize the results of this section, we outline three fundamental relations: eqn. (3.35) for tensor F, eqn. (3.36) for tensor f, and the linear material relation (3.33) linking F with f. These relations constitute a conceptual base for constructing material composites in space-time. We see that this base is substantially relativistic.

3.4 Material tensor s: discussion. Two types of dynamic materials

This tensor is characterized by equation (3.32) in the case of isotropic dielectrics; this equation allows for a clear geometric interpretation. We observe that a purely spatial rotation does not affect either of the tensors $a_{12}a_{12} + a_{13}a_{13} + a_{23}a_{23}$ or $a_{14}a_{14} + a_{24}a_{24} + a_{34}a_{34}$; consequently, such a rotation does not affect s. This is understandable because the dielectric is assumed isotropic in a conventional sense, i.e. with respect to ordinary rotations in the 3D Euclidean space. However, if we apply spatio-temporal rotation involving the x_4-axis (i.e. introduce a material motion), then the situation becomes different. If the motion occurs with velocity $\mathbf{V} = V\mathbf{e}_3$, then, as shown in section 3.3, all tensors a_{ik} except a_{12} and a_{34} become affected, and the same holds true for s. This tensor, specified by (3.32), is therefore isotropic with respect to purely spatial rotations, and anisotropic with regard to spatio-temporal rotations initiated by the material motion. It will become *completely isotropic*, i.e. isotropic with respect to *all* rotations in 4-space, provided that $1/\mu c = \epsilon c$, i.e. $c^2 = 1/(\epsilon\mu)$. This case is exceptional: it holds for a vacuum where $\epsilon = \epsilon_0,\ \mu = \mu_0,\ c^2 = 1/(\epsilon_0\mu_0)$, and the s-tensor becomes proportional to a unit tensor (3.31):

$$s = \sqrt{\epsilon_0/\mu_0}e.$$

With this notable exception, all of the real materials are anisotropic in space-time.

We may now single out two independent types of spatio-temporal composites. We first consider spatio-temporal microstructures generated by two different, conventionally isotropic dielectric constituents occupying periodic cells in space-time but *motionless* in a laboratory frame. By the terminology introduced in section 1.2, this is a pure activation case. In this case, the material tensors s of original substances differ in their eigenvalues $1/\mu c,\ \ \epsilon c$ alone, whereas their eigentensors a_{ik} remain identical. Another conceivable formation will be a "spatio-temporal polycrystal": this one appears when the cells are occupied by fragments of one and the same conventionally isotropic dielectric (recall that every such dielectric is *anisotropic* in space-time!), and these fragments are brought to *a relative material motion*. By the terminology of section 1.2, this is a pure case of kinetization. We call this formation a spatio-temporal polycrystal because its property pattern represents a direct

analog of a conventional polycrystal assembled *in space* from fragments of the same anisotropic material, those fragments differing only in their orientation relative to the laboratory frame in space. In a spatio-temporal case, we have a similar situation, with the difference in orientation now occurring *in space-time* due to a relative material motion. Such motion may be arranged by various means; e.g., through a high-frequency background mechanical vibration in the form of the standing waves. Another special arrangement generating a desired motion (s.c. "caterpillar construction") will be described below in section 3.6.

As indicated above the material tensors s of original substances differ only in their eigenvalues in the case of activation, and only in their eigentensors in the case of kinetization. This does not mean, of course, that the *effective* material tensors of composites created by these procedures will preserve the same eigentensors (eigenvalues) as the original materials. The reason for that is, certainly, the microgeometry of an assemblage, i.e. the shape of spatio-temporal domains occupied, on a microscale, by different original constituents.

3.5 An activated dielectric laminate: one-dimensional wave propagation

In this and several subsequent sections, we shall examine propagation of a plane electromagnetic wave characterized by equations (3.4)-(3.7) and (3.21), through a heterogeneous medium distributed along the z-axis and representing an activated periodic laminate in a (z,t)-plane illustrated in Fig. 1.4. Materials 1 and 2 occupying the layers are specified as uniform isotropic dielectrics immovable in the (z,t)-frame and having properties

$$(\epsilon,\mu)=\begin{cases}(\epsilon_1,\mu_1)-\text{ material 1},\\(\epsilon_2,\mu_2)-\text{ material 2}.\end{cases}\tag{3.37}$$

We shall be looking for a smooth solution to this problem, i.e. for the functions u,v satisfying equations (3.7) and continuous across the interfaces separating materials 1 and 2 from each other. The continuity of u and v reflects the continuity of E' and H' calculated in the frame moving along with the interface (see (3.25), (3.4), and (3.6)):

$$E'=\Gamma(E+VB)=\Gamma(u_t+Vu_z),$$
$$H'=\Gamma(H+VD)=\Gamma(v_t+Vv_z);$$

of course, we assume that $V<c$ is chosen with observance of (2.5) where $a_i=1/\sqrt{\epsilon_i\mu_i}$ is the velocity of light in material i.[2] This problem differs from

[2] The velocity V of activation need not necessarily be subluminal because no signal is moving at such velocity. The case $V>c$, when the interface becomes spacelike, is discussed below in section 3.11.

the one discussed in section 2.2 only by notation, the relevant correspondence established by (3.8). However, in order to introduce the effective parameters generated by equations (2.11), we, contrary to (2.20), apply the *Lorentz* transform to define new coordinates z' and t'

$$z' = \gamma(z - wt), \;\; t' = \gamma\left(t - \frac{w}{c^2}z\right), \;\; \gamma = \frac{1}{\sqrt{1 - \frac{w^2}{c^2}}}. \tag{3.38}$$

The velocity w will be specified below.

In a new frame (z', t'), the system (2.11) takes on the form

$$\begin{gathered}(p + 2qw - rw^2)u_{z'} - \left[q + \left(\frac{p}{c^2} - r\right)w + q\frac{w^2}{c^2}\right]u_{t'} = \frac{1}{\gamma^2}v_{t'}, \\ \left[q + \left(\frac{p}{c^2} - r\right)w + q\frac{w^2}{c^2}\right]u_{z'} + \left(r - 2q\frac{w}{c^2} - p\frac{w^2}{c^4}\right)u_{t'} = \frac{1}{\gamma^2}v_{z'}\end{gathered} \tag{3.39}$$

Define w by

$$\frac{q}{c^2}w^2 + \left(\frac{p}{c^2} - r\right)w + q = 0; \tag{3.40}$$

the frame (3.38) then becomes proper (see section 2.2), and in this frame the system (3.39) takes the form

$$v_{t'} = (p + qw)u_{z'}, \;\; v_{z'} = \left(\frac{p}{c^2} + \frac{q}{w}\right)u_{t'}, \tag{3.41}$$

similar to (2.23).

Comparing (3.41) with (3.7), we treat the complex $p + qw$ as an inverse effective magnetic permeability $1/M$, and the factor $p/c^2 + q/w$ as an effective dielectric permittivity $\mathcal{E}$:

$$\mathcal{E} = \frac{p}{c^2} + \frac{q}{w}, \;\; \frac{1}{M} = p + qw. \tag{3.42}$$

For eigenvalues $\mathcal{E}c, 1/Mc$ of the effective s-tensor we obtain the expressions

$$\mathcal{E}c = \frac{p}{c} + \frac{qc}{w}, \;\; \frac{1}{Mc} = \frac{p}{c} + \frac{qw}{c}. \tag{3.43}$$

The first invariant $\mathcal{E}c + \frac{1}{Mc}$ of this tensor is given by

$$\mathcal{E}c + \frac{1}{Mc} = \frac{2p}{c} + \frac{qc}{w} + \frac{qw}{c} = \frac{p}{c} + rc; \tag{3.44}$$

here, we applied (3.40) to eliminate w.

By a direct inspection, and with reference to (3.40) and (2.24), we obtain the formula for the second invariant (determinant) of the effective s-tensor:

$$\frac{\mathcal{E}}{M} = \left(\frac{p}{c^2} + \frac{q}{w}\right)(p + qw) = pr + q^2 = 1/\theta; \tag{3.45}$$

this relation is the same as (2.26). If we notice that, by (3.40),

$$\frac{p}{c^2} + \frac{q}{w} = r - \frac{qw}{c^2},$$

and use (3.45), then equations (3.42) will be reduced to the form

$$\mathcal{E} = r - \frac{qw}{c^2}, \quad \frac{1}{M} = \theta^{-1}\left(r - \frac{qw}{c^2}\right)^{-1}, \tag{3.46}$$

similar to (2.25). The difference is because the equations (2.25) resulted from the Galilean transform (2.20), whereas (3.46) appear to be a consequence of the Lorentz transform (3.38). When $(V/c) \ll 1$, the same inequality holds for q/c and w/c, and the term qw/c^2 in (3.46) becomes negligible.

The quadratic equation (3.40) for w should have the real roots to ensure that the effective parameters $\mathcal{E}, M$ are real. The product of the roots equals c^2, so one of the real roots is $\leq c$; this particular root should be applied in (3.38).

To make the roots real it is necessary that

$$\left(\frac{p}{c^2} - r\right)^2 - \frac{4q^2}{c^2} \geq 0.$$

Clearly, this inequality holds for V sufficiently small. The general case will be discussed below, in section 3.8, where the analysis of an activated laminate will be continued.

3.6 A spatio-temporal polycrystallic laminate: one dimensional wave propagation

In this and the following sections, we consider the same periodic laminar microgeometry as in the previous section (see Fig. 1.4), but the filling of layers will be assumed different. The content of this section reproduces results published in the paper [11]. Specifically, we suppose that the layers are occupied by the same material with properties (ϵ, μ), but this material is brought into an individual motion along the z-axis within each layer. The period of lamination is combined of two layers: in the first, occupying the m_1th part of the period, the motion occurs with velocity v_1; in the second layer, the relevant parameters are specified as m_2 and v_2. As before, we shall speak about "material 1" and "material 2"; clearly, $m_1 + m_2 = 1$. We thus have a *discontinuous* velocity pattern along the z-axis; this pattern can be implemented through the use of the following feasible construction.

Assume that we have a linear arrangement of caterpillars placed one after another along the z-axis (Fig. 3.1). The tracks that are moved by caterpillars become electrically connected when they belong with the z-axis, and stay disconnected otherwise. The z-axis will then become occupied by material

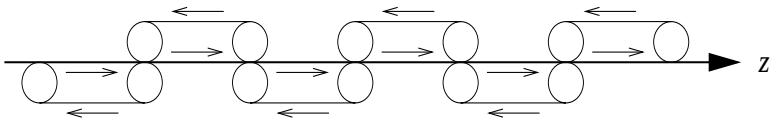

Fig. 3.1. The "caterpillar" construction.

fragments moving each at its own horizontal velocity, and the electric current will flow along the z-axis through the assemblage of electrically connected tracks. With this construction, the performance of the electromagnetic field in a transmission line combined of two such arrangements will be controlled directly by the maintained velocity pattern. This construction resembles an arrangement of belt transmissions distributed on a microscale along the same direction. In Appendix 3, we describe a *mechanical* arrangement capable of creating a discontinuous velocity pattern along an elastic bar, with uninterrupted transmission of energy and momentum from one section of the bar to another.

Under these assumptions, equations (2.11) and (2.16), as well as (3.40)-(3.46), continue to hold, with equations (2.15) replaced by the following relations:

$$\alpha = c\,\frac{\left\langle \frac{Q-T\tanh\psi}{W}\right\rangle}{\left\langle \frac{1}{W}\right\rangle},\quad \beta = \frac{\left\langle \frac{T-R\tanh\psi}{W}\right\rangle}{\left\langle \frac{1}{W}\right\rangle},\quad \theta = \frac{\left\langle \frac{1}{W}\right\rangle}{\left\langle \frac{\epsilon/\mu}{W}\right\rangle}. \tag{3.47}$$

In these formulae, parameters ψ, Q, T, R, W, ϕ are defined as

$$\begin{aligned}
&\tanh\psi = V/c,\\
&Q = \frac{1}{\mu c}\cosh^2\phi - \epsilon c\sinh^2\phi,\quad T = \left(\frac{1}{\mu c} - \epsilon c\right)\sinh\phi\cosh\phi,\\
&R = \frac{1}{\mu c}\sinh^2\phi - \epsilon c\cosh^2\phi,\quad W = -Q + 2T\tanh\psi - R\tanh^2\psi,\\
&\tanh\phi = v/c.
\end{aligned} \tag{3.48}$$

We assume here and below in this chapter (except section 3.11) that $V < c$. The reader will not be confused with the identity of the symbol v used for the material velocity in (3.48) and for the function v first appeared in equations (2.2). The meaning of this symbol will become clear from the context in each individual case.

Note the identities

$$Q = \epsilon c + 1/\mu c + R,\quad T^2 - QR = \epsilon/\mu\ . \tag{3.49}$$

The formulae (3.47) are derived in Appendix 2; they are quite general in a sense that they apply to the situation when material 1 and 2 differ in the values of ϵ, μ, and ϕ. In, particular, if $\phi_1 = \phi_2 = 0$, then these formulae are reduced to (2.15), with substitutions specified by (3.8). Also, if $\phi_1 = \phi_2 = \psi$,

then equations (3.47), (2.16), (3.40) and (3.42) indicate that $\mathcal{E} = \langle\epsilon\rangle, M = \langle\mu\rangle$, as it should be because of (2.17) and (3.8). We shall, however, consider another extreme, i.e. we assume, as mentioned above, that $\epsilon_1 = \epsilon_2 = \epsilon$, $\mu_1 = \mu_2 = \mu$, and $\phi = \phi_i$ for material i; this yields a polycrystallic laminate in space-time. For this composite formation, we shall establish bounds for its effective material parameters.

3.7 A spatio-temporal polycrystallic laminate: the bounds

As seen from (3.45) and from the third formula (3.47), the second invariant $\mathcal{E}/M$ of the effective material tensor for such a laminate preserves the value ϵ/μ of the second invariant common to both materials:

$$\frac{\mathcal{E}}{M} = \frac{\epsilon}{\mu} = \frac{1}{\theta}. \tag{3.50}$$

Therefore, the problem of bounds for $\mathcal{E}$ and M is reduced to the same problem for the first invariant $\mathcal{E}c + 1/Mc$ of the effective s-tensor.

Referring to (3.44) and (2.16), we represent the expression for $\mathcal{E}c + 1/Mc$ in the form:

$$\mathcal{E}c + \frac{1}{Mc} = \frac{c}{\beta V - \alpha}\left[\left(\frac{V^2}{c^2} - 1\right)\frac{1}{\theta} - \left(\frac{\alpha^2}{c^2} - \beta^2\right)\right]. \tag{3.51}$$

By observing that (see (3.47), (3.48))

$$\beta V/c - \alpha/c = \frac{1}{\langle 1/W\rangle}\langle (T\tanh\psi - R\tanh^2\psi - Q + T\tanh\psi)/W\rangle = \frac{1}{\langle 1/W\rangle},$$

we reduce (3.51) to

$$\mathcal{E}c + \frac{1}{Mc} = (\tanh^2\psi - 1)\frac{\epsilon}{\mu}\langle\frac{1}{W}\rangle - \left\langle\frac{Q - T\tanh\psi}{W}\right\rangle^2 \Big/ \left\langle\frac{1}{W}\right\rangle + \left\langle\frac{T - R\tanh\psi}{W}\right\rangle^2 \Big/ \left\langle\frac{1}{W}\right\rangle. \tag{3.52}$$

Because, by (3.49),

$$\frac{\epsilon}{\mu}\left\langle\frac{1}{W}\right\rangle = \left\langle\frac{T^2 - QR}{W}\right\rangle,$$

we rewrite the first term at the rhs of (3.52) as

$$(\tanh^2\psi - 1)\frac{\epsilon}{\mu}\left\langle\frac{1}{W}\right\rangle = \tanh^2\psi\left\langle\frac{T^2-QR}{W}\right\rangle - \left\langle\frac{T^2+R^2\tanh^2\psi - 2TR\tanh\psi}{W}\right\rangle$$
$$+\left\langle\frac{QR+R^2\tanh^2\psi-2TR\tanh\psi}{W}\right\rangle = \tanh^2\psi\left\langle\frac{T^2-QR}{W}\right\rangle$$
$$-\left\langle\frac{(T-R\tanh\psi)^2}{W}\right\rangle - \langle R\rangle = \tanh^2\psi\left\langle\frac{T^2-QR}{W}\right\rangle - \langle Q\rangle$$
$$-\left\langle\frac{(T-R\tanh\psi)^2}{W}\right\rangle + \epsilon c + \frac{1}{\mu c} = \epsilon c + \frac{1}{\mu c} - \left\langle\frac{(T-R\tanh\psi)^2}{W}\right\rangle$$
$$+\left\langle\frac{(Q-T\tanh\psi)^2}{W}\right\rangle.$$

The expression (3.52) for $\mathcal{E}c + 1/Mc$ now takes on the form

$$\mathcal{E}c + 1/Mc = \epsilon c + \frac{1}{\mu c} + \left\langle\frac{(Q-T\tanh\psi)^2}{W}\right\rangle - \left\langle\frac{Q-T\tanh\psi}{W}\right\rangle^2 \Big/ \left\langle\frac{1}{W}\right\rangle$$
$$- \left[\left\langle\frac{(T-R\tanh\psi)^2}{W}\right\rangle - \left\langle\frac{T-R\tanh\psi}{W}\right\rangle^2 \Big/ \left\langle\frac{1}{W}\right\rangle\right]. \quad (3.53)$$

Consider the quantity

$$F(x) = \langle x^2/W\rangle - \frac{\langle x/W\rangle^2}{\left\langle\frac{1}{W}\right\rangle},$$

with symbols x and W defined for each material. This quantity is equal to

$$F(x) = \frac{m_1 m_2}{\bar{W}}(\Delta x)^2,$$

where $\bar{W} = m_1 W_2 + m_2 W_1$, $\Delta x = x_2 - x_1$.

Equation (3.53) is now rewritten as

$$\mathcal{E}c + \frac{1}{Mc} = \epsilon c + \frac{1}{\mu c} + \frac{m_1 m_2}{\bar{W}}[(\Delta Q - \Delta T\tanh\psi)^2 - (\Delta T - \Delta R\tanh\psi)^2] \quad (3.54)$$

For the case of a polycrystal,

$$\Delta R = (1/\mu c)\Delta(\cosh^2\phi) - \epsilon c\Delta(\sinh^2\phi), \text{ etc.}$$

Since $\Delta Q = \Delta R$ by (3.49), we rewrite the third term in the rhs of (3.54) as

$$\frac{m_1 m_2}{\bar{W}}[(\Delta Q)^2 - (\Delta T)^2](1 - \tanh^2\psi). \quad (3.55)$$

Introduce the angle χ by $\tanh^2\chi = 1/(\epsilon\mu c^2) = a^2/c^2$; then

$$W = -Q + 2T\tanh\psi - R\tanh^2\psi = -\epsilon c\cosh^2\phi[\tanh^2\chi - \tanh^2\phi$$
$$+ 2(1-\tanh^2\chi)\tanh\phi\tanh\psi + (\tanh^2\chi\tanh^2\phi - 1)\tanh^2\psi]$$
$$= -\epsilon c\cosh^2\phi(1-\tanh\phi\tanh\psi)^2[\tanh^2\chi - \tanh^2(\phi-\psi)],$$

and the expression (3.55) becomes equal to

$$-\frac{m_1 m_2}{\epsilon c \bar{w}}(1-\tanh^2\psi)[(\Delta Q)^2-(\Delta T)^2], \tag{3.56}$$

with $\bar{w} = m_1 w_2 + m_2 w_1$,

$$w_i = \cosh^2\phi_i(1-\tanh\phi_i\tanh\psi)^2[\tanh^2\chi - \tanh^2(\phi_i-\psi)], \quad i=1,2.$$

With the reference to (3.48), we now calculate $(\Delta Q)^2-(\Delta T)^2$ as $(\epsilon c - 1/\mu c)^2$ $(-\sinh^2\phi_2\cosh^2\phi_2 + 2\sinh\phi_2\cosh\phi_2\sinh\phi_1\cosh\phi_1 - \sinh^2\phi_1\cosh^2\phi_1$ $+\cosh^4\phi_2 - 2\cosh^2\phi_2\cosh^2\phi_1 + \cosh^4\phi_1) = -(\epsilon c - 1/\mu c)^2\sinh^2(\phi_1-\phi_2)$, and (3.54) reduces to (see (3.55), (3.56))

$$\mathcal{E}c + \frac{1}{Mc} = \epsilon c + \frac{1}{\mu c} + \kappa, \tag{3.57}$$

$$\kappa = \frac{\epsilon c}{\bar{w}} m_1 m_2 (1-\tanh^2\psi)(1-\tanh^2\chi)^2\sinh^2(\phi_1-\phi_2). \tag{3.58}$$

Equations (3.57), (3.58) will become a focus of our analysis; we first assume that ϵ, μ are both positive; the results will later be reformulated to cover the case when these parameters are both negative.

We now consider two admissible cases listed below.

i Subrelativistic case

This term applies when $\chi \geq \phi_i - \psi$, and, consequently, $w_i \geq 0$ for both $i=1$ and $i=2$. If the determinants w_i are both non-negative, then, in a co-moving coordinate frame in which the interface is at rest, the material motion on both sides of it occurs at the speed less than the speed of light in the relevant material. This situation matches the case $V^2 < \min\left(a_1^2, a_2^2\right)$ in inequality (2.5).

Because $\tanh\psi = V/c \leq 1$, we see that $\kappa \geq 0$, and the first invariant has the lower bound

$$\mathcal{E}c + \frac{1}{Mc} \geq \epsilon c + \frac{1}{\mu c}. \tag{3.59}$$

The upper bound appears as we find the maximum of κ as the function of m_1:

$$\max_{m_1}\kappa = \frac{\epsilon c}{\left(\sqrt{w_1}+\sqrt{w_2}\right)^2}(1-\tanh^2\psi)(1-\tanh^2\chi)^2\sinh^2(\phi_1-\phi_2); \tag{3.60}$$

the maximizing value of m_1 equals

$$m_1 = \frac{\sqrt{w_1/w_2}}{1+\sqrt{w_1/w_2}}.$$

Consider the limit value of $\max_{m_1}\kappa$ attained as $\phi_1 = \psi, \phi_2 = \chi+\psi = \chi+\phi_1$; then $w_2 \to 0$, and we get

$$\lim \max_{m_1} \kappa = \epsilon c(1 - \tanh^2 \chi) = \epsilon c - \frac{1}{\mu c}, \tag{3.61}$$

with the relevant value $\lim m_1 = 1$; observe that the rhs of (3.61) is positive because $a = 1/\sqrt{\epsilon\mu} < c$. This result is not paradoxical since material 2 then disappears more slowly than the value w_2 tends to zero (observe that we are considering the value of m_1 *maximizing* k all the time!). If we first go to $m_1 = 1$, and *then apply* the limit $w_2 \to 0$, then the limit value of κ would become zero indicating that we *first* withdraw material 2.

Bearing (3.61) in mind and referring to (3.57) and to the conservation law (3.49), we conclude that the original point $P(\epsilon c, 1/\mu c)$ on the hyperbola (Fig. 3.2) is now replaced by the point P_1 with coordinates

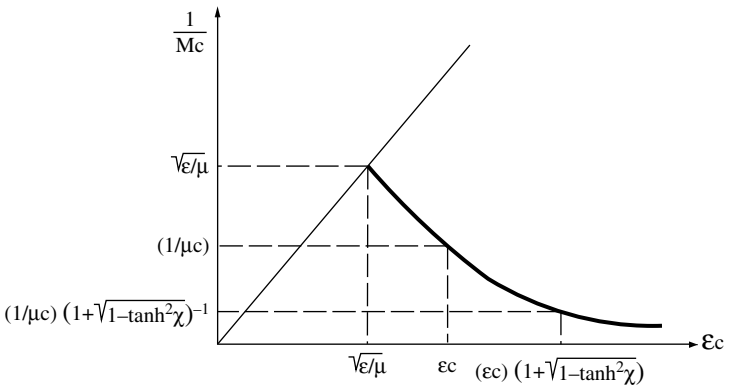

Fig. 3.2. The hyperbola $\mathcal{E}/M = \epsilon/\mu$.

$$\mathcal{E}_1 c = \epsilon c \left(1 + \sqrt{1 - \tanh^2 \chi}\right), \quad \frac{1}{M_1 c} = \frac{1}{\mu c} \frac{1}{1 + \sqrt{1 - \tanh^2 \chi}};$$

with this point we associate a new angle χ_1 defined by

$$\tanh^2\chi_1 = \frac{1}{c^2\mathcal{E}_1 M_1} = \frac{1-\sqrt{1-\tanh^2\chi}}{1+\sqrt{1-\tanh^2\chi}};$$

we notice that

$$1-\tanh^2\chi_1 = \frac{2\sqrt{1-\tanh^2\chi}}{1+\sqrt{1-\tanh^2\chi}} \geq \sqrt{1-\tanh^2\chi}.$$

Since the values of $\mathcal{E}_1$ and M_1 are real, the velocity w is also real, as it is seen from (3.43). This means that there exists a proper frame (3.38) with the eigenvalues $\mathcal{E}_1 c$ and $1/M_1 c$ of a material tensor s.

Repeating this procedure with P_1 as a starting point, we arrive at the next step at a new point P_2 with coordinates

$$\mathcal{E}_2 c = \mathcal{E}_1 c\left(1+\sqrt{1-\tanh^2\chi_1}\right) = \epsilon c\left(1+\sqrt{1-\tanh^2\chi}\right)\left(1+\sqrt{1-\tanh^2\chi_1}\right)$$
$$\geq \epsilon c[1+(1-\tanh^2\chi)^{1/2}][1+(1-\tanh^2\chi)^{1/4}],$$
$$\frac{1}{M_2 c} \leq \frac{1}{\mu c}[1+(1-\tanh^2\chi)^{1/2}]^{-1}[1+(1-\tanh^2\chi)^{1/4}]^{-1},$$

and so on. Because the infinite product

$$(1+x)(1+x^{1/2})(1+x^{1/4})\ldots, \quad x \leq 1,$$

is divergent, we manage to cover the whole branch $\mathcal{E}c \geq \epsilon c,\ \ 1/Mc \leq 1/\mu c$ of hyperbola $\mathcal{E}/M = \epsilon/\mu,\ \ \mathcal{E}, M > 0$, and the first invariant $\mathcal{E}c + 1/Mc$ has no finite upper bound in this case. Summarizing, we conclude that in case (i),

$$\infty \geq \mathcal{E}c + \frac{1}{Mc} \geq \epsilon c + \frac{1}{\mu c}. \tag{3.62}$$

Remark 3.1. The point P_2 in the above construction corresponds to the rank two polycrystallic laminate, etc.; we thus apply laminates of *multiple rank* to attain the relevant part of hyperbola $\mathcal{E}/M = \epsilon/\mu$.

Remark 3.2. The above procedure fails to work when $\chi = \infty$, i.e. when the original material represents the vacuum.

ii Relativistic (Cherenkov) case

For this case, $\chi \leq \phi_i - \psi$, and all w_i become ≤ 0. The material motion on both sides of the interface then occurs at the speed exceeding the speed of light in the relevant material, but, of course, remaining less than c. In this situation, the Cherenkov radiation occurs; it matches the case $V^2 > \max\left(a_1^2, a_2^2\right)$ in (2.5). The function κ is then ≤ 0; its minimum with respect to m_1 is given by the formula

$$\min_{m_1}\kappa = -\frac{\epsilon c}{\left(\sqrt{|\ w_1\ |}+\sqrt{|\ w_2\ |}\right)^2}(1-\tanh^2\psi)(1-\tanh^2\chi)^2\sinh^2(\phi_1-\phi_2).$$

This quantity attains its minimum in ϕ_1 and ϕ_2 when $\phi_1 = \psi+\chi,\ \ \phi_2 = \infty$, or when $\phi_1 = \infty,\ \ \phi_2 = \psi + \chi$. Assume that $\phi_2 \to \infty$ (i.e. material 2 moves at speed approaching c); then

$$\begin{aligned}\lim_{\phi_2\to\infty}\min_{m_1}\kappa &= -\epsilon c\frac{1+\tanh\psi}{1-\tanh\psi}(1-\tanh^2\chi)\lim_{\phi_2\to\infty}\frac{\sinh^2(\phi_1-\phi_2)}{\cosh^2\phi_2}\\ &= -\epsilon c e^{2(\psi-\phi_1)}(1-\tanh^2\chi).\end{aligned}$$

Because $\chi \le \phi_1 - \psi$, we obtain the lower bound for κ by taking $\phi_1 = \chi+\psi$:

$$\begin{aligned}\kappa &\ge \min_{m_1}\kappa \ge -\epsilon c e^{-2\chi}(1-\tanh^2\chi)\\ &= -\epsilon c(1-\tanh\chi)^2 = -\left(\sqrt{\epsilon c}-\frac{1}{\sqrt{\mu c}}\right)^2.\end{aligned}$$

Returning to (3.50), we conclude that in the relativistic case

$$\epsilon c + \frac{1}{\mu c} \ge \mathcal{E}c + \frac{1}{Mc} \ge \epsilon c + \frac{1}{\mu c} - \left(\sqrt{\epsilon c}-\frac{1}{\sqrt{\mu c}}\right)^2 = 2\sqrt{\frac{\epsilon}{\mu}}. \tag{3.63}$$

Remark 3.3. The limit $\phi_2 \to \infty$ cannot be attained for particles with non-zero proper mass because it would require an infinite energy input. But the point $\mathcal{E}c = 1/Mc = \sqrt{\epsilon/\mu}$ corresponding to a completely isotropic dielectric can, in principle, be approached as close as desired by making ϕ_2 sufficiently large.

Corollary 3.4. *Given two materials (3.37) with positive material parameters $\epsilon_1, \dots, \mu_2 > 0$, we may assemble a static laminate by taking $V = 0$ in the construction of section 3.5. By (3.45), (2.29), and (3.8), the effective properties $\mathcal{E}$ and M of such laminate will be specified as*

$$\mathcal{E} = \langle\epsilon\rangle, \quad M = \langle\mu\rangle. \tag{3.64}$$

These formulae represent a hyperbolic segment in $(\mathcal{E}c, 1/Mc)$-plane, with endpoints $(\epsilon_1 c, 1/\mu_1 c)$ and $(\epsilon_2 c, 1/\mu_2 c)$. As shown in the present section, each point $(\epsilon c, 1/\mu c)$ of this segment generates a branch of hyperbola $\mathcal{E}/M = \epsilon/\mu$ belonging to the first quadrant $\mathcal{E}, M \ge 0$. The hyperbolic strip

$$\epsilon_2/\mu_2 > \mathcal{E}/M > \epsilon_1/\mu_1, \quad \mathcal{E}, M \ge 0 \tag{3.65}$$

is shown in Fig.3.3, it appears to be attainable by laminates assembled in space-time from materials 1 and 2.

Remark 3.5. The analysis of this section remains valid, with obvious changes, when the material constants of the original dielectric are both assumed negative. In this case we should, however, consider the branch of hyperbola

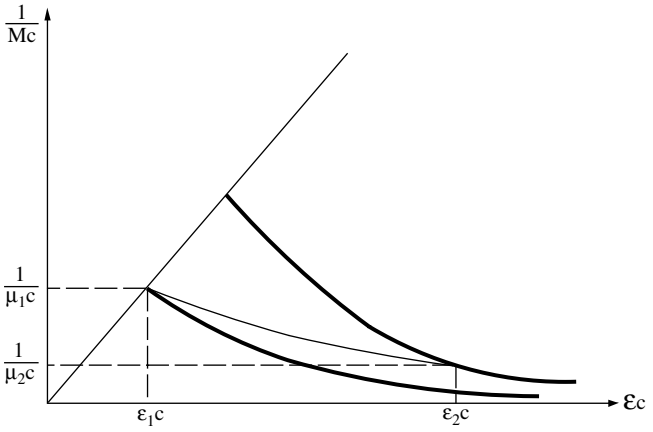

Fig. 3.3. The hyperbolic strip $\epsilon_2/\mu_2 > \mathcal{E}/M > \epsilon_1/\mu_1, \;\; \mathcal{E}, M \geq 0.$

$\mathcal{E}/M = \epsilon/\mu$ belonging with the *third* quadrant $\mathcal{E}, M \leq 0$ (Fig. 3.4). The bounds (3.62) and (3.63) are now replaced by

$$-\infty \leq \mathcal{E}c + \frac{1}{Mc} \leq \epsilon c + \frac{1}{\mu c},$$

$$\epsilon c + \frac{1}{\mu c} \leq \mathcal{E}c + \frac{1}{Mc} \leq -2\sqrt{\frac{\epsilon}{\mu}},$$

and the hyperbolic strip (3.65) is transformed to

$$\epsilon_2/\mu_2 > \mathcal{E}/M > \epsilon_1/\mu_1, \quad \mathcal{E}, M \leq 0.$$

This strip is shown in Fig. 3.4.

In the following section, the possibility of effective material constants to become negative will be confirmed for a particular spatio-temporal assemblage.

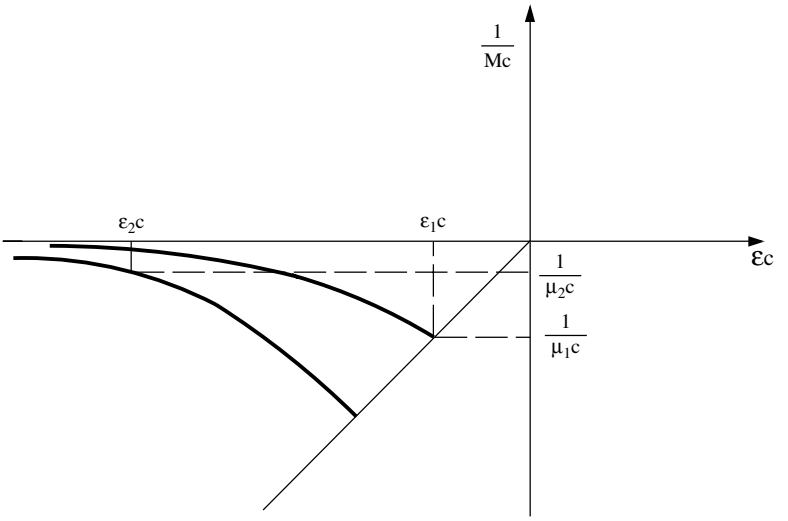

Fig. 3.4. The hyperbolic strip $\epsilon_2/\mu_2 > \mathcal{E}/M > \epsilon_1/\mu_1$, $\mathcal{E}, M \leq 0$.

3.8 An activated dielectric laminate: negative effective material properties

So far through our discussion of spatio-temporal composites, we have been assuming that the material constants of the primary constituents are positive. As to the effective parameters, they not necessarily remained positive. As observed in section 2.5, the characteristic parameter r of an activated laminate, actually, its effective density (see (2.25)), may, under special circumstances, become negative. We shall investigate this possibility in detail in this section, this time in the context of an activated dielectric laminate considered in section 3.5. Material of this and the next sections follows the paper [12].

Referring to (3.43), (2.26), (2.15), (2.29), and (3.8), we arrive, after some calculation, to the following formulae for the invariants $I_1 = \mathcal{E}c + \frac{1}{Mc}$ and $I_2 = \mathcal{E}/M$ of an effective s-tensor:

$$I_1 = \mathcal{E}c + \frac{1}{Mc} = \frac{\bar{\epsilon}\bar{\mu} + \frac{c^2}{a_1^2 a_2^2}}{\bar{\epsilon}\mu_1\mu_2 c\left[V^2 - \frac{1}{\bar{\epsilon}}\left(\frac{\bar{1}}{\mu}\right)\right]}(V^2 - h), \tag{3.66}$$

$$h = \frac{c^2\left(\frac{\bar{1}}{\epsilon}\right)\left(\frac{\bar{1}}{\mu}\right) + a_1^2 a_2^2}{c^2 + a_1^2 a_2^2 \bar{\epsilon}\bar{\mu}}, \tag{3.67}$$

$$I_2 = \frac{\mathcal{E}}{M} = \frac{\left\langle\frac{1}{\mu}\right\rangle}{\left\langle\frac{1}{\epsilon}\right\rangle}\frac{V^2 - \frac{1}{\bar{\mu}}\left(\frac{\bar{1}}{\epsilon}\right)}{V^2 - \frac{1}{\bar{\epsilon}}\left(\frac{\bar{1}}{\mu}\right)}. \tag{3.68}$$

Desiring to investigate the sign of I_1, we first notice that $h < c^2$. Assuming the contrary, we admit that $f(c^2) < 0$ where

$$f(\lambda) \equiv \lambda^2 + \lambda \left[a_1^2 a_2^2 \bar{\epsilon}\bar{\mu} - \left(\frac{\bar{1}}{\epsilon}\right)\left(\frac{\bar{1}}{\mu}\right)\right] - a_1^2 a_2^2.$$

Clearly, the equation $f(\lambda) = 0$ has the real roots of opposite signs, with the product $-a_1^2 a_2^2$. We check that $f(a_1^2) = 2m_1 a_1^2(a_1^2 - a_2^2) < 0$, and $f(a_2^2) = 2m_2 a_1^2(a_2^2 - a_1^2) > 0$ since $a_2 > a_1$; this means that a_2^2 exceeds the positive root of $f(\lambda) = 0$. Because $f(+\infty) = +\infty$, and $c^2 > a_2^2$, we conclude that $f(c^2) > 0$.

The velocity w of the proper frame (3.38) is real when (see (3.40), (3.44), (3.45))

$$(\mathcal{E}c + 1/Mc)^2 - 4\frac{\mathcal{E}}{M} \geq 0.$$

In view of (3.66), (3.68), this inequality may be rewritten as

$$\left(\bar{\epsilon}\bar{\mu} + \frac{c^2}{a_1^2 a_2^2}\right)^2 (V^2 - h)^2 \geq 4\frac{c^2}{a_1^2 a_2^2}\bar{\epsilon}\bar{\mu}\left[V^2 - \frac{1}{\bar{\mu}}\left(\frac{\bar{1}}{\epsilon}\right)\right]\left[V^2 - \frac{1}{\bar{\epsilon}}\left(\frac{\bar{1}}{\mu}\right)\right].$$

If we introduce parameter σ by the formula

$$\sigma = \frac{c^2}{a_1^2 a_2^2 \bar{\epsilon}\bar{\mu}},$$

and rewrite (3.67) as

$$h = \frac{\sigma\bar{\epsilon}\bar{\mu}\left(\frac{\bar{1}}{\epsilon}\right)\left(\frac{\bar{1}}{\mu}\right) + 1}{\sigma + 1}\,\frac{1}{\bar{\epsilon}\bar{\mu}}, \tag{3.69}$$

then the said inequality takes on the form:

$$(1+\sigma)^2(V^2 - h)^2 \geq 4\sigma\left[V^2 - \frac{1}{\bar{\mu}}\left(\frac{\bar{1}}{\epsilon}\right)\right]\left[V^2 - \frac{1}{\bar{\epsilon}}\left(\frac{\bar{1}}{\mu}\right)\right]. \tag{3.70}$$

We now look for the possibility for parameters $\mathcal{E}c, 1/Mc$ to become negative. Equations (3.66)-(3.70) are valid for arbitrary ϵ, μ; however, we first assume that these parameters are positive. The product (3.68) is non-negative due to (2.5), (2.52), and (3.8). As to the sum (3.66), it may be negative if either (i) $V^2 < (1/\bar{\epsilon})(\overline{1/\mu})$ and $V^2 > h$, or (ii) $V^2 > (1/\bar{\epsilon})(\overline{1/\mu})$ and $V^2 < h$. The second possibility can be made consistent with (3.70), as shown by the following argument. Referring to (2.5) and to the third inequality (2.52) together with (3.8), we conclude that V^2 should be taken greater than a_2^2. This may come to agreement with $V^2 < h$ since h may exceed a_2^2 if the value of σ is sufficiently large. In fact, if $\sigma \to \infty$, then h monotonically increases, approaching the value $(\overline{1/\epsilon})(\overline{1/\mu})$ which may exceed a_2^2 for the irregular case (see (2.59) and (3.8)). Considering this case and choosing V^2 within the interval (a_2^2, h), we

observe that, for sufficiently large values of σ, the lhs of (3.70) prevails. Fig. 3.5 represents the plot of $1/M$ versus $\mathcal{E}$, with V variable along the curve. A model value for c is taken equal to $10a_2$. The interval (1.0541, 1.5851) of V from (3.70) corresponds to negative values of both effective parameters, while for $V > 1.9755$ those parameters become positive. A more detailed discussion of numerical results follows below in section 3.10.

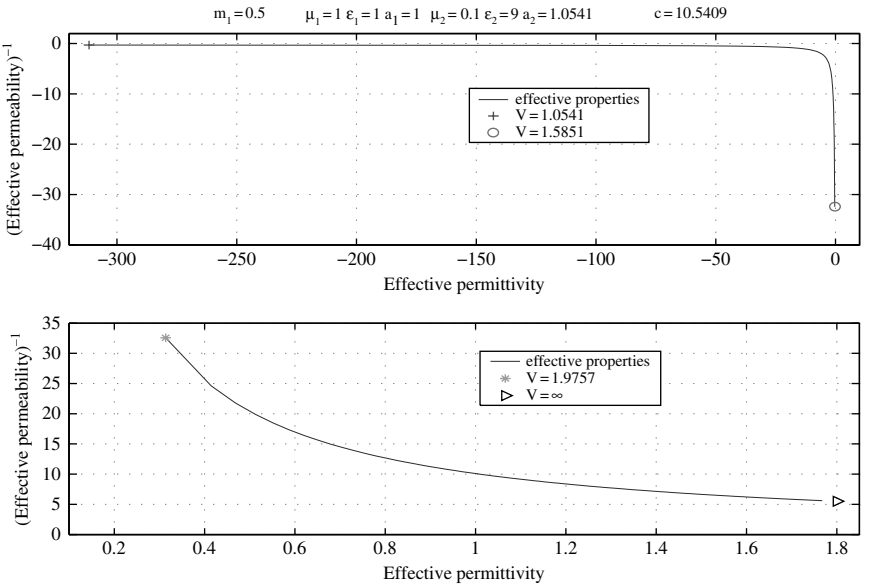

Fig. 3.5. Effective permittivities and permeabilities of dielectric laminate with $(\epsilon_1, \mu_1) = (1, 1), (\epsilon_2, \mu_2) = (9, 0.1), m_1 = 0.5$, for variable V.

The effective wave impedance $\mathcal{E}/M$ versus V is plotted in Fig. 3.6.

Inequality (3.70) is important because it guarantees real values of the effective parameters $\mathcal{E}, M$ together with the velocity w of a proper coordinate frame. At the same time, once w is real, then $\mathcal{E}Mc^2 > 1$, i.e. the effective parameters are consistent with a relativistic concept.

To prove this, observe that inequality $\mathcal{E}Mc^2 > 1$ yields (see (3.43))

$$\frac{\frac{p}{c} + \frac{qc}{w}}{\frac{p}{c} + \frac{qw}{c}} > 1. \tag{3.71}$$

If the roots $w_{1,2}$ of (3.40) are real, then they are of the same sign. This sign may be taken positive with no lack of generality, by specifying the sign of q. The roots $w_{1,2}$ are positive if and only if

$$\left(\frac{p}{c^2} - r\right)\frac{c^2}{q} < 0,$$

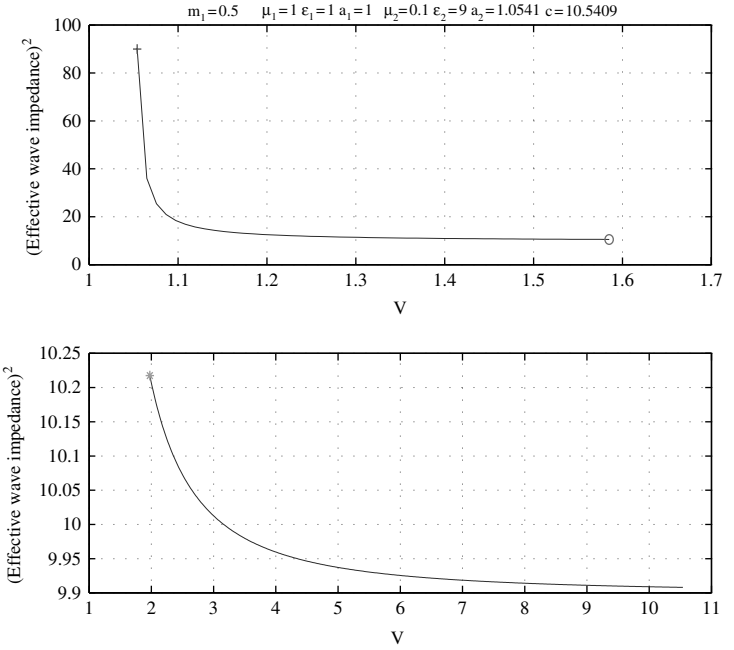

Fig. 3.6. Effective wave impedance versus V.

i.e.

$$\frac{p}{c^2} - r \gtrless 0 \quad \text{when} \quad q \lessgtr 0. \tag{3.72}$$

Now, if $\mathcal{E}, M > 0$, then, by (3.43) and (3.71) we conclude that

$$\frac{p}{c} + \frac{qc}{w} > \frac{p}{c} + \frac{qw}{c},$$

or

$$\frac{qc}{w} > \frac{qw}{c}.$$

For the positive root w that is less than c, this inequality means $q > 0$; inequality (3.72) then yields

$$\frac{p}{c^2} - r < 0. \tag{3.73}$$

By a similar argument, we find that if $\mathcal{E}, M < 0$, then $q < 0$, and

$$\frac{p}{c^2} - r > 0. \tag{3.74}$$

Now it is easy to check the validity of (3.73) or (3.74) for activated laminate in space-time. Particularly, referring to (2.29), (3.8), we find that

$$\frac{p}{c^2} - r = \left\{ \frac{\left\langle \frac{1}{\mu} \right\rangle}{c^2} \left(V^2 - \frac{1}{\bar{\epsilon}\bar{\mu}} \right) - \frac{\epsilon_1 \epsilon_2}{\bar{\epsilon}} \left[V^2 - \left(\frac{\bar{1}}{\epsilon} \right) \left(\frac{\bar{1}}{\mu} \right) \right] \right\} \frac{1}{V^2 - \frac{1}{\bar{\epsilon}} \left(\frac{\bar{1}}{\mu} \right)}.$$

Considering the irregular case (2.56), (2.59), (3.8), and choosing V^2 within the interval (a_2^2, h), we observe, with reference to (2.53) and (2.54), that $\frac{p}{c^2} - r > 0$, which yields $q < 0$ for $w > 0$. By (3.74), this means that $\mathcal{E}, M < 0$, as indicated above in this section.

If $\mathcal{E}Mc^2 > 1$, then the effective phase velocity $1/\sqrt{\mathcal{E}M}$ in a proper frame does not exceed c. By a standard relativistic rule, this property holds in any other frame moving with velocity below c relative to the proper frame; particularly, this property should hold in a laboratory frame where the phase velocities are specified by (2.50). At the same time this formula together with (3.8) shows that one of such velocities tends to infinity when $V^2 \to \left(\frac{\bar{1}}{\epsilon}\right)\left(\frac{\bar{1}}{\mu}\right)$; we conclude that if V^2 is too close to $\left(\frac{\bar{1}}{\epsilon}\right)\left(\frac{\bar{1}}{\mu}\right)$, then inequality (3.70) must be violated. In other words, once V^2 is chosen in the interval $\left(a_2^2, \left(\frac{\bar{1}}{\epsilon}\right)\left(\frac{\bar{1}}{\mu}\right)\right)$, it should not stay too close to its right end point.

To confirm this, we represent inequality (3.70) in the form

$$\phi(V^2) \geq 0, \tag{3.75}$$

with

$$\phi(y) = (1-\sigma)^2 y^2 - 2Ky + L, \quad K = h(1+\sigma)^2 - 2\sigma\left[\left(\frac{\bar{1}}{\epsilon}\right)\frac{1}{\bar{\mu}} + \frac{1}{\bar{\epsilon}}\left(\frac{\bar{1}}{\mu}\right)\right], \tag{3.76}$$

$$L = (1+\sigma)^2 h^2 - 4\sigma \frac{1}{\bar{\epsilon}\bar{\mu}}\left(\frac{\bar{1}}{\epsilon}\right)\left(\frac{\bar{1}}{\mu}\right). \tag{3.77}$$

The function $\phi(y)$ attains its minimum at

$$y = y_* = \frac{K}{(1-\sigma)^2};$$

the minimum value equals

$$\phi(y_*) = L - \frac{K^2}{(1-\sigma)^2}.$$

The value y_* approaches $\left(\frac{\bar{1}}{\epsilon}\right)\left(\frac{\bar{1}}{\mu}\right)$ as $\sigma \to \infty$; at the same time, by (3.68), (3.76), and (3.77), the asymptotic value of $\phi(y_*)$ becomes

$$\phi(y_*) \sim -4\sigma \frac{1}{\bar{\epsilon}\bar{\mu}}\left(\frac{\bar{1}}{\epsilon}\right)\left(\frac{\bar{1}}{\mu}\right)\left[\bar{\epsilon}\bar{\mu}\left(\frac{\bar{1}}{\epsilon}\right)\left(\frac{\bar{1}}{\mu}\right) + 1\right], \tag{3.78}$$

as $\sigma \to \infty$. On the other hand, by (3.75) and (3.69),

$$\phi(0) = L \sim \sigma^2 \frac{1}{(\bar{\epsilon}\bar{\mu})^2}\left[\bar{\epsilon}\bar{\mu}\left(\frac{\bar{1}}{\epsilon}\right)\left(\frac{\bar{1}}{\mu}\right) + 1\right]^2. \tag{3.79}$$

Because $\phi(\pm\infty) = +\infty$, we conclude that the smallest positive root of $\phi(y)$ belongs, for large values of σ, to the interval $[0, y_*]$; this root approaches y_* as $\sigma \to \infty$, i.e. it approaches $\left(\frac{\bar{1}}{\epsilon}\right)\left(\frac{\bar{1}}{\mu}\right)$. For the irregular case (2.56), (2.59), (3.8), the said root may exceed a_2^2, and the interval between a_2^2 and the root will meet our requirements: with V^2 in this interval, inequality (3.75) will be satisfied.

We conclude that negative values of $\mathcal{E}, M$ may be created if parameter σ is large enough, i.e. if the phase velocities a_1 and a_2 of light in original materials are much smaller than c.

The difference $V^2 - \left(\frac{\bar{1}}{\epsilon}\right)\left(\frac{\bar{1}}{\mu}\right)$ should not take zero value for another substantial reason: if it does, then the formula (2.50) itself becomes wrong because the asymptotic formulae for $\mu_{1,2}$ produced for $\omega\delta/a \ll 1$ in Appendix 1 appear in this case to be inaccurate; correct calculation requires a better approximation of $\mu_{1,2}$ given by higher powers of $\omega\delta/a$.

The above discussion is related to the case when material constants of original constituents are all positive; it applies, word for word, to the case when those constants are all negative. With such constituents, we may then construct activated laminate with the effective constants $\mathcal{E}, M$ that are both positive.

3.9 An activated dielectric laminate: the energy considerations. Waves of negative energy

In this section, we revisit the formulae for the wave energy introduced in section 2.6, to study transformation of energy in the case of negative effective parameters. We will obtain alternative expressions for the average and effective energy densities and show that these expressions *may become negative* along with the effective material parameters. This observation demonstrates that the low frequency *waves may carry negative energy* - the phenomenon peculiar to wave propagation through material media that are not in thermodynamic equilibrium.

We start with calculating the average electromagnetic energy density in a laminate; this quantity is defined as $\langle w_e + w_m \rangle$, where (see section 3.5) the symbols

$$w_e = \frac{1}{2}\epsilon u_t^2, \quad w_m = \frac{1}{2\mu}u_z^2$$

have, respectively, the sense of electric and magnetic energy densities.

Because of the continuity of u and v across the layers' interface, the derivatives (c.f. (2.3), (2.4))

$$\begin{aligned} u_\tau &= u_t + Vu_z, \\ v_\tau &= v_t + Vv_z = \epsilon V u_t + \tfrac{1}{\mu}u_z \end{aligned} \tag{3.80}$$

are also continuous. We use this to express u_t, u_z as functions of ϵ, μ, V, and the continuous derivatives, u_τ, v_τ:

$$\begin{aligned} u_t &= -\tfrac{a^2}{V^2-a^2}u_\tau + \tfrac{V}{\epsilon(V^2-a^2)}v_\tau, \\ u_z &= \tfrac{V}{V^2-a^2}u_\tau - \tfrac{1}{\epsilon(V^2-a^2)}v_\tau. \end{aligned}$$

The value of $\langle w_e\rangle$ is thus calculated as

$$\begin{aligned} \langle w_e\rangle &= \tfrac{1}{2}\left\langle \epsilon\left(\tfrac{a^2}{V^2-a^2}\right)^2\right\rangle u_\tau^2 - \left\langle \tfrac{a^2}{(V^2-a^2)^2}\right\rangle V u_\tau v_\tau \\ &+\tfrac{1}{2}\left\langle \tfrac{1}{\epsilon(V^2-a^2)^2}\right\rangle V^2 v_\tau^2; \end{aligned} \tag{3.81}$$

in this formula, the derivatives u_τ, v_τ remain unaffected by averaging and stay identical with their average values. The latter are linked with the average values $\langle u_t\rangle, \langle u_z\rangle, \langle v_t\rangle, \langle v_z\rangle$ through the formulae (see (2.11), (2.16), and (3.8)).

$$\begin{aligned} &u_\tau = \langle u_t\rangle + V\langle u_z\rangle, \\ &v_\tau = \langle v_t\rangle + V\langle v_z\rangle = (p+qV)\langle u_z\rangle - (q-rV)\langle u_t\rangle = \alpha c\langle u_z\rangle + \beta\langle u_t\rangle. \end{aligned} \tag{3.82}$$

Note that these formulae relate the *average* values of $u_t, \ldots, v_z$, and are therefore different from those in (3.80) which relate the pointwise values and hold along the layers' interfaces. As mentioned in section 2.2, we preserve below the symbols $u_t, \ldots, v_z$ without corner brackets, introduced for the pointwise values, also for the average values; the appropriate meaning will follow from the context.

By eliminating u_τ, v_τ from (3.81) with the aid of (3.82), we arrive at the following expression for $\langle w_e\rangle$:

$$\begin{aligned} \langle w_e\rangle &= \frac{1}{2}\left\langle \epsilon\frac{\left(\frac{V}{\epsilon}\beta - a^2\right)^2}{(V^2-a^2)^2}\right\rangle u_t^2 + \left\langle \frac{\epsilon}{(V^2-a^2)^2}\left(\frac{V}{\epsilon}\beta - a^2\right)\left(\frac{c\alpha}{\epsilon} - a^2\right)\right\rangle V u_t u_z \\ &+ \frac{1}{2}\left\langle \epsilon\frac{\left(\frac{c\alpha}{\epsilon} - a^2\right)^2}{(V^2-a^2)^2}\right\rangle V^2 u_z^2. \end{aligned} \tag{3.83}$$

By a similar argument, we calculate $\langle w_m\rangle$ as

$$\begin{aligned} \langle w_m\rangle &= \frac{1}{2}\left\langle \frac{1}{\mu}\frac{\left(V - \frac{\beta}{\epsilon}\right)^2}{(V^2-a^2)^2}\right\rangle u_t^2 + \left\langle \frac{1}{\mu}\frac{\left(V - \frac{\beta}{\epsilon}\right)\left(V^2 - \frac{c\alpha}{\epsilon}\right)}{(V^2-a^2)^2}\right\rangle u_t u_z \\ &+ \frac{1}{2}\left\langle \frac{1}{\mu}\frac{\left(V^2 - \frac{c\alpha}{\epsilon}\right)^2}{(V^2-a^2)^2}\right\rangle u_z^2. \end{aligned} \tag{3.84}$$

The sum $\langle w_e\rangle + \langle w_m\rangle = \langle w_e + w_m\rangle$ - clearly positive - represents an average value $\langle W_{tt}\rangle$ of the electromagnetic energy density $W_{tt} = w_e + w_m$ measured

in a laboratory frame. An average value $\langle W_{zt}\rangle$ of the momentum density $W_{zt} = \epsilon u_t u_z$, originally dependent on pointwise values of u_t, u_z, is given by the formula

$$\langle W_{zt}\rangle = \langle \epsilon u_t u_z\rangle = \left\langle \epsilon \frac{\left(V - \frac{\beta}{\epsilon}\right)\left(V\frac{\beta}{\epsilon} - a^2\right)}{(V^2 - a^2)^2} \right\rangle u_t^2$$

$$+ \left\langle \frac{\epsilon}{(V^2 - a^2)^2}\left[\left(V\frac{\beta}{\epsilon} - a^2\right)\left(V^2 - \frac{c\alpha}{\epsilon}\right) + V\left(V - \frac{\beta}{\epsilon}\right)\left(\frac{c\alpha}{\epsilon} - a^2\right)\right]\right\rangle u_t u_z$$

$$+ \left\langle \epsilon V \frac{\left(\frac{c\alpha}{\epsilon} - a^2\right)\left(V^2 - \frac{c\alpha}{\epsilon}\right)}{(V^2 - a^2)^2} \right\rangle u_z^2. \tag{3.85}$$

Like equations (3.83) and (3.84), this formula contains the average values of u_t, u_z. The energy flux density $W_{tz} = -(1/\mu)u_t u_z$ has an average value

$$\langle W_{tz}\rangle = -\left\langle \frac{1}{\mu} u_t u_z \right\rangle = -\left\langle \frac{1}{\mu} \frac{\left(V - \frac{\beta}{\epsilon}\right)\left(V\frac{\beta}{\epsilon} - a^2\right)}{(V^2 - a^2)^2} \right\rangle u_t^2$$

$$- \left\langle \frac{1}{\mu(V^2 - a^2)^2}\left[\left(V\frac{\beta}{\epsilon} - a^2\right)\left(V^2 - \frac{c\alpha}{\epsilon}\right) + V\left(V - \frac{\beta}{\epsilon}\right)\left(\frac{c\alpha}{\epsilon} - a^2\right)\right]\right\rangle u_t u_z$$

$$- \left\langle \frac{V}{\mu} \frac{\left(\frac{c\alpha}{\epsilon} - a^2\right)\left(V^2 - \frac{c\alpha}{\epsilon}\right)}{(V^2 - a^2)^2} \right\rangle u_z^2, \tag{3.86}$$

and the momentum flux density $\langle W_{zz}\rangle$ equals -$\langle W_{tt}\rangle$. It is easy to check that $\langle W_{tt}\rangle = \langle T_{tt}\rangle, \langle W_{zt}\rangle = \langle T_{zt}\rangle$, etc., where the rhs are given by equations (2.86), etc., of section 2.6, with obvious substitutions (3.8). We again obtain interpretation for the quantities $\langle T_{\tau\tau}\rangle, \langle T_{\tau\eta}\rangle$ introduced in section 2.6: they appear to be equal, respectively, to $\langle W_{\tau\tau}\rangle, \langle W_{\tau\eta}\rangle$.

We consider the action density Λ specified in that section by (2.73); an alternative expression is given by

$$\Lambda = w_e - w_m = \frac{1}{2}(u_t v_z - u_z v_t). \tag{3.87}$$

Here, we used the pointwise values of $u_t, \ldots, v_z$. For laminates, the action density is quasi-affine, i.e. its averaged value $\langle\Lambda\rangle$ is equal to the action density of the averaged field $\bar{\Lambda}$ (the *effective action density*). This result follows from the chain of equalities

$$\langle\Lambda\rangle = \frac{1}{2}\langle u_t v_z - u_z v_t\rangle = \frac{1}{2}\langle u_{t'} v_{z'} - u_{z'} v_{t'}\rangle$$

$$= \frac{1}{2}[u_{t'}\langle v_{z'}\rangle - \langle u_{z'}\rangle v_{t'}] = \frac{1}{2}[\langle u_{t'}\rangle\langle v_{z'}\rangle - \langle u_{z'}\rangle\langle v_{t'}\rangle] = \bar{\Lambda}. \tag{3.88}$$

We used here the Lorentz-invariance of action, with the primed frame z', t' moving along with the property interfaces and preserving continuity of tangential fields $\mathbf{E}' = \mathbf{E} + (\mathbf{V} \times \mathbf{B}) = (u_t + V u_z)\mathbf{j} = u_{t'}\mathbf{j}$, and $\mathbf{H}' = \mathbf{H} - (\mathbf{V} \times \mathbf{D}) = (v_t + V v_z)\mathbf{i} = v_{t'}\mathbf{i}$. We confirm this result also by a direct inspection based on (3.83) and (3.84), and, by using (2.16); the calculation shows that

$$\langle w_e - w_m \rangle = \langle \Lambda \rangle = \bar{\Lambda} = \frac{1}{2} r u_t^2 + q u_t u_z - \frac{1}{2} p u_z^2. \tag{3.89}$$

This relation matches the formula (2.90) in section 2.6. The effective action density serves as the integrand (Lagrangian) for the functional

$$\int\int \bar{\Lambda} dz dt$$

generating (2.11) as Euler equations and (2.91) as components of an effective energy-momentum tensor; these components satisfy the system (2.92). In (2.90) and (2.91), we used the symbol u_0 instead of u.

For $V \neq 0$, the quasi-affinity property (3.88) does not extend in an analogous fashion to the components of the energy-momentum tensor, i.e. the energy density, the energy density flux, etc. For example we have seen in section 2.6 that an averaged energy density $\langle W_{tt} \rangle = \langle T_{tt} \rangle$ in a laboratory frame is *not equal* to $\bar{W}_{tt}$.

However, if we consider a co-moving Galilean frame (2.20) traveling at velocity $w = V$ relative to a laboratory, then, in such a frame,

$$\langle W_{\tau\tau} \rangle = \bar{W}_{\tau\tau}, \quad \langle W_{\tau\eta} \rangle = \bar{W}_{\tau\eta}. \tag{3.90}$$

This follows from equations (2.102), (2.104) together with the remark after eqn. (3.86).

As stated in section 2.6, equation (2.75) indicates that the net rate of increase of the energy of the electromagnetic field in a unit segment is equal to the work committed, per unit time, by an external agent against the variable property pattern. This work is expressed by the right hand side of (2.75). In the case of activated laminate, both ϵ and μ (or ρ and k^{-1}) satisfy the equation $(\cdot)_t + V(\cdot)_z = 0$; from (2.76) we conclude that the term

$$-\frac{1}{2}\left[\epsilon_t u_t^2 - \left(\frac{1}{\mu}\right)_t u_z^2\right] \tag{3.91}$$

is equal to the expression

$$-V\left(\frac{\partial}{\partial t} W_{zt} + \frac{\partial}{\partial z} W_{zz}\right).$$

At the first glance, the presence of the work term (3.91) might be interpreted as equivalent to the change in the energy density W_{tt} of the field in

the laboratory frame by the value VW_{zt}, and to a simultaneous change in the energy flux W_{tz} by the value VW_{zz} (cf. (2.105)):

$$\frac{\partial}{\partial t}(W_{tt} + VW_{zt}) + \frac{\partial}{\partial z}(W_{tz} + VW_{zz}) = 0.$$

By applying averaging to this equation and by referring to (2.99), we arrive at the equation

$$\frac{\partial}{\partial t}(\bar{W}_{tt} + V\bar{W}_{zt}) + \frac{\partial}{\partial z}(\bar{W}_{tz} + V\bar{W}_{zz}) = 0,$$

following from (2.92). The combination $\bar{W}_{tt} + V\bar{W}_{zt}$ - the average energy density $\langle W_{\tau\tau}\rangle$ *in a co-moving frame* (2.20) - might then be interpreted, *in a laboratory frame*, as the averaged net energy density composed of the energy $\langle W_{tt}\rangle$ of the electromagnetic wave minus the energy $-V\langle W_{zt}\rangle$ needed to overcome the variable property pattern.

This interpretation is valid only in part, however. The effective energy density $\bar{W}_{tt} + V\bar{W}_{zt}$ in a co-moving frame (2.20) may be calculated by (2.91) for the d'Alembert waves $u_i = u(z - v_i t)$, $i = 1, 2$, where v_i are the roots of the quadratic equation (2.51). We get

$$\bar{W}_{tt} + V\bar{W}_{zt} = u'^2(rv - q)(v - V), \tag{3.92}$$

the prime here denotes differentiation with respect to the whole argument.

If the original materials are identical ($\epsilon_1 = \epsilon_2 = \epsilon$, $\mu_1 = \mu_2 = \mu$), then $p = \frac{1}{\mu}, q = 0, r = \epsilon$ by (2.29) and (3.8), and $v_{1,2} = \pm a$, $a = 1/\sqrt{\epsilon\mu}$; the energy $\bar{W}_{tt} + V\bar{W}_{zt}$ then becomes equal to

$$\bar{W}_{tt} + V\bar{W}_{zt} = u'^2\epsilon v(v - V). \tag{3.93}$$

This expression depends on V, a purely kinematic effect related exclusively to the frame and not associated with the variability of the property pattern. When $v = a$ (a "slow" wave in the moving frame), then $\bar{W}_{tt} + V\bar{W}_{zt}$ becomes negative if $V > a$ (Sturrock [13]); when $v = -a$ (a "fast" wave in the moving frame), then $\bar{W}_{tt} + V\bar{W}_{zt}$ remains positive for $V > 0$. We see that, for a *uniform* property pattern, when the work (3.91) is zero, the quantity $\bar{W}_{tt} + V\bar{W}_{zt}$ is not equal to $\bar{W}_{tt}$ which is, in this case, the same as $\langle W_{tt}\rangle$.

If the original substances are different in their material parameters, then the energy (3.92) should be calculated for $v = v_{1,2}$ given by (2.50):

$$v_{1,2} = -\frac{V\left[\bar{\epsilon}\bar{\mu} - \left(\frac{\bar{1}}{a^2}\right)\right] \mp \frac{1}{a_1 a_2}\sqrt{\bar{\epsilon}\bar{\mu}\left[V^2 - \frac{1}{\bar{\epsilon}}\left(\frac{\bar{1}}{\mu}\right)\right]\left[V^2 - \frac{1}{\bar{\mu}}\left(\frac{\bar{1}}{\epsilon}\right)\right]}}{\frac{1}{a_1^2 a_2^2}\left[V^2 - \left(\frac{\bar{1}}{\epsilon}\right)\left(\frac{\bar{1}}{\mu}\right)\right]}.$$

In particular, if we consider the irregular case $\epsilon_2 > \epsilon_1, \mu_2 < \mu_1, a_2 > a_1$, then calculations show that $\bar{W}_{tt} + V\bar{W}_{zt}$ *may become negative for both waves*

$v = v_1$ and $v = v_2$ if $a_2^2 \le V^2 \le (\overline{1/\epsilon})(\overline{1/\mu})$. The velocity V then also falls into the interval (v_1, v_2). This may occur when the d'Alembert waves become coordinated with v_1 and v_2 being both positive.

To prove this, observe that

$$\bar{\epsilon}\bar{\mu} - \left(\frac{\bar{1}}{a^2}\right) = -m_1 m_2 \Delta\epsilon \Delta\mu;$$

this quantity is positive for the irregular case. If $V > 0$ and $a_2^2 < V^2 < \left(\overline{1/\epsilon}\right)\left(\overline{1/\mu}\right)$, then $v_2 > v_1 > 0$, and

$$\begin{aligned} V - v_{1,2} &= \frac{a_1^2 a_2^2}{V^2 - \left(\frac{\bar{1}}{\epsilon}\right)\left(\frac{\bar{1}}{\mu}\right)} \left\{ \frac{1}{a_1^2 a_2^2} V \left[V^2 - \left(\frac{\bar{1}}{\epsilon}\right)\left(\frac{\bar{1}}{\mu}\right)\right] + V\left[\bar{\epsilon}\bar{\mu} - \left(\frac{\bar{1}}{a^2}\right)\right] \right. \\ &\quad \left. \mp \frac{1}{a_1 a_2} \sqrt{\bar{\epsilon}\bar{\mu}\left[V^2 - \frac{1}{\bar{\epsilon}}\left(\frac{\bar{1}}{\mu}\right)\right]\left[V^2 - \frac{1}{\bar{\mu}}\left(\frac{\bar{1}}{\epsilon}\right)\right]} \right\} \\ &= \frac{1}{V^2 - \left(\frac{\bar{1}}{\epsilon}\right)\left(\frac{\bar{1}}{\mu}\right)} \left\{ V(V^2 - \overline{a^2}) \mp a_1 a_2 \sqrt{\bar{\epsilon}\bar{\mu}\left[V^2 - \frac{1}{\bar{\epsilon}}\left(\frac{\bar{1}}{\mu}\right)\right]\left[V^2 - \frac{1}{\bar{\mu}}\left(\frac{\bar{1}}{\epsilon}\right)\right]} \right\}. \end{aligned}$$

Direct calculation shows that

$$\begin{aligned} V^2(V^2 - \overline{a^2})^2 - a_1^2 a_2^2 \bar{\epsilon}\bar{\mu}\left[V^2 - \frac{1}{\bar{\epsilon}}\left(\frac{\bar{1}}{\mu}\right)\right]\left[V^2 - \frac{1}{\bar{\mu}}\left(\frac{\bar{1}}{\epsilon}\right)\right] \\ = (V^2 - a_1^2)(V^2 - a_2^2)\left[V^2 - \left(\frac{\bar{1}}{\epsilon}\right)\left(\frac{\bar{1}}{\mu}\right)\right]; \end{aligned}$$

this quantity is negative if $a_1^2 < a_2^2 < V^2 < (\overline{1/\epsilon})(\overline{1/\mu})$. Because $V > 0$, we conclude that $v_1 - V < 0$, and $v_2 - V > 0$, as expected.

The energy density $\bar{W}_{\tau\tau}$ in a moving frame (2.20) is given by (3.92), and the energy flux density $\bar{W}_{\tau\eta}$ in the same frame calculated by (3.90) , (2.99), and (2.91) as

$$\bar{W}_{\tau\eta} = u'^2 (rv - q)(v - V)^2; \tag{3.94}$$

as above, we consider here a solution $u(z - vt)$ with $v = v_{1,2}$ being the roots of (2.51). We now find the group velocities of waves in a moving frame to be equal to

$$\frac{\bar{W}_{\tau\eta}}{\bar{W}_{\tau\tau}} = v - V,$$

with $v = v_1(v_2)$ for the first (second) wave. By (2.29), (2.50) and (3.8) we find

$$rv_{1,2} - q = \pm \frac{\epsilon_1 \epsilon_2}{\bar{\epsilon}} a_1 a_2 \frac{\sqrt{\bar{\epsilon}\bar{\mu}\left[V^2 - \frac{1}{\bar{\epsilon}}\left(\frac{\bar{1}}{\mu}\right)\right]\left[V^2 - \frac{1}{\bar{\mu}}\left(\frac{\bar{1}}{\epsilon}\right)\right]}}{V^2 - \frac{1}{\bar{\epsilon}}\left(\frac{\bar{1}}{\mu}\right)},$$

with upper (lower) sign related to the first (second) wave. If $V^2 > a_2^2$, then

$$rv_1 - q > 0, \quad rv_2 - q < 0.$$

We see that, for irregular case,

a) $\bar{W}_{\tau\tau} < 0, \bar{W}_{\tau\eta} > 0$ for the first wave ($v = v_1$),
b) $\bar{W}_{\tau\tau} < 0, \bar{W}_{\tau\eta} < 0$ for the second wave ($v = v_2$).

With respect to a moving frame, the first wave travels from right to left, at a negative group velocity $v_1 - V$; the second wave travels from left to right, at a positive group velocity $v_2 - V$. Both waves carry a negative energy. This comes into contrast with the case of uniform material moving at superluminal speed $V > a$: as mentioned above, the "slow" ("fast") wave then has a negative (positive) energy.

Physically speaking, the appearance of waves of negative energy is associated with the Cherenkov radiation [14]. Consider a "boost" co-moving frame in which the material interfaces remain at rest. An incident wave propagating through a moving heterogeneous medium, initiates dipoles concentrated on material interfaces and vibrating at the wave frequency. This vibration initiates the Cherenkov radiation in a medium moving at superluminal speed $V > a_{1,2}$ at each part of it, including interfaces, and this radiation carries the energy away from the wave. This loss of energy should be compensated by a material motion if we want the velocity V to be maintained uniform. But we do not explicitly account for this supplemental energy in our equations since we do not consider the effect produced by electromagnetic forces on the material motion. For this reason, the energy of radiation formally comes from the wave energy in a boost frame; as a consequence, this energy becomes negative.

If we add the energy stored in the flow, the overall energy density in a system "flow plus wave" will again become positive.

This argument applies to uniform material also, but in that case it affects only one out of two travelling waves. In a material laminate, both waves carry negative energy due to the presence of dipoles sitting on the interfaces and adding up to the radiation produced by polarization currents that always develop in every conventional dielectric.

3.10 Numerical examples and discussion

In this section, we focus on activated laminates made up of two materials, (ϵ_1, μ_1) and (ϵ_2, μ_2), to illustrate theoretical results given in the previous sections. We use a numerical method to simulate the heterogeneous problem described by equations (3.7). The effective behaviour of a disturbance through such a laminate is shown in contour plots later in this section. Material of this section reproduces, in most part, the results of S.L. Weekes published in [15].

Directly computing the numerical solution to wave propagation through fast range ($V^2 > a_2^2$) dynamic laminates has proven to be a challenging problem. A more standard conservative finite difference approach analogous to the one taken in [12] for the slow range ($V^2 < a_1^2$) and for static laminates yields an unstable scheme. Numerical results are degraded since accuracy is quickly lost due to the growth of short waves which enter into the computation as truncation and round-off error. In [12], an approach is taken that successfully circumvents the appearance of these instabilities in the case of temporal laminates when $V = \infty$.

For the fast range laminates, we make the following change of coordinates: $\tau = t - \frac{z}{V}$, $\zeta = z$ yielding the PDE system (c.f. (3.7))

$$\epsilon u_\tau + \frac{1}{V} v_\tau = v_\zeta,$$

$$\mu v_\tau + \frac{1}{V} u_\tau = u_\zeta.$$

In ζ, τ coordinates, the fast range dynamic material is as a temporal material where the property pattern depends on τ alone and has period δ. When a wave is incident on the pattern interfaces, $\tau = n\delta$ or $\tau = (n + m_1)\delta$ for n an integer, two new waves arise which both move into the new material. These waves are of the same wave number as the incident wave when looked upon in the new coordinate system. However, short wave modes unavoidably introduced into the computation will grow and destroy the fidelity of the results. We perform a spectral decomposition of the initial data, and at very regular intervals in the course of the numerical computation, we filter out those wave modes that lie without the rangle initially present. This spectral approach has proved successful and we illustrate some of the results below.

We consider a rank one activated laminate made up of two isotropic dielectrics. We take the material parameters to be

$$(\epsilon_1, \mu_1) = (1, 1) \quad (\epsilon_2, \mu_2) = (9, 0.1); \tag{3.95}$$

thus $a_1 = 1$, $a_2 = 1.0541$ on a scale with $c = 10a_2$. Take the mixing factor to be $m_1 = 0.5$, so

$$(1/\bar{\epsilon})(\overline{1/\mu}) = 1.1, \quad (\overline{1/\epsilon})(\overline{1/\mu}) = 3.0556,$$

$$h = 2.9757, \quad \sigma = 36.3636,$$

from (3.67) and the formula for σ given in section 3.8. For the fast range laminates, the effective permittivity and permeability, $\mathcal{E}$ and M, are real and the effective material is isotropic when either

$$a_2 = 1.0541 < V < 1.5853, \quad \text{or} \quad V > 1.9755,$$

from (3.70). In the first range, the effective values are both negative as predicted, whereas the values are positive in the second range. Figure 3.5 represent the plots of $1/M$ versus $\mathcal{E}$ as V varies within the acceptable ranges. Figure 3.7 plots the corresponding energy densities computed from (3.92) for each of the d'Alembert waves (2.50) represented by solid and dashed curves.

Figs. 3.8 and 3.9 show contour plots of u when an initial Gaussian pulse,

$$u(z,0) = e^{-z^2}, \;\; v(z,0) = 0,$$

propagates through a fast range laminate with material parameters given in (3.95), and $m_1 = 0.5$. We note that these are the results that come from the direct, detailed computation of the unhomogenized equations, not from computing solutions to the effective equations. The figures show the results for u in z, t coordinates when $V = 1.3$ and $V = 4$. The horizontal axis gives the z-values, while time is on the vertical axis.

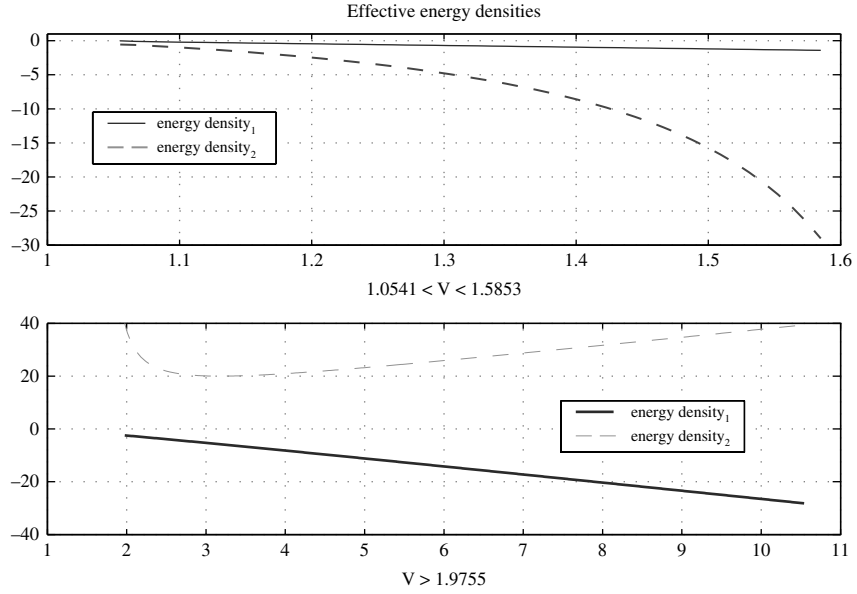

Fig. 3.7. Effective energy densities of dielectric laminate with $(\epsilon_1, \mu_1) = (1,1), (\epsilon_2, \mu_2) = (9, 0.1), m_1 = 0.5$, for variable V.

Calculations show that for $V = 1.3$, the theoretical values for v_1, v_2 are 1.09324 and 2.7147 - coordinated wave motion as seen clearly in Fig. 3.8. Looking at the numerical results in the contour plot of Fig. 3.8, we estimate that the slower moving disturbance travels at a velocity 1.0895, and the faster wave has velocity 2.7133. From Figs. 3.3–3.7, we expect that the effective material coefficients when $V = 1.3$ are negative as are the energy densities. We find that $\mathcal{E} = -4.0293$ and $M = -0.3532$. The energy densities $\bar{W}_{tt} + V\bar{W}_{zt}$

given by (3.92) are -0.69835 and -4.77846 using the theoretical values for the effective velocities; the energy densities are $-0.71917, -4.77023$ using the numerical values of v_i in (3.92).

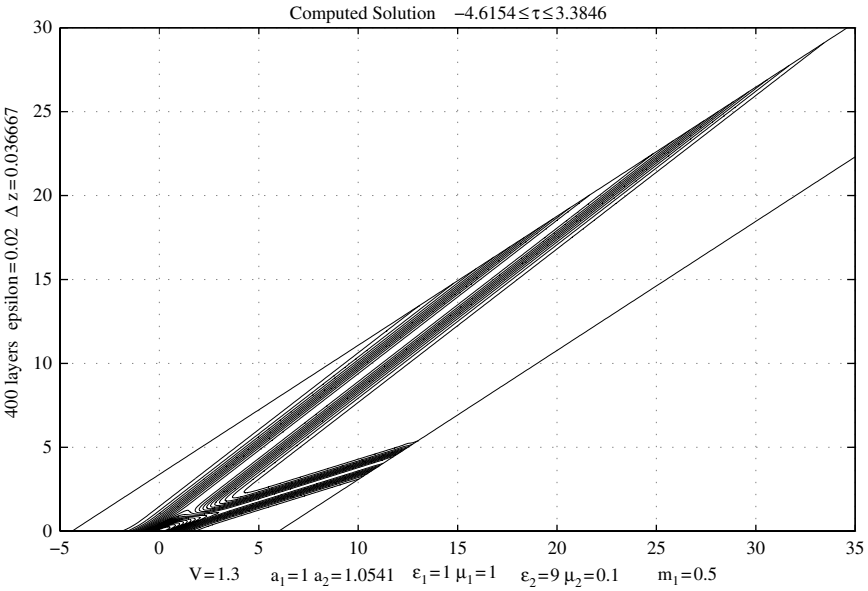

Fig. 3.8. Wave propagation through a fast range laminate where $V = 1.3$ yields a homogenized material with negative effective coefficients.

For $V = 4$, the theoretical values for v_1, v_2 are 1.4001 and -2.6362 - no coordination. Looking at the numerical results in the contour plot of Fig. 3.9, we find that the disturbances travel with velocities 1.4 and -2.6296. The effective material properties, $\mathcal{E}$ and M, are both positive as indicated in Fig. 3.5, and take the values 1.5582 and 0.1564 respectively. As given in Fig. 3.7, the energy densities are of opposite signs when $V = 4$, and from (3.92) they take the values -8.20495 and 20.94315 using the theoretical values of v_i, and -8.20633 and 20.9587, using the numerically computed values of the effective velocities.

The values of the energy densities that have been calculated incorporate contributions due both to the frame motion and to the variable property pattern. To single out contribution caused specifically by the variable property pattern, one has to subtract the value of the energy density calculated by the formula (3.93) for a pure material from the corresponding value of $\bar{W}_{tt} + V\bar{W}_{zt}$ calculated by (3.92) for the variable material pattern. In Figs. 3.10 and 3.11, we show how the energy densities of both waves that develop in an activated laminate vary as the fraction of material 1 (i.e. m_1) in the mixture increases from 0 to 1.

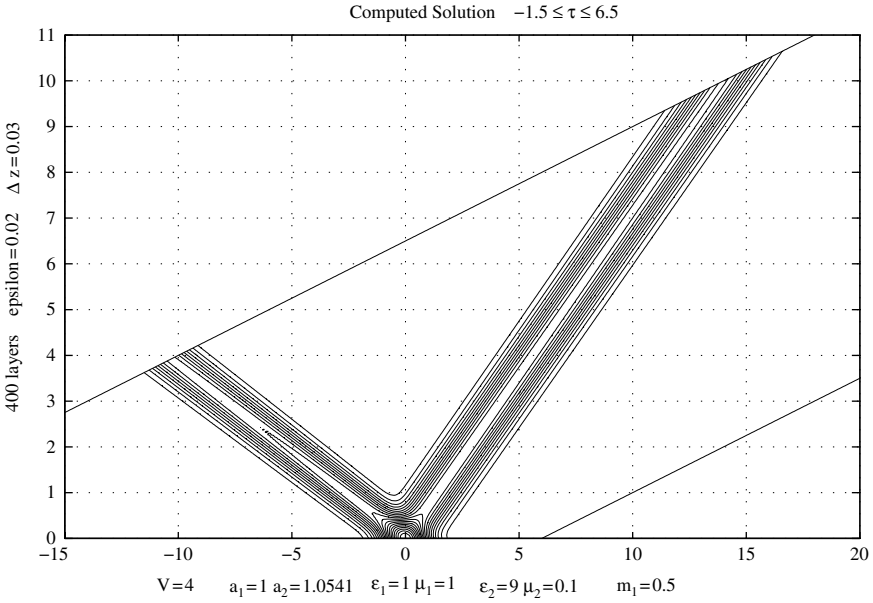

Fig. 3.9. Wave propagation through a fast range laminate where $V = 4.0$ yields a homogenized material with positive effective coefficients.

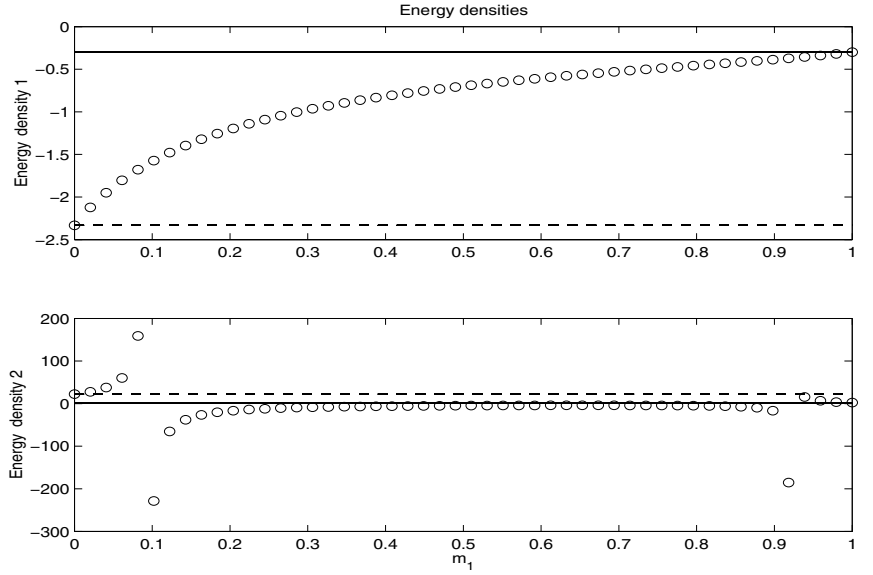

Fig. 3.10. Energy densities of composites vs. m_1, for $V = 1.3$. Solid line is energy density of pure material 1, dashed line is energy density of pure material 2.

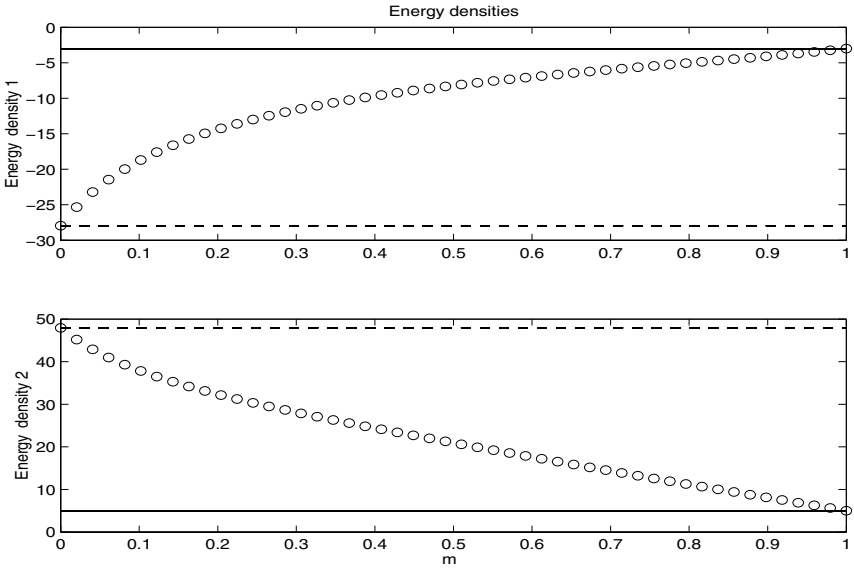

Fig. 3.11. Energy densities of composites vs. m_1, for $V = 4.0$. Solid line is energy density of pure material 1; dashed line is energy density of pure material 2.

For pure materials, as discussed in section 3.9, one wave is "fast" and the other "slow". The upper/lower plot is associated with the wave that is "slow"/"fast" for the pure materials of (3.95). For a "slow" wave, the energy density remains negative for all m_1; a "fast" wave has energy density negative in the presence of coordination in a laboratory frame, and positive in the absence of it. The energy densities of pure materials are indicated on these plots. It is clearly seen that the energy contribution due to the variable property pattern goes to zero as the property pattern becomes uniform, i.e. $\epsilon_2 \to \epsilon_1$ and $\mu_2 \to \mu_1$, or vice versa.

Dielectric substances with negative ϵ and μ represent the so-called "left-handed materials". This name has been introduced by Veselago in his paper [1] that opened a new chapter in both theoretical and experimental study of such substances. Historically, the idea of left-handed materials ascends to Lamb who discussed in [2] the mechanical device conducting the waves with phase moving in the direction opposite from that of the energy flow. This feature is one of many special characteristics of left-handed materials. Later, an interest to them was demonstrated by many authors, starting from Mandelstam [[3],[4],[5]]. This interest has recently become much more pronounced because a great many ways have been found to practically implement left-handed materials within some selected frequency bands. In our example the left-handed medium is a non-equilibrium, thermodynamically open system possessing negative energy.

A vast bibiolography on left-handed media may be found in [6].

3.11 Effective properties of activated laminates calculated via Lorentz transform. Case of spacelike interface

So far in this and the previous chapters the effective parameters of activated laminates were calculated for a subluminal slope of the interface, i.e. $V < c$; in other words, the interface was assumed to be timelike. We basically applied the Galilean transform (2.6) toward such calculation and arrived at eqs. (2.10), (2.13) for A, B, C, D, and, as a consequence, at eqs. (2.29) for p, q, r, θ.

These formulae remain the same if we apply the Lorentz transform (3.38) toward their derivation instead of its simplified Galilean version (2.6). However, desiring to calculate the *effective properties* as the invariants with respect to a Lorentz group, we applied in section 3.5 the full Lorentz transform. It was still assumed that $V < c$, i.e. the laminates' interfaces are timelike.

For all of these reasons, we use the present section to show firstly that eqs. (2.10), (2.13) never become affected if we use, instead of (2.6), the full Lorentz transform (3.38) in the procedure of section (2.2). Secondly, we consider the case of superluminal (spacelike) interface in the laminates, and arrive, for this case, at a system (2.11) with appropriately modified expressions for p, q, r.

The first of these problems is simple. By using (3.38), we introduce the frame (z', t') and reduce the original system (2.2) to the form (we preserve symbols ρ, k for material constants, and $a = \sqrt{k/\rho}$ for the phase velocity):

$$u_{z'} = \frac{V}{c^2}\frac{a^2 - c^2}{a^2 - V^2}u_{t'} + \frac{1}{c^2}\frac{c^2 - V^2}{\rho(a^2 - V^2)}\, v_{t'},$$
$$v_{z'} = \frac{1}{c^2}\frac{k(c^2 - V^2)}{a^2 - V^2}u_{t'} + \frac{V}{c^2}\frac{a^2 - c^2}{a^2 - V^2}v_{t'}. \tag{3.96}$$

By applying averaging to this system and by using the continuity of u, v across the interfaces z'=const, we arrive at the system (see (2.10), (2.13))

$$u_{z'} = Mu_{t'} - \left(1 - \frac{V^2}{c^2}\right) Cv_{t'},$$
$$v_{z'} = -\left(1 - \frac{V^2}{c^2}\right) Du_{t'} + Mv_{t'}, \tag{3.97}$$

where

$$M = -\frac{AV}{c^2} + BV. \tag{3.98}$$

In (3.97) the field variables u, v are already assumed averaged over the period $x - Vt = \delta$ of laminate. We now again apply the Lorentz transform (3.38) to return to the original frame (z, t):

$$u_{z'} = \gamma\left(u_z + \frac{V}{c^2}u_t\right), \quad u_{t'} = \gamma(u_t + Vu_z), \quad \gamma = \left(1 - \frac{V^2}{c^2}\right)^{-1/2}, \tag{3.99}$$

etc. This yields, after some calculation and with the reference to (2.10), (2.13),

$$\begin{aligned} BVv_t + Av_z &= D(u_t + Vu_z), \\ C(v_t + Vv_z) &= BVu_t + Au_z; \end{aligned} \tag{3.100}$$

by (2.12), this system is easily reduced to (2.11).

We now consider the case of superluminal (spacelike interface); the corresponding velocity V is greater than c : $V > c$. Introduce the Lorentz frame (z', t') moving at velocity $\bar{V} = c^2/V$; clearly $\bar{V} < c$. In a new frame, the system (2.2) becomes

$$u_{t'} = V\frac{a^2 - c^2}{a^2 - V^2}u_{z'} + \frac{c^2 - V^2}{\rho(a^2 - V^2)}v_{z'},$$

$$v_{t'} = \frac{k(c^2 - V^2)}{a^2 - V^2}u_{z'} + V\frac{a^2 - c^2}{a^2 - V^2}v_{z'}.$$

This system appears if we exchange symbols z' and t' in (3.96) and drop the factor $\frac{1}{c^2}$ at the rhs of each equation.

We now average this system over the period $t - \frac{1}{V}x = \delta$; as a result, we obtain

$$\begin{aligned} u_{t'} &= c^2 M u_{z'} - c^2\left(1 - \frac{V^2}{c^2}\right)Cv_{z'}, \\ v_{t'} &= -c^2\left(1 - \frac{V^2}{c^2}\right)Du_{z'} + c^2 M v_{z'}. \end{aligned} \tag{3.101}$$

If we now use (3.101) to return to the original (z, t)-frame, then, after calculation, this system takes the form (3.100). We see that the averaged system (2.11) preserves its shape for superluminal laminates, with symbols p, q, r defined, as before, by eqs. (2.29).

References

1. Veselago, V.G.: The electrodynamics of substances with simultaneously negative values of eps and mu. Soviet Phys. Usp. **10**, 509 (1968), Usp. Fiz. Nauk **92**, 517–526 (1967)
2. Lamb, H.: On group velocity. Proc. London Math. Soc. **1**, 473–479 (1904)
3. Mandelstam, L.I.: Group velocity in crystalline arrays. Zh. Eksp. Teor. Fiz. **15**, 475–478 (1945)
4. —: Complete Collected Works. Akad. Nauk SSSR, Moscow, **2** 334 (1947)
5. —: Complete Collected Works. Akad. Nauk SSSR, Moscow, **5** 419 (1950)
6. http://www.wave-scattering.com/negative.html
7. Sommerfeld, A.: Elektrodynamik. Geest & Portig, Leipzig (1964)
8. Lurie, K.A.: The problem of effective parameters of a mixture of two isotropic dielectrics distributed in space-time and the conservation law for wave impedance in one-dimensional wave propagation. Proc. R. Soc. Lond. A **454**, 1767–1779 (1998)
9. Minkowski, H.: Nachr. Ges. Wiss. Göttingen, S. 53 (1908); also: Raum und Zeit, Phys. Z., Bd. 10, S. 104 (1909).
10. Einstein, A.: Zur Elektrodynamik bewegter Körper. Ann d. Physik, **17**, 891 (1905)
11. Lurie, K.A.: Bounds for the electromagnetic material properties of a spatio-temporal dielectric polycrystal with respect to one-dimensional wave propagation. Proc. R. Soc. Lond. A **456**, 1547–1557 (2000)
12. Lurie, K.A., and Weekes, S.L.: Effective and averaged energy densities in one-dimensional wave propagation through spatio-temporal dielectric laminates with negative effective values of ϵ and μ. In "Nonlinear Analysis and Applications: to V. Lakshmikantham on his 80th Birthday", R. Agarwal and D. O'Regan, eds., Kluwer, 767–789 (2004)
13. Sturrock, P.A.: In what sense do slow wave carry negative energy? J. Appl. Phys., **31**, 2052–2056 (1960)
14. Nezlin, M.V.: Negative-energy waves and the anomalous Doppler effect. Sov. Phys. Usp., **19**, no. 11, 946–954 (1976)
15. Weekes, S.L.: A stable scheme for the numerical computation of long wave propagation in temporal laminates. J. Comput. Phys., **176**, 345–362 (2002)

4

G-closures of a Set of Isotropic Dielectrics with Respect to One-Dimensional Wave Propagation

4.1 Preliminary considerations. Terminology

In this book, we study the spatio-temporal composites, i.e. material formations assembled from conventional constituents distributed on a periodic microscale in space and time. We are particularly interested in the propagation of long waves through such formations (the term "long" in this context means "long compared with the period of a microstructure"). Depending on the microgeometry of a mixture and on the material parameters of its constituents, a composite may or may not allow for the long waves travel through it without damping or amplification. In the first case, we call a composite *stable*, otherwise we term it *unstable*.

These terms require a more precise characterization which we will now give for laminates of arbitrary rank. The waves through such media are known to be *modulated* waves, i.e. the high frequency carriers having the period of a material pattern, and the amplitude distribution taking the form of a low frequency envelope. This is clearly revealed by the Floquet analysis carried out in section 2.4 particularly for activated laminar assemblage. The "long waves" mentioned above represent the amplitude waves incorporated in modulated waves as their envelopes. Such waves are mathematically detected through homogenization. They travel at velocities that are qualified as the group velocities of modulated waves. The equations that govern their propagation demonstrate no dispersion in our case, so the relevant group velocities coincide with the phase velocities. This performance is characteristic of stable composites. In the absence of stability, there are no travelling waves whatsoever. The stable and unstable scenarios reveal themselves through the effective properties of spatio-temporal composites.

Any laminate is a material assemblage endowed with a specific geometric framework implemented on a microscale. This framework depends on parameters, such as the volume fractions and the slopes of interfaces separating, within a microstructure, one material assemblage from another. Specifically,

one may consider a laminate of higher rank depending on a number of latent parameters.

Such parameters may only take values that belong with some specific ranges (we call such values admissible). Inequalities $m_i \geq 0, \;\; i = 1, 2, \;\; m_1 + m_2 = 1$, as well as inequality (2.5) represent examples of the admissible ranges.

The property of a composite to be stable or unstable depends on the values taken by parameters of the microstructure.

If a composite is stable for all of the admissible values of its parameters, then it will be termed *uniformly stable*.[1] An example of an uniformly stable composite is given by an activated rank one dielectric laminate assembled from two immovable materials with material constants $\epsilon_i, \mu_i, \;\; i = 1, 2$, having the same sign. The effective material tensor s_0 of such a laminate has the determinant (see (2.26), (2.15), and (3.8))

$$\det s_0 = \left\langle \frac{y}{\langle y \rangle} \det s \right\rangle, \tag{4.1}$$

where $\langle \cdot \rangle = m_1 \langle \cdot \rangle_1 + m_2 (\cdot)_2, \;\; m_1, m_2 \geq 0, \;\; m_1 + m_2 = 1$, and

$$\begin{aligned} \det s &= \epsilon/\mu, \\ y &= (\Delta)^{-1}, \\ \Delta &= \epsilon(V^2 - a^2), \;\; a^2 = (\epsilon\mu)^{-1}. \end{aligned} \tag{4.2}$$

Here, $m_i, \quad i = 1, 2$ denotes the volume fraction of the ith material in a laminate, and the symbol Δ in (4.2) and below in this chapter stands for $\rho\Delta$ in eqs. (2.15).

The expression $\Delta = \epsilon V^2 - \mu^{-1}$ differs by a positive factor from the action density

$$\Lambda = \epsilon u_t^2 - \mu^{-1} u_z^2,$$

evaluated for the "wave" $u = u(z - Vt)$ travelling at velocity V. The symbol V in (4.2) denotes the speed of the interface separating materials 1 and 2 in the laminate. The admissible values of this speed are assumed to lie outside the banned interval $(\min \mid a_i \mid, \quad \max \mid a_i \mid)$ to ensure smoothness of the solution $u = u(z, t)$ of the Maxwell's system (see (2.5)). When $V^2 < \min_i a_i^2$ and $\epsilon > 0$, the expression (4.2) for Δ is negative; when $V^2 > \max_i a_i^2$ and $\epsilon > 0$, this expression becomes positive.

The sign of Δ is switched to opposite if $\epsilon < 0$. We observe that if materials 1 and 2 in a composite have all of their material constants ϵ_i, μ_i of the same sign, then $y_i/\langle y \rangle \geq 0, \; i = 1, 2$. By introducing symbols

$$\kappa_i = m_i y_i / \langle y \rangle, \tag{4.3}$$

we conclude that the values $\kappa_i \geq 0, \;\; \kappa_1 + \kappa_2 = 1$ are admissible, and equation (4.1) then shows that $\det s_0$ is a convex combination of $\det s_i, \; i = 1, 2$, i.e. it

[1] In [1], the term "absolutely stable" was introduced instead of "uniformly stable". In this text we prefer the latter term as conceptually more appropriate.

is positive when $\det s_i > 0$. As a consequence, the phase velocities of waves through a composite are real for all admissible m_i and V, and a composite is absolutely stable. If, however, material 1 has both material constants ϵ_1, μ_1 positive, and the material 2 has both of them negative ("materials of opposite signs"), and if $\langle \Delta^{-1} \rangle^{-1} \neq 0$, then the admissible values κ_1 and κ_2 appear to be of opposite signs (though, as before, $\kappa_1 + \kappa_2 = 1$). The determinant

$$\det s_0 = \kappa_1 \det s_1 + \kappa_2 \det s_2 \tag{4.4}$$

in this case takes values that lie outside the interval $(\det s_1, \det s_2)$; by a due choice of κ_1, this determinant may be made negative, and the phase velocity made complex, so a composite may become unstable. We conclude that an activated laminate assembled from immovable materials of opposite signs fails to be uniformly stable.

Other examples of composites lacking the absolute stability may be given by laminates of a higher rank.

In this chapter we are looking for a formal characterization of a set GU of *all uniformly stable composites* assembled from an arbitrary set U of originally given isotropic dielectrics. The analysis is carried out with regard to wave propagation in one spatial dimension. The set GU so defined will be termed a stable G-closure of the original set U.

As a starting point, we describe in section 4.2 the set GU of all admissible composites produced in one spatial dimension and time by a single original isotropic dielectric. Based on this description, we construct in the subsequent sections the stable G-closures for some more complex original sets U. We first build a G-closure for a binary set U: $\{(\epsilon, \mu) = (\epsilon_i, \mu_i), \quad i = 1, 2\}$, and later - for an arbitrary set U. We also give characterization for the sets $G_m U$ - the stable G-closures with specified volume fractions m_i of participating constituents. Material of this chapter is based on papers [1],[2],[3],[4].

4.2 Conservation of the wave impedance through one-dimensional wave propagation. A stable *G*-closure of a single isotropic dielectric

In the preceding sections, we have been interested in the effective properties of a special microstructure - a polycrystallic laminate in one spatial dimension and time. Particularly, with regard to such laminates, we noticed that their second invariant $\mathcal{E}/M$ preserves the value ϵ/μ related to the original (paternal) substance (see (3.50)). Equations (2.26) and (3.45), that hold for general laminates, also show, together with (2.15), that for original constituents possessing the common value of ϵ/μ, the second invariant $\mathcal{E}/M$ of a general laminate preserves the same value. Remarkably, it turns out that this result remains in effect in a far more general context, specifically, it holds true for *any admissible microstructure* in one spatial dimension and time. We here quote

as "admissible" any microstructure that allows for solution to the relevant hyperbolic problem (2.2) belonging to the Sobolev space W_2^1.

To prove this conjecture, consider two linearly independent solutions $u(1)$, $v(1)$, and $u(2), v(2)$ of the system (2.2), (3.8). These solutions are assumed continuous in time over the domain $(0,T)$; they belong to the Sobolev space $W_2^1(\mathcal{D})$ where $\mathcal{D}$ is the relevant domain in one spatial dimension. The functions $u(1),\ldots,v(2)$ represent two independent test fields generated by two linearly independent sources. The tensors F and f for one-dimensional waves propagating along the z-axis belong with the subspace (a_{23}, a_{24}) of the space a_{ik}; such tensors are given by (3.21), with a material tensor s specified by

$$s = -\frac{1}{\mu c} a_{23} a_{23} - \epsilon c a_{24} a_{24}. \tag{4.5}$$

Consider the tensor

$$O = a_{23} a_{24} - a_{24} a_{23};$$

the expression

$$F(1) \,:\, O \,:\, F(2) = 2c^2 (u_{x_3}(1) u_{x_4}(2) - u_{x_4}(1) u_{x_3}(2)) = 2c^2 \det(\nabla u(1), \nabla u(2))$$

is quasiaffine in $W_2^1(\mathcal{D}) \cup C(0,T)$. This means that the weak limit of the sequence

$$2c^2 \det(\nabla u^{(r)}(1),\ \nabla u^{(r)}(2))$$

generated by the partitioning (r) of $\mathcal{D} \times (0,T)$ into admissible subdomains occupied by material 1 and 2, is equal to the same expression

$$2c^2 \det(\nabla u^{(0)}(1), \nabla u^{(0)}(2))$$

calculated for the weak limits $u^{(0)}(i)$ of solutions $u^{(r)}(i)$. We formally get

$$\lim wk 2c^2 \det(\nabla u^{(r)}(1), \nabla u^{(r)}(2)) = 2c^2 \det(\nabla u^{(0)}(1), \nabla u^{(0)}(2)), \tag{4.6}$$

$$\lim wk u^{(r)}(i) = u^{(0)}(i), \quad i = 1, 2\ .$$

A similar behavior is demonstrated by the expression

$$\begin{aligned} f(2) \,:\, O \,:\, f(1) &= 2c^2 (v_{x_3}(1) v_{x_4}(2) - v_{x_4}(1) v_{x_3}(2)) \\ &= 2c^2 \det(\nabla v(1), \nabla v(2)). \end{aligned}$$

This is also quasiaffine, i.e.

$$\lim wk 2c^2 \det(\nabla v^{(r)}(1), \nabla v^{(r)}(2)) = 2c^2 \det(\nabla v^{(0)}(1), \nabla v^{(0)}(2)), \tag{4.7}$$

where

$$\lim wk v^{(r)}(i) = v^{(0)}(i), \quad i = 1, 2\ .$$

The reason for the quasiaffinity of said expressions is because they represent divergent combinations; for instance,

$$u_{x_3}(1)u_{x_4}(2) - u_{x_4}(1)u_{x_3}(2) = \frac{\partial}{\partial x_3}(u(1)u_{x_4}(2)) - \frac{\partial}{\partial x_4}(u(1)u_{x_3}(2)),$$

and the vector

$$u(1)[u_{x_4}(2)\mathbf{e}_3 - u_{x_3}(2)\mathbf{e}_4]$$

has a continuous normal component across the interface separating two different materials.

Because $f = s \,:\, F$, we refer to (3.21), (4.5), and rewrite (4.7) as

$$\lim wk \det s^{(r)} \det(\nabla u^{(r)}(1), \nabla u^{(r)}(2)) = \det s_0 \det(\nabla u^{(0)}(1), \nabla u^{(0)}(2)),$$

where s_0 is an effective material tensor of a composite. By (4.5), this relation is the same as

$$\det s_0 = \frac{\lim wk \det s^{(r)} \det(\nabla u^{(r)}(1), \nabla u^{(r)}(2))}{\lim wk \det(\nabla u^{(r)}(1), \nabla u^{(r)}(2))}. \tag{4.8}$$

Assume now that

$$\det s^{(r)} = \epsilon/\mu = \text{const}(r); \tag{4.9}$$

equation (4.8) then shows that

$$\det s_0 = \epsilon/\mu.$$

The validity of this result is based on a single assumption (4.9); in all other respects, the tensors $s^{(r)}$ may be different. In particular, they may have different pairs of values ϵ and μ taken separately, as well as orientation of their principal axes in space-time. If we consider continuous solutions and if the original materials satisfy (4.9), then the second invariant ϵ/μ remains preserved through the mixing in one spatial dimension and time, with any admissible microgeometry, and with any type of composite involved.

Combining this with the bounds produced in section 3.7 for spatio-temporal polycrystals in one spatial dimension, we may now specify the G-closure of all possible composites generated in one spatial dimension and time by an arbitrary set of isotropic dielectrics having positive values of ϵ and μ and the same value of ϵ/μ. Such a set is characterized as an arc of the hyperbola

$$\mathcal{E}/M = \epsilon/\mu, \tag{4.10}$$

lying in the first quadrant $\mathcal{E}c > 0, 1/Mc > 0$ under the diagonal $\mathcal{E}c = 1/Mc$. The point on the diagonal is exceptional; also, if all of the original constituents have their parameters ϵ and μ negative, then the relevant G-closure is given by (4.10), with $\mathcal{E}c < 0, \quad 1/Mc < 0$; the hyperbolic arc then belongs to the third quadrant and goes above the diagonal.

4.3 A stable G-closure of a set U of two isotropic dielectrics with respect to one-dimensional wave propagation

The original set U will be first assumed consisting of two different materials with positive material properties $\epsilon_i, \mu_i, \ \ i = 1, 2$. As shown in section 3.7, every such material generates a set of spatio-temporal polycrystals; their effective constants $\mathcal{E}, M$ fill the hyperbola $\mathcal{E}/M = \epsilon_1/\mu_1, \ \ \mathcal{E} > 0, \ M > 0$ for the first material, and $\mathcal{E}/M = \epsilon_2/\mu_2, \ \mathcal{E} > 0, M > 0$ for the second. Fig. 4.1 reproduces these hyperbolas in the first quadrant of $(\mathcal{E}c, \ 1/Mc)$-plane, with the assumption $\epsilon_1/\mu_1 > \epsilon_2/\mu_2$. All points on each hyperbola are attainable except the point $\mathcal{E}c = 1/Mc$ on the diagonal; the relevant polycrystals are absolutely stable, and therefore, each hyperbola represents a stable G-closure of a set of differently oriented fragments of the same original material.

We wish to characterize the set GU of all absolutely stable composites made from two originally available materials *possessing different values of* ϵ/μ. The materials on the hyperbolas mentioned above obviously belong with the required set.

To characterize this set in full, suppose first that the properties $\epsilon_1, \ldots, \mu_2$ satisfy inequalities $\epsilon_1 > \epsilon_2 > 0, \ \ \mu_1 > \mu_2 > 0, \ \ \epsilon_1/\mu_1 > \epsilon_2/\mu_2$ (a regular case, by the terminology of section 2.5; see also (3.8)).

Materials 1 and 2 are marked as points P_1 and P_2 in Fig. 4.1. A static laminate ($V = 0$) produced from them is absolutely stable; its effective parameters $\mathcal{E} = \langle\epsilon\rangle, \ \ M = \langle\mu\rangle$ occupy the hyperbolic segment P_1P_2 not shown in Fig. 4.1. Each point on this segment generates its own hyperbola $\mathcal{E}/M =$ const, $\mathcal{E}, M \geq 0$; we thus create absolutely stable composites occupying the portion of a hyperbolic strip

$$\epsilon_1/\mu_1 \geq \mathcal{E}/M \geq \epsilon_2/\mu_2 \tag{4.11}$$

below diagonal in the first quadrant of the $(\mathcal{E}c, 1/Mc)$-plane. The eigenvalues $\mathcal{E}c, 1/Mc$ of all such composites remain real and positive.

Assume now that parameters ϵ, μ of the original materials are so chosen that $\epsilon_1 > \epsilon_2 > 0, \ \ \mu_2 > \mu_1 > 0$, but $\epsilon_1\mu_1 \geq \epsilon_2\mu_2$ (an irregular case, see section 2.5); the new materials are marked as points Q_1 and Q_2 in Fig. 4.1. We may treat them as spatio-temporal polycrystals generated by the same original materials 1 and 2; these polycrystals will now be used as original substances that participate in a spatio-temporal activated laminate. Then, as shown in section 3.8, by a due choice of V and m_1 in such a laminate, we shall obtain *the real negative* values for both $\mathcal{E}$ and M, those values also belonging to the strip (4.11) but this time to that part of it that lies above diagonal in the third quadrant. By taking $\epsilon_1\mu_1 = \epsilon_2\mu_2$, we may completely cover this part of the strip; the relevant composites again appear to be absolutely stable.

We claim that the *entire* strip (4.11), with both parts of it reproduced in Fig. 4.1, actually *represents* a stable G-closure of a set of two isotropic

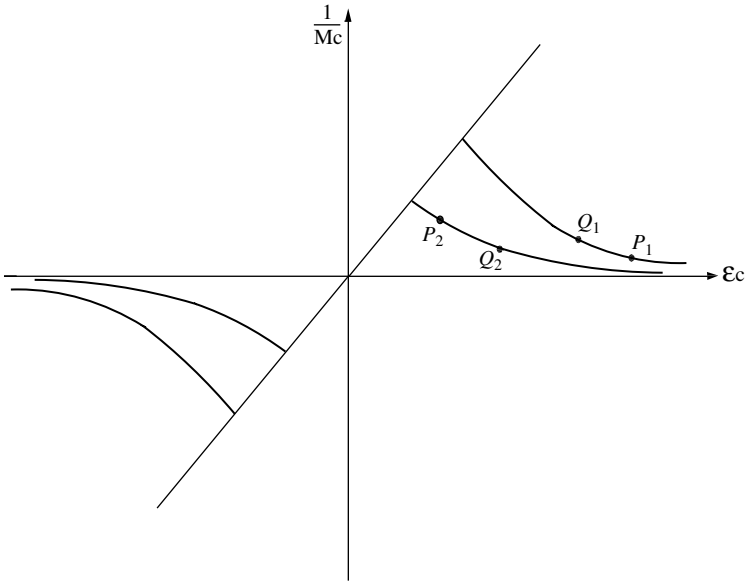

Fig. 4.1. A stable G-closure of a set of two isotropic dielectrics of the same sign.

dielectrics of the same sign: (ϵ_1, μ_1) and (ϵ_2, μ_2), $\epsilon_1/\mu_1 > \epsilon_2/\mu_2$. In other words, no point in the $(\mathcal{E}c, 1/Mc)$-plane that does not fall into (4.11) can ever be attained by uniformly stable spatio-temporal composites generated by those materials. The proof is based on a general formula (4.8) for $\mathcal{E}/M$ discussed in the next section.

4.4 The second invariant $\mathcal{E}/M$ as an affine function; a stable G-closure of an arbitrary set U of isotropic dielectrics

Equation (4.8) defines $\mathcal{E}/M = \det s_0$ as a linear combination of $\det s^{(r)}$. If $\det s^{(r)}$ takes the same value ϵ/μ for all materials involved, then $\det s_0 = \epsilon/\mu$, i.e. we obtain the conservation law mentioned in section 4.2. In a more general context, equation (4.8) means that (c.f. (4.2))

$$\det s_0 = \frac{\langle y \det s \rangle}{\langle y \rangle} = \left\langle \frac{y}{\langle y \rangle} \det s \right\rangle . \tag{4.12}$$

Here we introduced the symbol y for $\det(\nabla u(a), \nabla u(b))$; this symbol is the same as the one introduced by (4.2); we shall see below that this new definition of y reduces to that one in (4.2) for a laminate considered in section 4.1. Because $\langle y/\langle y \rangle \rangle = 1$, we conclude that $\det s$ is an *affine* function with regard

to the mixing procedure in space-time. If all of the factors $y/\langle y\rangle$ are non-negative, then the affinity becomes convexity, and we get

$$\max_U \det s \geq \det s_0 \geq \min_U \det s. \tag{4.13}$$

The symbol $y = \det(\nabla u(a), \nabla u(b))$ is invariant with respect to a Lorentz transform. If this invariant has the same sign for all material constituents participating in a composite, then this composite is uniformly stable. Consider two original materials that both belong to a strip (4.11), possibly, to its branches located in different quadrants of the $(\mathcal{E}c, 1/Mc)$-plane. Each of those materials is uniformly stable; we ask if a rank one laminate assembled from these materials preserves this property. As shown in section 4.1, this question may receive either positive or negative answer, depending on the circumstances. We now give an additional illustration of this alternative, this time in a close connection with a general formula (4.8).

We assume that materials 1 and 2 are characterized each by its individual pair $\epsilon_i, \mu_i,\ i = 1, 2$, of dielectric and magnetic constants, and that materials are moving with individual velocities $v_i,\quad i = 1, 2$, relative to a laboratory frame. The electromagnetic wave propagation through each material is governed by equations (2.11) where p, q, r are defined by the formulae

$$p = Qc,\ \ q = -T,\ \ r = \frac{1 - \frac{\mu}{\epsilon}T^2}{\frac{\mu}{\epsilon}\,Qc}, \tag{4.14}$$

with Q, T given by (3.48). In Q, as well as in T, we have to set $\epsilon = \epsilon_i, \mu = \mu_i, v = v_i(\phi = \phi_i)$, and, accordingly, $p = p_i,\ q = q_i,\ r = r_i$ for material i.

Equations (4.14) follow from (2.16), (3.47) if we set $V = 0$ and take $m_i = 1$ for material i. Consider a rank one laminate assembled from materials 1 and 2, and let its interface move with velocity V relative to a laboratory frame. Both solutions $u(a)$ and $u(b)$ are subjected to the compatibility conditions

$$[u_t + Vu_z]_2^1 = 0,\ \ [pu_z - qu_t + V(qu_z + ru_t)]_2^1 = 0,$$

expressing the continuity of u and v across the interface. By using these conditions, we obtain after a simple calculation that

$$L_1[u_{1z}(a)u_{1t}(b) - u_{1t}(a)u_{1z}(b)] = L_2[u_{2z}(a)u_{2t}(b) - u_{2t}(a)u_{2z}(b)],$$

or

$$L_1 y_1 = L_2 y_2. \tag{4.15}$$

Here,

$$L_i = r_i V^2 - 2q_i V - p_i,\ \ i = 1, 2,$$

differs by a positive factor from the action density $\Lambda_i = (1/2)(r_i u_t^2 + 2q_i u_t u_z - p_i u_z^2)$ in a material i evaluated for the "wave" $u = u(z - Vt)$.

Remark 4.1. According to (4.12), only the ratio $y/\langle y\rangle$ is significant; we therefore may define y_i as L_i^{-1} to satisfy (4.15); the symbol y then takes on the form (4.2) for a laminate assembled of immovable materials.

Equation (4.15) shows that the symbol y preserves its sign across the interface if the action density Λ_i does the same.

The phase velocities $a_i^{(1)}, a_i^{(2)}$ of waves $u = u(z - a_i t)$ propagating in material i are found to be the roots of

$$a_i^2 - 2\frac{q_i}{r_i}\, a_i - \frac{p_i}{r_i} = 0,$$

and for L_i we obtain

$$L_i = r_i(V - a_i^{(1)})(V - a_i^{(2)}), \quad i = 1, 2.$$

We shall have precisely two characteristics departing from the interface in any of the four modes presented in Figs. 4.2-4.5.

In all of those cases, the expression $L_i/r_i = (V - a_i^{(1)})(V - a_i^{(2)})$ has the same signs for $i = 1$ and $i = 2$. We conclude that if the signs of r_1 and r_2 are the same, then the signs of y_1 and y_2 are identical too, and the composite is uniformly stable; otherwise there is no uniform stability.

Given (4.14) and the formulae (3.48) for Q, T, it is easy to show that the sign of r_i is identical with that of

$$\epsilon_i(1 - \tanh^2\phi_i \tanh^2\chi_i),$$

where $\tanh\phi_i = v_i/c \leq 1$, and $\tanh\chi_i = 1/c\sqrt{\epsilon_i\mu_i} \leq 1$. We conclude that $\mathrm{sgn} r_i = \mathrm{sgn}\epsilon_i$, and the laminate is uniformly stable only if it is assembled from materials of the same sign. This conclusion does not differ from the one obtained in section 4.1 for immovable original substances.

A uniformly stable composite made from materials 1 and 2 cannot be represented in a $(\mathcal{E}c, 1/Mc)-$ plane by a point lying outside the strip (4.13). The structure of equation (4.12) makes this point clear. Failure to fall within (4.13) means that the symbols y do not preserve their sign within a microstructure, and the affine function $\det s_0$ is therefore not convex. In the case of a binary composite, equation (4.12) is equivalent to (4.3); as explained in section 4.1, this means the absence of uniform stability because the symbols κ_i (see (4.3)) then appear to be of opposite signs. We conclude that all composites that are uniformly stable should correspond to points within the strip (4.13); on the other hand, this strip may be represented at each point by a uniformly stable composite. This confirms the claim made at the end of section 4.3.

Corollary 4.2. *It follows from the above argument that inequalities (4.13) define a stable G-closure GU of an arbitrary set U of original materials: this one is formed as a union of hyperbolic strips generated by the elements of U with the extremal values of* $\det s = \epsilon/\mu$.

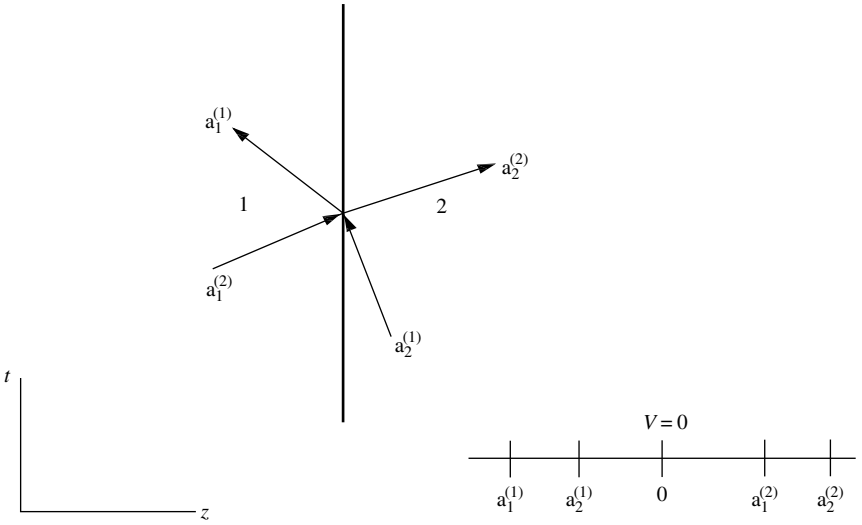

Fig. 4.2. Case $a_1^{(1)} < a_2^{(1)} < V < a_1^{(2)} < a_2^{(2)}$.

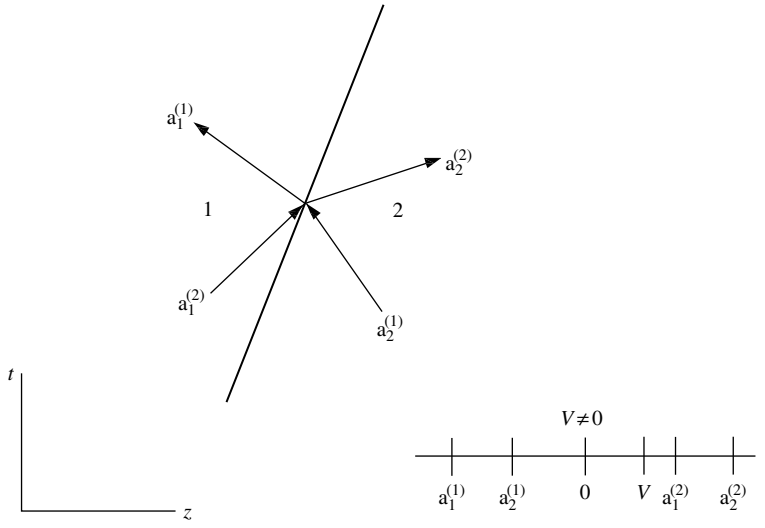

Fig. 4.3. Case $a_1^{(1)} < a_2^{(1)} < V < a_1^{(2)} < a_2^{(2)}$.

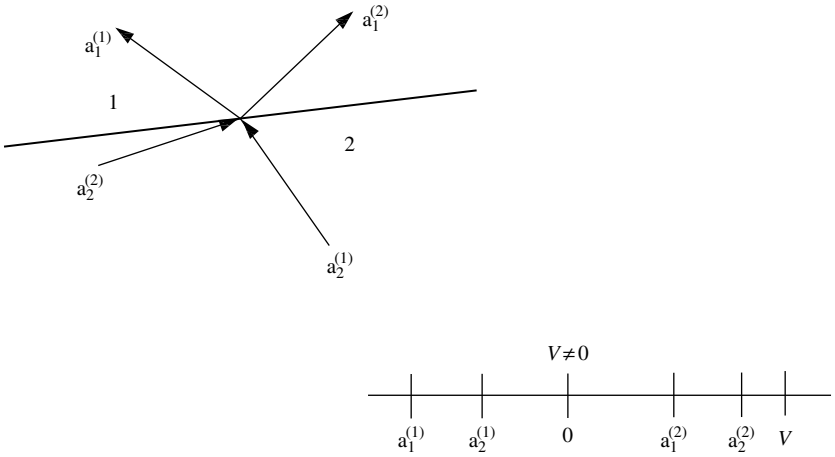

Fig. 4.4. Case $a_1^{(1)} < a_2^{(1)} < V < a_1^{(2)} < a_2^{(2)} < V$.

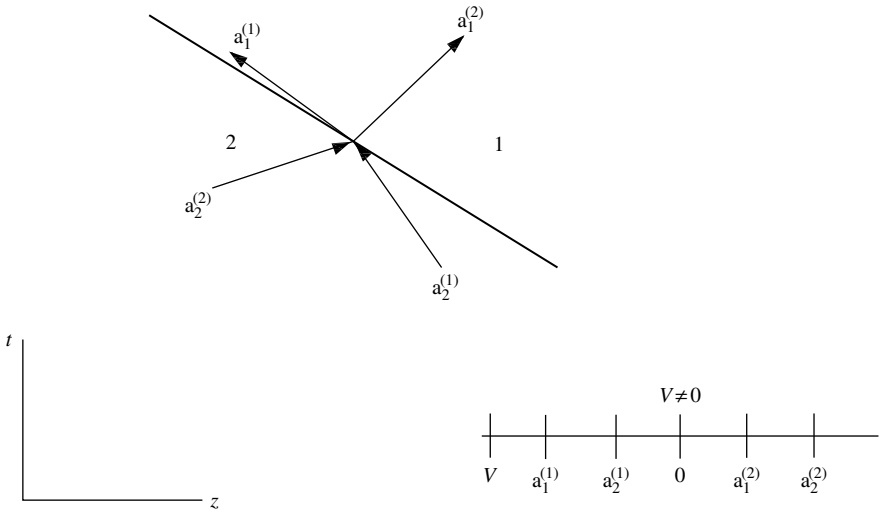

Fig. 4.5. Case $V < a_1^{(1)} < a_2^{(1)} < a_1^{(2)} < a_2^{(2)}$.

4.5 A stable G_m-closure of a set U of two isotropic dielectrics

As in section 4.1, assume that the set U includes only two admissible materials: s_1, and s_2, and suppose that these materials remain immovable in an activated uniformly stable laminate. Equation (4.4) includes parameters κ_i defined by (4.3). Because of a uniform stability, $\kappa_i \geq 0, \kappa_1 + \kappa_2 = 1$, so these parameters may be interpreted as "weighted volume fractions". While the genuine volume fractions, m_i, remain fixed, the weighted fractions κ_i may still be variable due to the dependency of y upon parameters of the microstructure. By (4.2)),

$$y_i = \frac{1}{\epsilon_i(V^2 - a_i^2)}.$$

Assume that $a_2^2 \geq a_1^2$; then inequality (2.5) allows for two admissible ranges for V^2: $0 \leq V^2 < a_1^2$ (slow range), and $a_2^2 \leq V^2 < c^2$ (fast range). For a slow range, the fraction $\kappa_1(V^2)$ increases from $\kappa_1(0) = \frac{m_1\mu_1}{\langle\mu\rangle}$ to $\kappa_1(a_1^2 - 0) = 1$, whereas for a fast range it increases from $\kappa_1(a_2^2 + 0) = 0$ to $\kappa_1(c^2) = \frac{m_1\epsilon_2(c^2 - a_2^2)}{\bar{\epsilon}c^2 - \left(\frac{\bar{1}}{\mu}\right)}$; here we used a usual notation $(\bar{\cdot}) = m_1(\cdot)_2 + m_2(\cdot)_1$.

Because $\epsilon_i\mu_i c^2 \geq 1, \;\; i = 1, 2$, we have

$$\kappa_1(c^2) - \kappa_1(0) = \frac{m_1 m_2 c^2}{\left[\bar{\epsilon}c^2 - \left(\frac{\bar{1}}{\mu}\right)\right]\langle\mu\rangle}(\epsilon_2\mu_2 - \epsilon_1\mu_1) \leq 0,$$

and there is a gap in the values of $\kappa_1(V^2)$ generated by the values of $V^2 \leq c^2$ consistent with (2.5) (Fig. 4.6). This gap shrinks to zero when $a_1 = a_2$. The latter can be achieved by manufacturing polycrystals produced by either one of the original materials. We conclude that, for any fixed $m_1 \in (0, 1)$, the values of κ_1 may cover the entire interval $(0, 1)$ due to a proper choice of V, i.e. due to a proper motion of the material pattern. In other words, a stable G_m-closure of a set of two isotropic dielectrics coincides with a stable G-closure of the same set.

4.6 Comparison with an elliptic case

The results obtained in this chapter about the stable hyperbolic G (G_m)-closures allow for an interesting comparison with analogous conclusions that work in a similar elliptic situation [2],[3],[4],[5]. We begin this comparison with polycrystals in $2D$, with both dimensions being spatial in an elliptic case, and one spatial, one temporal in a hyperbolic case.

Consider a stationary problem of temperature distribution in a planar domain. The domain is occupied by an ordinary polycrystal assembled on a fine scale by mixing differently oriented fragments of an anisotropic heat

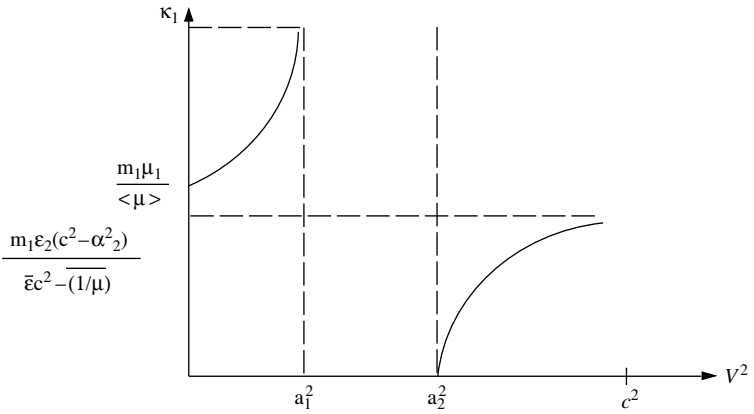

Fig. 4.6. A gap in the values $\kappa_1(c^2)$ and $\kappa_1(0)$.

conductor (paternal material), with principal heat conductances d_1, d_2. The effective conductances λ_1, λ_2 of such a polycrystal are known to satisfy the conservation relation $\lambda_1\lambda_2 = d_1d_2$.

This result, originally obtained in [2], demonstrates a remarkable formal analogy with eq. (4.10) that holds for a spatio-temporal polycrystal in one spatial dimension and time. There is, however, a fundamental difference between the two statements, this difference related to the attainability issue. In the elliptic case, only that part of the hyperbola $\lambda_1\lambda_2 = d_1d_2$ is attainable that spreads from (d_1, d_2) toward the diagonal [3]; the rest of the hyperbola cannot be attained. This is understandable because a spatial mixture of differently oriented fragments of a paternal material *cannot become more anisotropic* than this material itself. Because of this *irreversibility* property, only the paternal material may serve as initial substance capable of producing all mixtures that occupy the attainable portion of the hyperbola. This property establishes an hierarchy of materials on the attainable portion; only those substances that are placed on the hyperbola further away from the diagonal, may generate substances staying closer to it, *not vice versa*.

In a hyperbolic case, the situation is different. As explained in section 3.7, the spatio-temporal laminar polycrystal may correspond to points that lay either closer to the diagonal, or further away from it, than the original anisotropic (in space-time) substance. Unlike statics, the process of mixing in space-time appears to be *reversible*; this process does not introduce any hierarchy of materials. This contrast in the material performance of polycrystals entails a sharp difference between the elliptic and the stable hyperbolic

$G(G_m)$-closures. In the elliptic case, the G-closure of a set U formed in $2D$ by two anisotropic materials $(d_1^{(1)}, d_2^{(1)})$ and $(d_1^{(2)}, d_2^{(2)})$ is illustrated in Fig. 4.7. It is described as *a part* of the strip $d_1^{(1)} d_2^{(1)} \le \lambda_1 \lambda_2 \le d_1^{(2)} d_2^{(2)}$ bounded in the transverse direction by the segment $Q_1 Q_2$ of the diagonal at one end and by *a special curve* $N_1 N_2$ at another end, this curve representing a rank one laminate assembled from original materials [3]. As to an elliptic G_m-closure, this one is also different from its hyperbolic counterpart. Such a closure was explicitly found in [4] for the set U consisting of two isotropic dielectrics. It represents only a portion of a G-closure, but, certainly $GU = \cup G_m U$. In the hyperbolic case, as shown above in this chapter, the G-closure and G_m-closure are identical; both are described as a *whole* strip (4.11) in the first and the third quadrants. The only transverse bound for the strip is now given by two segments of the diagonal.

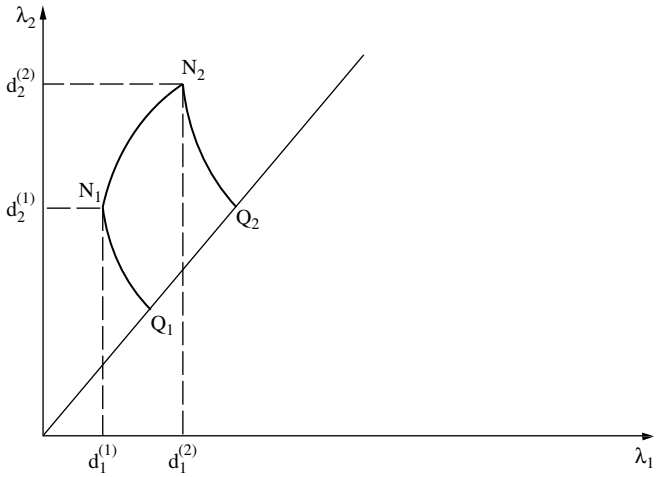

Fig. 4.7. G-closure of a binary set of two anisotropic heat conductors in a plane.

The mentioned difference in G-closures is fundamental; it is intrinsic in the very nature of the elliptic and hyperbolic cases. The key reason is that the first is governed by the variational principle of *minimal stored energy*, while the second emerges from the principle of *stationary action*. In the latter principle, the energy is not as fundamental as in the former one: in dynamics, energy is not invariant with regard to the Galilean (Lorentz) group; it represents just a component of the energy-momentum tensor. The energy is pumped

into a dynamic material through its implementation, which is not the case for the static (spatial) material assemblages. This feature makes the energy an important characteristic of material formation in space-time.

In both elliptic and hyperbolic design, we work with material tensors. These tensors are chacterized by their sets of eigenvalues and eigentensors. Eigenvalues represent invariant material properties that are responsible for the reaction of a substance to the external fields. In both statics and dynamics, they directly affect the amount of energy stored in a system. Eigentensors are a different story. They appear as we work in a proper frame of reference; transition to this frame is different in elliptic and hyperbolic situations as far as the energy issue is concerned. In the elliptic context, this transition (Euclidean rotation) is free. In the hyperbolic context, this transition (Minkowskian rotation) means a material motion, and therefore costs energy. The hyperbolic $G(G_m)$-closures introduced above in this chapter, include Minkowskian rotations and, consequently, require the energy supply from the external sources. This supply was never taken into account above as a restriction, i.e. the bounds obtained in this chapter for $G(G_m)$-closures remain valid if the energy supply is unlimited. This setting is, however, not very practical. Realistically, we have to introduce restriction upon the energy *measured in a laboratory frame* and needed to create and maintain dynamic materials with optimal performance in a given environment. This restriction is essential because in its absence an optimization problem may easily allow for a trivial solution with infinite energy expenditure. We may therefore put forward the problem of finding *G-closures of limited energy* in a laboratory frame for the sets U of available materials originally immovable in this frame. The restriction upon energy will create additonal bounds for the effective properties of dynamic materials. Finding such bounds still remains an open problem.

References

1. Lurie, K.A.: A stable spatio-temporal G-closure and G_m-closure of a set of istoropic dielectrics with respect to one-dimensional wave propagation. Wave Motion, **40**, 95-110 (2004)
2. Dykhne, A.M.: Conductivity of a two-dimensional two-phase systems. Sov. Phys. JETP, **32**, 63-65 (1971)
3. Lurie, K.A., and Cherkaev, A.V.: G-closure of a set of anisotropically conducting media in the two-deimensional case. J. Optim. Theory and Applications, **42**, 1984, 283-304; Corrig. **53**, 319 (1987)
4. Lurie, K.A., and Cherkaev, A.V.: Exact estimates of conductivity of composites formed by two isotropically conducting media taken in prescribed proportion. Proc. R. Soc. Edinburgh A **99**, no. 1-2, 71-87 (1984)
5. Lurie, K.A., Fedorov, A.V., and Cherkaev, A.V.: On the existence of solutions to some problems of optimal design for bars and plates. Ioffe Institute Tech. Rep. 668, Leningrad, 43 pp (1980); also J. Optim. Theory and Applications, **42**, 247-282 (1984)

5

Rectangular Microstructures in Space-Time

5.1 Introductory remarks

In the preceding chapters, the concept of spatio-temporal composites (dynamic materials) has been developed specifically for laminar microstructures. For such formations, the existence of a low frequency limit was demonstrated in Chapter 2 through the use of the Floquet theory. This attempt has proven to be successful because laminates are substantially one-dimensional assemblages, and the effective parameters for them can therefore be specified relatively easily through a direct calculation.

In the present chapter, we discuss more general rectangular microstructures in one spatial dimension and time. For such microstructures, the Floquet theory is generally not applicable. We begin our analysis with the case of separation of variables, for which the Floquet procedure works, and then proceed to a "checkerboard" assemblage, with the Floquet approach no longer possible. In this latter case, however, some important conclusions follow when the wave impedances of all material constituents participating in the assemblage are assumed to be the same. The kinematics of disturbances is especially simple in this case; it reveals the possibility to judge about the transformation of energy and impulse at each encounter with the interfaces separating, in a microstructure, one material from another. Particularly, we see that, in certain cases, energy is systematically added to the disturbance travelling through such encounters; as a consequence, the energy demonstrates an exponential growth. The relevant checkerboard assemblages may therefore appear to be non-transparent because in order for disturbances to pass through them, one has to waste an infinite amount of energy. Material of this chapter reproduces the content of the paper [1].

5.2 Statement of a problem

Consider a doubly-periodic material distribution in the (z,t)-plane given by the pattern in Fig. 5.1. The rectangle $-\ell_1 < z < \ell_2, -t_1 < t < t_2$ represents the basic cell of periodicity with periods $\delta = \ell_1 + \ell_2$ in z and $\tau = t_1 + t_2$ in t. Rectangle i for $i = 1,2,3,4$ is occupied by a uniform material i having density $\rho_{(i)}$ and stiffness $k_{(i)}$. In an electromagnetic context, $\rho_{(i)}$ and $k_{(i)}$ would represent dielectric permittivity and the reciprocal of magnetic permeability. All materials are assumed immovable in a laboratory frame z,t.

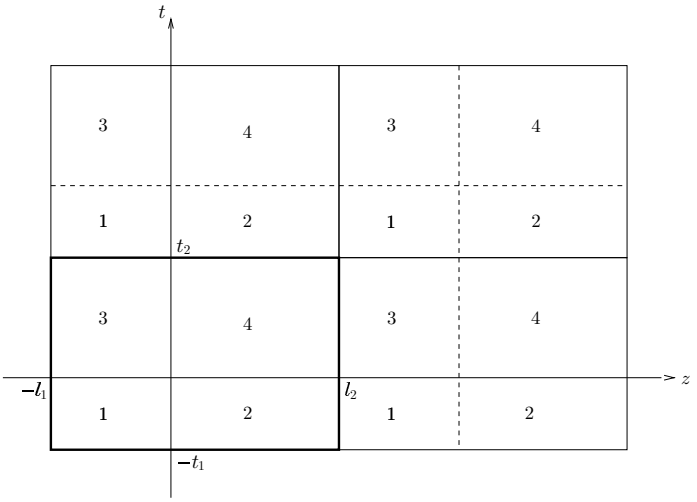

Fig. 5.1. Rectangular microstructure in z-t.

In this assemblage, we consider wave motion governed in each material by the linear second order equation (see (2.1))

$$(\rho u_t)_t - (k u_z)_z = 0, \tag{5.1}$$

or, equivalently, by the system (see (2.2))

$$v_t = k u_z, \quad v_z = \rho u_t, \tag{5.2}$$

with ρ, k taking values $\rho_{(i)}, k_{(i)}$ within material i. The waves pass from one material to another. maintaining the continuity of u and v across the interfaces separating the rectangles. The purpose of this chapter is to study propagation of dynamic disturbances through such an assemblage. Both spatial and temporal periods, δ and τ, will be assumed of the same order of magnitude, i.e. $\delta/\tau = O(a)$, where $a = \sqrt{k/\rho}$ denotes the phase speed within any material constituent.

For each material, we have an elementary solution of (5.2),

$$u = \left(Ae^{-\lambda\frac{z}{a}} + Be^{\lambda\frac{z}{a}}\right)\left(Ce^{-\lambda t} + De^{\lambda t}\right),$$
$$v = \gamma\left(Ae^{-\lambda\frac{z}{a}} - Be^{\lambda\frac{z}{a}}\right)\left(Ce^{-\lambda t} - De^{\lambda t}\right), \tag{5.3}$$

where $\gamma = \sqrt{k\rho}$ denotes the wave impedance of the substance, and λ is a separation parameter.

Consider a layer $-t_1 < t < 0$ occupied by a δ-periodic sequence of materials $1, 2$ in z separated by vertical interfaces $z = -\ell_1,\ \ z = 0,\ \ z = \ell_2$, etc. as seen in Fig. 5.1. Assume that the values λ, C, and D are constant along the layer; A and B satisfy the compatibility conditions

$$\begin{aligned}
A_{(1)} + B_{(1)} &= A_{(2)} + B_{(2)} \\
\gamma_{(1)}(A_{(1)} - B_{(1)}) &= \gamma_{(2)}(A_{(2)} - B_{(2)}), \\
e^{\mu\delta}\left(A_{(1)}e^{\lambda\frac{\ell_1}{a_{(1)}}} + B_{(1)}e^{-\lambda\frac{\ell_1}{a_{(1)}}}\right) &= A_{(2)}e^{-\lambda\frac{\ell_2}{a_{(2)}}} + B_{(2)}e^{\lambda\frac{\ell_2}{a_{(2)}}}, \\
\gamma_{(1)}e^{\mu\delta}\left(A_{(1)}e^{\lambda\frac{\ell_1}{a_{(1)}}} - B_{(1)}e^{-\lambda\frac{\ell_1}{a_{(1)}}}\right) &= \gamma_{(2)}\left(A_{(2)}e^{-\lambda\frac{\ell_2}{a_{(2)}}} - B_{(2)}e^{\lambda\frac{\ell_2}{a_{(2)}}}\right)
\end{aligned} \tag{5.4}$$

where the subscripts "(1)" and "(2)" relate to the relevant materials. The first pair of equations comes from the continuity conditions on $z = 0$. The second pair comes from continuity on $z = \ell_2$ where the Floquet relations

$$u(z) = e^{\mu\delta}u(z - \delta), \qquad v(z) = e^{\mu\delta}v(z - \delta), \tag{5.5}$$

are used to express solutions at $z = \ell_2$ in terms of solutions at $z = -\ell_1$.

As shown in Appendix 1, the system (5.4) is satisfied if the Floquet exponent μ takes either one of two values $\mu_{1,2}$ such that

$$\mu_{1,2}\,\delta = \pm\chi(\theta_1, \theta_2), \tag{5.6}$$

with χ, θ_1, θ_2 defined by

$$\begin{aligned}
\cosh\chi &= \cosh\theta_1\cosh\theta_2 + \sigma\sinh\theta_1\sinh\theta_2, \\
\sigma &= \frac{\gamma_{(1)}^2 + \gamma_{(2)}^2}{2\gamma_{(1)}\gamma_{(2)}}, \qquad \theta_i = -\lambda\,\delta\,m_i/a_{(i)},
\end{aligned}$$

and

$$m_1 = \ell_1/\delta, \qquad m_2 = \ell_2/\delta.$$

In the low frequency limit, $|\ \lambda\delta/a_{(1)}\ | \ll 1$, we get (see (2.69))

$$\mu_{1,2} = \pm\lambda\sqrt{\left\langle\frac{1}{k}\right\rangle_m \langle\rho\rangle_m}, \tag{5.7}$$

where

$$\langle\xi\rangle_m = m_1\xi_{(1)} + m_2\xi_{(2)} \tag{5.8}$$

denotes the arithmetic mean of ξ.

The Floquet solution is given by the formulae (see section 2.4)

$$\begin{aligned} u &= [M_1 e^{\mu_1 z} P(\mu_1, z) + M_2 e^{\mu_2 z} P(\mu_2, z)](Ce^{-\lambda t} + De^{\lambda t}), \\ v &= [M_1 e^{\mu_1 z} Q(\mu_1, z) + M_2 e^{\mu_2 z} Q(\mu_2, z)](Ce^{-\lambda t} - De^{\lambda t}), \end{aligned} \tag{5.9}$$

with $P(\mu, z), Q(\mu, z)$ specified as

$$P(\mu, z) = \begin{cases} e^{-\left(\mu + \frac{\lambda}{a_{(1)}}\right)(z - j\delta)} + Ie^{-\left(\mu - \frac{\lambda}{a_{(1)}}\right)(z - j\delta)}, & (j - m_1)\delta < z < j\delta, \\ & j = 1, 2, \ldots \\ Ke^{-\left(\mu + \frac{\lambda}{a_{(2)}}\right)(z - j\delta)} + Le^{-(\mu - \frac{\lambda}{a_{(2)}})(z - j\delta)}, & j\delta < z < (j + m_2)\delta, \\ & j = 0, 1, 2, \ldots, \end{cases} \tag{5.10}$$

$$Q(\mu, z) = \begin{cases} \gamma_{(1)} \left[-e^{-(\mu + \frac{\lambda}{a_{(1)}})(z - j\delta)} + Ie^{-(\mu - \frac{\lambda}{a_{(1)}})(z - j\delta)} \right], & (j - m_1)\delta < z < j\delta, \\ & j = 1, 2, \ldots \\ \gamma_{(2)} \left[-Ke^{-(\mu + \frac{\lambda}{a_{(2)}})(z - j\delta)} + Le^{-(\mu - \frac{\lambda}{a_{(2)}})(z - j\delta)} \right], & j\delta < z < (j + m_2)\delta, \\ & j = 0, 1, 2, \ldots. \end{cases} \tag{5.11}$$

Here μ takes the values μ_1, μ_2, and I, K, L are solutions of the system

$$\begin{aligned} -I + K + L &= 1, \\ I + (K - L)(\gamma_{(2)}/\gamma_{(1)}) &= 1, \\ -Ie^{\theta_1} + Ke^{\theta_2 \mp \chi} + Le^{-\theta_2 \mp \chi} &= e^{-\theta_1}, \end{aligned} \tag{5.12}$$

with the upper (lower) sign of $\mp$ related to $\mu_1(\mu_2)$. Both $P(\mu, z), Q(\mu, z)$ are δ-periodic in z. System (5.9) specifies the modulated waves with $e^{\mu z}$ being the modulation factor and $P(\mu, z), Q(\mu, z)$ representing the short wave carriers. Eqs. (5.10)-(5.12) reproduce those of (2.43)-(2.49) in section 2.4.

Consider the layer $0 < t < t_2$. We observe that equations (5.3)–(5.12) remain valid for it as well with obvious modifications. The symbols $A, \ldots, D, I, K, L, P, Q, \theta_1, \theta_2, \chi, \mu_1, \mu_2, \lambda$ should be replaced by the relevant symbols $\bar{A}, \ldots, \bar{D}, \bar{I}, \bar{K}, \bar{L}, \bar{P}_1, \bar{Q}_1, \bar{\theta}_1, \bar{\theta}_2, \bar{\mu}_1, \bar{\mu}_2, \bar{\chi}, \bar{\lambda}$, and material constants k, ρ, a, γ take values $k_{(3)}, \ldots, \gamma_{(3)}$ and $k_{(4)}, \ldots, \gamma_{(4)}$, in materials 3 and 4.

For the layer $t_2 < t < t_2 + t_1$, we apply equations (5.3)–(5.12) with $A, \ldots, \lambda$ replaced by $\bar{\bar{A}}, \ldots, \bar{\bar{\lambda}}$, and $k, \ldots, \gamma$ taking values $k_{(1)}, \ldots, \gamma_{(1)}$ and $k_{(2)}, \ldots, \gamma_{(2)}$ in materials 1 and 2.

On the interface $t = 0$, we have compatibility conditions expressing the continuity of u and v:

$$
\begin{aligned}
&[M_1 e^{\mu_1 z} P(\mu_1, z) + M_2 e^{\mu_2 z} P(\mu_2, z)](C + D) \\
&\qquad = [\bar{M}_1 e^{\bar{\mu}_1 z} \bar{P}(\bar{\mu}_1, z) + \bar{M}_2 e^{\bar{\mu}_2 z} \bar{P}(\bar{\mu}_2, z)](\bar{C} + \bar{D}) \\
&[M_1 e^{\mu_1 z} Q(\mu_1, z) + M_2 e^{\mu_2 z} Q(\mu_2, z)](C - D) \\
&\qquad = [\bar{M}_1 e^{\bar{\mu}_1 z} \bar{Q}(\bar{\mu}_1, z) + \bar{M}_2 e^{\bar{\mu}_2 z} \bar{Q}(\bar{\mu}_2, z)](\bar{C} - \bar{D}). \quad (5.13)
\end{aligned}
$$

A similar system holds on the interface $t = t_2$.

Clearly, equations (5.13) are satisfied only if the coefficients of $C + D$ and $\bar{C} + \bar{D}$, as well as of $C - D$ and $\bar{C} - \bar{D}$, are constant multiples of each other. It will be shown in the next section that this happens if the material layout represented in Fig. 5.1 is such that the system (5.2) allows for separation of variables.

5.3 Case of separation of variables

The variables z, t are separated in (5.2) if $\rho(z,t)$ and $k(z,t)$ appear to be products of functions that depend on the single variable z and the single variable t alone:

$$\rho = \rho^Z(z)\rho^T(t), \qquad k = k^Z(z)k^T(t). \tag{5.14}$$

We look for $u(z,t)$, the solution of (5.1), in the form of a product $u^Z(z)u^T(t)$. Then u^Z and u^T will be solutions of

$$(k^Z u^Z_z)_z - \lambda^2 \rho^Z u^Z = 0, \qquad (\rho^T u^T_t)_t - \lambda^2 k^T u^T = 0, \tag{5.15}$$

with a separation constant λ.

Assume now that each of the two pairs of functions ρ^Z, k^Z and ρ^T, k^T takes different values in the relevant base intervals of periodicity $-\ell_1 < z < \ell_2$, $-t_1 < t < t_2$:

$$\rho^Z, k^Z = \begin{cases} \rho_1^Z, k_1^Z, & -\ell_1 < z < 0, \\ \rho_2^Z, k_2^Z, & 0 < z < \ell_2, \end{cases} \tag{5.16}$$

$$\rho^T, k^T = \begin{cases} \rho_1^T, k_1^T, & -t_1 < t < 0, \\ \rho_2^T, k_2^T, & 0 < t < t_2. \end{cases} \tag{5.17}$$

In other words, we have the following characterization of materials $1, \ldots, 4$ (see Fig. 5.1).

$$
\begin{aligned}
&\text{Material 1:} \quad \rho_{(1)} = \rho_1^Z \rho_1^T, \quad k_{(1)} = k_1^Z k_1^T, \\
&\text{Material 2:} \quad \rho_{(2)} = \rho_2^Z \rho_1^T, \quad k_{(2)} = k_2^Z k_1^T, \\
&\text{Material 3:} \quad \rho_{(3)} = \rho_1^Z \rho_2^T, \quad k_{(3)} = k_1^Z k_2^T, \\
&\text{Material 4:} \quad \rho_{(4)} = \rho_2^Z \rho_2^T, \quad k_{(4)} = k_2^Z k_2^T. \quad (5.18)
\end{aligned}
$$

Note that ρ_j^Z, ρ_j^T and k_j^Z, k_j^T for $j = 1, 2$ have dimensions of the square roots of ρ and k, respectively.

Equations (5.2) allow for the following elementary solutions:

$$u = \left(Ae^{-\lambda\frac{z}{a^Z}} + Be^{\lambda\frac{z}{a^Z}}\right)\left(Ce^{-\lambda a^T t} + De^{\lambda a^T t}\right),$$
$$v = \gamma^Z\left(Ae^{-\lambda\frac{z}{a^Z}} - Be^{\lambda\frac{z}{a^Z}}\right)\gamma^T\left(Ce^{-\lambda a^T t} - De^{\lambda a^T t}\right), \tag{5.19}$$

with symbols

$$a^Z = \sqrt{k^Z/\rho^Z}, \quad a^T = \sqrt{k^T/\rho^T}, \quad \gamma^Z = \sqrt{k^Z\rho^Z}, \quad \gamma^T = \sqrt{k^T\rho^T},$$

specified by (5.16) and (5.17). Note the relation between the symbols in this section and the phase velocities and wave impedances in section 5.2:

$$a_{(i)} = a^Z_{(i)}a^T_{(i)}, \qquad \gamma = \gamma^Z_{(i)}\gamma^T_{(i)}.$$

The values of $(a^Z_{(i)})^2, (a^T_{(i)})^2, (\gamma^Z_{(i)})^2$ and $(\gamma^T_{(i)})^2$ related to various materials are summarized in Table 5.1.

Material	$(a^Z)^2$	$(a^T)^2$	$(\gamma^Z)^2$	$(\gamma^T)^2$
1	k_1^Z/ρ_1^Z	k_1^T/ρ_1^T	$k_1^Z\rho_1^Z$	$k_1^T\rho_1^T$
2	k_2^Z/ρ_2^Z	k_1^T/ρ_1^T	$k_2^Z\rho_2^Z$	$k_1^T\rho_1^T$
3	k_1^Z/ρ_1^Z	k_2^T/ρ_2^T	$k_1^Z\rho_1^Z$	$k_2^T\rho_2^T$
4	k_2^Z/ρ_2^Z	k_2^T/ρ_2^T	k_2^Z/ρ_2^Z	$k_2^T\rho_2^T$

Table 5.1. Values of a^Z, a^T, γ^Z, and γ^T related to materials $1, 2, 3, 4$ in a rectangular microstructure.

Consider the layer $-t_1 < t < 0$ occupied by a δ-periodic sequence of materials 1 and 2. Referring to Table 5.1, we observe that a^T and γ^T are *the same* for both materials. The Floquet solutions for this layer are therefore specified by equations (5.6)–(5.9), with obvious modifications generated by equations (5.15). In particular, the long wave Floquet exponent μ in (5.7) becomes

$$\mu_{1,2} = \pm\mu = \pm\lambda\sqrt{\left(\frac{m_1}{k_1^Z} + \frac{m_2}{k_2^Z}\right)\left(m_1\rho_1^Z + m_2\rho_2^Z\right)} = \pm\lambda\sqrt{\left\langle\frac{1}{k^Z}\right\rangle_m\langle\rho^Z\rangle_m}. \tag{5.20}$$

These values do not depend on k_1^T and ρ_1^T. The functions $P(\mu, z), Q(\mu, z)$ in (5.9) have the structure given by equations (5.10), (5.11) with $\gamma_{(1)}, \cdots, a_{(2)}$ replaced by $\gamma^Z_{(1)}, \cdots, a^Z_{(2)}$, respectively. The solution (5.9) then becomes

$$u = [M_1e^{\mu_1 z}P(\mu_1, z) + M_2e^{\mu_2 z}P(\mu_2, z)]\left(Ce^{-\lambda a^T_{(1)}t} + De^{\lambda a^T_{(1)}t}\right),$$
$$v = [M_1e^{\mu_1 z}Q(\mu_1, z) + M_2e^{\mu_2 z}Q(\mu_2, z)]\left(Ce^{-\lambda a^T_{(1)}t} - De^{\lambda a^T_{(1)}t}\right). \tag{5.21}$$

The factors in the square brackets represent the Floquet solutions related to the first equation (5.15) and generated by a δ-periodic sequence of materials distributed along the z-axis and possessing properties (ρ_1^Z, k_1^Z) and (ρ_2^Z, k_2^Z). Equations (5.21) are related to the layer $-t_1 < t < 0$; their structure is similar to that of (5.19). When we pass to the next layer $0 < t < t_2$, the solution preserves this structure, the z-dependent factors in the square brackets remain *the same*, as seen from Table 5.1, whereas $a_{(1)}^T$ gives way to $a_{(2)}^T$, and $\gamma_{(1)}^T$ is replaced by $\gamma_{(2)}^T$. We now apply the Floquet procedure to a τ-periodic sequence of layers perpendicular to the t-axis, and arrive at the final solution

$$u = [M_1 e^{\mu_1 z} P(\mu_1, z) + M_2 e^{\mu_2 z} P(\mu_2, z)] \\ \left[N_1 e^{\nu_1 t} R(\nu_1, t) + N_2 e^{\nu_2 t} R(\nu_2, t)\right], \quad (5.22)$$

$$v = [M_1 e^{\mu_1 z} Q(\mu_1, z) + M_2 e^{\mu_2 z} Q(\mu_2, z)] \\ \left[N_1 e^{\nu_1 t} S(\nu_1, t) + N_2 e^{\nu_2 t} S(\nu_2, t)\right], \quad (5.23)$$

with low frequency Floquet exponents

$$\nu_{1,2} = \pm\nu = \pm\lambda \sqrt{(n_1 k_1^T + n_2 k_2^T)\left(\frac{n_1}{\rho_1^T} + \frac{n_2}{\rho_2^T}\right)} = \pm\lambda \sqrt{\langle k^T \rangle_n \left\langle \frac{1}{\rho^T} \right\rangle_n} \quad (5.24)$$

where

$$n_1 = t_1/\tau, \qquad n_2 = t_2/\tau.$$

The τ-periodic functions $R(\nu, t), S(\nu, t)$ are specified by the expressions for P and Q in (5.10) and (5.11) with t used instead of z, ν instead of μ, $a_{(1)}$ replaced by $(a_{(1)}^Z)^{-1}$, $a_{(2)}$ by $(a_{(2)}^T)^{-1}$, $\gamma_{(1)}$ replaced by $\gamma_{(1)}^T$ and $\gamma_{(2)}$ by $\gamma_{(2)}^T$; also, n_i should replace m_i, and τ replace δ.

By (5.20) and (5.24), we conclude that a general solution (5.22), (5.23) is a combination of modulated waves with envelopes

$$e^{\mu z \pm \nu t}$$

propagating, in the case of low frequency, with group velocities

$$\pm\nu/\mu = \pm \sqrt{\langle k^T \rangle_n \left\langle \frac{1}{k^Z} \right\rangle_m^{-1} \langle \rho^Z \rangle_m^{-1} \left\langle \frac{1}{\rho^T} \right\rangle_n} \quad (5.25)$$

The factors μ and ν represent the Floquet exponents generated by the periodic dependency of the property pattern. The "double Floquet" behavior is a consequence of the separation of variables in our problem.

In the next section, we examine another case of wave propagation through a rectangular material structure in space-time. Specifically, we choose a checkerboard assemblage made up of two materials having the same wave impedance. For this particular class of structures, we will be able to make some conclusions about the effective velocities of wave propagation.

5.4 Checkerboard assemblage of materials with equal wave impedance

We consider here a special case of the rectangular spatio-temporal material structure as represented in Fig. 5.1. Suppose material 3 is the same as material 2, and material 4 is the same as material 1; we call such a layout a 'checkerboard'. In addition, we will later assume that the two materials 1 and 2 have the same value of the wave impedance γ. It is easy to see that the variables in (5.2) cannot be separated in this case.

Within a pure material, the general solution of (5.2) can be easily constructed from the values of the two Riemann invariants $R = u - v/\gamma$ and $L = u + v/\gamma$ which are respectively governed by the scalar advection equations

$$R_t + a\, R_z = 0, \tag{5.26}$$

and

$$L_t - a\, L_z = 0, \tag{5.27}$$

with $a = \sqrt{k/\rho}$ being the phase speed of the material. We look at an elementary solution for which $L = 0$, and $R = 2u$; by (5.26), we get

$$u = Ae^{\lambda(t-z/a_{(1)})}, \qquad v = -\gamma_{(1)} Ae^{\lambda(t-z/a_{(1)})}, \tag{5.28}$$

representing, for imaginary λ, a wave which travels through material 1 in a positive z-direction. When such a wave reaches an interface $z = 0$ separating material 1 from material 2, it splits into a reflected wave

$$u = \frac{\gamma_{(1)} - \gamma_{(2)}}{\gamma_{(1)} + \gamma_{(2)}}\, Ae^{\lambda(t+z/a_{(1)})}, \qquad v = \gamma_{(1)} \frac{\gamma_{(1)} - \gamma_{(2)}}{\gamma_{(1)} + \gamma_{(2)}}\, Ae^{\lambda(t+z/a_{(1)})}, \tag{5.29}$$

which heads to the left, back into material 1, and a transmitted wave

$$\bar{u} = \frac{2\gamma_{(1)}}{\gamma_{(1)} + \gamma_{(2)}}\, Ae^{\lambda(t-z/a_{(2)})}, \qquad \bar{v} = -\frac{2\gamma_{(1)}\gamma_{(2)}}{\gamma_{(1)} + \gamma_{(2)}}\, Ae^{\lambda(t-z/a_{(2)})}, \tag{5.30}$$

which continues through the interface material 2. When a wave (5.28) reaches a 'horizontal' interface $t = 0$ separating material 1 from material 2, two waves are generated which both move into material 2. The general solution is

$$\bar{\bar{u}} = \frac{A}{2}\left[\frac{\gamma_{(2)} - \gamma_{(1)}}{\gamma_{(2)}}\, e^{-\bar{\lambda}(t+z/a_{(2)})} + \frac{\gamma_{(2)} + \gamma_{(1)}}{\gamma_{(2)}}\, e^{\bar{\lambda}(t-z/a_{(2)})}\right] \tag{5.31}$$

$$\bar{\bar{v}} = \frac{A}{2}\left[\big(\gamma_{(2)} - \gamma_{(1)}\big)\, e^{-\bar{\lambda}(t+z/a_{(2)})} - \big(\gamma_{(2)} + \gamma_{(1)}\big)\, e^{\bar{\lambda}(t-z/a_{(2)})}\right], \tag{5.32}$$

where $\bar{\lambda} = \lambda a_{(2)}/a_{(1)}$.

For our special checkerboard structure, we assume that materials 1 and 2 have the same wave impedance, $\gamma_{(1)} = \gamma_{(2)} = \gamma$. In this case, there is no

reflected wave (5.29), and there is only one transmitted wave in (5.31), (5.32). The incident wave (5.28) passes through interfaces undiminished in amplitude but with a change in frequency or wave number. In this and the next sections, we shall only consider waves propagating in the positive z-direction. Waves propagating in the negative z-direction are independent and follow a similar analysis.

The goal is to study and understand how disturbances propagate through this checkerboard microstructure. To do this, we simulate numerically wave motion through several material arrangements, and then make some conjectures based on our experimental observations. The units of space and time in the examples below are chosen so that the periods of the assemblage along the z and t axes are both unity, that is, $\delta = \tau = 1$. When $m_1 = 0$ or $m_1 = 1$, we have a temporal laminate; if $n_1 = 0$ or 1, then this is a static laminate. Since wave impedance $\gamma_{(i)} = \sqrt{k_{(i)}\rho_{(i)}}$ is assumed to be the same throughout the entire structure, we distinguish between the two constituent materials via their phase speeds $a_{(i)} = \sqrt{k_{(i)}/\rho_{(i)}}$. Without loss of generality, we take $\gamma_{(1)} = \gamma_{(2)} = 1$.

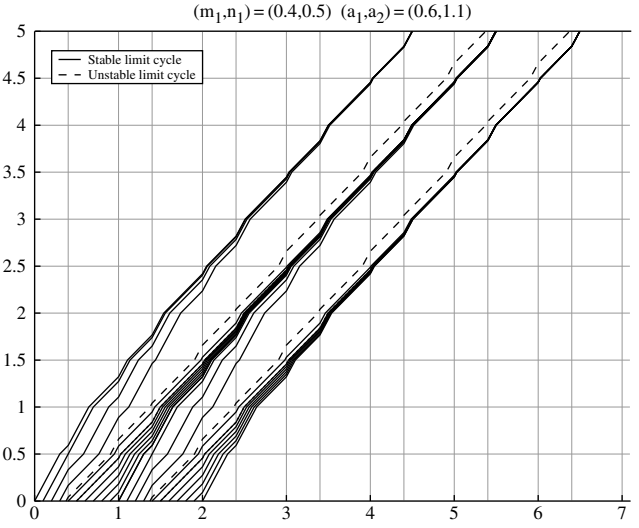

Fig. 5.2. Limit cycles in the checkerboard structure with $a_{(1)} = 0.6, a_{(2)} = 1.1, m_1 = 0.4, n_1 = 0.5$.

In the first experiment, we consider the structure with parameters $m_1 = 0.4, n_1 = 0.5, a_{(1)} = 0.6$, and $a_{(2)} = 1.1$. Fig. 5.2 represents the paths of right-going disturbances which originate on the interval $[0, 2]$ at time 0. Time is measured along the vertical axis of this figure. The vertical and horizontal lines define the checkerboard arrangement. It is clear to see that within each period, the group of paths in Fig. 5.2 separates into two distinct

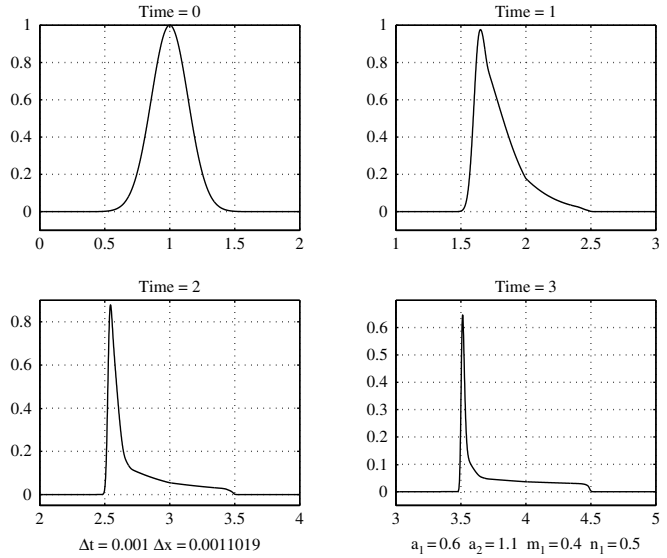

Fig. 5.3. Evolution of a disturbance through a structure with $m_1 = 0.4, n_1 = 0.5, a_{(1)} = 0.6$, and $a_{(2)} = 1.1$.

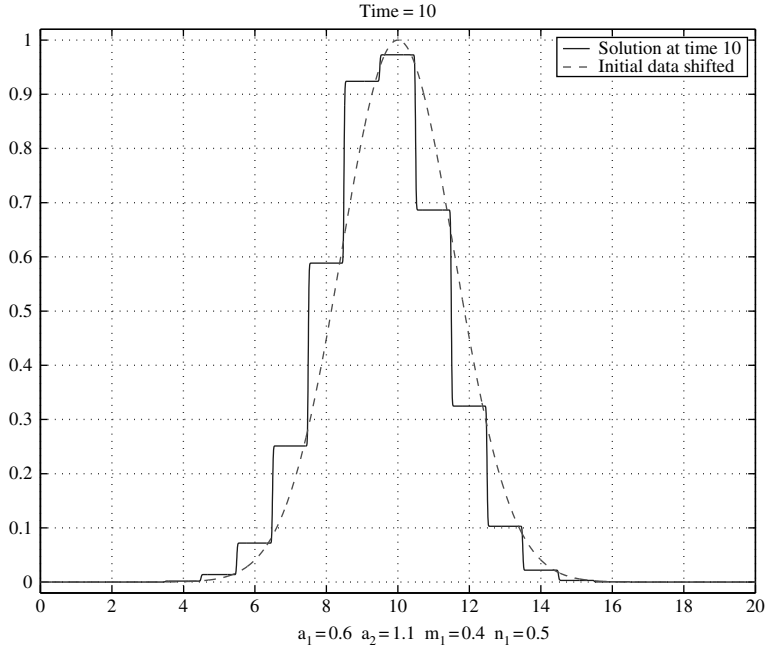

Fig. 5.4. Solution at time 10 of a disturbance with wide support through a structure with $m_1 = 0.4, n_1 = 0.5, a_{(1)} = 0.6, a_{(2)} = 1.1$, and initial data shifted right 10 units.

arrays that each converges to its own limiting path ("limit cycle") after a few time periods. The limit paths are called cycles because the trajectory pattern cycles or repeats. Such cycles are parallel to each other and have a common average slope equal to 1. Each cycle is stable; it attracts trajectories which originate on the initial manifold at the left and the right of the point of origination of the cycle itself. In the example given, the cycles originate around $z = 0.5$ and $z = 1.5$ at time 0, and are indicated by the paths in bold. There is one limit cycle per spatial period. Successive stable limit cycles are separated by an unstable limit cycle. After close numerical inspection, we find that unstable cycles originate, at time 0, at points $n + 0.375$ for integers n, and at $n + 0.495$ for stable limit cycles.

This convergence phenomenon manifests itself through concentration of the initial disturbance, and is illustrated in the solution profile sequence of Figure 5.3. The vertical axis is u, and z is on the horizontal axis. The profiles are computed from system (5.2) via a finite volume scheme which is a blend of the techniques used in [2] and [3]. The initial disturbance is a Gaussian; we may regard it as having support on $[0.5, 1.5]$. We show evolution profiles up to time 3; the speed of the disturbance is seen to be 1. As the disturbance travels through the checkerboard material, the information that was initially spread over the region $[0.5, 1.35]$ has, roughly speaking, by time 3, concentrated within the narrower region $[3.5, 3.65]$. The data is compressed as expected by the trajectory behaviour illustrated in Fig. 5.2. The information that was initially associated with z values in $[1.35, 1.37]$ has, by time 3, been spread over the interval $[3.65, 4.4]$ giving an almost constant state, while the rest of the solution changes more rapidly over $[4.4, 4.5]$.

In Fig. 5.4, we plot the solution at time 10 of a Gaussian disturbance with support about 10 times wider than that in Fig. 5.3, which has gone through the same checkerboard structure as above. The solution is piecewise constant taking values of the initial data at $z = n + 0.37$ for $n = -5, \cdots, 5$. To see this, we also plot the initial data shifted to the right 10 units. The constant states occupy a space interval of length $\delta = 1$ since there is only one stable limit cycle per period.

Next, we consider the structure with the same values of a_i, m_i as before but with $n_1 = 0.8$. Unlike the first structure, the paths in Figs. 5.5 and 5.6 do not demonstrate stable convergence to isolated asymptotic routes. Instead, the trajectories engage in a regular pattern of drift towards and then away from would-be limit cycles. This trend is periodic and the wavelength of this pattern is about 10 times the period of the structure itself. From the trajectories, we compute that the average speed of the disturbances is roughly 0.9.

If we reduce n_1 to 0.1, we see very little remnants of the existence of limit cycles. The wave trajectories more or less occupy the entire strip. See Fig. 5.7. The average asymptotic speed of these paths is roughly 0.77.

The four parameters $a_{(1)}, a_{(2)}, m_1, n_1$ determine the checkerboard material, and hence determine the manner in which disturbances travel through such structures. In the three examples presented above, $a_{(1)}, a_{(2)}$ and m_1 were

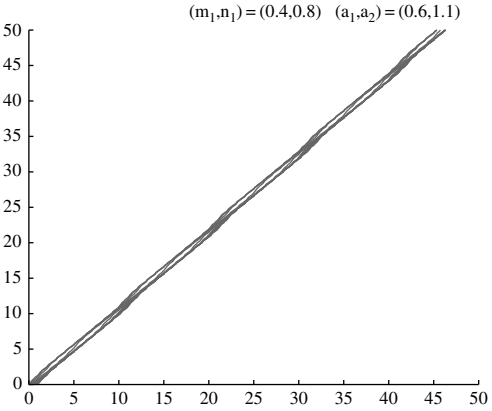

Fig. 5.5. Low frequency pattern in trajectories through structure with $m_1 = 0.4, n_1 = 0.8, a_{(1)} = 0.6$, and $a_{(2)} = 1.1$.

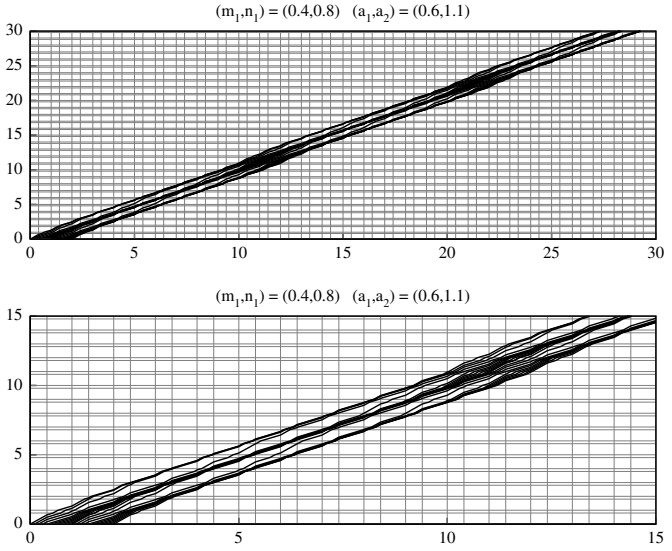

Fig. 5.6. Closer view of wave trajectories through structure with $m_1 = 0.4, n_1 = 0.8, a_{(1)} = 0.6$, and $a_{(2)} = 1.1$.

fixed, and by varying the value of n_1 only, we are able to see different trajectory behaviour and different average speeds. In Fig. 5.8, we plot graphs of average speed versus n_1 for a sequence of m_1 values. Define the speed in the structures as $f(m_1, n_1)$. Notice that $f(m, n) = f(1 - m, 1 - n)$. This is so because, in space-time, each period of the structure with volume fractions (m, n) is made up of an $m \times n$ and an $(1-m)\times(1-n)$ rectangles of material 1, and the rest is filled with material 2. Thus, the checkerboard structure with volume fractions (m, n) is the same as that with volume fractions $(1 - m, 1 - n)$.

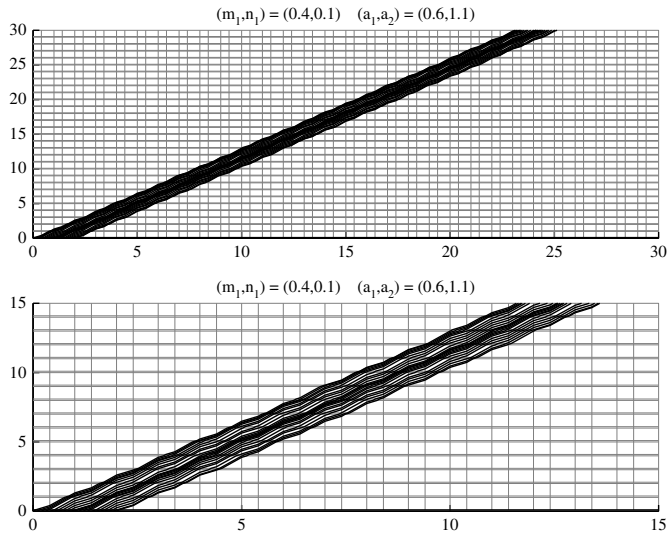

Fig. 5.7. Structure with $m_1 = 0.4, n_1 = 0.1, a_{(1)} = 0.6$, and $a_{(2)} = 1.1$.

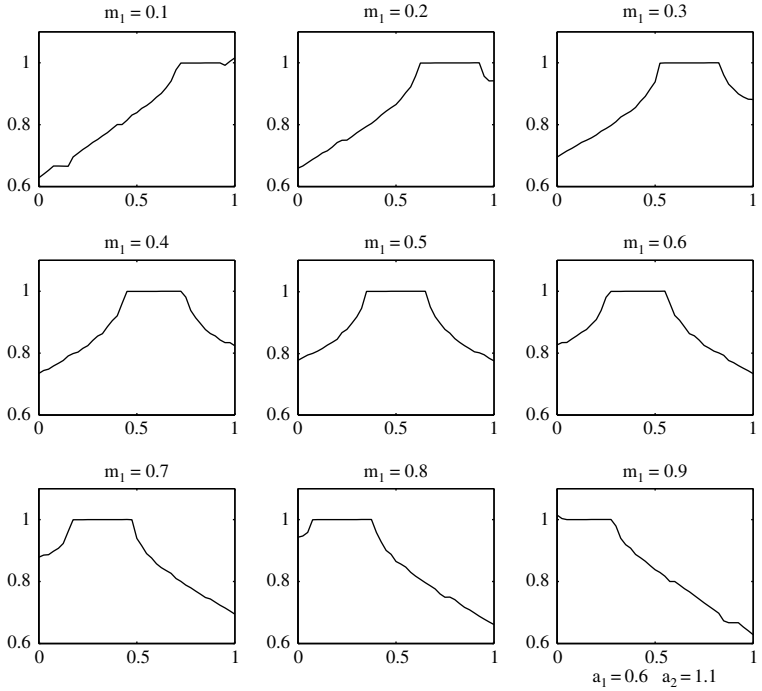

Fig. 5.8. Wave speed as a function of m_1 and n_1 for $a_{(1)} = 0.6$ and $a_{(2)} = 1.1$.

In several of the plots, we see intervals of n_1 for which $f(m_1, n_1)$ is constant for a given m_1 value; we call these "plateaux" and refer to the associated

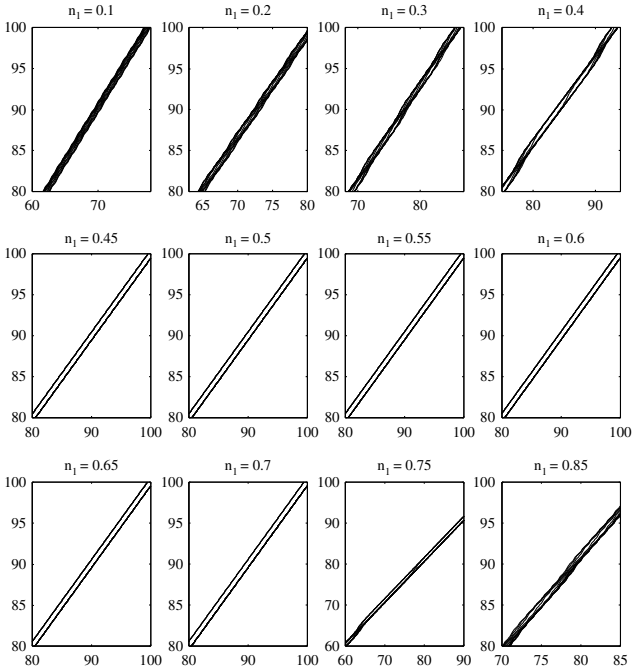

Fig. 5.9. Trajectories in material with $a_{(1)} = 0.6, a_{(2)} = 1.1, m_1 = 0.4$ and n_1 as indicated.

structures as "being on a plateau". By inspecting the plots in Fig. 5.8, it is seen that for $a_{(1)} = 0.6$ and $a_{(2)} = 1.1$, there are always plateaux corresponding to a speed equal to unity. In the first example of this section where we observed the existence of stable limit cycles, we had $(m_1, n_1) = (0.4, 0.5)$. The propagation speed in such a structure is $1{=}f(0.4, 0.5)$, and this material puts us on the plateau of the fourth plot of the series shown in Fig. 5.8. The other structures shown in Fig. 5.6 and 5.7 are not on a plateau and do not exhibit limit cycles.

Fig. 5.9 gives portions of trajectories which originate on $[0, 1]$ at time 0 in twelve checkerboard structures distinguished only by their values of n_1. The other parameter values are $a_{(1)} = 0.6, a_{(2)} = 1.1, m_1 = 0.4$. By comparing the values of n_1 which yield limit cycles with the location of the plateau in the velocity-n_1 graph for $m_1 = 0.4$ in Fig. 5.10, we propose the following hypothesis:

A structure is on a plateau if and only if the structure yields stable limit cycles.

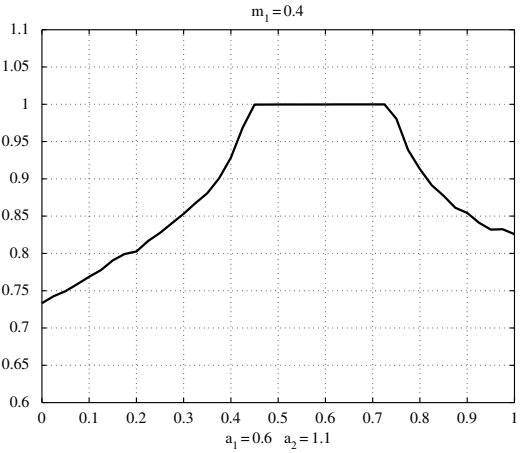

Fig. 5.10. Speed versus n_1 in material with $a_{(1)} = 0.6, a_{(2)} = 1.1, m_1 = 0.4$.

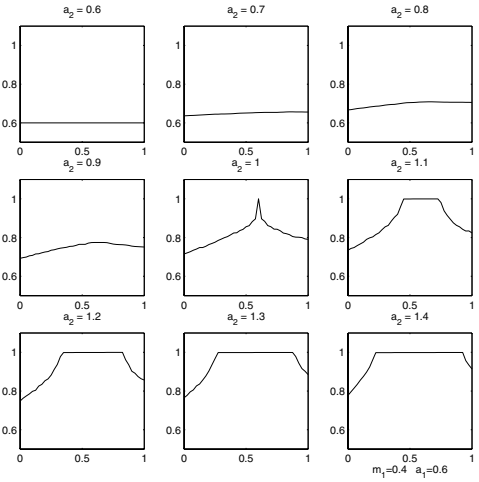

Fig. 5.11. Wave speed as a function of $a_{(2)}$ and n_1, for $a_{(1)}$ between 0.6 and 1.4.

In Fig. 5.11 and 5.12, we see how speeds vary with n_1 for distinct values of $a_{(2)}$, with $a_{(1)} = 0.6, m_1 = 0.4$. Note that $a_{(2)} = 1$ is a crucial case, since there will always be a trajectory that moves with constant speed $1 = \delta/\tau$ because it passes through the corners of the checkerboard so as to remain always in material 2 and never be deflected by entering material 1. Furthermore, when $a_{(1)}, a_{(2)} < 1$, there are no limit cycles with speed 1.

The limit cycle to which an array of trajectories converges is such that if it passes through the point (z, t) in the z-t plane, then it also passes through the point $(z + q\delta, t + p\tau)$ for some integers p, q. We take the speed of travel to be $\frac{q}{p}(\frac{\delta}{\tau})$. So, in our computed examples, the speeds should be rational numbers

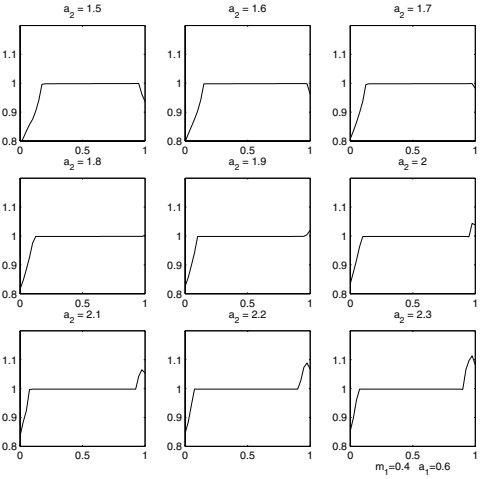

Fig. 5.12. Wave speed as a function of $a_{(2)}$ and n_1, for $a_{(1)}$ between 1.5 and 2.3.

since $\delta = \tau = 1$. Fig. 5.13 suggests that for $a_{(1)} = 0.6, a_{(2)} = 0.9, m_1 = 0.15$ there are at least 2 clear plateaux (maybe 3) indicating values of n_1 for which limit cycles have rational speeds. Figs. 5.14 and 5.15 in which n_1 takes the values of 0.55 and 0.2, respectively, support the observation that there are limit cycles for the structures on the plateaux and that the associated cycle speeds are 3/4 and 2/3.

Fig. 5.16 shows the solution at time 30 of a disturbance through the checkerboard structure with parameters $a_{(1)} = 0.6, a_{(2)} = 0.9, m_1 = 0.15, n_1 = 0.2$. The initial data shifted to the right 20 units is also shown. Compare this figure to Fig. 5.4. The trajectory paths in Fig. 5.15 show that there are 3 stable limit cycles per period and so we see that the piecewise constant solution consists of 3 constant states per spatial period $\delta = 1$. In general, for a structure on a plateau, the asymptotic solutions in the limit $t \to \infty$ for non-zero values of the ratio of the period of the structure to the characteristic wavelength of the disturbance are discontinuous. However, when this ratio approaches zero, the solution generated by continuous initial data tends to become continuous for finite t.

Figs. 5.17, 5.18 and 5.19 have randomly generated values for $a_{(1)}, a_{(2)}, m_1, n_1$ which give limit cycles. The limit cycles travel at rational speeds as expected by our hypothesis.

These observations are in accordance with Poincaré's theorem indicating the existence of the average speed termed the *rotation number* in Poincaré's formulation. It is known that this speed is rational if and only if the phase curve of the differential equation

$$\frac{dz}{dt} = a$$

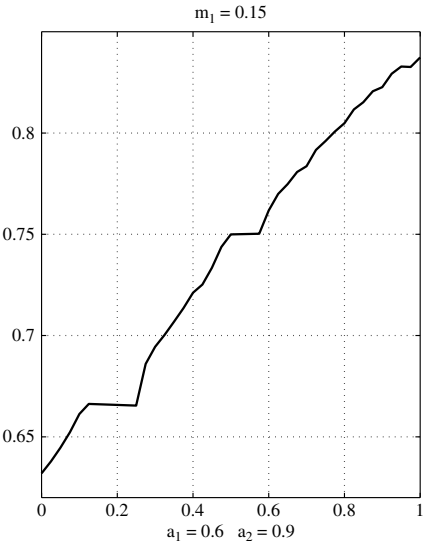

Fig. 5.13. Limit cycles have speeds that are rational multiples of $\delta/\tau = 1$. Here, $a_{(1)} = 0.6, a_{(2)} = 0.9, m_1 = 0.15$.

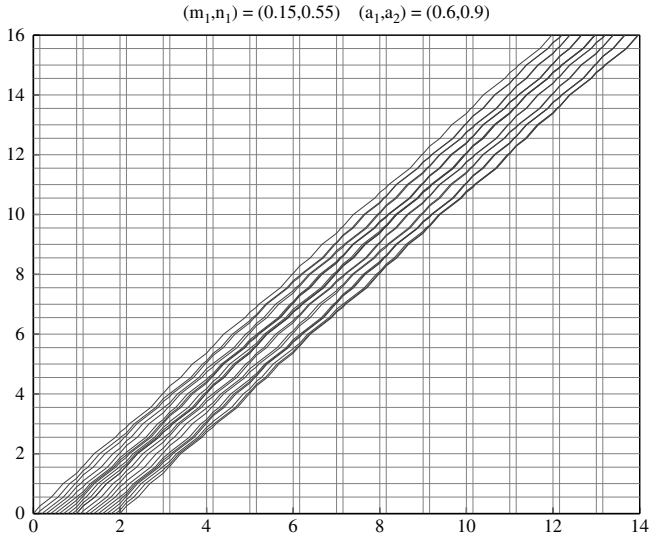

Fig. 5.14. Wave speed = 3/4 when $a_{(1)} = 0.6, a_{(2)} = 0.9, m_1 = 0.15$, and $n_1 = 0.55$.

is closed on the torus. At the same time, this rational value of rotation number persists over a range of structural parameters giving what we have called plateaux. This range can be wide enough, thus securing stability of rational rotation numbers.

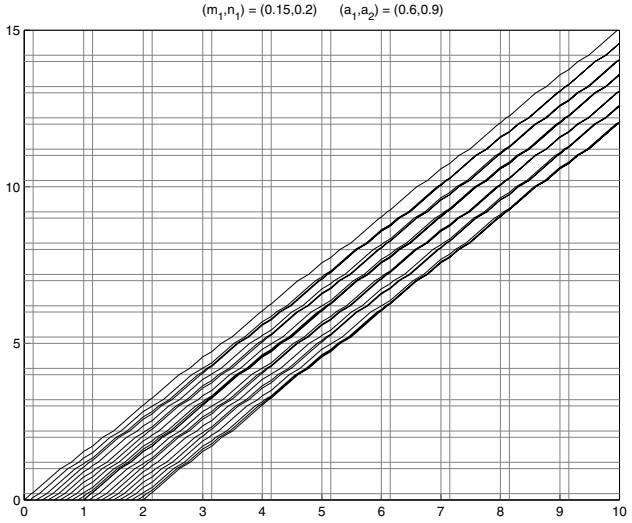

Fig. 5.15. Wave speed $= 2/3$ when $a_{(1)} = 0.6, a_{(2)} = 0.9, m_1 = 0.15$, and $n_1 = 0.2$.

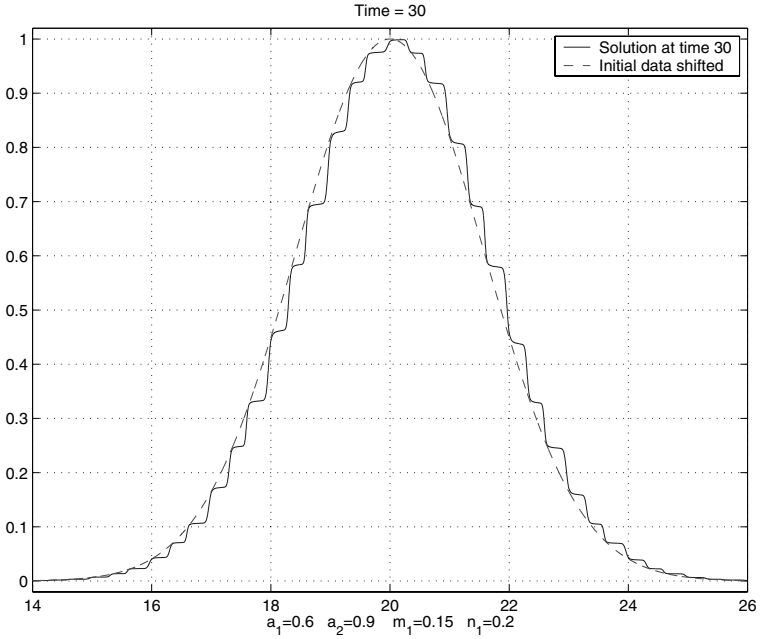

Fig. 5.16. Solution at time 30 of a disturbance with wide support through a structure with $a_{(1)} = 0.6, a_{(2)} = 0.9, m_1 = 0.15, n_1 = 0.2$, and initial data shifted right 20 units.

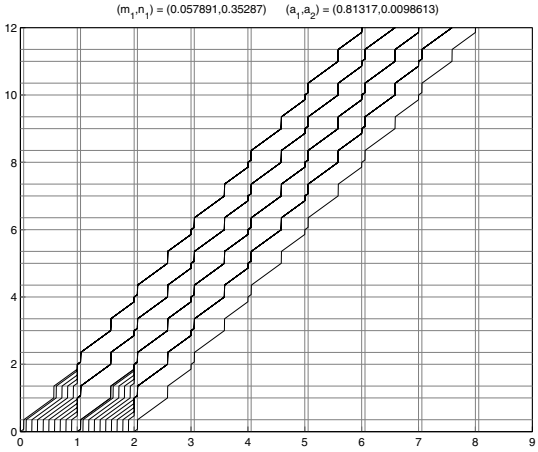

Fig. 5.17. Wave speed $= 1/2$. Use $m_1 = 0.0579, n_1 = 0.3529, a_{(1)} = 0.8132, a_{(2)} = 0.0099$ (randomly generated parameters).

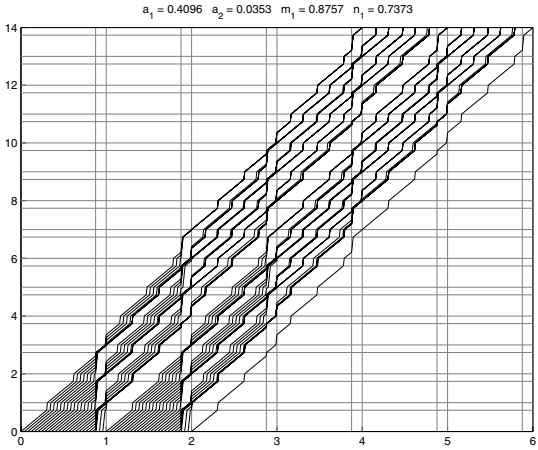

Fig. 5.18. Wave speed $= 2/7$. Use $m_1 = 0.8757, n_1 = 0.7373, a_{(1)} = 0.4096, a_{(2)} = 0.0353$ (randomly generated parameters).

5.5 Energy transformation in the presence of limit cycles

The formation of limit cycles illustrated in Fig. 5.2 is accompanied by a special energy/momentum exchange between the dynamic material and the environment. An attentive look, as in Fig. 5.2, reveals interesting behavior of characteristics that go close enough to the limit cycle: they enter material 1 (leave material 2) across a *vertical* interface, and leave material 1(enter material 2) across a *horizontal* interface. Because of this special kinematics, a

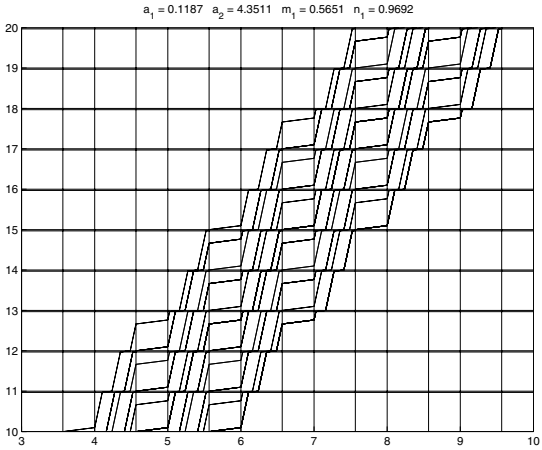

Fig. 5.19. Wave speed = 2/5. Use $m_1 = 0.5651, n_1 = 0.9692, a_{(1)} = 0.1187, a_{(2)} = 4.3511$ (randomly generated parameters).

bunch of parallel characteristics *gains* some finite portion of energy from the outside agent each time it enters material 2; this happens because an external agent performs at this moment a finite work against the inertial and elastic forces. To show this, consider equation (2.75) and integrate it over a narrow horizontal strip $z_0 < z < z_1,\ t_* - \epsilon < t < t_* + \epsilon$ containing the interface $t = t_*$ that separates material 1 below it from material 2 above it. The rhs of (2.75) becomes, after integration,

$$\frac{1}{2}\int_{z_0}^{z_1} dz \int_{t_*-\epsilon}^{t_*+\epsilon} \left[\frac{\partial}{\partial t}\left(\frac{1}{\rho}\right)\left(\rho\frac{\partial u}{\partial t}\right)^2 + \frac{\partial k}{\partial t}\left(\frac{\partial u}{\partial z}\right)^2\right] dt \qquad (5.33)$$
$$= \frac{1}{2}\int_{z_0}^{z_1} \left\{\left[\frac{1}{\rho}\right]_{(1)}^{(2)}\left(\rho\frac{\partial u}{\partial t}\right)^2 + [k]_{(1)}^{(2)}\left(\frac{\partial u}{\partial z}\right)^2\right] dz,$$

this equation specifies the work mentioned above; the quantities $\rho\frac{\partial u}{\partial t}$ and $\frac{\partial u}{\partial z}$ in its rhs may be taken, due to their continuity, at either side of the interface. Because materials 1 and 2 belong with the regular range (2.55), we conclude that the expression (5.33) is positive. The integral of the lhs of (2.75) equals

$$\int_{z_0}^{z_1}\int_{t_*-\epsilon}^{t_*+\epsilon}\left(\frac{\partial}{\partial t}W_{tt} + \frac{\partial}{\partial z}W_{tz}\right) dtdz = \int_{z_0}^{z_1} [W_{tt}]_{t_*-\epsilon}^{t_*+\epsilon}\, dz + \int_{t_*-\epsilon}^{t_*+\epsilon} [W_{tz}]_{z_0}^{z_1}\, dt \qquad (5.34)$$

By assuming that $[W_{tz}]_{z_0}^{z_1}$ is bounded, we pass to the limit $\epsilon \to 0$; equation (2.75) then shows that

$$\left[\int_{z_0}^{z_1} W_{tt} dz\right]_{t_*-0}^{t_*+0} = \frac{1}{2}\int_{z_0}^{z_1}\left\{\left[\frac{1}{\rho}\right]_{(1)}^{(2)}\left(\rho\frac{\partial u}{\partial t}\right)^2 + [k]_{(1)}^{(2)}\left(\frac{\partial u}{\partial z}\right)^2\right] dz;$$

in other words, the energy

$$\int_{z_0}^{z_1} W_{tt} dz$$

increases by the amount (5.33) when we move across the horizontal interface from material 1 to material 2.

We now apply a similar procedure to a narrow vertical strip $z_* - \epsilon < z < z_* - \epsilon,\ t_0 < t < t_1$, containing the interface $z = z_*$ that separates material 2 on its left from material 1 on its right. The integral of the rhs of (2.75)

$$-\frac{1}{2}\int_{t_0}^{t_1} dt \int_{z_*-\epsilon}^{z_*+\epsilon} \left[\frac{\partial \rho}{\partial t}\left(\frac{\partial u}{\partial t}\right)^2 - \frac{\partial k}{\partial t}\left(\frac{\partial u}{\partial z}\right)^2\right] dz$$

equals zero because $\frac{\partial \rho}{\partial t} = \frac{\partial k}{\partial t} = 0$ within the strip. The integral of lhs of (2.75) equals

$$\int_{t_0}^{t_1}\int_{z_*-\epsilon}^{z_*+\epsilon}\left(\frac{\partial W_{tt}}{\partial t} + \frac{\partial W_{tz}}{\partial z}\right) dz dt = \int_{z_*-\epsilon}^{z_*+\epsilon} [W_{tt}]_{t_0}^{t_1}\, dz + \int_{t_0}^{t_1} [W_{tz}]_{z_*-\epsilon}^{z_*+\epsilon}\, dt.$$

Passing to the limit $\epsilon \to 0$ and bearing in mind the supposed boundedness of W_{tt} within the strip $[z_* - \epsilon,\ z_* + \epsilon]$, we conclude that

$$\int_{t_0}^{t_1} [W_{tz}]_{z_*-0}^{z_*+0}\, dz = 0.$$

In other words, the energy density flux W_{tz} remains continuous across the vertical interface.

Through the rest of this section, we will assume that the spatial and temporal periods τ and δ of the microstructure are both equal to ϵ.

Consider now the bunch of characteristics that pass in a close vicinity of a limit cycle (Fig. 5.20). As they approach the cycle, the horizontal distance between two neighboring characteristics decreases from h at moment $t = 0$ to $h\alpha$ at moment $t = n_1\epsilon$ and $h\alpha^2$ at moment $t = \epsilon$, where $\alpha = \tan\phi_1/\tan\phi_2 = a_{(1)}/a_{(2)} = 0.545$ (Fig. 5.2).

Integrate equation (2.75) over the domain *ABCDEA* (Fig. 5.20) bounded by two horizontal segments *AE* and *CD*, and by three segments *AB, BC,* and *DE* of characteristics. The horizontal segment *AE* is traversed along its *top side* $t = +0$, whereas the segment *CD* is traversed along its *bottom side* $t = n_1\epsilon - 0$. Because the energy density flux W_{tz} remains continuous across the vertical segment *EB* and because the energy density flux is zero on the segments *AB, BC* and *DE*, we conclude that the energy

$$w_1 = \int_A^E W_{tt}\Big|_{t=+0} dz$$

is the same as the energy

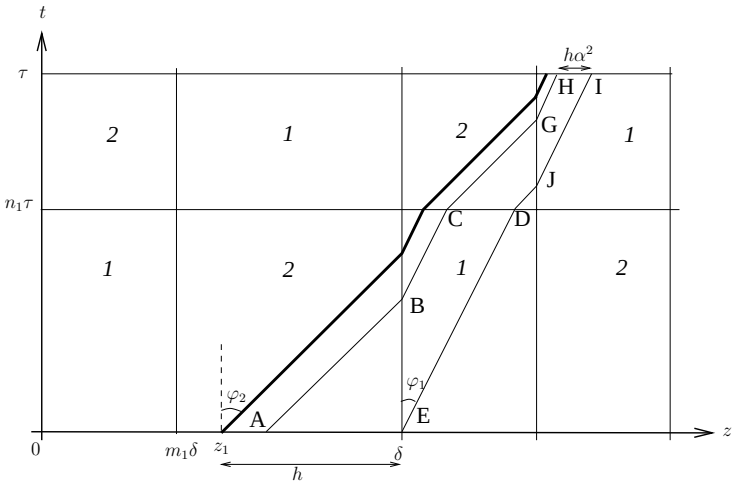

Fig. 5.20. The bunch of characteristics in the vicinity of a limit cycle. The spatial and temporal periods of the microstructure are taken equal to ϵ, other parameters specified as $a_{(1)} = 0.6, a_{(2)} = 1.1, m_1 = 0.4, n_1 = 0.5$.

$$\int_C^D W_{tt}\Big|_{t=n_1\epsilon-0} dz.$$

On the other hand, when we go across the segment CD from its bottom side $t = n_1\epsilon - 0$ occupied by material 1 to its top side $t = n_1\epsilon + 0$ occupied by material 2, then the energy increases from the value w_1 to the value (see (5.33))

$$\begin{aligned} w_2 &= w_1 + \frac{1}{2}\int_C^D \left\{ \left[\frac{1}{\rho}\right]_1^2 \left(\rho\,\frac{\partial u}{\partial t}\right)^2 + [k]_1^2 \left(\frac{\partial u}{\partial z}\right)^2 \right\} dz \\ &= w_1 + \frac{1}{2}[k]_1^2 \int_C^D \left\{ \frac{1}{k_{(1)}\rho_{(1)}} \left(\rho_{(1)}\,\frac{\partial u}{\partial t}\right)^2_{t=n_1\epsilon-0} + \left(\frac{\partial u}{\partial z}\right)^2_{t=n_1\epsilon-0} \right\} dz \\ &= \frac{a_{(2)}}{a_{(1)}} w_1 = \frac{1}{\alpha} w_1. \end{aligned} \tag{5.35}$$

In the latter calculation, we used the relation $k_{(1)}\rho_{(1)} = k_{(2)}\rho_{(2)}$ following from the identity of the wave impedances of materials 1 and 2.

By a similar argument applied to the domain bounded by the contour $CGHIJD$ in Fig. 5.20, we conclude that the energy w_3 on the top side of the segment HI is linked with the energy w_1 on the top side of the segment AE by the relation

$$w_3 = \frac{1}{\alpha^2} w_1;$$

that is, it increases by the factor $\frac{1}{\alpha^2}$ through each temporal period. Because $\alpha < 1$, the energy grows exponentially as the bunch of disturbances approaches

the limit cycle. The rectangular microstructure with materials possessing identical wave impedance may therefore accumulate energy when the characteristic pattern contains the limit cycles. In other words, such a microstructure may resemble a swing where the energy is pumped into the system at duly chosen instants of time. The difference is that, in our case, the accumulation occurs at *all* frequencies, whereas, in the case of a swing, it develops only for those frequencies that exceed a certain threshold value.

We see that a energy accumulation in a checkerboard is maintained due to a special geometry of the characteristic pattern that is properly adjusted to a checkerboard material assemblage. Such accumulation persists unlimitedly if the energy supply from outside is unbounded. We may say that the disturbance then demonstrates stability with regard to the phase (the convergence of characteristics to limit cycles), but it appears to be unstable in the sense of energy. However, this instability will disappear (there will be no energy accumulation), if the energy supply from outside has limits. The checkerboard microstructure with originally fixed parameters will then no longer be maintained, and the disturbance will be stabilized following a concrete scenario generated by the mechanism of termination of energy pumping. Particularly, the microstructure may become laminar, in which case no accumulation of energy may occur. This is illustrated by temporal laminates where the energy of low frequency wave *pumped* into the system as the disturbance goes across an interface from material 1 to material 2, is balanced by the energy *taken away* from the system at the subsequent interface where material 2 is followed by material 1. In this respect, the system resembles a simple harmonic oscillator in which the energy periodically takes the form of potential or kinetic, but the total energy stored in the system is preserved.

Returning to the rectangular microstructure, it is interesting to note, as mentioned at the end of the previous section, that the solution tends to become continuous as $\delta, \tau \to 0$, whereas the energy needed to maintain propagation of waves through a microstructure that produces limit cycles may become infinite. Of course, in such circumstances, there is no homogenization in its standard version applicable to laminates.

5.6 Numerical analysis of energy accumulation

We now give a numerical illustration of the energy accumulation phenomenon discussed above. We consider the structure defined by

$$a_{(1)} = 0.55,\ a_{(2)} = 2a_{(1)},\ m_1 = 0.5, n_1 = 0.5,\ \gamma_{(1)} = \gamma_{(2)} = 1. \tag{5.36}$$

Fig. 5.21 shows the paths of trajectories for (5.36); these paths are similar to those shown in Fig. 5.2. The unstable limit cycles for right-going waves originate at $z = 0.45+n$; the left-going ones begin at $(m_1-0.45)+n = 0.05+n$ for any integer n. They are represented as heavy dashed lines in the figure.

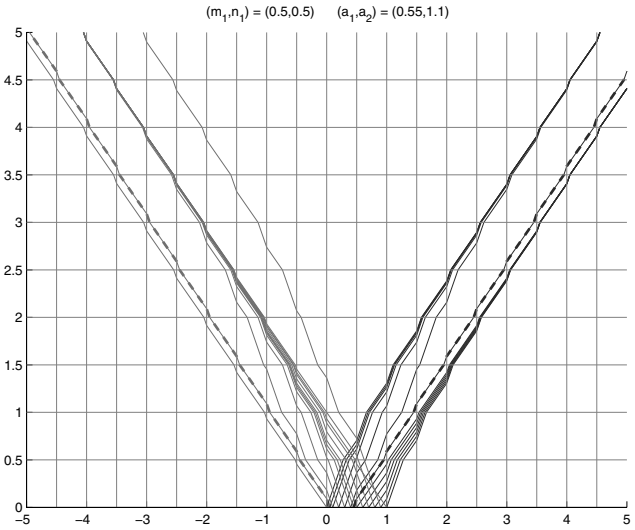

Fig. 5.21. Characteristic paths through checkerboard material (5.36).

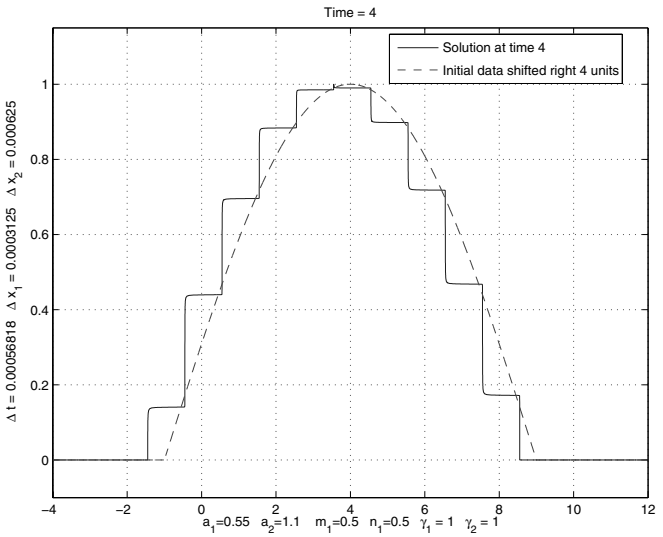

Fig. 5.22. Solution at time 4 to $a_{(1)} = 0.55, a_{(2)} = 2a_1, m_1 = 0.5, n_1 = 0.5$.

We consider the problem (5.26), (5.27) for the structure (5.36) with initial data

$$R(z,0) = \begin{cases} \cos(\pi z/10) & \mid z \mid \leq 5, \\ 0 & \text{otherwise}, \end{cases}$$

$$L(z,0) = 0.$$

The solution is thus made up only of right-going waves since the left characteristic information $L(z,t)$ is zero. The resulting profile at time 4 is shown in Fig. 5.22. The initial data shifted right 4 units is also shown. These two curves coincide most significantly at $0.45 + n$ for $n = -1, 0, 1, \ldots, 8$. The constant states in the evolved solution take on the values of the right going Riemann invariant $R(z,t)$ associated with the unstable limit cycles. The energy

$$E(t) = \frac{1}{2}\int_{-\infty}^{\infty}\left[\rho\left(\frac{\partial u}{\partial t}\right)^2 + k\left(\frac{\partial u}{\partial z}\right)^2\right]dz = \frac{1}{2}\int_{-\infty}^{\infty}\left[\rho\left(\frac{\partial u}{\partial t}\right)^2 + \frac{1}{k}\left(\frac{\partial v}{\partial t}\right)^2\right]dz$$

changes as shown in Fig. 5.23. According to (5.35) and (5.36), it should double each time the checkerboard structure switches and ideally should grow as

$$E(t) = E(0)r^{\bar{t}}, \quad \bar{t} = \begin{cases} t & \mathrm{mod}(t,\tau) \neq n\tau \\ t + n\tau & \text{otherwise.} \end{cases}$$

The computed energy matches well with the curve. The limit cycles alone do not guarantee the energy accumulation. The structure defined by

$$a_{(1)} = 0.25,\ a_{(2)} = 2a_{(1)},\ m_1 = 0.3,\ n_1 = 0.2,\ \gamma_{(1)} = \gamma_{(2)} = 1 \tag{5.37}$$

features the limit cycles (see Fig. 5.24). The right going characteristic paths are reproduced (with some magnification) in Fig. 5.25 for time range ($t = 21, t = 30$). We see that the paths not necessarily enter (leave) material 2 across horizontal (vertical) interfaces; as a consequence, there appears to be no energy accumulation: the energy changes as shown in Fig. 5.26. The solution profile at time 10 is replicated in Fig. 5.27.

5.7 Some remarks about discontinuous solutions for laminates

So far through this and preceding chapters we were discussing continuous solutions to the wave system (2.2). Particularly for a laminate, such solutions exist if a structure satisfies ineqs. (2.5). In this section we give a brief account of some phenomena that arise in laminates once these inequalities are violated.

Assuming, as in section 2.1, that $a_2 > a_1$, consider an interface 12 (Fig. 5.28) moving at velocity V such that $a_1 < V < a_2$ (Fig. 2.4); these inequalities violate (2.5). Immovable materials 1(2) are located, respectively, on the left (right) side of the interface; we see that three characteristics depart away from the interface, while only one arrives onto it.

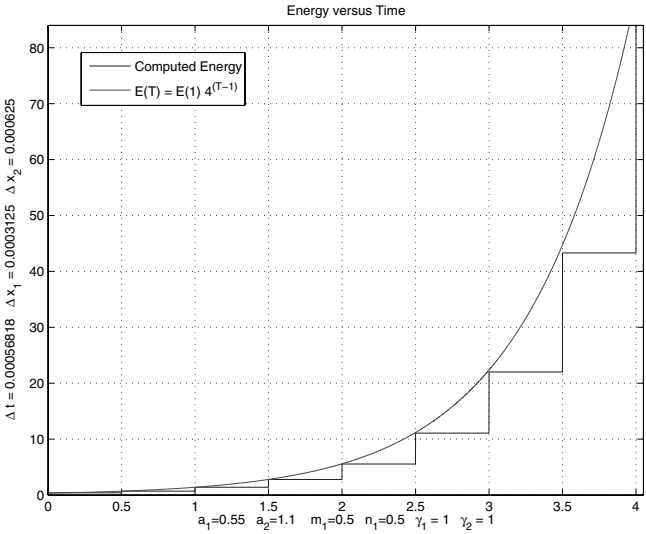

Fig. 5.23. Energy variation up to time 4 for $a_{(1)} = 0.55, a_{(2)} = 2a_{(1)}, m_1 = 0.5, n_1 = 0.5$.

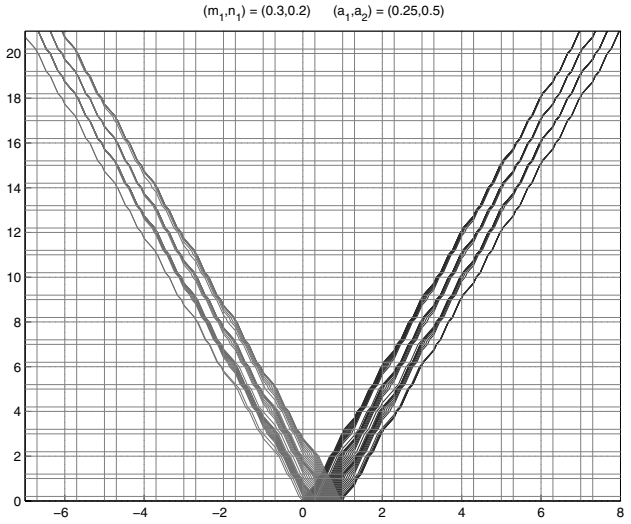

Fig. 5.24. Characteristic paths through checkerboard material (5.37).

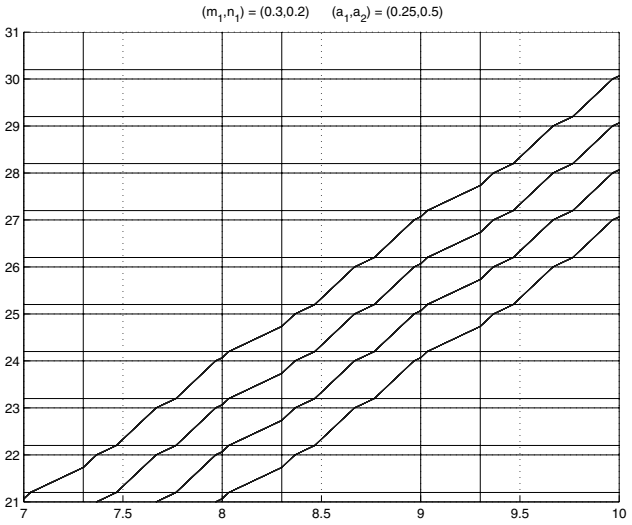

Fig. 5.25. Right going characteristic paths through material (5.37).

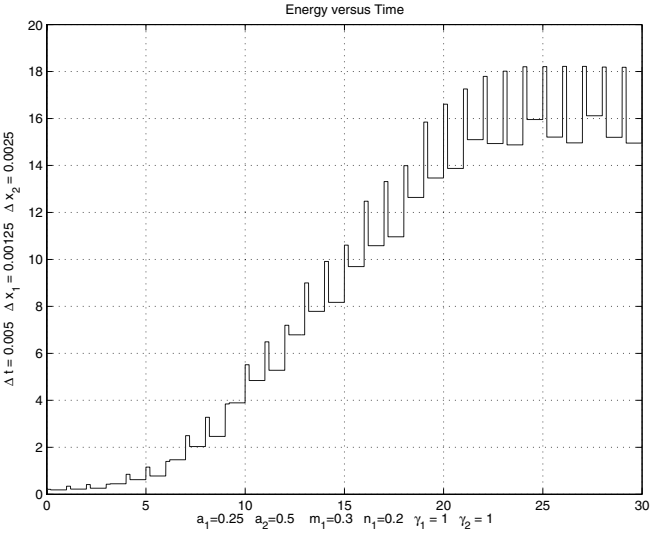

Fig. 5.26. Energy variation in material (5.37).

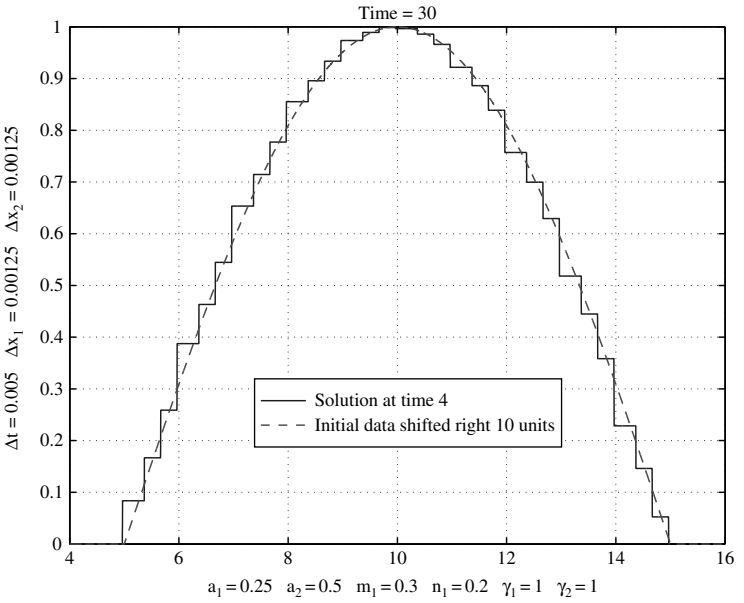

Fig. 5.27. Solution at time 10 to material (5.37).

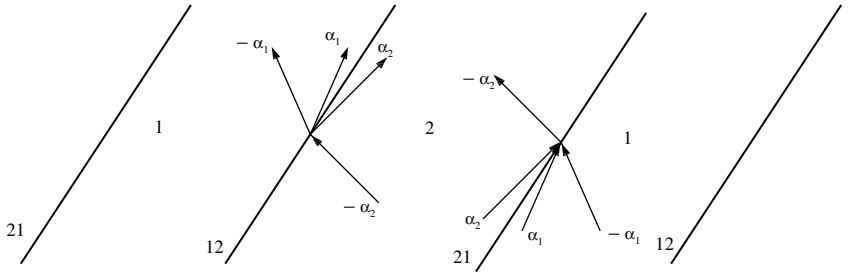

Fig. 5.28. The pattern of characteristics in a laminate violating ineqs. (2.5)

.

One of the departing characteristics (with phase velocity $-a_1$) carries through material 1 the Riemann invariant wave $L(z,t)$ (see (5.28)). The values of $L(z,t)$ arrive at 12 after travelling through material 2 at velocity $-a_2$. We may say that these two waves (characteristics) belong with the same L-family because they both travel from right to left. Similarly, we define the R-family of characteristics, a_1 and a_2, travelling from left to right; they both carry the values of another Riemann invariant $R(z,t)$ and *depart* from 12 into materials 1 and 2, respectively.

In a laminate, the interface 12 is followed by a parallel interface 21 (Fig. 5.28), with material 2(1) on its left (right) side. The characteristics $-a_1$ and $-a_2$ of the L-family carry the values of $L(z,t)$ through this interface, while the characteristics a_1 and a_2 of the R-family both bring the values of $R(z,t)$ onto the interface and *collide* along it. This pattern of characteristics shows that in order to formulate a transmission problem correctly, we have to set three additional conditions along 12, and one condition along 21, in each case the number of conditions matching the number of departing characteristics. Such conditions should reflect the physics of the problem. Generally, we expect the appearance of a strong discontinuity in the values of $R(z,t)$ maintained along the interface 21, because of a collision between characteristics a_1 and a_2 belonging with the same R-family.

To get a clear idea of such additional conditions, one may consider the case when materials 1 and 2 have the same values of the wave impedance: $\gamma_1 = \gamma_2$. In this case (see section 5.4), the R- and L-waves are governed each by their own equation (5.26) and (5.27), and additional conditions for them may be formulated independently of each other. Let us assume, as in a familiar case of ineqs. (2.5), that $L(z,t)$ is continuous across any interface. Then, the L-disturbance will travel through materials 1 and 2 along the characteristics $-a_1$ and $-a_2$, respectively, i.e. along the L-family. We may say that the R-family is not involved in this transport at all. Instead, this family may carry the R-waves originating independently from each other on both sides of the interface 12. The R-wave originating on side 1 of it propagates with velocity a_1 into material 1, and arrives at the neighboring interface 21 from its 1-side. Another R-wave, originating on side 2 of 12, propagates with velocity a_2 into material 2, and arrives at another neighboring interface 21 from its 2-side. Because of the periodicity of a laminate structure we see that on 21, there is maintained a stationary shock caused by the difference in values of $R(z,t)$ brought onto this interface from the opposite sides of it.

The R-waves are thus generated by independent sources of disturbance on both sides of 12. Once there is no such sources, there will be no R-waves, and the disturbance will all be reduced to $L(z,t)$. Eq. (5.27) governing it may be averaged, with continuous solutions $L(z,t)$, to the form

$$L_t + \left(V - \frac{1}{\left\langle \frac{1}{V+a} \right\rangle} \right) L_z = 0.$$

Here, the symbol L stands for the value of L averaged over the period δ of laminate. One should mention that there may be shocks maintained along the interfaces 21 over limited periods of time due to the influence of non-zero initial R-disturbance $R(z, 0)$. After such periods, in the absence of independent sources along 12, the shock waves on 21 will disappear.

References

1. Lurie, K.A., and Weekes, S.L.: Wave propagation and energy exchange in a spatio-temporal material composite with rectangular microstructure. J. Math. Analysis and Applications, **314** No. 1, 286–310 (2006)
2. Weekes, S.L.: Numerical computation of wave propagation in dynamic materials. Applied Numerical Mathematics **37**, 417–440 (2001)
3. Weekes, S.L.: A stable scheme for the numerical computation of long wave propagation in temporal laminates, J. Computational Physics, **176**, 345–362 (2002)

6

Some Applications of Dynamic Materials in Electrical Engineering and Optimal Design

6.1 A plane electromagnetic wave propagation through an activated laminate in 3D

So far in this book we discussed the wave propagation in a single spatial dimension. In the first four sections of this chapter, we shall discuss a more general case of electromagnetic waves travelling in 3D-space through an activated laminate structure with laminates perpendicular to the z-axis and moving along it.

The wave vector $\mathbf{k}$ of a plane electromagnetic wave will be assumed belonging with the (x, z)-plane, this plane being therefore the plane of incidence. Two independent polarizations of the wave will be examined:

(i) an *electric* polarization, with the electric field vector $\mathbf{E}$ normal to the plane $(\mathbf{e}_1, \mathbf{e}_3)$ of incidence:

$$\mathbf{E} = E_2\mathbf{e}_2, \quad \mathbf{B} = B_1\mathbf{e}_1 + B_3\mathbf{e}_3; \tag{6.1}$$

(ii) a *magnetic* polarization, with the magnetic inductance vector $\mathbf{B}$ normal to the plane of incidence:

$$\mathbf{B} = B_2\mathbf{e}_2, \ \ \mathbf{E} = E_1\mathbf{e}_1 + E_3\mathbf{e}_3. \tag{6.2}$$

The material relations in materials 1 and 2 participating in laminate are given by

$$\mathbf{D} = \epsilon_i\mathbf{E}, \ \ \mathbf{H} = (1/\mu_i)\mathbf{B}, \ \ i = 1, 2, \tag{6.3}$$

with the index i related to the ith material.

An activated periodic laminate represents a material assemblage that depends on the fast variable $(z - Vt)/\delta$ where δ is a period. We shall assume that the electromagnetic field is independent of y for both polarizations. With this assumption, the Maxwell's equations (3.1) and (3.2) combined with material relations (6.3) are reduced to

$$E_{2z} = (\mu H_1)_t, \;\; E_{2x} = -(\mu H_3)_t, \;\; H_{1z} - H_{3x} = (\epsilon E_2)_t, \tag{6.4}$$

for an electric polarization, and to

$$H_{2x} = (-\epsilon E_1)_t, \;\; H_{2x} = (\epsilon E_3)_t, \;\; E_{1z} - E_{3x} = -(\mu H_2)_t, \tag{6.5}$$

for a magnetic polarization.

Eqs. (6.5) appear if we replace $\mathbf{E}$ by $\mathbf{H}, \mathbf{H}$ by $-\mathbf{E}, \mu$ by ϵ, and ϵ by μ in eqs. (6.4).

By introducing potential u through the formulae

$$E_2 = u_t, \;\; B_1 = u_z, \;\; B_3 = -u_x, \tag{6.6}$$

we satisfy the first two of eqs. (6.4); the third one together with (6.3), (6.6) yields

$$\left(\frac{1}{\mu}u_x\right)_x + \left(\frac{1}{\mu}u_z\right)_z = (\epsilon u_t)_t; \tag{6.7}$$

this equation will now be subjected to homogenization.

6.2 The homogenized equations. Elimination of the cutoff frequency in a plane waveguide

The standard technique of homogenization (see Appendix 4) applied to eq. (6.7) produces the following equation for the value of u averaged over the period δ of the microstructure (the symbol u is preserved for this quantity)

$$pu_{zz} - 2qu_{zt} - ru_{tt} + \ell u_{xx} = 0. \tag{6.8}$$

The symbols p, q, r are defined by (2.16)(see also (2.29)); the symbol ℓ is $\langle \mu^{-1} \rangle$. The lhs of (6.8) differs by the term ℓu_{xx} from the lhs of the equation that appears as we apply homogenization to the equation

$$\left(\frac{1}{\mu}u_z\right) = (\epsilon u_t)_t$$

related to plane waves with the wave vector directed perpendicularly to the layers, i.e. along the z-axis. The plane wave solution $\exp[i(gx + hz + \omega t)]$ to (6.8) depends on parameters g, h, ω satisfying the dispersive relation

$$h^2 p - 2h\omega q - r\omega^2 + \ell g^2 = 0. \tag{6.9}$$

The discriminant Δ of this quadratic equation for h takes on the form

$$\Delta = \omega^2(pr + q^2) - g^2 p\ell = \omega^2\theta^{-1} - g^2 p\ell. \tag{6.10}$$

As shown in Appendix 4, ℓ is always positive, and θ is positive in observance of (2.5). When $V = 0$, the product $p\ell$ is positive, and Δ becomes positive if $\omega^2 >$

$\omega_*^2 = g^2 p\ell\theta$ (cutoff frequency). However, if $V \neq 0$, then the discriminant Δ can be made positive, *regardless of the frequency*, by an appropriate adjustment of parameters of a material filling.

To show this, consider the expression (2.29) (see also (3.8)) for p, and assume that $V^2 < a_1^2 < a_2^2$. The denominator $V^2 - \frac{1}{\tilde{\epsilon}}\left(\frac{\tilde{1}}{\mu}\right)$ is then negative; as to the numerator $V^2 - \frac{1}{\tilde{\epsilon}\tilde{\mu}}$, this one may become positive if the original material parameters $\epsilon_1, \ldots, \mu_2$ fall into the irregular range (2.56), e.g. if $\epsilon_2 > \epsilon_1, \mu_2 < \mu_1$, but still $\epsilon_2\mu_2 > \epsilon_1\mu_1$. By a due choice of the volume fraction m_1, the value of $1/(\tilde{\epsilon}\tilde{\mu})$ may then be made less than a_1^2. If we now place V^2 within the interval $(1/(\tilde{\epsilon}\tilde{\mu}), a_1^2)$, then p will become negative, making the discriminant Δ positive. This means that the electromagnetic waves much longer than δ progress without damping along a planar waveguide bounded by two parallel conducting planes and filled by a duly activated laminate. In other words, in such a waveguide there is no cutoff frequency, and the travelling waves along it exist regardless of the transverse dimensions.

As to the roots h_1, h_2 of (6.9), they are real if $\Delta > 0$; the roots have opposite signs if

$$p(\omega^2 r - g^2\ell) > 0, \tag{6.11}$$

and have the same sign otherwise. For the case mentioned above, $1/(\tilde{\epsilon}\tilde{\mu}) < V^2 < a_1^2 < a_2^2$, we have $p < 0, r > 0$, and the roots have opposite signs if $\omega^2 < \omega_{**}^2 = \ell g^2/r$; if, on the contrary, $\omega^2 > \omega_{**}^2$, then the roots have the same sign, and coordinated wave propagation occurs. In the latter case, the common direction of propagation may be switched to opposite as the velocity V of the property pattern changes sign.

6.3 The effective material tensor and homogenized electromagnetic field

The material relations (6.3) are incorporated in a tensor equation

$$f = s \,:\, F, \tag{6.12}$$

linking the electromagnetic tensors F and f with the aid of a material tensor s. For a plane electromagnetic wave, the electromagnetic tensors are defined as (we omit $\sqrt{2}$ in (3.19) and (3.20))

$$\begin{aligned} F &= cB_3 a_{12} + cB_1 a_{23} - iE_2 a_{24}, \\ f &= H_3 a_{12} + H_1 a_{23} - icD_2 a_{24}, \end{aligned} \tag{6.13}$$

for an electric polarization, and

$$\begin{aligned} F &= -cB_2 a_{13} - iE_1 a_{14} - iE_3 a_{34}, \\ f &= -H_2 a_{13} - icD_1 a_{14} - icD_3 a_{34}, \end{aligned} \tag{6.14}$$

for a magnetic polarization.

The material equations (6.3) are related to the immovable original materials characterized as isotropic dielectrics; they generate material tensors

$$s = -\frac{1}{\mu_i c}(a_{12}a_{12} + a_{23}a_{23}) - \epsilon_i c a_{24}a_{24}, \quad i = 1, 2, \tag{6.15}$$

$$s = -\frac{1}{\mu_i c}a_{13}a_{13} - \epsilon_i c(a_{14}a_{14} + a_{34}a_{34}), \quad i = 1, 2, \tag{6.16}$$

for the electric and magnetic polarizations, respectively.

A dielectric composite that appears after homogenization is no more isotropic. For an electric (magnetic) polarization, such composite acquires different magnetic permeabilities (dielectric permittivities) along the x- and z-axes. For an electric polarization, the effective tensor will be represented as

$$s = -\frac{1}{M_1 c}a'_{12}a'_{12} - \frac{1}{Mc}a'_{23}a'_{23} - \mathcal{E}c a'_{24}a'_{24}, \tag{6.17}$$

with $M_1, M, \mathcal{E}$ being the effective material constants, and tensors a'_{st} defined as $a'_{12} = a_{12}$, $a'_{23} = a_{23}\cosh\chi + ia_{24}\sinh\chi$, $a'_{24} = -ia_{23}\sinh\chi + a_{24}\cosh\chi$, with χ being an appropriate rotation angle in 4-space. By substituting (6.17) into (6.12) and by using (6.13), we arrive at the following material relations

$$\begin{aligned}
H_1 &= [(1/Mc)\cosh^2\chi - \mathcal{E}c\sinh^2\chi]cB_1 + [(1/Mc) - \mathcal{E}c]E_2\sinh\chi\cosh\chi,\\
H_3 &= B_3/M_1,\\
cD_2 &= -[(1/Mc)\sinh^2\chi - \mathcal{E}c\cosh^2\chi]E_2 - [(1/Mc) - \mathcal{E}c]cB_1\sinh\chi\cosh\chi.
\end{aligned} \tag{6.18}$$

The Maxwell's equation $H_{1z} - H_{3x} = D_{2t}$ together with eqs. (6.6) and (6.3) now yield

$$\frac{1}{M_1}u_{xx} + c\left(\frac{1}{Mc}\cosh^2\chi - \mathcal{E}c\sinh^2\chi\right)u_{zz} + 2\left(\frac{1}{Mc} - \mathcal{E}c\right)\sinh\chi\cosh\chi\, u_{zt} + \frac{1}{c}\left(\frac{1}{Mc}\sinh^2\chi - \mathcal{E}c\cosh^2\chi\right)u_{tt} = 0.$$

By comparing this with (6.8), we obtain the formulae

$$\begin{aligned}
\frac{1}{M_1} &= \ell,\\
c\left(\frac{1}{Mc}\cosh^2\chi - \mathcal{E}\cosh^2\chi\right) &= p,\\
\left(\frac{1}{Mc} - \mathcal{E}c\right)\sinh\chi\cosh\chi &= -q,\\
\frac{1}{c}\left(\frac{1}{Mc}\sinh^2\chi - \mathcal{E}c\cosh^2\chi\right) &= -r,
\end{aligned} \tag{6.19}$$

and eqs. (6.18) and (6.6) now show that

$$\begin{aligned} H_1 &= pu_x - qu_t, \\ H_3 &= -\ell u_x, \\ D_2 &= ru_t + qu_z. \end{aligned} \tag{6.20}$$

Eqs. (6.19) allow us to express $\mathcal{E}, M, \chi$ in terms of p, q, and r.

6.4 The transport of effective energy

The mean (over the period) value of the complex Poynting vector is given by

$$\mathbf{S} = \mathbf{E} \times \mathbf{H}^*.$$

For an electric polarization, the $\mathbf{e}_3$-component of $\mathbf{S}$ equals (see (6.6),(6.20))

$$\mathbf{S} \cdot \mathbf{e}_3 = -E_2 H_1^* = -u_t(pu_z^* - qu_t^*) = -\omega(ph - q\omega).$$

The mean value of the complex effective energy density

$$\begin{aligned} \bar{T}_{44} = \frac{1}{2}\mathbf{B} \cdot \mathbf{H}^* + \frac{1}{2}\mathbf{D} \cdot \mathbf{E}^* = \frac{1}{2}u_z(pu_z^* - qu_t^*) \\ + \frac{1}{2}u_x \ell u_x^* + \frac{1}{2}(zu_t + qu_z)u_t^* = \frac{1}{2}h(ph - q\omega) + \frac{1}{2}\ell g^2 \\ + \frac{1}{2}\omega(r\omega + gh) = \frac{1}{2}(ph^2 + r\omega^2 + \ell g^2) = \omega(r\omega + gh). \end{aligned}$$

allows us to calculate the group velocity $v_{gr} = (\mathbf{S} \cdot \mathbf{e}_3)/\bar{T}_{44}$

$$v_{gr} = -\frac{ph - q\omega}{r\omega + gh}. \tag{6.21}$$

This formula also follows from (6.9) with v_{gr} defined as $-d\omega/dh$.

We shall characterize the sign of v_{gr} for the case when the cutoff frequency is eliminated; as shown in section 6.2, in this case $p < 0, r > 0$, and the roots

$$h_{1,2} = \frac{\omega q \pm \sqrt{\omega^2\theta^{-1} - g^2 p\ell}}{p}$$

of (6.9) are both real because

$$\omega^2\theta^{-1} - g^2 p\ell = \omega^2 q^2 + \omega^2 pr - g^2 p\ell > 0.$$

In section 6.2 it was also shown that

(i) $h_1 h_2 < 0$ if $\omega^2 pr - g^2 p\ell > 0$,
(ii) $h_1 h_2 > 0$ if $\omega^2 pr - g^2 p\ell < 0$.

Consider the case (i): $h_1 h_2 < 0$. With no loss of generality, assume that $q > 0$; then $h_1 < 0, h_2 > 0$. We have

$$\begin{aligned} r\omega + qh_1 &= \frac{\omega\theta^{-1} + q\sqrt{\omega^2\theta^{-1} - g^2 p\ell}}{p} < 0, \\ ph_1 - q\omega &= \sqrt{\omega^2\theta^{-1} - g^2 p\ell} > 0, \\ r\omega + qh_2 &= \frac{\omega\theta^{-1} - q\sqrt{\omega^2\theta^{-1} - g^2 p\ell}}{p} > 0, \\ ph_2 - q\omega &= -\sqrt{\omega^2\theta^{-1} - g^2 p\ell} < 0. \end{aligned} \tag{6.22}$$

The group velocity $v_{gr}(h)$ appears to be positive for both waves. We conclude that the energy propagates in the same direction as the phase for the h_1-wave, and in the opposite direction for the h_2-wave.

Consider now the case (ii): $h_1 h_2 > 0$. In this case, both waves travel in the same direction; the roots $h_{1,2}$ are both negative if $q > 0$. Inequalities (6.22) remain valid also in this case; for the first two and the last of those inequalities it is obvious; the third inequality requires some calculation:

$$\begin{aligned} \omega^2\theta^{-2} - q^2(\omega^2\theta^{-1} - g^2 p\ell) &= \omega^2(p^2 r^2 + 2prq^2 + q^4) \\ - \omega^2 q^2(pr + q^2) + g^2 q^2 p\ell &= p(\omega^2 pr^2 + \omega^2 rq^2 + g^2 q^2 \ell). \end{aligned} \tag{6.23}$$

The expression in parentheses at the rhs equals $\omega^2 r\theta^{-1} + g^2 q^2 \ell$, which is positive since $\ell > 0$.

6.5 On the necessary conditions of optimality in a typical hyperbolic control problem with controls in the coefficients

6.5.1 Introduction

When the investigation of the coefficient control of linear elliptic equations was initiated in the mid-sixties and early seventies [1],[2], it has been realized that the analysis of the necessary conditions reveals the specific ill-posedness of the original problem. Particularly in most of the practical situations, such conditions were found to be contradictory and therefore incapable of being satisfied unless the problem is given a revised formulation based on relaxation. Later on, it has been demonstrated [3] that the composite structures actually implement such relaxation since they precisely fill the gap peculiar to the original version of the necessary conditions.

A similar goal is pursued in the following sections, this time for a typical hyperbolic optimization problem with controls in the coefficients. The analysis of the necessary conditions shows that the ill-posedness of the above type arises in hyperbolic problems as well, and relaxation is required to make

the relevant necessary conditions non-contradictory. Particularly, the spatio-temporal laminates introduced and examined in the previous chapters may work towards this goal. As an example, we discuss below a design problem in space-time for a kinetic dynamic material.

6.5.2 Statement of the problem

We consider a material control problem for a hyperbolic system that governs the one-dimensional electromagnetic wave propagation through a moving dielectric medium. The electromagnetic field of a plane electromagnetic wave propagating along the z-axis is represented by the tetrade of vectors $\mathbf{E}(z,t)$, $\mathbf{B}(z,t)$, $\mathbf{H}(z,t)$, $\mathbf{D}(z,t)$, each vector possessing one non-zero component in the (x,y,z)-frame (cf. (3.4)):

$$\mathbf{E} = E\mathbf{j}, \quad \mathbf{B} = B\mathbf{i}, \quad \mathbf{H} = H\mathbf{i}, \quad \mathbf{D} = D\mathbf{j}. \tag{6.24}$$

As in section 3.1, we introduce the vector potentials

$$\mathbf{A} = -u(z,t)\mathbf{j}, \quad \mathbf{A}^* = v(z,t)\mathbf{i}; \tag{6.25}$$

by taking

$$E = u_t, \quad B = u_z, \quad H = v_t, \quad D = v_z, \tag{6.26}$$

we satisfy the Maxwell's equations (3.1), (3.2); the electromagnetic tensors F and f will then be given, respectively, by the expressions (cf. (3.21))

$$\begin{aligned} F &= \sqrt{2}c(u_{x_3}a_{23} + u_{x_4}a_{24}), \\ f &= \sqrt{2}ic(v_{x_4}a_{23} - v_{x_3}a_{24}). \end{aligned} \tag{6.27}$$

As in Chapter 3, we use a standard notation $x_1 = x$, $x_2 = y$, $x_3 = z$, $x_4 = ict$ for Minkowskian coordinates, the symbol c being the velocity of light in vacuum. Through a_{23}, a_{24} we denote an orthonormal pair of skew-symmetric 2nd rank tensors in Minkowskian space introduced in section 3.3:

$$a_{23} = (1/\sqrt{2})(\mathbf{e}_2\mathbf{e}_3 - \mathbf{e}_3\mathbf{e}_2), \quad a_{24} = (1/\sqrt{2})(\mathbf{e}_2\mathbf{e}_4 - \mathbf{e}_4\mathbf{e}_2), \tag{6.28}$$

with $\mathbf{e}_1 = \mathbf{i}, \mathbf{e}_2 = \mathbf{j}, \mathbf{e}_3 = \mathbf{k}, \mathbf{e}_4$ being the orthonormal system of unit vectors along the axes $x_1, \ldots, x_4$. The tensors a_{23}, a_{24} satisfy the relationships

$$a_{23} \,:\, a_{23} = a_{24} \,:\, a_{24} = -1, \quad a_{23} \,:\, a_{24} = 0;$$

these tensors define the subspace in the space of second rank skew-symmetric tensors in Minkowskian space that is substantial for one-dimensional wave propagation.

The material equation for a linear dielectric medium is given by eq. (3.33):

$$f = s \,:\, F; \tag{6.29}$$

this equation includes the fourth rank material tensor s. For an isotropic dielectric immovable with respect to a laboratory frame $\mathbf{e}_1, \ldots, \mathbf{e}_4$, the part of the s-tensor substantial for one-dimensional wave propagation is given by

$$s = -(1/\mu c)a_{23}a_{23} - \epsilon c a_{24}a_{24};$$

here ϵ and μ denote, respectively, the dielectric permittivity and magnetic permeability of the material. If the material is moving with velocity v relative to the laboratory frame,[1] then eq. (6.29) still holds, but with tensor s specified by the expression

$$s = -(1/\mu c)a'_{23}a'_{23} - \epsilon c\, a'_{24}a'_{24}, \tag{6.30}$$

where tensors $a'_{23},\ a'_{24}$ are defined by eqs. (6.28) with unit vectors $\mathbf{e}_1, \ldots, \mathbf{e}_4$ replaced by the vectors $\mathbf{e}'_1, \ldots, \mathbf{e}'_4$ linked with $\mathbf{e}_1, \ldots, \mathbf{e}_4$ through the Lorentz transform. If the material motion occurs along the x_3-axis (which is assumed below), then the relevant transform is given by the formulae

$$\mathbf{e}'_1 = \mathbf{e}_1,\ \ \mathbf{e}'_2 = \mathbf{e}_2,\ \ \mathbf{e}'_3 = \mathbf{e}_3\mathrm{cosh}\phi + \mathbf{e}_4 i\mathrm{sinh}\phi,\ \ \mathbf{e}'_4 = -\mathbf{e}_3 i\mathrm{sinh}\phi + \mathbf{e}_4\mathrm{cosh}\phi,$$

with corresponding relations for a'_{23}, a'_{24} (cf. (3.22)):

$$a'_{23} = a_{23}\mathrm{cosh}\phi + a_{24}i\mathrm{sinh}\phi,\ \ a'_{24} = -a_{23}i\mathrm{sinh}\phi + a_{24}\mathrm{cosh}\phi. \tag{6.31}$$

The angle ϕ is defined in these formulae by $\mathrm{tanh}\phi = v/c \leq 1$. Eq. (6.30) specifies s in terms of the tensors a'_{23}, a'_{24} related to the "primed" frame $\mathbf{e}'_1, \ldots, \mathbf{e}'_4$ moving with velocity v relative to the frame $\mathbf{e}_1, \ldots, \mathbf{e}_4$. In the primed frame, the material stays at rest. The expression (6.30) may be rewritten in terms of the laboratory tensors a_{23}, a_{24} as

$$s = -Qa_{23}a_{23} - iT(a_{23}a_{24} + a_{24}a_{23}) + Ra_{24}a_{24}, \tag{6.32}$$

with the coefficients Q, T, R defined by eqs. (3.48):

$$\begin{aligned} Q &= (1/\mu c)\ \mathrm{cosh}^2\phi - \epsilon c\ \mathrm{sinh}^2\phi, \\ T &= ((1/\mu c) - \epsilon c)\mathrm{sinh}\phi\mathrm{cosh}\phi, \\ R &= (1/\mu c)\mathrm{sinh}^2\phi - \epsilon c\ \mathrm{cosh}^2\phi. \end{aligned} \tag{6.33}$$

Note that always $R < 0$ because $\epsilon c \geq 1/\mu c$. Given eqs. (6.27), we refer to eqs. (6.32) and (6.33) and replace (6.29) by the following system:

$$\begin{aligned} iv_{x_4} &= Qu_{x_3} + iTu_{x_4}, \\ -iv_{x_3} &= iTu_{x_3} - Ru_{x_4}. \end{aligned} \tag{6.34}$$

Getting back to variables z, t, we rewrite this system as

[1] The reader will not be confused to find the symbol v denoting the material velocity identical with the symbol v introduced in (6.25) to denote the magnetic potential.

$$v_t = Qcu_z + Tu_t,$$
$$v_z = -Tu_z - (R/c)u_t. \tag{6.35}$$

When $\phi = 0$ (immovable material), this system reduces to

$$v_t = (1/\mu)u_z, \quad v_z = \epsilon u_t.$$

The system (6.35) may be rewritten in the following standard form [1],[2]:

$$u_z = \zeta^1,$$
$$u_t = \zeta^2,$$
$$v_z = -T\zeta^1 - (R/c)\zeta^2, \tag{6.36}$$
$$v_t = Qc\zeta^1 + T\zeta^2.$$

Here, we introduced the parametric variables ζ^1, ζ^2. The form (6.36) is convenient for the analysis of optimal control problems.

A typical boundary value problem for eqs. (6.36) arises if we consider the domain $\Sigma : a \le z \le b, \ 0 \le t \le t_1$, and introduce the initial and boundary conditions:

$$u(z,0) = u_0(z), \quad v(z,0) = v_0(z), \quad a \le z \le b,$$
$$u(a,t) = u_a(t), \quad u(b,t) = u_b(t), \quad 0 \le t \le t_1. \tag{6.37}$$

We shall assume that $u_0(z), v_0(z), u_a(t), u_b(t)$ are continuous and shall be looking for a *smooth* solution to this problem, i.e. the solution belonging to $W_1^2(\Sigma)$.

Introduce the cost functional

$$I = \int_a^b g(u(z,t_1), v(z,t_1))dz \tag{6.38}$$

with g differentiable with respect to each argument. We shall consider I as a functional of s with u, v calculated as solutions to the boundary value problem (6.36), (6.37). Assume that we have an admissible set $\mathcal{S}$ of material tensors $s : s \subset \mathcal{S}$; among the elements of this set we wish to find the element(s) for which the functional I takes its minimum value. The set S will be that of tensors S specified by (6.32)) and (6.33), with ϕ taking values in $(-\infty, \infty)$.

6.5.3 The necessary conditions of optimality

Following a standard scheme [1],[2] we introduce the Lagrange multipliers $\xi_1, \eta_1, \xi_2, \eta_2$, and construct the expression for the increment ΔI subject to constraints (6.36) and (6.37). We begin with the identity

$$\iint_\Sigma \{\xi_1(\Delta u_z - \Delta\zeta^1) + \eta_1(\Delta u_t - \Delta\zeta^2)$$
$$+ \xi_2[\Delta v_z + \Delta(T\zeta^1) + (1/c)\Delta(R\zeta^2)]$$
$$+ \eta_2[\Delta v_t - c\Delta(Q\zeta^1) - \Delta(T\zeta^2)]\}dzdt = 0,$$

that holds due to (6.36). Here, $\Delta(\cdot)$ denotes the increment of $(\cdot)$, i.e. the difference between the admissible and optimal values of the relevant quantity. In view of a possible appearance of a line Γ of discontinuity of the material tensor s, the double integral is represented as a sum of integrals over the subdomains Σ_1 and Σ_2 separated by some unknown curve Γ with unit tangent $T(z_s, t_s)$ and unit normal $N(t_s, -z_s)$.

By integrating by parts and by using the continuity of u, v across Γ, we rewrite the previous identity in the following form

$$\begin{aligned}
&\oint_\gamma \Delta u(\xi_1 t_s - \eta_1 z_s)ds \\
&\quad + \oint_\gamma \Delta v(\xi_2 t_s - \eta_2 z_s)ds + \oint_\Gamma \Delta u[\xi_1 t_s - \eta_1 z_s]_1^2 ds + \oint_\Gamma \Delta v[\xi_2 t_s - \eta_2 z_s]_1^2 ds \\
&\quad - \oint_\Gamma [(\partial u/\partial N)(\xi_1 t_s - \eta_1 z_s) + (\partial v/\partial N)(\xi_2 t_s - \eta_2 z_s)]_1^2 \Delta N ds \\
&\quad - \iint_\Sigma \{(\xi_{1z} + \eta_{1t})\Delta u + (\xi_{2z} + \eta_{2t})\Delta v + \xi_1 \Delta\zeta^1 + \eta_1 \Delta\zeta^2 \\
&\quad - \xi_2[\Delta(T\zeta^1) + (1/c)\Delta(R\zeta^2)] + \eta_2[c\Delta(Q\zeta^1) + \Delta(T\zeta^2)]\} dz dt = 0.
\end{aligned} \tag{6.39}$$

Here and below, γ denotes the contour of Σ, and $[\cdot]_1^2$ is the difference between the limit values of the relevant quantity on both sides of Γ. The last two members in the figure brackets in a double integral may be conveniently rewritten as

$$\begin{aligned}
&- \xi_2[T\Delta\zeta^1 + (R/c)\Delta\zeta^2] + \eta_2[Qc\Delta\zeta^1 + T\Delta\zeta^2] \\
&- \xi_2[(\Delta T)Z^1 + (1/c)(\Delta R)Z^2] + \eta_2[c(\Delta Q)Z^1 + (\Delta T)Z^2].
\end{aligned} \tag{6.40}$$

The symbols $Z^1 = U_z$, $Z^2 = U_t$ are referred to the admissible values of parametric variables $\zeta^1 = u_z$ and $\zeta^2 = u_t$.

Referring to the stationarity conditions

$$\xi_{1z} + \eta_{1t} = 0, \quad \xi_{2z} + \eta_{2t} = 0,$$

$$\xi_1 - \xi_2 T + \eta_2 Qc = 0, \quad \eta_1 - \xi_2(R/c) + \eta_2 T = 0,$$

we introduce potentials ω_1, ω_2 to satisfy their first pair:

$$\xi_i = -\omega_{it}, \ \ \eta_i = \omega_{iz}, \ \ i = 1, 2; \tag{6.41}$$

the second pair now takes the form:

$$\begin{aligned}
\omega_{1t} &= Qc\omega_{2z} + T\omega_{2t}, \\
\omega_{1z} &= -T\omega_{2z} - (R/c)\omega_{2t},
\end{aligned} \tag{6.42}$$

similar to (6.35).

We also apply conditions along Γ:

$$[\xi_1 t_s - \eta_1 z_s]_1^2 = [\xi_2 t_s - \eta_2 z_s]_1^2 = 0, \tag{6.43}$$

or, equivalently,

$$[\omega_{1s}]_1^2 = [\omega_{2s}]_1^2 = 0, \tag{6.44}$$

and

$$[(\partial u/\partial N)(\xi_1 t_s - \eta_1 z_s) + (\partial v/\partial N)(\xi_2 t_s - \eta_2 z_s)]_1^2 = 0. \tag{6.45}$$

In view of (6.41) and (6.44), the latter condition may be rewritten as

$$\omega_{1s}[\partial u/\partial N]_1^2 + \omega_{2s}[\partial u/\partial N]_1^2 = 0,$$

or, given the continuity of $\partial u/\partial s, \partial v/\partial s$ across Γ,

$$\omega_{1s}[\partial u/\partial N]_1^2 + \omega_{2s}[\partial v/\partial N]_1^2 - \omega_{1N}[\partial u/\partial s]_1^2 - \omega_{2N}[\partial v/\partial s]_1^2 = 0.$$

Applying (6.41) and (6.36), we rewrite this condition as

$$\xi_1[\zeta^1]_1^2 + \eta_1[\zeta^2]_1^2 - \xi_2[T\zeta^1 + (R/c)\zeta^2]_1^2 + \eta_2[Qc\zeta^1 + T\zeta^2]_1^2 = 0. \tag{6.46}$$

In this formula, the Lagrange multipliers $\xi_1, \ldots, \eta_2$ may be taken on either side (1 or 2) of the curve Γ. Eq. (6.46) serves as an additional condition used to specify the unknown interface Γ.

The multipliers $\xi_1, \ldots, \eta_2$ also satisfy the natural boundary conditions

$$\xi_2(a,t) = \xi_2(b,t) = 0, \quad 0 \le t \le t_1,$$

$$\left.\begin{aligned} \eta_1(z,t_1) &= -g_u(u(z,t_1), v(z,t_1)), \\ \eta_2(z,t_1) &= -g_v(u(z,t_1), v(z,t_1)). \end{aligned}\right\} \quad a \le z \le b. \tag{6.47}$$

The increment ΔI of the cost functional (6.38) may be expressed as

$$\begin{aligned} \Delta I &= \int_a^b [g(U(z,t_1), V(z,t_1)) - g(u(z,t_1), v(z,t_1))]dz \\ &= \int_a^b [g(U(z,t_1), V(z,t_1)) - g(u(z,t_1), v(z,t_1)) \\ &- g_u(u(z,t_1), v(z,t_1))\Delta u - g_v(u(z,t_1), v(z,t_1))\Delta v]dz \\ &+ \int_a^b [g_u(u(z,t_1).v(z,t_1))\Delta u + g_v(u(z,t_1), v(z,t_1))\Delta v]dz. \end{aligned} \tag{6.48}$$

The first two integrals in (6.39)

$$\int_\gamma [(\xi_1 t_s - \eta_1 z_s)\Delta u + (\xi_2 t_s - \eta_2 z_s)\Delta v]ds,$$

are reduced, by (6.37), to the form

$$\int_{\gamma_1} [\eta_1 \Delta u + \eta_2 \Delta v] ds,$$

where γ_1 denotes the top side $t = t_1, a \le z \le b$, of the rectangle Σ; on this side, $z_s = -1$. The last expression equals

$$-\int_a^b [\eta_1 \Delta u + \eta_2 \Delta v] dz;$$

by (6.47), it is equivalent to

$$\int_a^b [g_u \Delta u + g_v \Delta v] dz.$$

Referring to (6.47), we conclude that the expression (6.48) for ΔI reduces to

$$\begin{aligned} \Delta I = \int_a^b & [g(U(z,t_1), V(z,t_1)) - g(u(z,t_1), v(z,t_1)) \\ & - g_u(u(z,t_1), v(z,t_1))\Delta u - g_v(u(z,t_1), v(z,t_1))\Delta v] dz \\ & - \int_{\gamma_1} [(\xi_1 t_s - \eta_1 z_s)\Delta u + (\xi_2 t_s - \eta_2 z_s)\Delta v] ds. \end{aligned} \tag{6.49}$$

Due to the assumed continuity of u, v (as well as of U, V)), we observe that if the control ϕ is exposed to a local change in a narrow strip D_δ of length δ and width δ^2, then the first integral in (6.49) becomes of order δ^2 whereas the last integral remains of order δ. By (6.39),(6.40), (6.44) and (6.45) we conclude that, as $\delta \to 0$, the main part of ΔI is given by the formula

$$\Delta I = \int\int_{D\delta} E dz dt, \tag{6.50}$$

with

$$\begin{aligned} E &= \xi_2[(\Delta T)Z^1 + (1/c)(\Delta R)Z^2] - \eta_2[c(\Delta Q)Z^1 + (\Delta T)Z^2] \\ &= -\omega_{2t}[(\Delta T)U_2 + (1/c)(\Delta R)U_t] - \omega_{2z}[c(\Delta Q)U_z + (\Delta T)U_t] \end{aligned} \tag{6.51}$$

The integral in (6.50) appeared as a result of transformation of the last integral in (6.49). The admissible values $Z^1 = U_z, Z^2 = U_t$ of the parametric variables should be determined along with u, v once the increment Δs of a material tensor is specified. As indicated before, we assume that $\Delta s \neq 0$ within a narrow strip D_δ of the length δ and width δ^2 in a (z,t)-plane. The increment ΔI then differs from the integral

$$\int\int_{D\delta} E dz dt$$

by terms of higher order of magnitude in δ, so the inequality

$$E \ge 0 \tag{6.52}$$

will be necessary for a strong relative minimum of I.

6.6 Transformation of the expression for ΔI : the strip test

To eliminate Z^1, Z^2 from (6.50), we apply a strong local variation $\Delta s = \bar{s} - s$ of a material tensor s. Here and below, the bar over any symbol will relate to an admissible value of the relevant quantity; the symbol with no bar will relate to its optimal value. For the material tensor s defined by (6.32), an admissible value $\bar{s}$ is given by the expression

$$\bar{s} = -\bar{Q}a_{23}a_{23} - i\bar{T}(a_{23}a_{24} + a_{24}a_{23}) + \bar{R}a_{24}a_{24}, \tag{6.53}$$

with coefficients $\bar{Q}, \bar{T}$ and $\bar{R}$ defined by eqs. (6.33), with ϕ replaced by $\bar{\phi}$.

The strong variation will be assumed non-zero within a narrow strip D_δ of width δ^2 and length δ, where δ is a small parameter: $\delta \to 0$. In other words, the strip is occupied by an admissible material moving with velocity $\bar{v}$. The direction cosines of the strip will be z_τ, t_τ, their ratio z_τ/t_τ denoted by V. As in Chapter 3 (section 3.6 and below), we will assume that $V < c$.

The symbols Z^1, Z^2 may now be eliminated from (6.50) by virtue of the compatibility conditions

$$\begin{aligned} &Z^1 z_\tau + Z^2 t_\tau = \zeta^1 z_\tau + \zeta^2 t_\tau, \\ &-[\bar{T}Z^1 + (\bar{R}/c)Z^2]z_\tau + [\bar{Q}cZ^1 + \bar{T}Z^2]t_\tau \\ &= -[T\zeta^1 + (R/c)\zeta^2]z_\tau + [Qc\zeta^1 + T\zeta^2]t_\tau, \end{aligned} \tag{6.54}$$

expressing the continuity of u, v across the strip's interface.

The determinant $\bar{D}$ of this system

$$\bar{D} = -(\bar{R}/c)z_\tau^2 + 2\bar{T}z_\tau t_\tau - \bar{Q}ct_\tau^2 \tag{6.55}$$

may be rewritten as

$$\bar{D} = -\bar{R}ct_\tau^2[\tanh\psi - \tanh(\bar{\phi} + \bar{\theta})][\tanh\psi - \tanh(\bar{\phi} - \bar{\theta})], \tag{6.56}$$

where

$$\tanh\psi = V/c, \;\; \tanh\bar{\phi} = \bar{v}/c, \;\; \tanh\bar{\theta} = 1/c\sqrt{\bar{\epsilon}\bar{\mu}}.$$

Here $1/\sqrt{\bar{\epsilon}\bar{\mu}}$ denotes the speed of light in an admissible material.

For Z^1 and Z^2, we obtain

$$Z^1 = \zeta^1 \, (D/\bar{D}) + (-\Delta(R/c)z_\tau + (\Delta T)t_\tau) \, (\zeta^1 z_\tau + \zeta^2 t_\tau)(1/\bar{D}),$$

$$Z^2 = \zeta^2(D/\bar{D}) + ((\Delta T)z_\tau - \Delta(Qc)t_\tau)(\zeta^1 z_\tau + \zeta^2 t_\tau)(1/\bar{D}),$$

where D is defined by the same expressions as (6.55), (6.56), with the bars removed.

The integrand E in (6.50) now becomes equal to

$$E = \{[\xi_2(\Delta T) - \eta_2 \Delta(Qc)]\zeta^1 + [\xi_2 \Delta(R/c) - \eta_2 \Delta T]\zeta^2\}(D/\bar{D})$$
$$+ \{[\xi_2 \Delta T - \eta_2 \Delta(Qc)][-\Delta(R/c)z_\tau + (\Delta T)t_\tau]$$
$$+ [\xi_2 \Delta(R/c) - \eta_2 \Delta T][(\Delta T)z_\tau - \Delta(Qc)t_\tau]\}(\zeta^1 z_\tau + \zeta^2 t_\tau)(1/\bar{D}).$$

Referring to (6.36) and (6.41), we reduce this expression after some calculation to the form

$$E = [-\Delta(Qc)u_z\omega_{2z} - \Delta(R/c)u_t\omega_{2t} - \Delta T(u_z\omega_{2t} + u_t\omega_{2z})](D/\bar{D})$$
$$+ [\Delta(Qc)\Delta(R/c) - (\Delta T)^2](1/\bar{D})(u_z z_\tau + u_t t_\tau)(\omega_{2z} z_\tau + \omega_{2t} t_\tau), \quad (6.57)$$

or, equivalently,

$$E = -\Delta(Qc)u_z\omega_{2z} - \Delta(R/c)u_t\omega_{2t} - \Delta T(u_z\omega_{2t} + u_t\omega_{2z})$$
$$- (1/\bar{D})[\Delta(Qc)u_z t_\tau - \Delta(R/c)u_t z_\tau - (\Delta T)(u_z z_\tau - u_t t_\tau)][\Delta(Qc)\omega_{2z} t_\tau$$
$$- \Delta(R/c)\omega_{2t} z_\tau - (\Delta T)(\omega_{2z} z_\tau - \omega_{2t} t_\tau)]. \quad (6.58)$$

By a standard argument, we require that $E \geq 0$ for a strong relative minimum. This inequality should hold for all admissible slopes $V = z_\tau/t_\tau$ of the strip of variation.

The range of values of ψ ($\tanh\psi = V/c$) admissible for the strip test $E \geq 0$, is defined by

$$D/\bar{D} = R[\tanh\psi - \tanh(\phi + \theta)][\tanh\psi - \tanh(\phi - \theta)]/(\bar{R}$$
$$[\tanh\psi - \tanh(\bar{\phi} + \bar{\theta})][\tanh\psi - \tanh(\bar{\phi} - \bar{\theta}]) \geq 0. \quad (6.59)$$

Since both $R, \bar{R} < 0$, this inequality means that the velocity V of motion of the interface separating optimal and admissible materials should, in both materials, stay in the same relation to the phase velocities $(v \pm 1/\sqrt{\epsilon\mu})/(1 \pm v/c^2\sqrt{\epsilon\mu})$ of light in the relevant moving medium. Particularly, if V exceeds both of the phase velocities in an optimal material, it should also exceed them in admissible material.

The range of the values for $\phi, \bar{\phi}$ admissible for the strip test $E \geq 0$ is given by one of the following two pairs of inequalities:

$$\psi - \theta < \phi < \psi + \theta, \quad \psi - \bar{\theta} < \bar{\phi} < \psi + \bar{\theta}, \quad (6.60)$$

or

$$\phi < \psi - \theta, \quad \bar{\phi} < \psi - \bar{\theta}. \quad (6.61)$$

These ranges guarantee a regular transmission of dynamic disturbances across a strip of variation; we stress that *both* inequalities in each pair (6.60) or (6.61) should apply simultaneously. Because $R, \bar{R} < 0$, we see from (6.56) that D and $\bar{D}$ are both negative for case (6.60), and both positive for (6.61).

The angle ψ in both (6.60) and (6.61) may take arbitrary values on the real axis $(-\infty, +\infty)$.

In what follows we shall consider various options offered by the requirement $E \geq 0$ implemented with the observance of (6.60) or (6.61). No special assumptions will be made about u and ω_2 entering the expressions (6.57) and (6.58) for E. These functions become more specific once a set of boundary conditions for ω_2 is generated by a selected cost functional, i.e., the one introduced by (6.38).

6.7 A polycrystal in space-time

It will be assumed in this section that all of the tensors s (see (6.30)) that constitute an admissible set S have the same pair of eigenvalues $\epsilon c, 1/\mu c$; as to their eigentensors a'_{23}, a'_{24}, they may be different for any two tensors in S. This difference is due to the relative material motion of fragments of the same isotropic dielectric moving at different velocities. An assemblage of such fragments constitutes a spatio-temporal material polycrystal. The admissible ranges for $\phi, \bar{\phi}$ are specified by (6.60), (6.61); we want to find the angle ϕ that gives the functional I the least possible value, which means the inequality $E \geq 0$ following from a strip test.

Define w and Δw, respectively, as

$$w = -Qcu_z\omega_{2z} - (R/c)u_t\omega_{2t} - T(u_z\omega_{2t} + u_t\omega_{2z}), \tag{6.62}$$

$$\Delta w = -(\Delta Q)cu_z\omega_{2z} - \Delta(R/c)u_t\omega_{2t} - \Delta T(u_z\omega_{2t} + u_t\omega_{2z}). \tag{6.63}$$

This expression for Δw includes first order terms in $\Delta\phi = \bar{\phi} - \phi$ at the rhs of (6.57). We find the stationary values ϕ as those making such terms vanish: $\partial w/\partial\phi = 0$. With the reference to (6.33) we obtain, after some calculation,

$$(u_z\omega_{2t} + u_t\omega_{2z})\tanh^2\phi + 2(cu_z\omega_{2z} + \frac{1}{c}u_t\omega_{2t})\tanh\phi + (u_z\omega_{2t} + u_t\omega_{2z}) = 0. \tag{6.64}$$

To characterize the roots of this equation we have to consider three different situations as suggested by the expression for the discriminant of (6.64)

$$\Phi = c^2\left(u_z^2 - \frac{1}{c^2}u_t^2\right)\left(\omega_{2z}^2 - \frac{1}{c^2}\omega_{2t}^2\right). \tag{6.65}$$

1. Case when $\Phi > 0$, and both parentheses in (6.65) are positive. Then

$$\tanh\phi = -\tanh\frac{\alpha+\beta}{2},$$

or

$$\phi = -\frac{\alpha+\beta}{2}. \tag{6.66}$$

Here, α and β are, respectively, the angles defined by

$$\frac{u_z}{\sqrt{u_z^2 - \frac{1}{c^2}u_t^2}} = \cosh\alpha, \quad \frac{\frac{1}{c}u_t}{\sqrt{u_z^2 - \frac{1}{c^2}u_t^2}} = \sinh\alpha,$$
$$\frac{\omega_{2z}}{\sqrt{\omega_{2z}^2 - \frac{1}{c^2}\omega_{2t}^2}} = \cosh\beta, \quad \frac{\frac{1}{c}\omega_{2t}}{\sqrt{\omega_{2z}^2 - \frac{1}{c^2}\omega_{2t}^2}} = \sinh\beta. \tag{6.67}$$

2. Case when $\Phi > 0$, and both parentheses in (6.65) are negative. Then, again, ϕ is given by eqn. (6.66), but with α, β defined by

$$\frac{\frac{1}{c}u_t}{\sqrt{\frac{1}{c^2}u_t^2 - u_z^2}} = \cosh\alpha, \quad \frac{u_z}{\sqrt{\frac{1}{c^2}u_t^2 - u_z^2}} = \sinh\alpha,$$
$$\frac{\frac{1}{c}\omega_{2t}}{\sqrt{\frac{1}{c^2}\omega_{2t}^2 - \omega_{2z}^2}} = \cosh\beta, \quad \frac{\omega_{2z}}{\sqrt{\frac{1}{c^2}\omega_{2t}^2 - \omega_{2z}^2}} = \sinh\beta. \tag{6.68}$$

3. Case when $\Phi < 0$. Then eqn. (6.64) has no real roots, and the function $w(\phi)$ is monotonic on the real ϕ-axis.

Referring to (6.62) and (6.33), we conclude that, as $\phi \to \pm\infty$, the expression w asymptotically becomes

$$w \sim -ce^{\pm 2\phi} x\sigma_\pm\tau_\pm, \quad x = \frac{1}{\mu c} - \epsilon c, \tag{6.69}$$

with

$$\sigma_\pm = u_z \pm \frac{1}{c}u_t, \quad \tau_\pm = \omega_{2z} \pm \frac{1}{c}\omega_{2t}. \tag{6.70}$$

Because $x < 0$, the sign of w at $\phi \to \pm\infty$ is the same as that of the product $\sigma_+\tau_+(\sigma_-\tau_-)$. Particularly, for cases 1 and 2, when $\sigma_+\tau_-\sigma_-\tau_- > 0$, this means that $w(\pm\infty)$ are of the same sign. More specifically, $w\mid_{\phi\to\infty} = w\mid_{\phi\to-\infty} = \pm\infty$ if $\sigma_+\tau_+, \sigma_-\tau_-$ are both positive (negative).

For case 3, when $\sigma_+\tau_+\sigma_-\epsilon_- < 0$, the values $w(+\infty)$ and $w(-\infty)$ have opposite signs. Specifically, we get

$$w\big|_{\phi\to+\infty} = +\infty, \quad w\big|_{\phi\to-\infty} = -\infty \text{ if } \sigma_+\tau_+ > 0, \quad \sigma_-\tau_- < 0.$$
$$w\big|_{\phi\to+\infty} = -\infty, \quad w\big|_{\phi\to-\infty} = +\infty \text{ if } \sigma_+\tau_+ < 0, \quad \sigma_-\tau_- > 0. \tag{6.71}$$

Minimum of $w(\phi)$ in case 3 is therefore $-\infty$, i.e. ineq. $E \geq 0$ can take place with $\phi = \pm\infty$. We now have to consider the cases 1 and 2.

We calculate Δw (see (6.63)) for these cases. For a polycrystal, we have

$$\begin{aligned}\Delta Q = \Delta R &= x\Delta(\cosh^2\phi) = x\Delta\left(\frac{1}{1-\tanh^2\phi}\right)\\ &= x\frac{1}{(1-\tanh^2\bar\phi)(1-\tanh^2\phi)}(\tanh^2\bar\phi - \tanh^2\phi),\end{aligned} \tag{6.72}$$

$$\begin{aligned}\Delta T &= x\Delta(\sinh\phi\cosh\phi) = x\Delta\left(\frac{\tanh\phi}{1-\tanh^2\phi}\right)\\ &= x\frac{1}{(1-\tanh^2\bar\phi)(1-\tanh^2\phi)}\end{aligned}$$

$$(\tanh\bar\phi - \tanh\phi)(1+\tanh\phi\tanh\bar\phi),$$

and the expression for Δw takes the form (case 1)

$$\begin{aligned}\Delta w &= -(\Delta Q)cu_z\omega_{2z} - \frac{1}{c}(\Delta R)u_t\omega_{2t} - (\Delta T)(u_z\omega_{2t} + u_t\omega_{2z}) = -\sqrt{\sigma_+\sigma_-\tau_+\tau_-}\\ &\quad[(\Delta Q)c\cosh\alpha\,\cosh\beta + (\Delta Q)c\sinh\alpha\,\sinh\beta\\ &\quad-\,(\Delta T)c(\cosh\alpha\,\sinh\beta + \sinh\alpha\,\cosh\beta)]\\ &\quad= -c\sqrt{\sigma_+\sigma_-\tau_+\tau_-}[(\Delta Q)\cosh(\alpha+\beta) + \Delta T\sinh(\alpha+\beta)]\\ &\quad= -cx\frac{\sqrt{\sigma_+\sigma_-\tau_+\tau_-}}{(1-\tanh^2\bar\phi)(1-\tanh^2\phi)}(\tanh\bar\phi - \tanh\phi)\\ &\quad\big[(\tanh\bar\phi + \tanh\phi)\cosh(\alpha+\beta) + (1+\tanh\phi\tanh\bar\phi)\sinh(\alpha+\beta)\big]\\ &\quad= -cx\frac{\sqrt{\sigma_+\sigma_-\tau_+\tau_-}}{(1-\tanh^2\bar\phi)(1-\tanh^2\phi)}\cosh^2\frac{\alpha+\beta}{2}(\tanh\bar\phi - \tanh\phi)\\ &\quad\left[(\tanh\bar\phi + \tanh\phi)\left(1+\tanh^2\frac{\alpha+\beta}{2}\right) + (1+\tanh\phi\tanh\bar\phi)\cdot 2\tanh\frac{\alpha+\beta}{2}\right].\end{aligned} \tag{6.73}$$

When $\phi = -\frac{\alpha+\beta}{2}$, the expression in the square brackets reduces to

$$\left(1-\tanh^2\frac{\alpha+\beta}{2}\right)\left(\tanh\bar\phi + \tanh\frac{\alpha+\beta}{2}\right),$$

and Δw becomes equal to

$$\Delta w = -cx\frac{\sqrt{\sigma_+\sigma_-\tau_+\tau_-}}{(1-\tanh^2\bar\phi)\left(1-\tanh^2\frac{\alpha+\beta}{2}\right)}\left(\tanh\bar\phi + \tanh\frac{\alpha+\beta}{2}\right)^2 \tag{6.74}$$

Observe that this expression does not depend on ψ; also, since $x<0$, we have $\Delta w > 0$.

The terms in the second and third lines of (6.58) depend on ψ; we represent them as

$$W = -\frac{1}{\bar{D}}\Theta\Omega, \tag{6.75}$$

with

$$\begin{aligned}
\Theta &= (\Delta Q)cu_z t_\tau - \frac{1}{c}(\Delta R)u_t z_\tau - \Delta T(u_z z_\tau - u_t t_\tau),\\
\Omega &= (\Delta Q)c\omega_{2z} t_\tau - \frac{1}{c}(\Delta R)\omega_{2t} z_\tau - \Delta T(\omega_{2z} z_\tau - \omega_{2t} t_\tau).
\end{aligned} \tag{6.76}$$

Considering case 1, we refer to eqs. (6.67) and (6.70); a convenient expression for $\bar{D}$ is given by (6.56). By (6.67), (6.70) and (6.72), (6.66), the formulae (6.76) become

$$\begin{aligned}
\Theta &= c\sqrt{\sigma_+\sigma_-}t_\tau \cosh\alpha[\Delta Q(1-\tanh\alpha\tanh\psi) - \Delta T(\tanh\psi - \tanh\alpha)]\\
&= cx\frac{\sqrt{\sigma_+\sigma_-}t_\tau\cosh\alpha}{(1-\tanh^2\bar{\phi})\left(1-\tanh^2\frac{\alpha+\beta}{2}\right)}\left(\tanh\bar{\phi}+\tanh\frac{\alpha+\beta}{2}\right)\\
&\quad\left[\left(\tanh\bar{\phi}-\tanh\frac{\alpha+\beta}{2}\right)(1-\tanh\alpha\tanh\psi)\right.\\
&\quad-\left.\left(1-\tanh\frac{\alpha+\beta}{2}\tanh\bar{\phi}\right)(\tanh\psi-\tanh\alpha)\right];\\
\Omega &= cx\frac{\sqrt{\tau_+\tau_-}t_\tau\cosh\beta}{(1-\tanh^2\bar{\phi})\left(1-\tanh^2\frac{\alpha+\beta}{2}\right)}\left(\tanh\bar{\phi}+\tanh\frac{\alpha+\beta}{2}\right)\\
&\quad\left[\left(\tanh\bar{\phi}-\tanh\frac{\alpha+\beta}{2}\right)(1-\tanh\beta\tanh\psi)\right.\\
&\quad-\left.\left(1-\tanh\frac{\alpha+\beta}{2}\tanh\bar{\phi}\right)(\tanh\psi-\tanh\beta)\right].
\end{aligned}$$

In view of (6.56), the expression (6.75) takes on the form

$$\begin{aligned}
W = -\frac{1}{\bar{D}}\Theta\Omega &= \frac{cx^2\sqrt{\sigma_+\sigma_-\tau_+\tau_-}\cosh\alpha\cosh\beta\left(\tanh\bar{\phi}+\tanh\frac{\alpha+\beta}{2}\right)^2}{\bar{R}[\tanh\psi-\tanh(\bar{\phi}+\theta)][\tanh\psi-\tanh(\bar{\phi}-\theta)]}\\
&\cdot\frac{\left(1-\tanh\frac{\alpha+\beta}{2}\tanh\bar{\phi}\right)^2}{(1-\tanh^2\bar{\phi})^2\left(1-\tanh^2\frac{\alpha+\beta}{2}\right)^2}KL,
\end{aligned} \tag{6.77}$$

with

$$
\begin{aligned}
K &= \tanh\left(\bar{\phi} - \frac{\alpha+\beta}{2}\right)(1 - \tanh\alpha\tanh\psi) - (\tanh\psi - \tanh\alpha) \\
&= (1 - \tanh\alpha\tanh\psi)\left[\tanh\left(\bar{\phi} - \frac{\alpha+\beta}{2}\right) - \tanh(\psi - \alpha)\right] \\
&= (1 - \tanh\alpha\tanh\psi)\left[1 - \tanh\left(\bar{\phi} - \frac{\alpha+\beta}{2}\right)\tanh(\psi - \alpha)\right]\tanh\left(\bar{\phi} - \psi + \frac{\alpha-\beta}{2}\right),
\end{aligned}
\tag{6.78}
$$

$$
\begin{aligned}
L &= \tanh\left(\bar{\phi} - \frac{\alpha+\beta}{2}\right)(1 - \tanh\beta\tanh\psi) - (\tanh\psi - \tanh\beta) \\
&= (1 - \tanh\beta\tanh\psi)\left[1 - \tanh\left(\bar{\phi} - \frac{\alpha+\beta}{2}\right)\tanh(\psi - \beta)\right]\tanh\left(\bar{\phi} - \psi - \frac{\alpha-\beta}{2}\right).
\end{aligned}
$$

Because $\bar{R} < 0$, the expression (6.77) for W has the sign of

$$
-\frac{KL}{[\tanh\psi - \tanh(\bar{\phi} + \theta)][\tanh\psi - \tanh(\bar{\phi} - \theta)]},
$$

or, by (6.78), the sign of

$$
-\frac{\tanh\left(\bar{\phi} - \psi + \frac{\alpha-\beta}{2}\right)\tanh\left(\bar{\phi} - \psi - \frac{\alpha-\beta}{2}\right)}{\tanh(\bar{\phi} - \psi + \theta)\tanh(\bar{\phi} - \psi - \theta)}. \tag{6.79}
$$

By (6.60), we have

$$
-\theta \le \bar{\phi} - \psi \le \theta,
$$

i.e.

$$
|\ \bar{\phi} - \psi\ | \le \theta; \tag{6.80}
$$

also, by (6.61), we have

$$
|\ \bar{\phi} - \psi\ | \ge \theta. \tag{6.81}
$$

The ratio in (6.80) does not exist when $\left|\bar{\phi} - \psi\right| = \theta$, unless $\theta = \left|\frac{\alpha-\beta}{2}\right|$; in the latter case, the said ratio reduces to unity. The expression (6.78) for W may then be calculated for every value of $\left|\bar{\phi} - \psi\right|$ belonging to the reference intervals (6.81) and (6.82), so the sum $E = \Delta w + W$ is well defined for *all admissible* values of $\left|\bar{\phi} - \psi\right|$. We conclude that the increment E of the functional exists and may become non-negative *if and only if* the phase velocity θ in a paternal material matches the half angle $(\alpha - \beta)/2$ between the complex vectors grad$u$ and gradω_2. This match may generally not occur, that is, our original problem may appear to be ill-posed.

We will find a way out of this contradiction if we assume that, along with a paternal material with phase velocity θ, there are also available the *spatio-temporal polycrystals* produced by mixing (on a microscale in space-time) different fragments of it participating in a relative material motion along the z-axis. As shown in Chapter 3, such polycrystals are characterized by the effective properties $\mathcal{E}, M$ that occupy the hyperbola $\mathcal{E}/M = \epsilon/\mu$ in the plane $(\mathcal{E}c, 1/Mc)$. Moving along this hyperbola, we will find a point that represents, in a proper frame, a material with a required value of the phase velocity. An additional freedom offered by such extension of the original set containing one paternal material, therefore works towards resolution of the above contradiction.

References

1. Lurie, K.A.: The Mayer-Bolza problem for multiple integrals and optimization of the behavior of systems with distributed parameters. Prikladnaya Matematika i Mekhanika (PMM) = Applied Mathematics and Mechanics, **27**, No. 2, 842–853 (1963)
2. Lurie, K.A.: The Mayer-Bolza problem for multiple integrals: some optimum problems for elliptic differential equations arising in magnetohydrodynamics. Topics in Optimization, G. Leitmann (ed), Academic Press, New York, 147–193 (1967)
3. Lurie, K.A.: On the optimal distribution of the resistivity tensor of the working medium in the channel of a MHD generator. Prikladnaya Matematika i Mekhanika (PMM) = Applied Mathematics and Mechanics, **34**, No. 2, 270–291 (1970)
4. Lurie, K.A.: Effective properties of smart elastic laminates and the screening phenomenon. International Journal of Solids and Structures, **34**, No. 13, 1633–1643 (1997)
5. Lurie, K.A.: G-closures of material sets in space-time and perspectives of dynamic control in the coefficients of linear hyperbolic equations. Journal of Control and Cybernetics, **27**, No. 2, 283–294 (1998)
6. Lurie, K.A.: Control in the coefficients of linear hyperbolic equations via spatio-temporal composites. In Homogenization, edited by V. Berdichevsky, V. Jikov, G. Papanicolaou, World Scientific, 285–315 (1999)
7. Lurie, K.A.: Applied optimal control theory of distributed systems. Plenum Press, 499 pp (1993)

Appendix: 1

Comment on eqs. (2.46), (2.49), and (2.50)

Consider a periodic array (2.43), (2.44) of segments distributed along the ζ-axis.

The segments have lengths $\ell_1 = m_1\delta$, $\ell_2 = m_2\delta$, and are occupied, respectively, by materials 1 and 2 immovable in the laboratory frame (z, t).

A general solution to the system (2.42) is given by

$$\left.\begin{aligned} \bar{u} &= Ae^{s\frac{\zeta}{V-a_1}} + Be^{s\frac{\zeta}{V+a_1}}, \\ \bar{v} &= -\gamma_1\left(Ae^{s\frac{\zeta}{V-a_1}} - Be^{s\frac{\zeta}{V+a_1}}\right), \end{aligned}\right\} -\ell_1 \le \zeta \le 0, \tag{A1.1}$$

$$\left.\begin{aligned} \bar{u} &= Ce^{s\frac{\zeta}{V-a_2}} + De^{s\frac{\zeta}{V+a_2}}, \\ \bar{v} &= -\gamma_2\left(Ce^{s\frac{\zeta}{Va_2}} - De^{s\frac{\zeta}{V+a_2}}\right), \end{aligned}\right\} 0 \le \zeta \le \ell_2. \tag{A1.2}$$

Here $\gamma_i = \rho_i a_i = k_i/a_i = \sqrt{k_i\rho_i}$, $i = 1, 2$.

By Floquet theory,

$$\bar{u}(\zeta) = e^{\mu\delta}\bar{u}(\zeta - \delta), \quad \bar{v}(\zeta) = e^{\mu\delta}\bar{v}(\zeta - \delta), \tag{A1.3}$$

where μ is the characteristic exponent. Given (A1.1) and (A1.3), we represent a solution in the interval $\ell_2 \le \zeta \le \ell_1 + \ell_2$ as

$$\begin{aligned} \bar{u} &= e^{\mu\delta}\left(Ae^{s\frac{\zeta-\delta}{V-a_1}} + Be^{s\frac{\zeta-\delta}{V+a_1}}\right), \\ \bar{v} &= -\gamma_1 e^{\mu\delta}\left(Ae^{s\frac{\zeta-\delta}{V-a_1}} - Be^{s\frac{\zeta-\delta}{V+a_1}}\right). \end{aligned}$$

The compatibility conditions

$$[u]_{\zeta=0^-}^{\zeta=0^+} = [v]_{\zeta=0^-}^{\zeta=0^+} = [u]_{\zeta=\ell_2-0}^{\zeta=\ell_2+0} = [v]_{\zeta=\ell_2-0}^{\zeta=\ell_2+0} = 0$$

produce a linear system

$$\begin{aligned} A + B &= C + D, \\ -\gamma_1(A - B) &= -\gamma_2(C - D), \end{aligned} \tag{A1.4}$$

$$e^{\mu\delta}\left(Ae^{-s\frac{\ell_1}{V-a_1}} + Be^{-s\frac{\ell_1}{V+a_1}}\right) = Ce^{s\frac{\ell_2}{V-a_2}} + De^{s\frac{\ell_2}{V+a_2}},$$

$$-\gamma_1 e^{\mu\delta}\left(Ae^{-s\frac{\ell_1}{V-a_1}} - Be^{-s\frac{\ell_1}{V+a_1}}\right) = -\gamma_2\left(ce^{s\frac{\ell_2}{V-a_2}} - De^{s\frac{\ell_2}{V+a_2}}\right),$$

with determinant

$$\begin{vmatrix} 1 & 1 & 1 & 1 \\ -\gamma_1 & \gamma_1 & -\gamma_2 & \gamma_2 \\ Ye^{-s\frac{\ell}{V-a_1}} & Ye^{-s\frac{\ell_1}{V+a_1}} & e^{s\frac{\ell_2}{V-a_2}} & e^{s\frac{\ell_2}{V+a_2}} \\ -\gamma_1 Ye^{-s\frac{\ell_1}{V-a_1}} & \gamma_1 Ye^{-s\frac{\ell_1}{V+a_1}} & -\gamma_2 e^{s\frac{\ell_2}{V-a_2}} & \gamma_2 e^{s\frac{\ell_2}{V+a_2}} \end{vmatrix}, \tag{A1.5}$$

where

$$Y = e^{\mu\delta}. \tag{A1.6}$$

By setting the determinant (A1.5) equal to zero, we obtain, after some calculation,

$$Y^2 e^{-2s\frac{V\ell_1}{V^2-a_1^2}} - 2Y[c_1c_2 + \sigma s_1 s_2] + e^{2s\frac{V\ell_2}{V^2-a_2^2}} = 0\,. \tag{A1.7}$$

Here we introduced notation

$$\begin{aligned} c_1 &= \frac{1}{2}\left(e^{-\frac{s\ell_1}{V-a_1}} + e^{-s\frac{\ell_1}{V+a_1}}\right), \\ c_2 &= \frac{1}{2}\left(e^{\frac{s\ell_1}{V-a_2}} + e^{s\frac{\ell_2}{V+a_2}}\right), \\ s_1 &= \frac{1}{2}\left(e^{-s\frac{\ell_1}{V-a_1}} - e^{-s\frac{\ell_1}{V+a_1}}\right), \\ s_2 &= \frac{1}{2}\left(e^{s\frac{\ell_2}{V+a_2}} - e^{s\frac{\ell_2}{V-a_2}}\right); \end{aligned}$$

parameter δ is defined by (2.47).

We now check by direct inspection that

$$e^{2s\frac{V\ell_1}{V^2-a_1^2}}[c_1c_2 + \sigma s_1 s_2] = e^{V\left(\frac{\theta_1}{a_1}+\frac{\theta_2}{a_2}\right)}(\cosh\theta_1\cosh\theta_2 + \sigma\sinh\theta_1\sinh\theta_2),$$

and

$$e^{2sV\left(\frac{\ell_1}{V^2-a_1^2}+\frac{\ell_2}{V^2-a_2^2}\right)} = e^{2V\left(\frac{\theta_1}{a_1}+\frac{\theta_2}{a_2}\right)},$$

with symbols θ_1, θ_2 defined by (2.47). Equation (A1.7) now takes on the form

$$Y^2 - 2Ye^{V\left(\frac{\theta_1}{a_1}+\frac{\theta_1}{a_2}\right)}(\cosh\theta_1\cosh\theta_2+\sigma\sinh\theta_1\sinh\theta_2)+e^{2V\left(\frac{\theta_1}{a_1}+\frac{\theta_2}{a_2}\right)} = 0. \quad \text{(A1.8)}$$

We look for the roots of this equation presented as

$$Y_{1,2} = e^{V\left(\frac{\theta_1}{a_1}+\frac{\theta_2}{a_2}\right)\pm\chi}. \quad \text{(A1.9)}$$

The sum of the roots equals

$$2e^{V\left(\frac{\theta_1}{a_1}+\frac{\theta_2}{a_2}\right)}\cosh\chi;$$

this becomes consistent with (A1.8) if parameter χ is defined by the equation

$$\cosh\chi = \cosh\theta_1\cosh\theta_2 + \sigma\sinh\theta_1\sinh\theta_2,$$

introduced in (2.47). By (A1.6) and (A1.9) we conclude that the characteristic exponents $\mu_{1,2}$ are specified as

$$\mu_{1,2}\delta = V\left(\frac{\theta_1}{a_1}+\frac{\theta_2}{a_2}\right) \pm \chi, \quad \text{(A1.10)}$$

in full accordance with (2.46).

By using (2.47), we, after some calculation, rewrite eq. (2.48) as

$$\chi = s\delta\frac{a_1a_2}{\Delta_1\Delta_2}\sqrt{(V^2\tilde{\rho}-\tilde{k})\left(V^2\left(\frac{\tilde{1}}{k}\right)-\left(\frac{\tilde{1}}{\rho}\right)\right)}; \quad \text{(A1.11)}$$

here Δ_i is defined by (2.28).

With reference to (2.47) and (A1.11), we rewrite (A1.10) as

$$\mu_{1,2}\delta = \frac{s\delta}{\Delta_1\Delta_2}\left[V(V^2-\widetilde{a^2}) \pm \sqrt{(V^2\tilde{\rho}-\tilde{k})\left(V^2\left(\frac{\tilde{1}}{k}\right)-\left(\frac{\tilde{1}}{\rho}\right)\right)}\right]. \quad \text{(A1.12)}$$

The system (2.49) for E, G, H now follows from the formulae for $P(\mu,\zeta), Q(\mu,\zeta)$ on p. 28 along with eqs. (2.45) and (A1.4). As to eqn. (2.50) for $v_{1,2} = V - \frac{s}{\mu_{1,2}}$, it follows from (A1.12) after some algebraic work.

Appendix: 2

Comment on eqs. (3.47)

If a plane electromagnetic wave travels along the z-axis, then its electromagnetic field is characterized by the electromagnetic tensors F and f specified by (3.21). The material tensor s participating in the constitutive relation (3.33) is given for an immovable material by the formula

$$s = -\frac{1}{\mu c} a_{23} a_{23} - \epsilon c a_{24} a_{24}.$$

If the dielectric is brought into motion with a uniform speed v along the x_3-axis, then the relevant expression for s becomes

$$s = -\frac{1}{\mu c} a'_{23} a'_{23} - \epsilon c a'_{24} a'_{24}, \tag{A2.1}$$

with the "primed" tensors a'_{23}, a'_{24} given by (c.f. (3.22))

$$a'_{23} = a_{23}\cosh\phi + i a_{24}\sinh\phi, a'_{24} = -i a_{23}\sinh\phi + a_{24}\cosh\phi,$$

and the angle ϕ defined by $\tanh\phi = v/c$. By referring to (3.21), (3.6) and (A2.1), we reduce the material relation (3.33) to the system of two equations

$$Q u_{x_3} + iT u_{x_4} = i v_{x_4}, \quad -T u_{x_3} - iR u_{x_4} = v_{x_3}, \tag{A2.2}$$

with parameters Q, T, R defined by (3.48). Consider now two dielectric media moving with different speeds v_1 and v_2 along the x_3-axis, and let these media be separated by a point moving with velocity $V < c$ along the same axis. This point of separation will trace the line L with the slope $\psi, \tanh\psi = V/c$, in the (z, t)-plane.

The derivative u_τ of u along this line equals

$$u_\tau = i u_{x_3} \tanh\psi - u_{x_4}; \tag{A2.3}$$

this derivative should be continuous across L along with a similar derivative of v [1]. Bearing this in mind, we eliminate u_{x_4}, v_{x_4} from (A2.2), and arrive at the system

$$u_{x_3} = iu_\tau \frac{R\tanh\psi - T}{W} + iv_\tau \frac{1}{W},$$
$$v_{x_3} = iu_\tau \frac{T^2 - QR}{W} + iv_\tau \frac{R\tanh\psi - T}{W},$$

with W defined by (3.48).

We now take average values of both sides of either equation bearing in mind the continuity of u_τ, v_τ. Returning to notation (A2.3), we arrive, after some calculation, at the system

$$\alpha u_z + \beta u_t = V v_z + v_t,$$
$$V u_z + u_t = \theta(\alpha v_z + \beta v_t), \tag{A2.4}$$

with α, β, θ defined by (3.47). A simple algebra reduces (A2.4) to a standard form (2.11).

Appendix: 3

A mechanical implementation of a discontinuous velocity pattern along an elastic bar

A discontinuous velocity distribution along the bar may be produced through the following arrangements suggested by B. P. Lavrov (B.P. Lavrov, private communication, 2003).

First Version

Consider a thin elastic band stretched by a tensile force. With respect to longitudinal vibrations, the band performs as an elastic bar, with material displacements occurring about the static equilibrium.

The band is split into many independent sections, each section fabricated as a closed loop mounted on four supporting rolls (see Fig. A3.1). One of the rolls serves as a carrier bringing the whole loop into motion, another bridle roll maintains the tension of the band. The upper rolls are suspended to the ceiling by the rods connected through hinges, so the entire section, being rectangular in statics, preserves the freedom of horizontal motion. Through such a motion, it becomes distorted and takes the shape of a parallelogram shown in Figure A3.2.

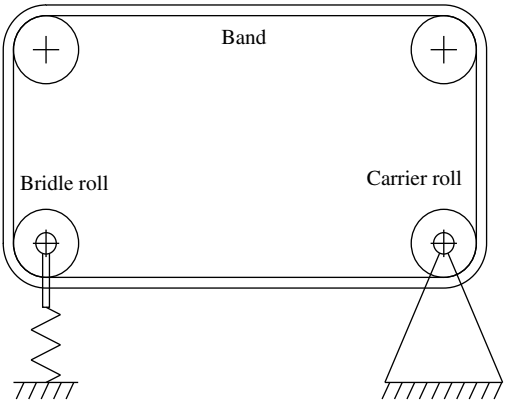

Fig. A3.1. A section of the elastic bar.

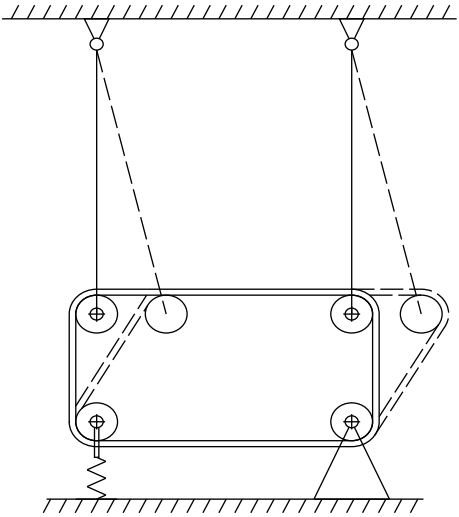

Fig. A3.2. A suspended section of the bar.

Two rolls out of four on each section have the axes common with rolls belonging to the adjacent sections (such rolls occupy the upper row in Fig. A3.3). All of the rolls rotate freely, without friction, about their axes. The

neighboring sections occupy alternating positions along the common rotation axes, so their respective bands come onto the rolls as shown in Fig. A3.3. The lower rolls in the alternating sections are placed at different horizontal levels to secure the access necessary for mounting the independent carrier and bridle rolls in order to maintain the required velocity and tension of the band.

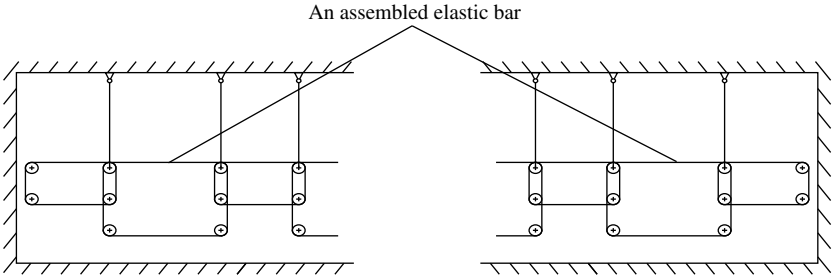

Fig. A3.3. An elastic bar as an assembly of sections.

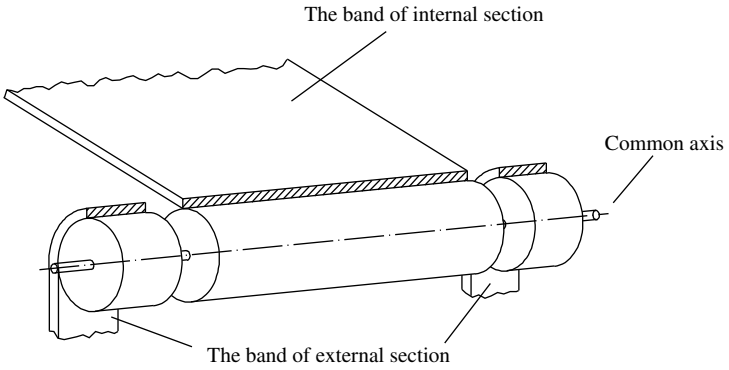

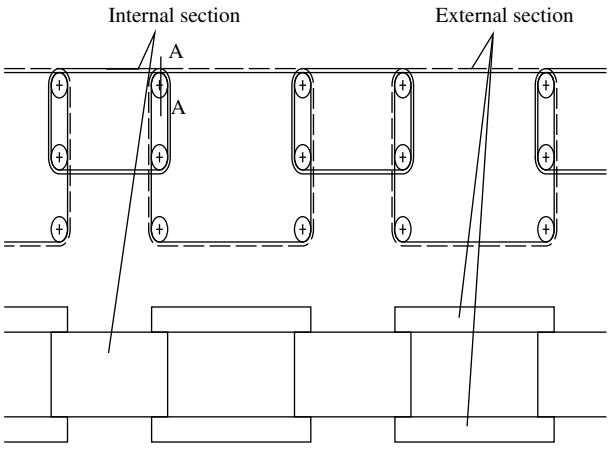

Fig. A3.4. Rolls from two adjacent sections mounted on the common axis.

The ultimate arrangement of an elastic bar is shown in Fig. A3.4. It is combined of the top horizontal parts of each section. The extreme left and right rolls of the arrangement are either attached to the walls, or connected to the devices that generate longitudinal vibrations or pulses.

The velocity of the band in each section may be independently sustained, both in magnitude and direction, by the use of the relevant single drive. The tension is, however, common to all sections; it is maintained by a tensile force generated by bridle rolls. To secure a reliable performance of a build up, the stress in the band should not exceed the yield force of the material.

Second Version

A bar is imitated by a gas (air) column. A segment of a pipeline is assembled of sections separated from each other by toroidal chambers (see Fig. A3.5). By manipulating compressions and rarefactions in the chambers, it is possible to produce, within each section, the velocity pattern variable in magnitude and direction.

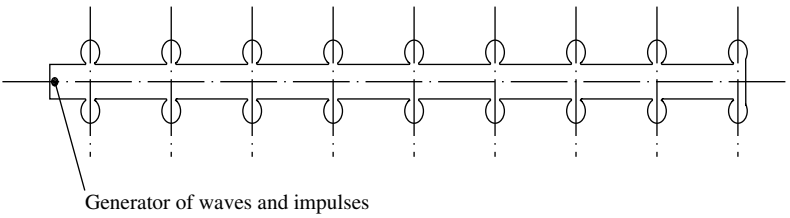

Fig. A3.5. A pipeline assembled of sections.

In particular, one may generate a standing wave and register variations of its frequency caused by the variable velocity distribution. The pressure may

be adjusted individually for each chamber, by virtue of reducing valves. The air should be able to leave some of the chambers, also through such valves.

A base pressure level in a system may be maintained by a common compressor; control of the pressure in various chambers may be carried out through individual reduction gears. The velocity of sound is affected by pressure, and may be accordingly controlled by pressure variations. There must be a way for the air to leave the system, also through the reduction gears.

Appendix: 4

Comment on eqn. (6.8)

We reproduce below a standard homogenization procedure for the wave equation

$$\mathrm{div}(\mu^{-1}\mathrm{grad}u) - (\epsilon u_t)_t = 0 \tag{A4.1}$$

in two spatial variables x, z, with the pattern of (ϵ, μ) defined as an activated laminate depending on the fast variable $(\xi x + \eta z - Vt)/\delta$, with period δ.

The asymptotics of solution of (A4.1) is sought for in the form

$$u(x,z,t) = u_0\left(x,z,t,\frac{\xi x+\eta z - Vt}{\delta}\right) + \delta u_1\left(x,z,t,\frac{\xi x+\eta z - Vt}{\delta}\right) + \delta^2 u_2\left(x,z,t,\frac{\xi x+\eta z - Vt}{\delta}\right). \tag{A4.2}$$

where $u_i(x,z,t,\zeta)$ is 1-periodic function of ζ, i.e. $u_i(x,z,t,\zeta{+}1) = u_i(x,z,t,\zeta)$, and $\xi = \cos\psi, \eta = \sin\psi$. By substituting (A4.2) into (A1.1) we obtain

$$\begin{aligned}
&-\delta^{-2}(\xi^2 L_{\zeta\zeta}u_0 + \eta^2 L_{\zeta\zeta}u_0 - V^2 M_{\zeta\zeta}u_0)\\
&-\delta^{-1}(\xi L_{x\zeta}u_0 + \eta L_{z\zeta}u_0 + \xi L_{\zeta x}u_0 + \eta L_{\zeta z}u_0 + \xi^2 L_{\zeta\zeta}u_1 \eta^2 L_{\zeta\zeta}u_1 + VM_{\zeta t}u_0 +\\
&+ VM_{t\zeta}u_0 - V^2 M_{\zeta\zeta}u_1) - \delta^0(L_{xx}u_0 + L_{zz}u_0 + \xi L_{x\zeta}u_1 + \eta L_{z\zeta}u_1\\
&+ \xi L_{\zeta x}u_1 + \eta L_{\zeta z}u_1 + \xi^2 L_{\zeta\zeta}u_2 + \eta^2 L_{\zeta\zeta}u_2 - M_{tt}u_0 + VM_{t\zeta}u_1 + VM_{\zeta t}u_1\\
&+ VM_{\zeta t}u_1 - V^2 M_{\zeta\zeta}u_2) + \delta r(x,z,t,\delta) = 0.
\end{aligned} \tag{A4.3}$$

Here

$$L_{\alpha\beta}u_i(x,z,t,\zeta) = \frac{\partial}{\partial\alpha}\left(\mu^{-1}(\zeta)\frac{\partial}{\partial\beta}u_i(x,z,t,\zeta)\right),$$

$$M_{\alpha\beta}u_i(x,z,t,\zeta) = \frac{\partial}{\partial\alpha}\left(\epsilon(\zeta)\frac{\partial}{\partial\beta}u_i(x,z,t,\zeta)\right),$$

$$r(x,z,t,\delta) = r_0(x,z,t,\delta) + \delta r_1(x,z,t,\delta),$$

$$r_0(x,z,t,\delta) = -L_{xx}u_1 - L_{zz}u_1 - \xi L_{x\zeta}u_2 - \eta L_{z\zeta}u_2 - \xi L_{\zeta x}u_2 - \eta L_{\zeta z}u_2 + M_{tt}u_2 - VM_{\zeta t}u_2,$$

$$r_1(x,z,t,\delta) = -L_{xx}u_2 - L_{zz}u_2 + M_{tt}u_0.$$

Let us require that the terms of orders $\delta^{-2}, \delta^{-1}, \delta^0$ vanish. Then

$$\xi^2 L_{\zeta\zeta}u_0 + \eta^2 L_{\zeta\zeta}u_0 - V^2 M_{\zeta\zeta}u_0 = 0, \tag{A4.4}$$

$$\xi L_{x\zeta}u_0 + \eta L_{z\zeta}u_0 + \xi L_{\zeta x}u_0 + \eta L_{\zeta z}u_0 + \xi^2 L_{\zeta\zeta}u_1 + \eta^2 L_{\zeta\zeta}u_1 + VM_{\zeta t}u_0 + VM_{t\zeta}u_0 - V^2 M_{\zeta\zeta}u_1 = 0, \tag{A4.5}$$

$$L_{xx}u_0 + L_{zz}u_0 + \xi L_{x\zeta}u_1 + \eta L_{z\zeta}u_1 + \xi L_{\zeta x}u_1 + \eta L_{\zeta z}u_1 + \xi^2 L_{\zeta\zeta}u_2 + \eta^2 L_{\zeta\zeta}u_2 - M_{tt}u_0 + VM_{t\zeta}u_1 + VM_{\zeta t}u_1 - V^2 M_{\zeta\zeta}u_2 = 0 \tag{A4.6}$$

It follows from (A4.4) that $\mu^{-1}(\zeta)\partial u_0(x,z,t,\zeta)/\partial\zeta - V^2\epsilon(\zeta)\partial u_0(x,z,t,\zeta)/\partial\zeta$ is independent of ζ, i.e. $\mu^{-1}(\zeta)\partial u_0/\partial\zeta - V^2\epsilon(\zeta)\partial u_0/\partial\zeta = C(x,z,t)$, therefore,

$$\frac{\partial u_0(x,z,t,\zeta)}{\partial\zeta} = \frac{C(x,z,t)}{\mu^{-1}(\zeta) - V^2\epsilon(\zeta)}. \tag{A4.7}$$

We adopt the following notation for the *mean over the period* in both the one-dimensional as well as many-dimensional case,

$$\langle f(x_1,\ldots,x_s,t,\zeta_1,\ldots,\zeta_s)\rangle = \int_0^1 \ldots \int_0^1 f(x_1,\ldots,x_s,t,\zeta_1,\ldots,\zeta_s)d\zeta_1\ldots d\zeta_s,$$

with the variables x and ζ considered independent in the last integral.

By applying the operator $\langle\cdot\rangle$ to the equality (A4.7), we see from the periodicity of $u_0(x,z,\zeta)$ in ζ that

$$\left\langle \frac{\partial u_0(x,z,t,\zeta)}{\partial\zeta} \right\rangle = \int_0^1 \frac{\partial u_0(x,z,t,\zeta)}{\partial\zeta} d\zeta = 0.$$

Thus $0 = C(x,z,t)\langle(\mu^{-1}(\zeta) - V^2\epsilon(\zeta))^{-1}\rangle$, and consequently, $C(x,z,t) = 0, \partial u_0/\partial\zeta = 0$, and $u_0(x,z,t,\zeta)$ is independent of ζ, i.e.

$$u_0(x,z,t,\zeta) = u_0(x,z,t). \tag{A4.8}$$

Referring to (A4.8), we rewrite (A4.5) as

$$\frac{\partial}{\partial\zeta}\left(\xi\mu^{-1}\frac{\partial u_0}{\partial x} + \eta\mu^{-1}\frac{\partial u_0}{\partial z} + \mu^{-1}\frac{\partial u_1}{\partial\zeta} + V\epsilon\frac{\partial u_0}{\partial t} - V^2\epsilon\frac{\partial u_1}{\partial\zeta}\right) = 0.$$

This implies that

$$\xi\mu^{-1}\frac{\partial u_0}{\partial x}+\eta\mu^{-1}\frac{\partial u_0}{\partial z}+\mu^{-1}\frac{\partial u_1}{\partial\zeta}+V\epsilon\frac{\partial u_0}{\partial t}-V^2\epsilon\frac{\partial u_1}{\partial\zeta}=C_1(x,z,t),$$

$$\begin{aligned}\frac{\partial u_1}{\partial\zeta}&=C_1\frac{1}{\mu^{-1}(\zeta)-V^2\epsilon(\zeta)}-\xi\frac{\mu^{-1}(\zeta)}{\mu^{-1}(\zeta)-V^2\epsilon(\zeta)}\frac{\partial u_0}{\partial x}\\&\quad-\eta\frac{\mu^{-1}(\zeta)}{\mu^{-1}(\zeta)-V^2\epsilon(\zeta)}\frac{\partial u_0}{\partial z}-V\frac{\epsilon(\zeta)}{\mu^{-1}(\zeta)-V^2\epsilon(\zeta)}\frac{\partial u_0}{\partial t}.\end{aligned}\tag{A4.9}$$

By applying the operator $\langle\cdot\rangle$, we get

$$\left\langle\frac{\partial u_1}{\partial\zeta}\right\rangle=-C_1C+\xi A\frac{\partial u_0}{\partial x}+\eta A\frac{\partial u_0}{\partial z}+VB\frac{\partial u_0}{\partial t},$$

where A, B, C are given by (2.13) and (2.10), with a standard substitution (3.8). Hence,

$$C_1(x,z)=\xi\frac{A}{C}u_{0_x}+\eta\frac{A}{C}u_{0_z}+V\frac{B}{C}u_{0_t},$$

and

$$\begin{aligned}\frac{\partial u_1}{\partial\zeta}&=u_{0_x}\frac{\xi}{\mu^{-1}-V^2\epsilon}\left(\frac{A}{C}-\mu^{-1}\right)+u_{0_z}\frac{\eta}{\mu^{-1}-V^2\epsilon}\left(\frac{A}{C}-\mu^{-1}\right)\\&\quad+u_{0_t}\frac{v}{\mu^{-1}-V^2\epsilon}\left(\frac{B}{C}-\epsilon\right).\end{aligned}$$

Taking into account this expression for $\frac{\partial u_1}{\partial\zeta}$, we integrate (A4.6) with respect to ζ over $[0,1]$, and use the periodicity of $u_1(\zeta), \mu^{-1}(\zeta)$ and $\epsilon(\zeta)$. This yields

$$\begin{aligned}&-u_{0_{tt}}\left(D-V^2\frac{B^2}{C}\right)+u_{0_{xx}}\left(\eta^2E-V^2D+\xi^2\frac{A^2}{C}\right)\\&+u_{0_{zz}}\left(\xi^2E-V^2D+\eta^2\frac{A^2}{C}\right)\\&+u_{0_{xz}}2\xi\eta\left(\frac{A^2}{C}-E\right)+u_{0_{xt}}2\xi V\left(\frac{AB}{C}-D\right)\\&+u_{0_{zt}}2\eta V\left(\frac{AB}{C}-D\right)=0,\end{aligned}\tag{A4.10}$$

where D is defined by (2.10) and (3.8), and E specified by

$$E=\left\langle\frac{1}{\mu}\frac{a^2}{V^2-a^2}\right\rangle.$$

Eq. (A4.10) represents the required averaged equation. When $\xi=0, \eta=1$, it reduces to (6.8).

Index